

**INVESTIGATING OF BIOCLOGGING IN HOMOGENOUS AND  
HETEROGENEOUS UNCONTAMINATED AND  
CONTAMINATED SANDS**

**A THESIS SUBMITTED FOR THE DEGREE OF DOCTOR OF  
PHILOSOPHY**

**By**

**PARIS ALSHIBLAWI**

**APRIL 2016**

**SCHOOL OF ENGINEERING**

**CARDIFF UNIVERSITY**

## ***DECLARATION***

This work has not previously been accepted in substance for any degree and is not concurrently submitted in candidature for any degree.

Signed..... (candidate)      Date.....

### **STATEMENT 1**

This thesis is being submitted in partial fulfilment of the requirements for the degree of Doctor of Philosophy (PhD).

Signed..... (candidate)      Date.....

### **STATEMENT 2**

This thesis is the results of my own independent work/investigation, except where otherwise stated. Other sources are acknowledged by explicit references.

Signed..... (candidate)      Date.....

### **STATEMENT 3**

I hereby give consent for my thesis, if accepted, to be available for photocopying and for inter-library loan, and for the title and summary to be made available to outside organisations.

Signed..... (candidate)      Date.....

## **ACKNOWLEDGMENTS**

The work presented in this thesis would not have been possible without my close association with many people who were always there when I needed them the most. I take this opportunity to acknowledge them and extend my sincere gratitude for helping me make this Ph.D. thesis a possibility.

I would like to start with the persons who made the biggest difference in my life, my senior supervisor Prof. Hywel Thomas and co-supervisor Dr. Michael Harbottle for the continuous support, motivation and invaluable academic guidance.

Special thanks for the Embassy of the Republic of Iraq/ Culture attaché for the financial support during my thesis. Great thanks to the Geotechnical technician Mr. Len Czekaj and the technical staff in Cardiff University.

My special thanks to all admin staff in the research office Mrs Chris Lee,

Ms Jeanette Whyte and Mrs Aderyn Reid.

Finally, I would like to thank my other friends who have been a source of moral support to me and have extended their helping hands without fail.

## **SUMMARY**

Bioclogging can be defined as the reduction of hydraulic conductivity and porosity of a saturated porous medium due to microbial growth. Wastewater disposals, artificial groundwater recharge, in-situ bioremediation of contaminated aquifers, construction of water reservoirs, or secondary oil recovery are all affected by this process. The potential for soil and groundwater contamination may increase by the rapid movement of the solutes through soil due to the presence of preferential flow which resulted in increasing bypassing of soil matrix and increasing pore water velocities.

On the other hand the presence of preferential flow could affect the clean-up process of the contaminated land by extending the remedial time. The reason behind that is the relatively quick contaminant clean-up in the high permeable zones compared to the slow contaminant clean-up in the low permeable layers. Therefore, this study aims to investigate the bioclogging process in porous media and the factors that can affect this process, also to understand how all aspects of flow are affected by the clogging process, and finally to investigate the potential of biological growth to control direction and location of subsurface hydraulic flow to overcome the problems of preferential flow.

The bioclogging process was investigated through a series of sand column experiments in homogeneous and heterogeneous porous media. Six sand fractions ranging from 63-1180  $\mu\text{m}$  were selected as a porous media. Two bacterial strains (*P. putida* mt-2 and *B. indica*) were used in this study. Different analytical methods such as loss on ignition and the total number of cells were used to analyse the soil samples. The outcomes of this study showed that the growth of bacteria in porous media can reduce the heterogeneity of the porous media, thereby reducing the impact of the preferential flow which could affect the clean-up process of the contaminated land.

Pore throat model with the incorporation of different bioclogging models such as the biofilm or plugs (Vandevivere *et al.*, 1995), micro-colony (Okubo and Matsumoto, 1979), and macroscopic (Clement *et al.*, 1996) models were applied to evaluate the results of the experimental work in heterogeneous porous media.

The changes in hydraulic conductivity and the porosity of porous media were modelled by assuming that the bioclogging occurs in the small pores which connect the large pores of the porous media.

Generally amongst the three bioclogging models, the current study showed that the measured values of the hydraulic conductivity relatively coincide with the predicted values obtained by using Vandevivere *et al.* (1995) model. Nevertheless, the predicted values of the hydraulic conductivity coincided to some extent with the measured values of the hydraulic conductivity for the large sand fractions. This corresponds with the findings of several previous studies which also confirmed that bioclogging models can only predict the change of the hydraulic conductivity for the large sand fractions. The failure of these models could be related to the assumptions made by each model, which could be less appropriate in fine-textured materials than they are in coarse textured ones. The second possible reason for the disparities between observations and model predictions is related to the assumption made in some of these models that the microorganisms which are responsible for clogging form biofilms of constant thickness which uniformly coated the surface of soil particles.

## Table of Contents

<i>List of Figures</i> .....	viii
<b>CHAPTER ONE</b> .....	1
<b>INTRODUCTION</b> .....	1
<b>1.1 Background of groundwater contamination</b> .....	1
<b>1.2 Aim and Objectives</b> .....	4
<b>1.3 Thesis outline</b> .....	5
<b>CHAPTER TWO</b> .....	8
<b>LITERATURE REVIEW AND BACKGROUND</b> .....	8
<b>2.1 Introduction</b> .....	8
<b>2.2 Microbial behaviour in porous media</b> .....	11
<b>2.2.1 Factors which affect microorganisms transport and growth</b> .....	12
<b>2.2.2 Extracellular polymeric substances (EPS)</b> .....	13
<b>2.2.3 Biofilms Formation</b> .....	14
<b>2.2.4 Biofilms application in environmental biotechnology</b> .....	18
<b>2.3 Soil heterogeneity and preferential flow paths</b> .....	20
<b>2.3.1 Behaviour of preferential flow in soil</b> .....	21
<b>2.3.2 The impact of preferential flow on groundwater remediation techniques</b> ....	23
<b>2.4 Bioclogging in porous media</b> .....	24
<b>2.4.1 Bioclogging in one dimension</b> .....	26
<b>2.4.2 Bioclogging in two dimensions</b> .....	32
<b>2.4.3 Factors influencing bioclogging in porous media</b> .....	38
<b>2.4.4 Bioclogging modelling approaches</b> .....	41
<b>2.4.5 The application of bioclogging in environmental biotechnology</b> .....	46
<b>2.4.6 Heavy metal removal in the presence of bacteria</b> .....	50
<b>CHAPTER THREE</b> .....	51
<b>MATERIALS AND METHODS</b> .....	51
<b>3.1 Introduction</b> .....	51
<b>3.2 Materials</b> .....	52
<b>3.2.1 Sand</b> .....	52
<b>3.2.2 Bacterial strain</b> .....	53
<b>3.3 Analytical methods</b> .....	55
<b>3.3.1 Soil tests</b> .....	55

3.3.2 Loss on ignition .....	64
3.3.3 Separation of cells from soil sample method .....	66
3.3.4 Bacteria counting using DAPI staining.....	66
3.3.5 Batch adsorption experiment.....	67
3.3.6 Inductively Coupled Plasma-Optical emission spectrometers ICP-OES method.....	69
3.4 Experimental methods.....	70
3.4.1 Preliminary experiments .....	70
3.5 Experimental work in homogeneous porous media.....	75
3.5.1 Set-up the bioclogging experiments in homogenous porous media .....	76
3.5.2 Different culture medium effect on bacterial growth in homogeneous soil ...	78
3.5.3 Flow rate effect on bacterial growth in homogeneous soil .....	79
3.5.4 Experiments of grain size effect on bioclogging in homogeneous porous media .....	79
3.6 Experimental work in heterogeneous porous media.....	81
3.6.1 Set-up the bioclogging experiments in heterogeneous porous media .....	81
3.6.2 Grain size effect on bioclogging in heterogeneous porous media .....	84
3.6.2 The effect of different zinc concentrations on bacterial growth .....	86
3.6.3 The heavy metals removal in the presence and absence of <i>B. indica</i> .....	87
<b>CHAPTER FOUR</b> .....	89
<b>RESULTS AND DISCUSSION OF BIOLOGGING EXPERIMENTS IN HOMOGENEOUS POROUS MEDIA</b> .....	89
4.1 Experimental results.....	89
4.1.1 Optimization of biofilm production.....	90
4.1.2 Flow rate effect .....	94
4.1.3 Grain size effect.....	97
4.2 Chemical and biological tests .....	106
4.2.1 Total number of cells .....	106
4.2.2 Loss on ignition analysis.....	108
4.3 Overall discussion .....	111
<b>CHAPTER FIVE</b> .....	120
<b>RESULTS AND DISCUSSION OF BIOLOGGING EXPERIMENTS IN HETEROGENEOUS POROUS MEDIA</b> .....	120
5.1 Experimental results.....	120
5.2 Grain size effect.....	120

5.3 Loss on ignition analysis.....	134
5.4 Total number of cells .....	138
5.5 Batch adsorption experiment.....	140
5.6 The effect of different zinc concentrations on bacterial growth in batch experiment .....	145
5.7 Zinc effect on bacterial growth in heterogeneous porous media .....	147
5.7.1 Loss on ignition analysis .....	150
5.8 Overall discussion .....	154
<b>CHAPTER SIX</b> .....	183
<b>THEORETICAL ANALYSIS OF THE EXPERIMENTAL WORK</b> .....	183
6.1 Introduction.....	183
6.2 Pore bioclogging model.....	184
6.3 Model calculations .....	189
6.4 Overall discussion .....	205
<b>CHAPTER SEVEN</b> .....	216
7.1 Introduction.....	216
7.1.2 Conclusions of the bioclogging experiments in homogeneous porous media .....	217
7.1.3 Conclusions of the bioclogging experiments in heterogeneous porous media .....	218
7.1.4 Conclusions of the theoretical analysis of the experimental works .....	221
7.2 Recommendations and Future works .....	222

## List of Tables

<b>Table 3.1:</b> Summary of hydraulic conductivity test for six sand fractions.....	59
<b>Table 3.2:</b> Compaction test results for six sand fractions.....	64
<b>Table 3.3:</b> The main Experiments in both homogenous and heterogeneous porous media.....	71
<b>Table 3.4:</b> Parameters of the bioclogging experiments in homogenous and heterogeneous porous media .....	74
<b>Table 4.1:</b> Comparisons between cell and EPS weights in batch experiment using six culture mediums with different concentrations of glucose (G) and ammonium sulphate (A).....	91
<b>Table 4.2:</b> The average of EPS weight under continuous nutrient feeding using three different culture mediums with different concentrations of glucose (G) and ammonium sulphate (A).....	92
<b>Table 6.1:</b> Parameters used in the bioclogging models.....	183

## List of Figures

<b>Figure 2.1:</b> The stages of biofilm formation (Armitage, 2005).....	16
<b>Figure 2.2:</b> Macro-pores in porous media.....	23
<b>Figure 2.3:</b> Progression of biofilm thickness ( <i>Ps. aeruginosa</i> ) for media of different diameter and composition (Cunningham <i>et al.</i> 1991).....	29
<b>Figure 2.4:</b> Change in hydraulic conductivity of each layer of sand (Seki, 2013)...	31
<b>Figure 2.5:</b> Effects of biofilm growth and shear stress on permeability ratio (Kim and Fogler, 2000).....	33
<b>Figure 2.6:</b> Pressure drop across micromodel during constant-rate injection of nutrient with 15 g/L sucrose (Stewart and Fogler, 2001).....	34
<b>Figure 2.7:</b> Illustration of a 3.2 mm x 4.3 mm area of the two SPIE patterns (Dupin and McCarty, 2000).....	35
<b>Figure 2.8:</b> Details of the sand box experiment (Kildsgaard and Engesgaard, 2000).....	36

<b>Figure 2.9:</b> The Brilliant Blue tracer distribution after 60 minutes on different days (Kildsgaard and Engesgaard, 2000).....	37
<b>Figure 2.10:</b> Relationship between the saturated hydraulic conductivity ratio and the bio-volume ratio for different grain size (Vandevivere <i>et al.</i> , 1995).....	40
<b>Figure 2.11:</b> Schematic diagram illustrating growth of micro-colonies. (A) A sparse distribution of micro-colonies after the initial inoculation of the porous medium. (B) A higher density of micro-colonies causing bioclogging of the pore throats (Seifert and Engesgaard, 2007).....	43
<b>Figure 2.12:</b> Permeable Reactive Barrier Example (EPA, 2001b).....	48
<b>Figure 3.1:</b> Sub-culture the <i>P. putida</i> mt-2 in 50 ml of nutrient broth.....	55
<b>Figure 3.2:</b> Sieve analysis graph of soil.....	56
<b>Figure 3.3:</b> Standard Permeameter of the constant and falling head method.....	58
<b>Figure 3.4:</b> The relation between dry density and water content for six sand fractions: A, B, C, D, E, F for 600, 425, 300, 212, 150 and 63 $\mu\text{m}$ .....	61-63
<b>Figure 3.5:</b> The relation between number of cells and optical density of <i>B. indica</i> .....	72
<b>Figure 3.6:</b> Schematic diagrams for bioclogging experiment in homogeneous soil.....	77
<b>Figure 3.7:</b> Photo of heterogeneous experiment structure.....	82
<b>Figure 3.8:</b> Schematic diagrams for the bioclogging experiment in heterogeneous porous media.....	84
<b>Figure 4.1:</b> Effect of different culture medium on the growth of <i>P. putida</i> mt-2, error bars represent standard deviation of measured hydraulic conductivity values, G and A refer to glucose and ammonium sulphate respectively.....	94
<b>Figure 4.2:</b> Effect of flow rate on hydraulic conductivity due to growth of <i>P. putida</i> mt-2, error bar represent standard deviation of measured hydraulic conductivity values.....	95

<b>Figure 4.3:</b> Flow rate effect on hydraulic conductivity due to the growth of <i>B. indica</i> , error bars represent standard deviation of measured hydraulic conductivity values.....	96
<b>Figure 4.4:</b> Change in hydraulic conductivity for three different sand fractions 600, 300, and 212 $\mu\text{m}$ in homogeneous soil due to the growth of <i>P. putida</i> mt-2, error bars represent standard deviation of measured hydraulic conductivity values.....	98
<b>Figure 4.5:</b> The changes of hydraulic conductivity with time due to the growth of <i>B. indica</i> for five sand fractions ranging from 150-1180 $\mu\text{m}$ on normal scale.....	100
<b>Figure 4.6:</b> Changes of hydraulic conductivity with time due to growth of <i>B. indica</i> at 12-22°C for five sand fractions ranging from 150-1180 $\mu\text{m}$ in logarithmic scale, error bars represent standard deviation of the measured hydraulic conductivity values.....	101
<b>Figure 4.7:</b> The changes of hydraulic conductivity with time due to the growth of <i>B. indica</i> for six sand fractions ranging from 63-1180 $\mu\text{m}$ .....	103
<b>Figure 4.8:</b> Changes of hydraulic conductivity with time due to growth of <i>B. indica</i> at 25°C for six sand fractions ranging from 63-1180 $\mu\text{m}$ at logarithmic scale, error bars represent standard deviation of the measured hydraulic conductivity values.....	104
<b>Figure 4.9:</b> Change in the hydraulic conductivity values with time at 25°C and 12-22°C.....	105
<b>Figure 4.10:</b> Comparison between total numbers of cells per gram of soil in control and biological conditions for six sand fractions at 25°C, error bars represent standard deviation of the total number of cells, data collected by the end of the each sand column experiment.....	107
<b>Figure 4.11:</b> The average of the total numbers of cells per gram under the biological conditions (live <i>B. indica</i> ) for six different sand fractions at 25°C, error bars represent standard deviation of the total cells numbers, the data collected the end of sand column experiment.....	107
<b>Figure 4.12:</b> Loss on ignition due to <i>B. indica</i> growth at 12-22°C for five sand fractions, error bars represent standard deviation of the measured loss on ignition values at the end of sand column experiment.....	108
<b>Figure 4.13:</b> Relation between the average loss on ignition due to <i>B. indica</i> growth and grain size, error bars represent the standard deviation of the measured loss on ignition values at the end of sand column experiment which carried out at 12-22°C.....	109

<b>Figure 4.14:</b> Loss on ignition due to <i>B. indica</i> growth at 25°C for six sand fractions ranging from 63 to 1180 μm, error bars represent standard deviation of the measured loss on ignition values at the end of sand column experiment.....	110
<b>Figure 4.15:</b> Relation between the average loss on ignition due to <i>B. indica</i> growth and grain size, error bars represent the standard deviation of the measured loss on ignition values at the end of sand column experiment which carried out at 25°C .....	110
<b>Figure 4.16:</b> The relation between the average loss on ignition and sand grain size on the actual x-axis, error bars represent the standard deviation of the measured loss on ignition values at the end of sand column experiment which carried out at 25°C.....	111
<b>Figure 4.17:</b> The flow rate effect on the growth of <i>P. putida</i> mt-2 and <i>B. indica</i> .....	114
<b>Figure 4.18:</b> The effect of grain size on hydraulic permeability due to the growth of <i>P. putida</i> mt-2 and <i>B. indica</i> for three sand fractions.....	117
<b>Figure 4.19:</b> The relation between the average of the loss on ignition and relative hydraulic conductivity due to the growth of <i>B. indica</i> at 25°C for six sand fractions.....	119
<b>Figure 5.1:</b> Changes in the hydraulic conductivity with time due to the growth of <i>B. indica</i> for five experiments using different sand fractions, A and A1 logarithmic and normal scale for EXP.(1), 5.1B and 5.1B1 for EXP.(2), C and C1 for EXP.(3), D and D1 for EXP.(4), and E and E1 for EXP.(5), error bars represent the standard deviation of the measured hydraulic conductivity value.....	(123-128)
<b>Figure 5.2:</b> Flow rate profile for all heterogeneous experiments(A:EXP(1), B:EXP(2), C:EXP(3), D:EXP(4), and E:EXP(5), error bars represent the standard deviation of the measured and calculated flow rates for different sand fractions.....	(130-132)
<b>Figure 5.3:</b> Loss on ignition values for all heterogeneous experiments, error bars represent the standard deviation of loss on ignition values .....	135
<b>Figure 5.4:</b> Relation between loss on ignition due to <i>B. indica</i> growth and grain size of sand for all heterogeneous experiments, error bars represent the standard deviation for loss on ignition values.....	136
<b>Figure 5.5:</b> Average of the total number of bacteria for all heterogeneous experiments, error bars represent the standard deviation for the total number of bacteria.....	138

**Figure 5.6:** The change of zinc after 24 hours of contact with four different soils: solution ratio for three sand fractions 600, 300, and 150  $\mu\text{m}$  .....140

**Figure 5.7:** Langmuir isotherm showing the variation of adsorption ( $C_e/q_e$ ) against the equilibrium concentration ( $C_e$ ) for adsorption of zinc ions onto soil particle: A for 600  $\mu\text{m}$ , B for 300  $\mu\text{m}$  and C for 150  $\mu\text{m}$  sand fractions..... (141-142)

**Figure 5.8:** Freundlich isotherm showing the variation of adsorption  $\ln(q_e)$  against the equilibrium concentration  $\ln(C_e)$  for adsorption of zinc ions onto soil particle: A for 600  $\mu\text{m}$ , B for 300  $\mu\text{m}$  and C for 150  $\mu\text{m}$  sand fractions..... (143-144)

**Figure 5.9:** The effects of different concentrations of zinc on the growth of *B. indica* in batch experiment, error bars represent the standard deviation of the optical density values.....146

**Figure 5.10:** The effect of zinc concentration on hydraulic conductivity of porous media due to *B. indica* growth in three different sizes of sand 600, 300 and 150  $\mu\text{m}$  in logarithmic scale, error bars represent the standard deviation of the hydraulic conductivity readings.....147

**Figure 5.11:** The effect of zinc concentration on hydraulic conductivity of porous media due to *B. indica* growth in three different sizes of sand 600, 300 and 150  $\mu\text{m}$  in normal scale, error bars represent the standard deviation of the hydraulic conductivity readings.....148

**Figure 5.12:** The effect of zinc concentration on hydraulic conductivity of porous media under control conditions (dead cells) in three different sizes of sand 600, 300 and 150  $\mu\text{m}$ , error bars represent the standard deviation of the measured hydraulic conductivity values.....148

**Figure 5.13:** Loss on ignition due to *B. indica* growth in three different sizes of sand 600, 300 and 150  $\mu\text{m}$  contaminated with zinc, error bars represent the standard deviation of the loss on ignition values.....150

<b>Figure 5.14:</b> Relation between losses on ignition due to <i>B. indica</i> growth and grain size of sand 600, 300 and 150 $\mu\text{m}$ , error bars represent the standard deviation of the loss on ignition values.....	150
<b>Figure 5.15:</b> Changes in zinc concentration in three sand fractions 600, 300 and 150 $\mu\text{m}$ for the biological conditions (live cells), error bars represent the standard deviation of the zinc concentrations.....	152
<b>Figure 5.16:</b> Changes in zinc concentration in three sand fractions 600, 300 and 150 $\mu\text{m}$ for the control conditions, error bars represent the standard deviation of the zinc concentrations.....	152
<b>Figure 5.17A:</b> The changes of the hydraulic conductivity via time in the 600 $\mu\text{m}$ in four heterogeneous experiments.....	155
<b>Figure 5.17B:</b> The changes of the hydraulic conductivity via time in the 425 $\mu\text{m}$ in two heterogeneous experiments.....	156
<b>Figure 5.17C:</b> The changes of the hydraulic conductivity via time in the 300 $\mu\text{m}$ in two heterogeneous experiments.....	157
<b>Figure 5.17D:</b> The changes of the hydraulic conductivity via time in the 212 $\mu\text{m}$ in two heterogeneous experiments.....	158
<b>Figure 5.17E:</b> The changes of the hydraulic conductivity via time in the 150 $\mu\text{m}$ in four heterogeneous experiments.....	159
<b>Figure 5.17F:</b> The changes of the hydraulic conductivity via time in the 63 $\mu\text{m}$ in one heterogeneous experiment.....	160
<b>Figure 5.18A-E:</b> Comparisons between the homogenous and heterogeneous experiments for the same sand fractions.....	(161-163)
<b>Figure 5.19</b> Ratio of low to high flow rate via time for all heterogeneous experiments. A: EXP.(1), B: EXP.(2), C: EXP.(3), D: EXP.(4) and E: EXP.(5).....	(164-166)
<b>Figure 5.20:</b> Relation between relative hydraulic conductivity and loss on ignition for the three columns of each set of sand fractions and for all heterogeneous experiments.....	(171-173)
<b>Figure 5.21:</b> Relation between loss on ignition values and relative hydraulic conductivity for six sand fractions.....	(174-177)
<b>Figure 5.22:</b> Comparison between the changes of the hydraulic conductivity values for three sand fractions in clean and contaminated porous media.....	180
<b>Figure 6.1:</b> (a) Body-centred cubic (b) Body-centred cubic unit cell (c) Section in body-centred cubic.....	185

**Figure 6.2:** The Pore body inside the body centred cubic unit cell.....187

**Figure 6.3:** Comparison between the predicted and the measured changes of the hydraulic conductivity with time for A: 600, B: 425, and C: 300  $\mu\text{m}$  sand fractions.....(191-192)

**Figure 6.4:** Comparison between the predicted and the measured changes of the hydraulic conductivity with time for A: 600, B: 425, and C: 150  $\mu\text{m}$  sand fractions.....(193-195)

**Figure 6.5:** Comparison between the predicted and the measured changes of the hydraulic conductivity with time for A: 600, B: 300, and C: 150  $\mu\text{m}$  sand fractions.....(196-197)

**Figure 6.6:** Comparison between the predicted and the measured changes of the hydraulic conductivity with time for A: 600, B: 212, and C: 150  $\mu\text{m}$  sand fractions.....(199-200)

**Figure 6.7:** Comparison between the predicted and the measured changes of the hydraulic conductivity with time for A: 212, B: 150 and C: 63  $\mu\text{m}$  sand fractions.....(202-203)

**Figure 6.8:** The relation between the relative hydraulic conductivity ( $K_{rel}$ ) and relative porosity ( $\eta_{rel}$ ) for the for EXP.(1) using three bioclogging models...(205-206)

**Figure 6.9:** The relation between the relative hydraulic conductivity ( $K_{rel}$ ) and relative porosity ( $\eta_{rel}$ ) for the for EXP.(2) using three bioclogging models...(206-207)

**Figure 6.10:** The relation between the relative hydraulic conductivity ( $K_{rel}$ ) and relative porosity ( $\eta_{rel}$ ) for the for EXP.(3) using three bioclogging models...(208-209)

**Figure 6.11:** The relation between the relative hydraulic conductivity ( $K_{rel}$ ) and relative porosity ( $\eta_{rel}$ ) for the for EXP.(4) using three bioclogging models...(209-210)

**Figure 6.12:** The relation between the relative hydraulic conductivity ( $K_{rel}$ ) and relative porosity ( $\eta_{rel}$ ) for the for EXP.(5) using three bioclogging models...(211-212)

## **INTRODUCTION**

### **1.1 Background of groundwater contamination**

Groundwater is one of the important resources that need to be managed carefully. Given the importance of this source of water to human-kind it has become necessary to keep it unpolluted to ensure safe current and future water supplies for the world. Serious public issues have been raised over the contamination of groundwater which is caused by organic chemicals, toxic heavy metals, and microbial pollutants because of the devastated influence on human health, water resources and food quality (Khan *et al.*, 2004).

As a result of groundwater pollution several remediation technologies have been implemented to limit and prevent the risk of this pollution. The clean-up process can be implemented in several ways, including the transfer of contaminated soil or groundwater into other places for final treatment, the destruction of the contaminants in their place. Removal is seen as transferring unresolved contaminant problems to another site (Brough *et al.*, 2001).

The most conventional remediation technologies available for soil and groundwater treatments include; pump and treat, soil washing, bioremediation, soil vapour extraction, precipitation, thermal desorption, stabilization, vitrification, and air stripping. Some of these technologies have many limitations and; one of these limitations is the soil heterogeneity. Soil heterogeneity refers to the variability of soil properties those results from natural cracks or different materials (Hicks and Nuttall, 2012).

Many laboratory and field studies confirmed that soil heterogeneity has a great influence on the in-situ remediation efficiency; the remediation timeframe is longer in heterogeneous soil than the homogenous soil (Reddy, 2008). The time required to clean the soil from the contaminants that are trapped in lower permeability layers will increase by increasing the difference in hydraulic conductivity between the lower permeability layer and the higher permeability layer (Ho and Udell, 1992). Ho and Udell (1992) reported that the heterogeneous nature of many subsurface layers results in rapid removal of trapped NAPL in the higher permeability layers followed by slow removal in the lower permeability layers.

Preferential flow can be defined as a relatively rapid movement of water and dissolved solutes along preferred pathways. In subsurface soil, this rapid movement of water and dissolved solutes along preferred pathways such as channels of higher conductivity formed by cracks, earthworm burrows and root channels through the soil allowing water to bypass part of the soil matrix, leading to faster transport of the solute into greater depths (Beven and Germann, 1982; Simunek and Van Genuchten, 2007; Hardie *et al.*, 2011). Soil heterogeneity could be one of the main causes of the occurrence of preferential flow that result in a significant spatial variation of water and solute flow (Nielsen *et al.*, 1973)

The existence of preferential flow due to the heterogeneity of saturated soil (EPA, 1996; Hendrickx and Flury, 2001) or instability of the wetting front in porous media (Bouwer, 1991) can affect the clean-up process of contaminated porous media through significantly extended remedial times (EPA, 1996), because the clean-up process may only occur in more permeable layers within the porous media. The lower permeability layer will require longer clean-up time than a more permeable medium. This behaviour

could be attributed to the rapid movement of the solute in high pore-water velocities due to the preferential flow, and the slow movement of solute in the less permeability layers which leads to minimise the efficiency of solute leaching (Cote *et al.*, 2003).

The potentially detrimental effect of preferential flow is not limited to contaminated land and pollution, but also extends to the agricultural sectors. The existence of preferential flow will cause a large amount of water and solute to be transported quickly and move to deep soil during irrigation, which will reduce the effect of pesticides and fertilize on the soil and led to more contamination of soil (Malone *et al.*, 2004). Pesticide contamination of drain tile discharges which are potentially significant pathways for the movement of fertilizers and pesticides to streams and ditches has also been widespread, affecting surface water quality.

Preferential flow in the unsaturated zone provides a route for water and solutes to bypass the soil matrix (Stone and Wilson, 2006). In order to overcome the presence of preferential flow which might affect the clean-up process in heterogeneous porous media, it is very important to reduce the soil heterogeneity, or reduce the difference in permeability for different soil layers. Recent researches defined bioclogging as the reduction in hydraulic conductivity due to the growth of microorganisms. Most of bioclogging studies indicated that biomass was able to reduce hydraulic conductivity up to three orders of magnitude (Taylor and Jaffé, 1990b). In general, most of the previous studies that investigated the bioclogging process did not come across the effect of the bacterial growth on the groundwater flow patterns in heterogeneous porous media or multi different permeable soil layers which is called as soil stratification. Soil stratification when the flow is parallel to soil layers need to be looked at on how the flow is diverted within bioclogging process. For this reason, it is so important to find out how the bacterial growth could affect soil heterogeneity, and

how these microorganisms could be able to clog the high permeable layers and divert the flow into the lower permeable layers.

## **1.2 Aim and Objectives**

The process by which changes in the flow pattern occurs as a result of bacterial growth in the soil is called bioclogging. So far, there is a lack of knowledge about the bioclogging process in heterogeneous porous media and the factors that can affect this process.

This thesis aims to study the bioclogging process in porous media and the factors that can affect this process, as well as understand how some aspects of flow are affected by the clogging process, and finally to investigate the potential of biological growth to control direction and location of subsurface hydraulic flow to overcome the problems of preferential flow.

The overall objectives of the thesis are listed as follows:

- Investigate the effect of bacterial growth on the hydraulic conductivity and porosity of homogeneous porous media (sand).
- Investigate the spatial distribution of bacterial growth and bioclogging in heterogeneous porous media.
- Investigate the effect of bacterial growth on hydraulic flow in heterogeneous porous media. Furthermore, investigate how bioclogging will alter the profile of hydraulic conductivity and explore how it could enhance flow-based remediation technologies such as pump and treat through controlling the fluid flow direction in heterogeneous porous media by clogging the highly permeable layers and divert the flow into the less permeable layers.

- Study the removal of heavy metals in heterogeneous porous media under biological and control conditions to make sure that bioclogging may help the process of clean-up the contaminated porous media.
- Calculate the theoretical hydraulic conductivity changes with time, through the development of mathematical bioclogging model in cooperation with the previous mathematical bioclogging models.

### **1.3 Thesis outline**

This thesis involves experimental and theoretical work to study bioclogging processes in both homogeneous and heterogeneous porous media as well as the factors that may affect this process such as the grain size, the optimum growth conditions for bacteria, and their spatial distribution.

Then bioclogging process could be applied to investigate how it can enhance the remediation efficiency by studying the removal of heavy metals in heterogeneous porous media.

**Chapter 2:** This chapter includes many sections; the first section included an introduction to the aim and the limitations of the groundwater remediation techniques such as soil heterogeneity.

The second section dealt with the microbial behaviour in porous media which included the factors which affect microorganisms transport and growth, Extracellular Polymeric Substances (EPS) production and biofilm formation. Biofilm applications in environmental biotechnology were also presented in this section.

The third section involves the description of soil heterogeneity and preferential flow paths. The heterogeneity of the soil can be lead to preferential flow phenomena that can affect the efficiency of the clean-up process in contaminated porous media. On the other hand the behaviour of preferential flow in porous media and the factors which

can lead to the existence of such this phenomena and the impact of preferential flow on groundwater remediation techniques was presented extensively.

The fourth section of this chapter has been allocated to study the bioclogging process in porous media. Furthermore, some previous bioclogging studies in one and two dimensions were also reviewed. In addition to that, the factors which could have an influence on bioclogging in porous media such as the grain size effect, temperature and bacterial growth conditions were described. Finally, applications of bioclogging in environmental biotechnology were described extensively.

**Chapter 3:** This chapter describes the details of the laboratory experiments that were performed in an attempt to study the bioclogging process in homogeneous and heterogeneous porous media.

The first section of this chapter was devoted to the study soil characteristic tests which involving the sieve analysis test, permeability test, and compaction and particle density tests.

The second section contains a description of the bacterial strains that are used, their technical culturing techniques, optimal growth conditions, and the ability of these bacterial strains to form biofilm in soil.

The third section involves the experimental works that examine the variation in hydraulic conductivity in homogeneous and heterogeneous porous media due to the bacterial growth, determine the effect of grain size on bioclogging process and also the spatial distribution of cells throughout the porous media. The last section describes the methods that were used to investigate the heavy metals removal from contaminated heterogeneous porous media.

**Chapter 4:** The results of experimental work in homogeneous porous media including the use of two bacterial strains (*Pseudomonas putida* and *Beijerinckia indica*) were

analysed and discussed. The optimal growth conditions of the first bacterial strain that used in this study (*P. putida*), and its ability to form biofilm in batch experiment and soil was investigated. *B. indica* was used as an alternative bacterial strain because of the ability of this strain to produce a huge amount of tough and adhesive exopolysaccharides material (EPS) (Dennis and Turner, 1998).

**Chapter 5:** The results of the experimental work in heterogeneous porous media which included the use of *B. indica* were analysed using some analytical methods such as loss on ignition and total number of bacteria and discussed.

**Chapter 6:** In this chapter, the overall results of the experimental work were analysed through developing Pore throat model with the incorporation of different bioclogging models such as the biofilm or plugs (Vandevivere *et al.*, 1995), micro-colony (Okubo and Matsumoto, 1979) and macroscopic (Clement *et al.*, 1996) models. The changes in hydraulic conductivity and the porosity of porous media was modelled by assuming that bioclogging occurs in the small pores which connect the large pores in the porous media due to the accumulation of biomass.

**Chapter 7:** This chapter summarizes the general conclusions and provides the outline of the possible future directions on which to expand upon this work.

## **LITERATURE REVIEW AND BACKGROUND**

### **2.1 Introduction**

Soil and groundwater remediation technologies aim to control and prevent soil and groundwater contamination. Most of these technologies are quite expensive and could lead to insufficient degradation of contaminants. Therefore, it is very important to find a cost effective alternative technology. In-situ groundwater bioremediation technology is considered one of the remediation technologies that promote the growth of indigenous microorganisms to enhance biodegradation of organic constituents in the saturated zone. Bioremediation technology generally needs a mechanism for stimulating and maintaining the activity of these microorganisms. This mechanism is usually a delivery system (Manual, 2004) which provides one or more of the following: An electron acceptor, electron donor and nutrients. Generally, electron acceptors and nutrients are the most important components of any delivery system as well as appropriate environmental conditions such as; pH, temperature, and oxygen which all take part in maintaining the survival and growth of microorganisms (Abu-Ashour *et al.*, 1994; Allaire *et al.*, 2009; Thomas and Ward, 1989).

Microbial technology is considered one of the cost effective and environmental technologies which include the use of the indigenous microorganisms which are fed on hydrocarbons. Nevertheless, some contaminants like heavy metals and minerals differ as they cannot be degraded but they can be transformed into other oxidation states in soil (Nies, 1999; Knox *et al.*, 2000; Tangahu *et al.*, 2011).

For example, in bioleaching technology, the ability of microorganisms to oxidize solid compounds and altering them into soluble elements became popular in heavy metals recovery (Vu *et al.*, 2009).

Different types of microbes such as, iron-oxidizing and reducing bacteria, manganese-oxidizing and reducing bacteria, sulphur-oxidizing and reducing bacteria can directly affect the mineral transformation by altering the chemical composition of several metals such as iron and sulphur (Gadd, 2007; Gadd and Raven, 2010).

Microbes can increase the metals mobility through a redox process which is defined as the reduction in oxygen levels and decrease in redox potentials by microbial consumption of oxygen, Fe (III) and Mn (IV) can be changed to Fe (II) and Mn (II) respectively (Gadd and Raven, 2010). The redox potential of a soil system is the measure of electron availability within the soil (Suslow, 2004).

Soil structure and stratification are important factors that have an impact on the efficiency of in-situ groundwater remediation techniques because they have a direct effect on flow rates and patterns of groundwater when water is extracted or injected through the soil (Elkateb *et al.*, 2003). This variance in soil permeability could enhance solute transport in the more permeable layers and reduce it in the less permeable layers; this flow behaviour is known as preferential flow (Brusseau and Rao, 1990; Allaire *et al.*, 2009).

Preferential flow behaviour can lead to a decrease in the effectiveness of clean-up process and extend remedial times for the less permeable layers, and it occurs not only due to the difference in soil permeability but also because of the macro-pores which are formed by cracks, earthworm burrows, root channels and other structural inhomogeneities (Bouwer, 1991).

In order to improve the groundwater remediation techniques and make them more efficient, the heterogeneity of the porous media can turn into homogeneity through control of the preferential flow paths; this technique was used in the microbial enhanced oil recovery which includes the use of microorganisms to selectively clog the high permeable layers (MacLeod *et al.*, 1988).

The growth of bacteria which involves division, multiplying and extracellular polysaccharides (EPS) production, can lead to clogging the soil pore when these organisms have enough nutrients and growth conditions to survive, this process is called bioclogging (Baveye *et al.*, 1998; Thullner, 2001; Ivanov and Chu, 2008; Seki, 2013). Bioclogging could happen when these microorganisms produce a sufficient amount of EPS that clog the pore volume, which results in a severe reduction in soil hydraulic conductivity (Taylor and Jaffé, 1990b; Cunningham *et al.*, 1991; Vandevivere and Baveye, 1992; Baveye *et al.*, 1998; Thullner, 2001). Furthermore bioclogging could occur when these microorganisms produce low solubility gases, e.g., N<sub>2</sub> by denitrification or CH<sub>4</sub> by fermentation (Oberdorfer and Peterson, 1985). These gases could directly retard flow transport and therefore, result in a decrease in hydraulic conductivity of porous media (Seki *et al.*, 1998).

Most of the previous studies have used heterogeneous porous media, as almost all porous media is heterogeneous, but none of these studies has focused on how the bacterial growth could affect soil heterogeneity, and how these microorganisms might be able to clog the high permeable layers and divert the flow into the lower permeable layers, thereby minimise the preferential flow.

## 2.2 Microbial behaviour in porous media

Previously, microorganisms have been described as plankton, freely-suspended cells and identified on the basis of their growth characteristics in nutritionally-rich culture media, but the discovery of microscopic observations of bacteria has changed this idea. The microscopic observation techniques showed unequivocally that more than 99.9 % of the bacteria grow in biofilms on a wide variety of surfaces (Costerton *et al.*, 1987; Davey and O'toole, 2000; Donlan and Costerton, 2002; Prakash *et al.*, 2003; Singh *et al.*, 2006).

Soils are composed of minerals and large numbers of microorganisms, a kilogram of soil has up to  $10^{12}$  of microbes (Mitchell and Santamarina, 2005), this huge number of microorganisms mainly dependent on the presence of carbon source which provides energy for grow and survival. Microbial activities linked to the availability of nutrients, which include sources of carbon for the cell mass, the source of energy to maintain life, water and a favorable environment (Mitchell and Santamarina, 2005). To some extent subsurface soil is considered as an ideal environment in which the microorganisms can live and survive. Hence a wide range of microorganisms including bacteria, fungi, algae, viruses and protozoa inhabits soil.

The release of petroleum products such as hydrocarbons into the soil is one of the main causes of groundwater and soil contamination (Holliger *et al.*, 1997). Hydrocarbons can be removed or degraded by using microorganisms, which have the ability to remove pollutants owing to their metabolic capabilities (Das and Chandran, 2010). There is a wide range of bacteria which exploit hydrocarbons as a food source (Yakimov *et al.*, 1997; Thullner *et al.*, 2002). Bacteria with the ability to degrade hydrocarbons are named hydrocarbon-degrading bacteria. Biodegradation of hydrocarbons can occur under aerobic and anaerobic conditions (Grishchenkov *et al.*,

2000). Although many bacteria are able to metabolize organic pollutants, a single bacterium does not possess the enzymatic capability to degrade all or even most of the organic compounds in a polluted soil. Mixed microbial communities have the most powerful biodegradation potential because the genetic information of more than one organism is necessary to degrade the complex mixtures of organic compounds present in contaminated areas (Fritsche and Hofrichter, 2005). Due to a whole range of factors: competition with microorganisms, insufficient supply with essential substrates, unfavourable external conditions (aeration, moisture, pH, temperature), and low bioavailability of the pollutant, biodegradation in natural conditions is lesser (Joutey *et al.*, 2013).

### **2.2.1 Factors which affect microorganisms transport and growth**

The microbes in porous media have the ability to travel, grow and survive depending mainly on many physical, chemical and biological factors such as particle size distribution, clay content, pH, temperature, moisture content, and nutrient supply (Crane and Moore, 1984; Yates and Yates, 1988; Stevik *et al.*, 2004; Mitchell and Santamarina, 2005; DeJong *et al.*, 2006).

The grain size of porous media is one of the significant factors that control the bacterial movement. In addition to the grain size, surface texture and charge of porous media, greatly influences the adhesion process (Stevik *et al.*, 2004). One of the chemical factors that have a great effect on bacterial movements and survival is the pH value; several studies reported that pH values that ranging from 3 to 4 could have a negative effect on the survival of indigenous soil bacteria (Yates and Yates, 1991). Moreover, temperature profoundly affects the bacterial survival as the survival of bacteria decreases with increasing temperature. Hendricks *et al.* (1979) reported that attachment of bacteria was substantially greater at higher temperatures. Transport of

bacteria through porous media can be controlled by several physico-chemical mechanisms (Ryan and Elimelech, 1996) including the following physical processes such as:

**Advection** is defined as the movement of bacteria within flowing water through the soil in a single direction (McCaulou *et al.*, 1994; Yates and Yates, 1991).

**Dispersion** is a secondary movement of microorganisms through porous media, which can be defined as the diffusing of bacteria between soil particles from areas of high density to areas of low density (McCaulou *et al.*, 1994).

**Straining** refers to the retaining of bacteria in pore throats, which are smaller than the size of bacteria and prevent the move of the bacteria across them, i.e. blocking the bacteria from moving in a free way through the porous media (Stevik *et al.*, 2004; Díaz *et al.*, 2010).

In addition to that, microbial transport in porous media can be controlled by *attachment and detachment* processes (Clement *et al.*, 1996). Attachment process can be defined as the deposition of bacteria on the solid-water and air-water interface (Gargiulo *et al.*, 2007), but when bacteria detach from the surface of the soil particles the process would be called *detachment* (Matthess and Pekdeger, 1981; Abu-Ashour *et al.*, 1994).

Furthermore, the gravitational deposition on surfaces of soil particles that normally occurs when bacteria density is greater than liquid density is known as *sedimentation* (Abu-Ashour *et al.*, 1994). Sedimentation could limit or facilitate microbial transport in porous media (Matthess and Pekdeger, 1981).

### **2.2.2 Extracellular polymeric substances (EPS)**

Most microorganisms have the ability to produce Extracellular Polymeric Substances (EPS) which are defined by (Vu *et al.*, 2009) as a complex mixture of biopolymers

primarily including polysaccharides, proteins, nucleic acids, lipids and humic substances. EPS is excreted by microbial cells to link the cells together and form biofilm (Chen-Charpentier *et al.*, 2009) to provide a safe and ideal environment for the bacteria cells against harsh conditions (Prakash *et al.*, 2003; Kokare *et al.*, 2009). EPS has a great effect on the survival of biofilm. EPS is highly hydrated because it can incorporate a large amount of water into its structure by hydrogen bonds (Prakash *et al.*, 2003). Because EPS prevents desiccation in some natural biofilms, many studies found out that slow bacterial growth will also enhance EPS production (Donlan and Costerton, 2002).

Different organisms produce differing amounts of EPS whose composition and quantity can be affected by the type and the growth rate of microorganisms, age of biofilms and shear stress (Mayer *et al.*, 1999). The EPS production rate increases with the increase of biofilm age (Prakash *et al.*, 2003) and with the increase of shear stress (Qi *et al.*, 2008).

Over the past few decades, the EPS had a wide range of applications in many areas such as food, pharmacology, and biomedication, because of the structural diversity and physical properties of EPS (Fialho *et al.*, 2008). Recently, several studies focused on the role of microorganisms and their EPS in the remediation of the contaminated soil.

### **2.2.3 Biofilms Formation**

Biofilms can be defined simply and broadly as communities of microorganisms that attach to a surface (Singh *et al.*, 2006). Typically, microbial cells can be accumulated by getting adhered to a wet surface and embedded in EPS to resist the harsh environmental circumstances (Augustin *et al.*, 2004; Donlan and Costerton, 2002; Prakash *et al.*, 2003; Hunter and Beveridge, 2005).

In general, biofilms are not only unstructured, homogeneous deposits of cells and accumulated slime, but also complicated communities of surface-associated cells surrounded by a self-produced polymer matrix containing open water channels (Donlan and Costerton, 2002; Prakash *et al.*, 2003; Kim *et al.*, 2012). Singh *et al.* (2006) reported that biofilm formation can occur due to the accumulation of either single or multiple species of bacteria, fungi, algae and protozoa. Biofilm structure consists of EPS and microbial cells, which both occupy approximately 85.0 % and 15.0 % respectively of the total volume of the biofilm structure (Hunter and Beveridge, 2005).

The development of biofilm can be divided into five stages including; reversible attachment, irreversible attachment, maturation-1 (log phase), maturation-2 (Plateau phase) and dispersion (Sauer *et al.*, 2002). During the reversible attachment which was considered to be unstable, some of the cells detached during this development stage after the initial attachment. In general, attachment process normally occurs most readily on surfaces which are rougher, more hydrophobic (Donlan and Costerton, 2002) due to the fact that with increasing the surface roughness the microbial colonization increase because of the high surface area of the rough surface (Characklis and Marshall, 1990). The irreversible attachment occurred when the cells become embedded in EPS and motility ceases in the attached cells. The maturation-1 stage or so called log phase occurs when cells initiated EPS production and become progressively layered, which means that cell clusters become thicker than 10 $\mu$ m. The fourth stage of biofilm developments (maturation-2) starts when cell clusters became thicker by approximately 100  $\mu$ m due to EPS production to reach the final stage of biofilm formation (dispersion), in which cells started to swim back into the bulk liquid to find better access to nutrients.

Conversely, another characterization of biofilm formation, development stages was suggested by Armitage (2005) as shown in Figure 2.1, three stages of biofilm formation, including, attachment stage, micro colonies stage and maturation stage can be detected. The initial stage occurred when cells became attached to the surface.

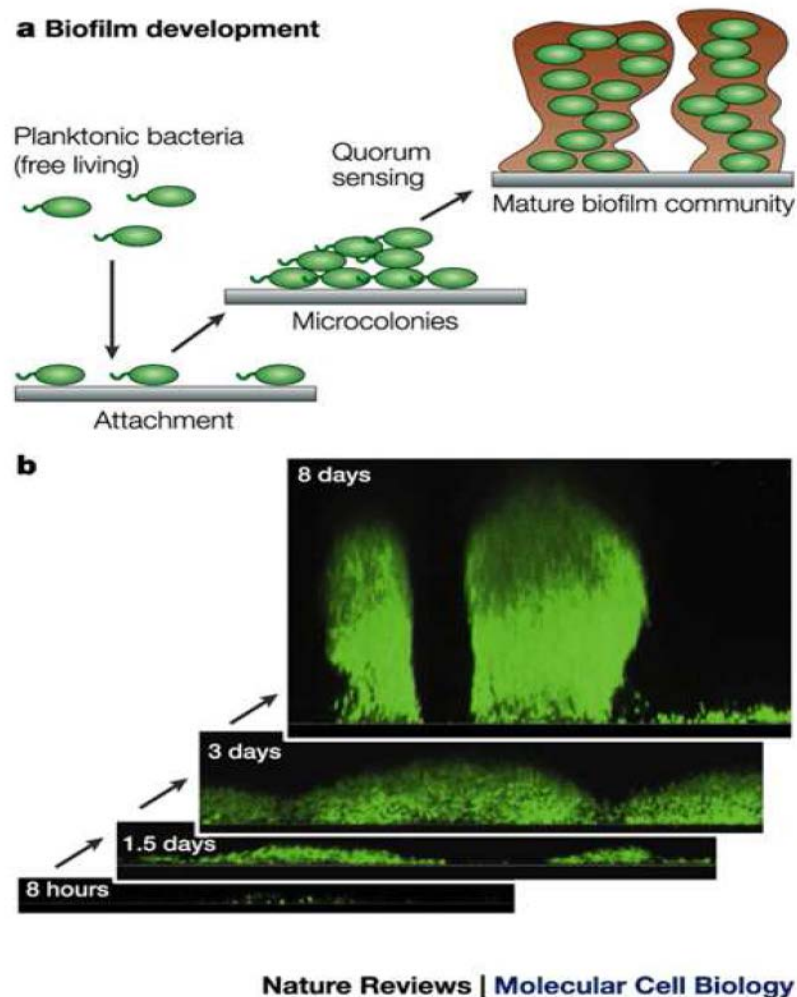


**Figure 2.1: The stages of biofilm formation (Armitage, 2005)**

Then by using quorum sensing (QS) which is the process that allows cells to communicate and share information with each other using chemical signalling of molecules (Rutherford and Bassler ,2012) cells started to colonize to reach the third stage which included the formation of mature biofilm.

Sometimes and for mechanical reasons only, some bacteria are shed from the colony or (more frequently); some bacteria stop producing EPS and are thus 'released' into the surrounding environment (Kavitha *et al.*, 2011). This dispersion occurs either by shedding of daughter cells from actively growing cells, or by detachment which refers to the releasing of large pieces of biofilm into the surrounding environment in response to nutrient availability (Bryers and Characklis, 1982). Several studies investigated the biofilm structure and the factors that highly affect it such as the type of carbon source or substrate, temperature, hydrodynamics and nutrient conditions (Stoodley *et al.*, 1999; Davey and O'Toole, 2000; Kim *et al.*, 2012).

The formation and development of biofilms in the environment mainly depend on the presence of the microorganisms, nutrient concentrations, energy sources and water, where biofilms in the subsurface environments may not form in case of absence these conditions (Stoodley *et al.*, 1999; Prakash *et al.*, 2003).

The influence of the hydrodynamics conditions and nutrients on biofilm structure was investigated by Stoodley *et al.* (1999) who reported that biofilm development is highly variable depending on two important factors; flow velocity and nutrient status. The results showed that the biofilm growing in laminar flow colonised the glass surface at a greater rate than the biofilm in turbulent flow but reached steady state earlier because the detachment rate was relatively low with respect to growth rate but steady state was reached sooner because of nutrient transfer limitations.

Another study performed by Villasenor *et al.* (2000) investigated the effect of different types of carbon on biofilm formation and indicated that the biofilm structure is highly affected by the concentration of carbon source. The results showed that reducing the substrate concentration results in a reduction in biomass concentration

and as a result the detachment of a growing biofilm becomes more likely to happen than that of a non-growing biofilm under the same detachment forces.

As for the effect of nutrient limitation on biofilm formation, Allan *et al.* (2002) confirmed that the substitution of the lactose carbon source by glucose gave lower planktonic cell phosphatase activity. In an attempt to investigate the effect of changing in nutrient conditions on biofilm formation, Rochex and Lebeault (2007) confirmed that increasing or decreasing nutrient levels decreases biofilm accumulation rate. The reason behind the reduction was the increase that took place in the biofilm erosion rate, which refers to the continual detachment of small particles of biofilm (Bryers and Characklis, 1982). These studies indicated that biofilm formation is controlled by detachment process in response to nutrient conditions.

#### **2.2.4 Biofilms application in environmental biotechnology**

Biofilms are beneficial in many industrial fields such as; bioremediation, microbial enhanced oil recovery, metal extraction and waste water technology (Van der Ruyt and van der Zon, 2009). A large amount of industrial and municipal wastewaters can be treated by using biofilm based reactor, which has the advantage of removing contaminants through a various mechanisms, including biological degradation (Yuan *et al.*, 2000), biosorption (Wang and Chen, 2009), bioaccumulation and biomineralisation (Singh *et al.*, 2006)

A biofilm barrier is one of the most efficient bioremediation techniques which were created to control the migration of contaminants in the contaminated plume (Komlos *et al.*, 2004). This will be implemented through the injection of microorganisms and sufficient nutrient selectively into the subsurface, thereby stimulating microorganisms to grow and form thick biofilm (Komlos *et al.*, 2004; Kim *et al.*, 2006).

Although biofilms are beneficial in many industrial fields, they can cause harm to human health and industrial productivity. For example, most biofilms are pathogenic, they have the of causing disease to humans, as well as causing corrosion in water pipes (Shafahi and Vafai, 2009).

#### ***2.2.4.1 In-situ implementation of biofilms***

Biofilms have become a focus of interests for the researchers in the field of bioremediation. In principle, in-situ bioremediation targets pollutant removal or attenuation under natural environmental conditions by implementation of microbial metabolic potential without the need for excavation of the contaminated samples (Jorgensen, 2007). In-situ bioremediation methods can be categorized into (1) biostimulation and (2) bioaugmentation (Omenn, 1992). Biostimulation can be used where the bacteria necessary to degrade the contaminants are present but conditions do not favour their growth (e.g., anaerobic bacteria in an aerobic aquifer, aerobic bacteria in an anaerobic aquifer, lack of appropriate nutrients or electron donors/acceptors). Bioaugmentation can be used when the bacteria necessary to degrade the contaminants do not occur naturally at a site or occur at too low of a population to be effective. There are several factors can affect in-situ applications of bioremediation such as the concentrations of contaminants, contaminant bioavailability, site characteristic, redox potential, pH, nutrients, and temperature. Contaminant concentrations directly influence microbial activity. When concentrations are too high, the contaminants may have toxic effects on the present bacteria. In contrast, low contaminant concentration may prevent induction of bacterial degradation enzymes. Contaminant bioavailability depends on the degree to which they sorb to solids or are sequestered by molecules in contaminated media, are

diffused in macropores of soil or sediment, and other factors such as whether contaminants are present in non-aqueous phase liquid (NAPL) form. Bioavailability for microbial reactions is lower for contaminants that are more strongly sorbed to solids, enclosed in matrices of molecules in contaminated media, more widely diffused in macropores of soil and sediments, or are present in NAPL form (ICSS, 2006). Site characteristics have a significant impact on the effectiveness of any bioremediation strategy. Site environmental conditions important to consider for bioremediation applications include pH, temperature, water content, nutrient availability, and redox potential. PH affects the solubility and biological availability of nutrients, metals, and other constituents; for optimal bacterial growth, pH should remain within the tolerance range for the target microorganisms (ESTCP, 2005). Bioremediation processes preferentially proceed at a pH of 6-8 (ICSS, 2006). Redox Potential and oxygen content typify oxidizing or reducing conditions. Redox potential is influenced by the presence of electron acceptors such as nitrate, manganese oxides, iron oxides and sulphate (ICSS, 2006). Nutrients are needed for microbial cell growth and division (ESTCP, 2005). Temperature directly affects the rate of microbial metabolism and consequently microbial activity in the environment. The biodegradation rate, to an extent rises with increasing temperature and slows with decreasing temperature (ESTCP, 2005).

### **2.3 Soil heterogeneity and preferential flow paths**

Soil heterogeneity can be attributed to the spatial soil variability, which is the variation of soil properties from one point to another in space due to different deposition conditions and different loading histories (Elkateb *et al.*, 2003). Soil heterogeneity affects the movement of solutes and makes it difficult to predict, and also affects

nutrients, and contaminants (Nielsen *et al.*, 1973). Several studies indicated that the development of preferential paths may be a natural consequence of soil heterogeneity under saturated conditions (Wang *et al.*, 2006). Preferential flow can be defined as a relatively rapid movement of water and dissolved solutes along preferred pathways; this rapid movement is responsible for faster transport of the solute through the porous media (Hendrickx and Flury, 2001; Simunek and Van Genuchten, 2007; Wang and Chen, 2009; Hardie *et al.*, 2011; Smith 2012).

### **2.3.1 Behaviour of preferential flow in soil**

Preferential flow can result from natural variability or heterogeneity of the saturated porous media (EPA, 1996; Hendrickx and Flury, 2001) or be due instability of the wetting fronts in porous media (Bouwer, 1991). The instability of the wetting front occurs when the rainfall intensity exceeds the infiltration capacity of soil, thereby water and solutes could transfer into the groundwater quickly as fingers (Liu *et al.*, 1994). However, preferential flow in soil is not restricted to the heterogeneity of the saturated porous media. Many studies have indicated that the occurrence of preferential flow can be detected in soil macro-pores like decayed root channels, cracks, and worm holes (Bouwer, 1991; Hendrickx and Flury, 2001).

According to the different physical field mechanisms (Hendrickx and Flury, 2001) preferential flow can be classified into three fundamental components, including macro-pore flow, funnel flow (heterogeneous), and unstable flow (finger) (Wang *et al.*, 2006; Jury and Horton, 2004).

The macro-pore flow is a preferential water movement which occurs due to the presence of soil macro-pores such as decayed root channels, cracks, worm holes. These macro-pores allow non-equilibrium conditions to develop during rapid water flow because of their large size and continuity (Hendrickx and Flury, 2001; Wang *et*

*al.*, 2006; Jarvis and Dubus, 2006). Jarvis and Dubus (2006) suggested that pore size bigger than 0.3 mm in diameter allows non-equilibrium flow and transport in porous media Figure 2.2.

Funnel flow takes place due to the presence of sloping geological layers which induce the pure water to flow laterally getting accumulated in a low region, while finger flow could occur when the underlying region is coarser (Wang *et al.*, 2006).

The occurrence of preferential flow in porous media causes several drawbacks. One of these drawbacks is the rapid movement of contaminants and microorganisms in porous media. Preferential flow provides a mechanism to bypass most of the porous media; the effects include enhanced solute transport in the soil (DiCarlo *et al.*, 1999). The potential soil and groundwater contamination may increase by the rapid movement of the solutes through soil due the presence of preferential flow. The existence of preferential flow increases the transfer of herbicides, fertilizers, heavy metals, and microorganisms into greater depths (Beven and Germann, 1982).

Furthermore, the presence of preferential flow paths can affect solute mobility significantly. The rapid movement of the solutes in high permeable layers and the slow movement of solutes in the less permeable layers both reduce the efficiency of the solute leaching (Cote *et al.*, 2003). In addition to that, microorganisms can migrate significantly through soil due to the presence of preferential flow, which results from a macro-pore feature like worm holes, cracks, and root channels (Abu-Ashour *et al.*, 1993).



**Figure 2.2: Macro-pores in porous media**

### **2.3.2 The impact of preferential flow on groundwater remediation techniques**

Groundwater remediation technologies such as pump and treat and in-situ bioremediation techniques which aim to control the movement of contaminant and to prevent the continued expansion of the contaminated zone (EPA, 1996 ; Bayer *et al.*, 2002) can be affected by preferential flow.

The efficiency of bioremediation, which is defined as any process that uses microorganisms or their enzymes to restore the environment altered by contaminants to its original condition could be affected by the existence of the preferential flow (Bayer *et al.*, 2002; Malone *et al.*, 2004; Ray *et al.*, 2004). The preferential flow, which happens due to natural phenomena such as rock fractures or joints, slows down the clean-up process, and therefore making the remedial times longer. The reason behind

that is the quick contaminant clean-up in the high permeable zones compared to the slow contaminant clean-up in the low permeable layers (EPA, 1996).

Pump and treat technique may face some phenomena such as; tailing and rebound problems. Tailing phenomenon refers to the progressively slower rate of dissolved contaminant concentration decline observed with continued operation of a pump and treat, whereas dissolved contaminant concentrations may rebound if pumping stopped, after temporarily attaining a clean-up standard (EPA, 1996). One of the reasons for tailing and rebound is the variable travel times associated with different flow paths or preferential flow paths taken by contaminants to an extraction well (EPA, 1996). The horizontal variations in the velocity of groundwater moving toward a pumping well (Keely, 1996) lead to tailing as higher concentrations of groundwater in slower path lines mix with lower concentrations in faster path lines (Palmer and Fish, 1992).

#### **2.4 Bioclogging in porous media**

The hydraulic conductivity reduction due to the microbial activities goes back to (Slichter, 1905). Afterwards, this finding was supported with evidence by (Nagata and Watanabe, 1990; Okubo and Matsumoto, 1979). In later years, other studies suggested that the reduction in the porous media properties such as porosity and permeability can change over time not only due to microbial activities but also due to physical and chemical activities (Taylor and Jaffé, 1990b; Vandevivere and Baveye, 1992; Kim and Fogler, 2000; Ross *et al.*, 2001). Physical clogging is the dominant type of clogging that can be observed during the artificial recharge which involves injecting water into an aquifer where it is stored for future use (Pyne, 1995). The physical clogging occurs when the water contains suspended solids of a size commensurate with that of the particles of the porous medium, which reduces the overall hydraulic conductivity of

the medium (Baveye *et al.*, 1998). Chemical clogging can occur due to the chemical interaction between dissolved salts and soil particle that can lead to reduce soil hydraulic conductivity (Rice, 1974). Metal precipitation could also lead to reducing the hydraulic conductivity of the porous media and cause clogging (Weidner *et al.*, 2012).

The microbial activities including the production of gas bubbles or the production of large amounts of biomass could plug the pores space of the porous medium, thus could lead to reducing the porosity and permeability of soil significantly (Soares *et al.*, 1991; Vandevivere and Baveye, 1992; Wu *et al.*, 1997; Baveye *et al.*, 1998; Thullner, 2001; Mitchell and Santamarina, 2005; Ivanov and Chu, 2008; Brovelli *et al.*, 2009).

The cells and the production of extracellular polymeric substances (EPS) can lead to a reduction in the saturated hydraulic conductivity by 2-3 orders of magnitude which consequently cause a severe clogging of the porous media in the presence of a sufficient amount of nutrients (Thullner, 2001; Vilcáez *et al.*, 2013). In addition to that, microbial activities which have the ability to induce mineral precipitation can enhance soil stability and also reduce the hydraulic conductivity (Ross *et al.*, 2001; DeJong *et al.*, 2006; Thullner, 2010). Changes in the flow pattern can be caused by bacterial plugging of the pore space (Kowalewski *et al.*, 2006) and by biopolymers (Crecente *et al.*, 2005), where severe bioclogging could change the flow from uniform to non-uniform flow (Engesgaard *et al.*, 2006).

Bioclogging can be divided into three stages: Phase (1) with no changes in flow properties, Phase (2) a significant change in dispersivity which refers to the tendency of the substrate to penetrate deeper into the column with time (Taylor and Jaffe, 1990) due to the biomass growth near the inlet of the column, and Phase (3) with added

growth of micro-colonies much deeper in the column leading to mass transfer of solutes from the water phase to bio-phase (Seifert and Engesgaard, 2007).

#### **2.4.1 Bioclogging in one dimension**

Many studies attempted to investigate bioclogging in porous media, and most of the experimental and theoretical studies investigated the bioclogging in one dimension. The most common experimental setup, is the laboratory column experiments (Vandevivere and Baveye, 1992; Komlos *et al.*, 1998; Seki *et al.*, 1998; Wu *et al.*, 1997; Seki *et al.*, 2002; Bielefeldt *et al.*, 2002; Seki, 2013; Zhong *et al.*, 2013). Such column studies include monitoring the change in hydraulic conductivity after packing them with porous media and microorganisms.

Some of the column studies correlated biomass growth with hydraulic conductivity reduction (Wu *et al.*, 1997); other studies linked the biofilm thickness with the permeability and porosity of porous media (Cunningham *et al.*, 1991), and biomass density with the reduction of hydraulic conductivity (Taylor and Jaffé, 1990a). Cunningham *et al.* (1991) observed that that more biomass grew in columns packed with larger size media, with 10 mm biofilm thickness on 0.12 mm diameter glass beads versus 37 mm biofilm thickness on 0.5 mm sand or glass beads. Taylor and Jaffé (1990) reported that for homogeneous sand media under aerobic conditions, the reduction in permeability can be described as a function of biomass density for densities less than about 0.4 mg/cm<sup>3</sup>.

Bioclogging process can be achieved for a large variety of growth conditions, so that several studies that investigated bioclogging in column studies used different type of porous media, microbial strains, growth culture medium, and flow conditions (Shaw *et al.*, 1985; Cunningham *et al.*, 1991; Vandevivere and Baveye, 1992; Wu *et al.*, 1997;

Seki *et al.*, 1998; Seki *et al.*, 2002; Bielefeldt *et al.*, 2002). Cunningham *et al.* (1991) tested a media consisted of 1-mm glass spheres, 0.70-mm sand, 0.54-mm sand, and 0.12-mm glass and sand. Bielefeldt *et al.* (2002) indicated that the maximum reduction of hydraulic conductivity did not correlate with the grain size when comparing results for sands with mean diameters of 0.19, 0.32, and 0.49mm. Vandevivere and Baveye, (1992) used different bacterial strains, the results showed that an EPS-producing bacterial strain caused clogging, whereas its non-EPS-producing mutant was not able to cause any clogging.

Several column studies investigated bioclogging in porous media through using different microbial strains. A study performed by Show *et al.* (1985) reported that the inoculation of *Pseudomonas* sp. into glass bead cores led to the formation of biofilm on the solid matrix, the biofilm formation was caused by the formation of micro-colony and bacterial production of EPS. This study was followed by MacLeod *et al.*(1988) with a bioclogging experiment that reported that the introduction of *Klebsiella pneumoniae* into glass bead cores led to significant reduction of the permeability of glass bead materials over than 99% due to the production of large amounts of polymer.

Taylor and Jaffe (1990) reported that the decrease of hydraulic conductivity by three orders of magnitude is attributed to the biomass accumulation, this finding was confirmed by Vandevivere and Baveye (1992a) who used four different strains of bacteria and reported that among the four strains only one bacterial strain which have a higher adhesion tended to reduce hydraulic conductivity of sand columns by three to four orders of magnitude in a period of a week because of the obstruction of flow channels with a large amount of biomass.

For provide a better understanding of the relationship between biomass accumulation and reduction of hydraulic conductivity, sand column experiments were conducted by Wu *et al.* (1997) to investigate the effect of enhanced biomass production by indigenous soil microbes on the hydraulic conductivity of river sand. The results showed that a reduction of hydraulic conductivity by one and one-half order of magnitudes was observed after the application of dextrose-nutrient solutions, and this noticeable reduction occurred due to biomass growth only and there was not fungal growth under the saturated conditions.

Other bioclogging experiments indicated that bacterial clogging has took place rapidly than fungal clogging (Seki *et al.*, 1998). This study followed by bioclogging experiments in glass bead columns due to bacteria and fungi showed that fungi are important clogging materials as well as bacteria because not only the number bacteria is increased at the clogged layers but also that of fungi (Seki *et al.*, 2002).

On the contrary, Kim (2004) observed that the reduction in porous media due to the biofilm formation in the fungus-soil mixture was faster than that of a bacterium soil mixture. In the same year, another bioclogging experiment was performed by Fuchs *et al.* (2004) to study biodegradation and bioclogging in the unsaturated porous soil beneath sewer leaks demonstrated that depositions of particulate matter as well as microbial growth are responsible for decreasing pore space and hydraulic conductivity.

As for substrate conditions and to investigate how biofilm influences the hydraulic properties of the porous media, a biofilm reactor was used by Cunningham *et al.* (1991) to estimate the effect of biofilm thickness on the medium porosity, permeability, and the friction factor; the results showed that biofilm thickness acquired quasi steady state after about 5 days of growth under high load substrate conditions,

and the maximum biofilm thickness varies with the particle size of porous media as shown in Figure 2.3.

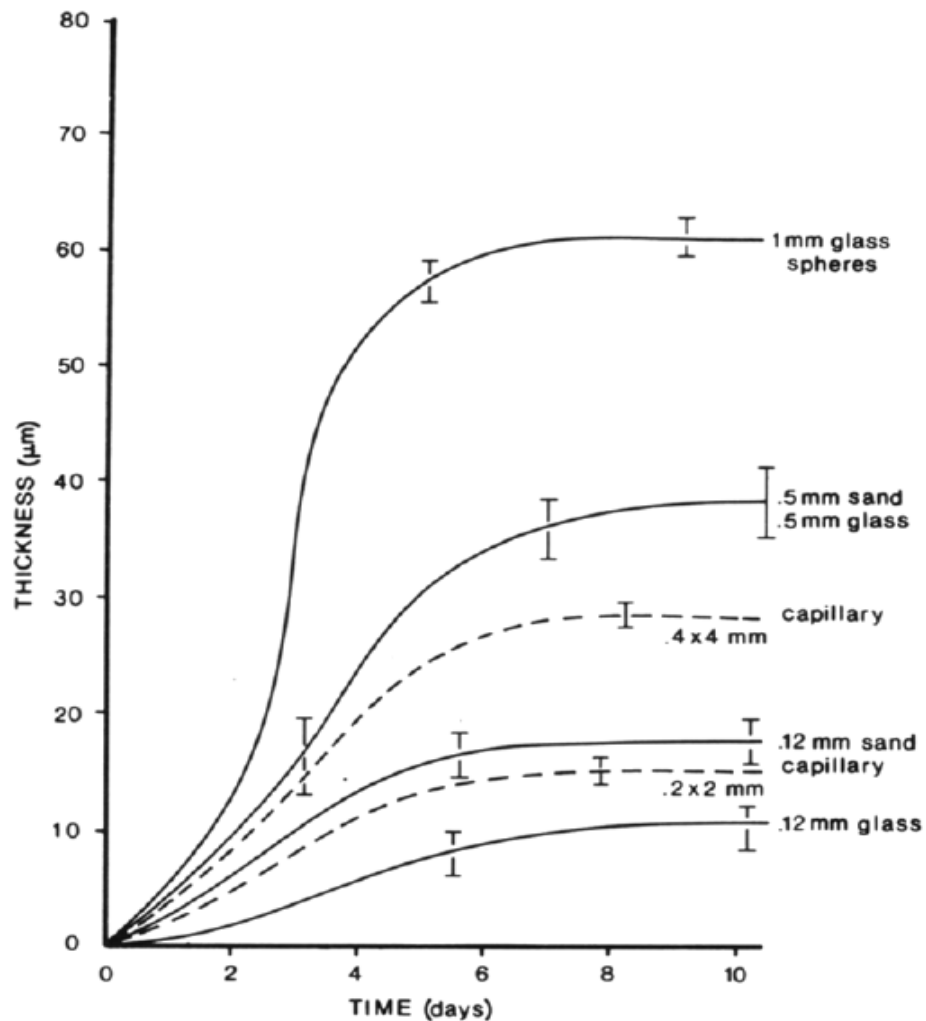


**Figure 2.3: Progression of biofilm thickness (*Ps. aeruginosa*) for media of different diameter and composition (Cunningham *et al.* 1991).**

Most of bioclogging experiments used high solubility compounds such as methanol and glucose, but Bielefeldt *et al.* (2002) used low solubility compounds (decane and naphthalene) which are different to other high solubility compounds such as (glucose and methanol) that biodegraded easily by indigenous bacteria. The study looked at the effect of biomass growth on the dissolved decane and naphthalene in simulated groundwater on the hydraulic conductivity and dispersivity. The outcome of this study

exhibited that natural soil bacteria degrading low concentrations of decane or naphthalene can highly influence the hydraulic conductivity and dispersivity of saturated porous media. The hydraulic conductivity of porous media decreased by 2 to 3 orders of magnitude due to clogging of pore spaces, whereas the dispersivity went up 2 to 5 times at high flow rate and long-term growth on decane or naphthalene.

Recently, and with regards to the impact of flow conditions on bioclogging, different column experiments were performed by Zhong *et al.* (2013) to study the changes in the biochemical and hydraulic parameters under discontinuous flow conditions during the bioclogging process. Depending on the finding of this study, the authors divided the bioclogging process into four stages: The first stage includes the occurrence of severe bioclogging at the inlet of the column. In the next stage, the bioclogging existed in the entire sand column, after that a rapid decrease in hydrodynamic dispersion occurred in the third stage, then the hydraulic parameters such as hydraulic conductivity, porosity, and hydrodynamic dispersion were all decreased steadily in the final stage.

A different clogging pattern was suggested by Seki (2013) through a series of column experiments indicated that bioclogging started from the inlet of the solution, but in some cases, it started from the bottom or the outlet of the column as shown in Figure 2.4.

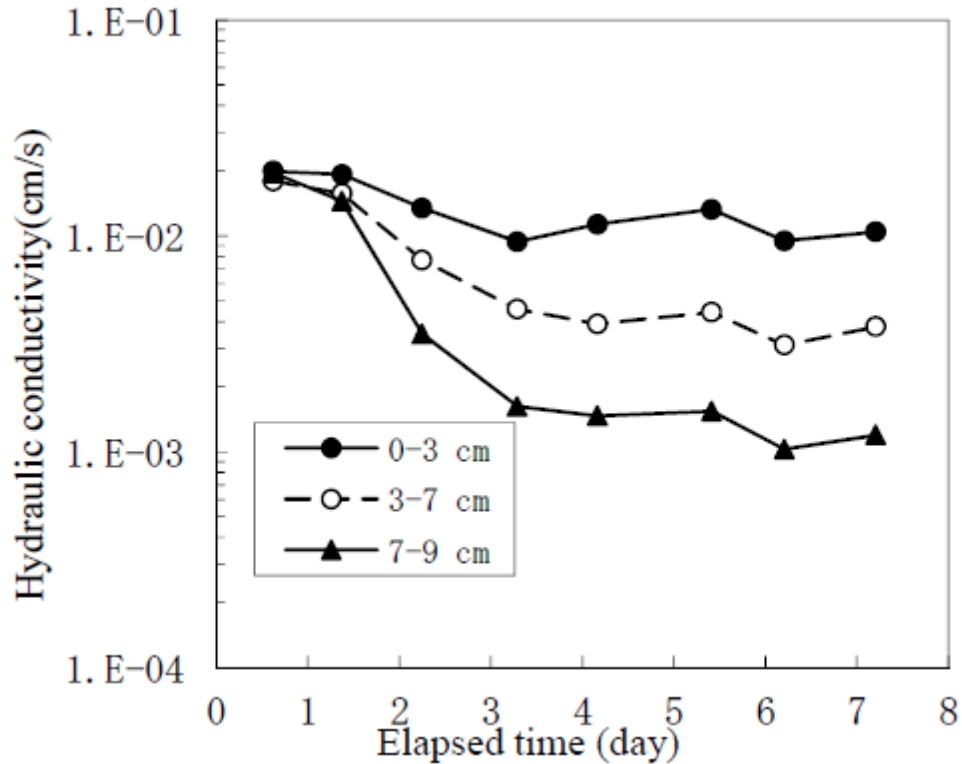


**Figure 2.4: Change in hydraulic conductivity of each layer of sand (Seki, 2013).**

These findings disagree with the early bioclogging experiments that supposed the occurrence of bioclogging near the inlet or injecting nutrients ports (Thullner *et al.*, 2002), this disparity could be related to the experiments design.

As regards to the porous media in bioclogging studies, most of bioclogging studies used sand and glass bead as a porous media, but only few studies concentrated on the effect of microbial activities on hydraulic properties of natural fractures. The effects of biofilm growth on flow and solute transport through a sandblasted glass parallel plate fracture were investigated by Hill and Sleep (2002). The experiment results showed that biomass initially grows in the fracture in discrete clusters, but forms a continuous biofilm over time and there was a reduction of hydraulic conductivity of a fracture by more than two orders of magnitude due to biomass growth.

The causes of hydraulic changes due to the microbial activity in naturally fractured chalk were studied by Arnon *et al.* (2005). The finding of this study indicated that the reductions in fractured chalk transmissivity which is referring to the amount of water that can be transmitted horizontally through a unit of width can be occurred primarily because of clogging by bacterial cells and EPS produced by the bacteria.

#### **2.4.2 Bioclogging in two dimensions**

Although column studies are useful for investigating bioclogging in porous media, some studies tried to scale up column experiments by investigating the bioclogging process in two dimensions instead of one dimension. Sand box experiments and micromodels or pore network models are the most common laboratory works that allocated to simulate the bioclogging process in two dimensions.

Generally, the pore networks consist of cylindrically shaped pores with a constant length, but varying radius arrange in a rectangular or cubic geometry to form a pore network grid (Suchomel *et al.*, 1998). In order to understand bacteria profile modification, Kim and Fogler (2000) performed micro-models which are a common option to visualize pore-scale processes during multi-phase flow. These models were proposed to investigate biomass accumulation and evolution in porous media under starvation conditions, they are two dimensional flow-channel networks etched in glass to simulate fluid flow in porous media. The observations of these micro-models identified four different evolution patterns as shown in Figure 2.5, including permeability reduction due to biomass accumulation in pore bodies and pore throats. The observations also exhibited an increase in permeability due to biomass sloughing caused by shear stress after nutrients termination.

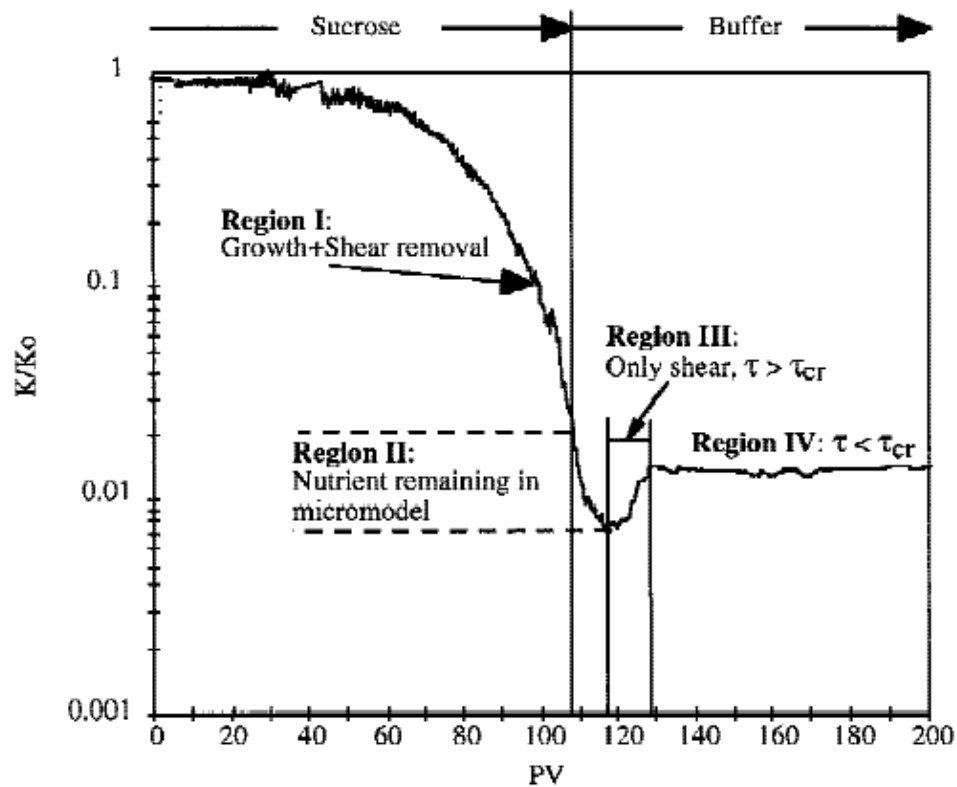


**Figure 2.5: Effects of biofilm growth and shear stress on permeability ratio (Kim and Fogler, 2000)**

Biomass plug development and propagation in porous media were studied by Stewart and Fogler (2001) through using two-dimensional micro-models and packed-bed experiments to simulate fluid flow in porous media and to determine the mechanisms associated with biomass plugging. The results arose from the combination of packed-bed and micro-models experiments, indicated that biomass plugging mechanisms correspond to three distinct regions or phases, including the exopolymer-induction phase, the plugging phase, and the plug-propagation phase. The results indicated that the exopolymer-producing conditions and highly differentiated in pressure drop was related to biomass distribution, and the production of exopolymer was the basic mechanisms associated with the plugging phase as shown in Figure 2.6.

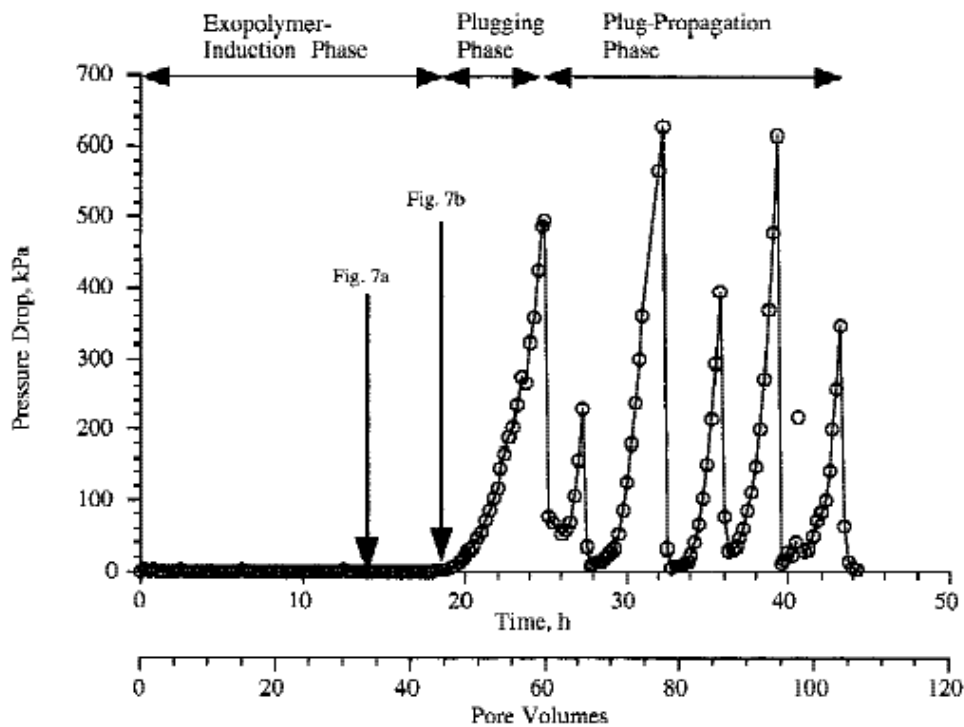


**Figure 2.6: Pressure drop across micromodel during constant-rate injection of nutrient with 15 g/L sucrose (Stewart and Fogler, 2001).**

Due to the difficulty in observing the bioclogging process in porous media, new micro-models apparatus as shown in Figure 2.7 was developed by Dupin and McCarty (2000). The apparatus allowing spatial and temporal observations of two-dimensional micro-models called Silicon Pore Imaging Elements (SPIEs). The observations suggested that weakly attaching organisms are likely to be washed out, while the stronger attaching organisms are likely to persist and reduce the porous media permeability and this finding was confirmed previously by Vandevivere and Baveye (1992).

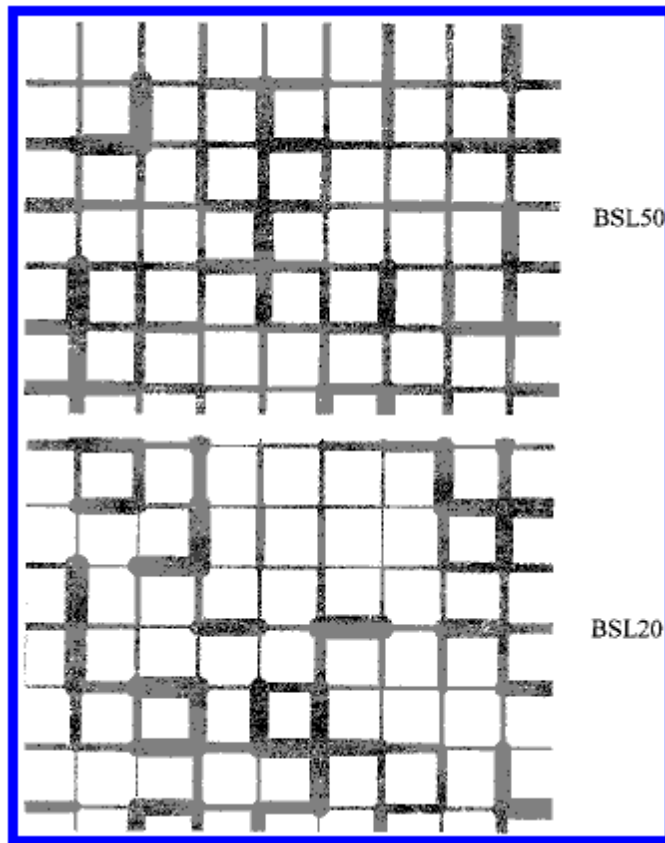


**Figure 2.7: Illustration of a 3.2 mm x 4.3 mm area of the two SPIE patterns (Dupin and McCarty, 2000).**

Instead of using the micro-model to visualize bioclogging in porous media, sand box experiments were built-up by Kildsgaard and Engesgaard (2002) to visualize the bioclogging process in two-dimension. The sand box packed with sand and inoculated with bacteria which grown by continuous nutrient injection (nitrate and acetate). Figure 2.8 shows a schematic diagram of the sand box. Tracer experiments carried out to visualize clogging in the sand box by using Brilliant Blue. The digital camera was used to record the tracer experiments. The results of this experiment showed that clogging evolved quickly in the sand box an asymmetry with plume fingers diverting around the main clogged area as shown in Figure 2.9.

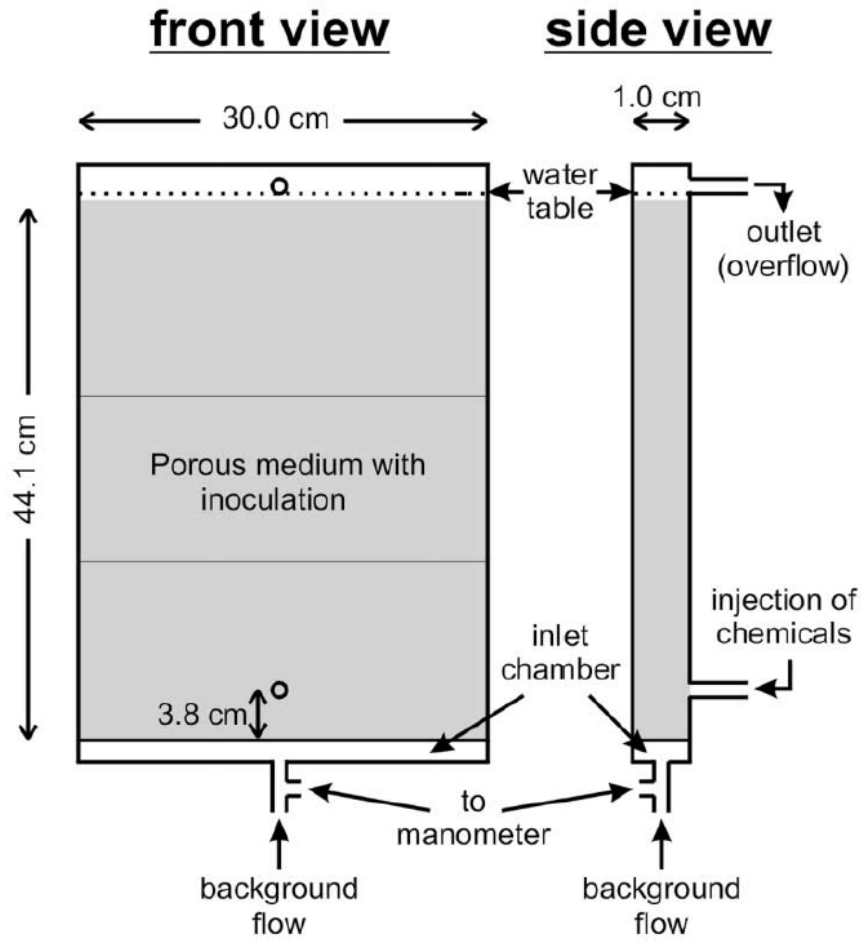
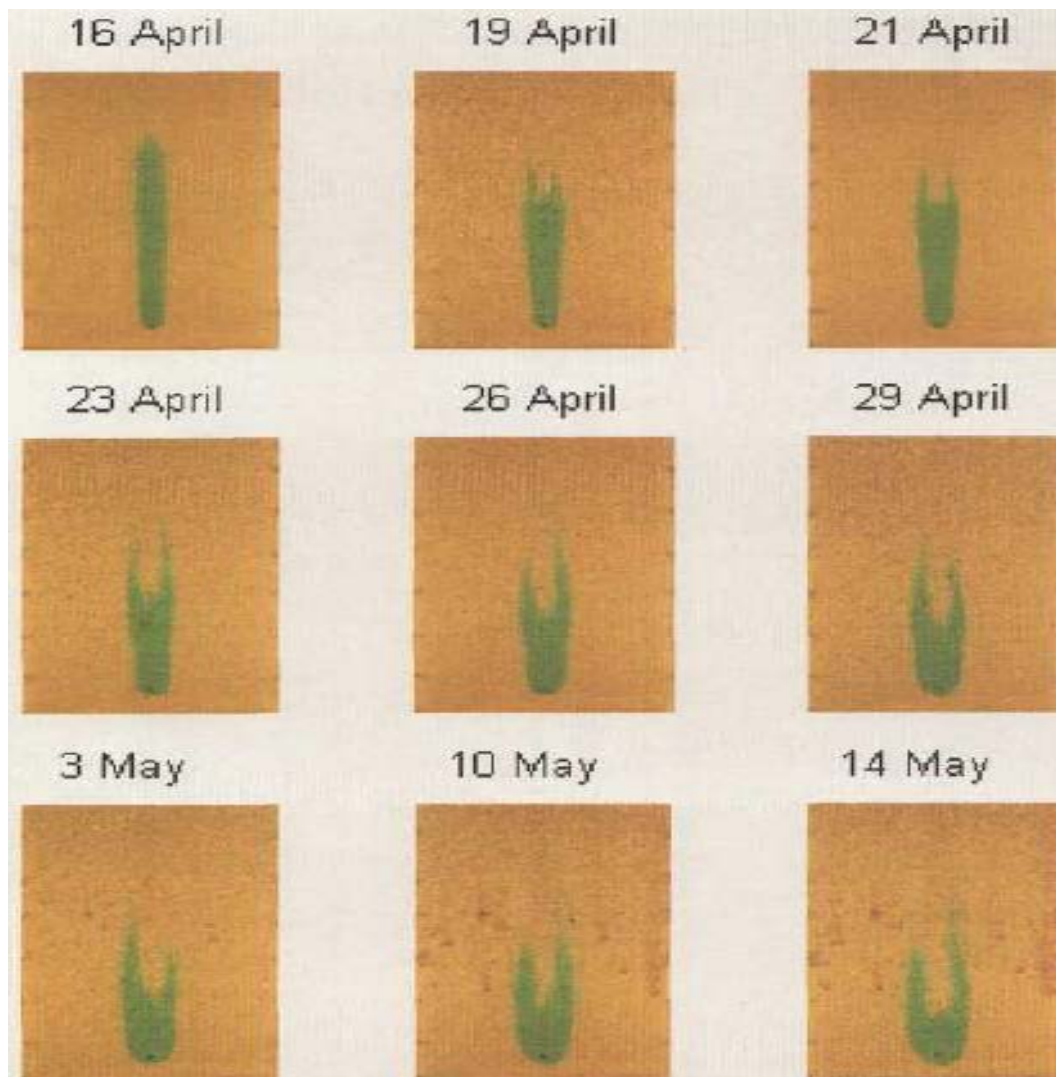


Figure 2.8: Details of the sand box experiment (Kildsgaard and Engesgaard, 2000).



**Figure 2.9: The Brilliant Blue tracer distribution after 60 minutes on different days (Kildsgaard and Engesgaard, 2000).**

Thullner *et al.* (2002) performed a two-dimensional flow cell to inspect the bacterial growth and its interaction with water flow field in a saturated porous medium. A flow cell filled with glass beads to simulate the porous media. The results of this study showed that flow bypassed the clogged area near the nutrients injection port. Clogging effect that happened locally did not change the whole system parameters because of flow bypass.

### **2.4.3 Factors influencing bioclogging in porous media**

Many studies investigated the environmental variables that have an impact on bioclogging processes, including oxygen and organic carbon availability in porous media, temperature, starvation conditions, and grain size (Vandevivere *et al.*, 1995; Cunningham *et al.*, 1991; Holm, 2000; Bielefeldt *et al.*, 2002; Sanin *et al.*, 2003; Seki *et al.*, 2005; Hand *et al.* 2008; Kim *et al.*, 2010).

Starvation conditions refer to the nutrient limitation conditions that could have a great effect on bioclogging. The starvation technique is used in secondary oil recovery, where the starved bacteria could penetrate through the porous media, thus the resuscitation of the bacteria can lead to improve the sealing of the high permeability zone (Cusack *et al.*, 1992). On the contrary, Sanin *et al.* (2003) reported that nitrogen starvation can lead to diminishing the attachment of bacteria to the porous media results in preventing clogging.

The influence of the environmental variables such as oxygen availability, sediment grain size, and organic carbon on bioclogging were investigated by Hand *et al.* (2008) who observed different clogging patterns for either aerobic and anaerobic bacteria. The results of this study showed that the anaerobic cells are more sensitive to carbon availability than the aerobic cells, since under the same carbon concentrations. An increase in pressure is clearly seen in the aerobic columns, but is barely recognizable in the anaerobic columns, which is indicative of bioclogging was slowest with using anaerobic bacteria.

With regard to the effect of grain size on bioclogging process, some studies did not find any effect of particle size on bioclogging (Holm, 2000; Bielefeldt *et al.*, 2002). Bielefeldt *et al.* (2002) found that the reduction of the hydraulic conductivity for three sand fractions 0.6 mm, 0.3 mm, 0.2 mm were nearly similar by the end of a sand

column experiment. Holm (2000) did not find an effect of the grain size on the clogging efficiency of the biomass for three sand types (fine sand with diameter of 0.0–0.4mm; medium sand with diameter of 0.3–0.6mm; coarse sand with diameter of 0.6–1.4 mm).

On the contrary, other studies concentrated on the importance of the grain size on the occurrence of bioclogging process (Vandevivere *et al.*, 1995; Cunningham *et al.*, 1991; Torbati *et al.*, 1986). Cunningham *et al.* (1991) measured the biofilm thickness and the saturated hydraulic conductivity of quartz sand and glass beads of different particle diameters (0.54 mm and 0.12 mm). They concluded that the large pores clog first due to the accumulation of biomass and the biofilm thickness increase with increasing the grain size. Cunningham *et al.* (1991) conclusions agreed with the finding of Torbati *et al.* (1986) who also concluded that bacteria prefers to clog larger pores first.

Based on the results of both Vandevivere and Baveye (1992b) and Cunningham *et al.* (1991), Vandevivere *et al.* (1995) found that for particle diameters ranging from 0.09 to 1.0mm the clogging efficiency is greater for smaller particle diameters than in large particle diameters as shown in Figure 2.10 which shows the reduction in hydraulic conductivity in different grain size of uniform soil.

This disagreement about the effect of grain size on bioclogging was associated with the tendency of biomass to form biofilms on the coarse-textured material than fine-textured material and this confirmed by the experimental observations of Cunningham *et al.* (1991) and Torbati *et al.* (1986). As a result, most of bioclogging models accurately predicted biological clogging in 1-mm glass beads, but were not able to model clogging in the finer fractions (Seki *et al.*, 1998).

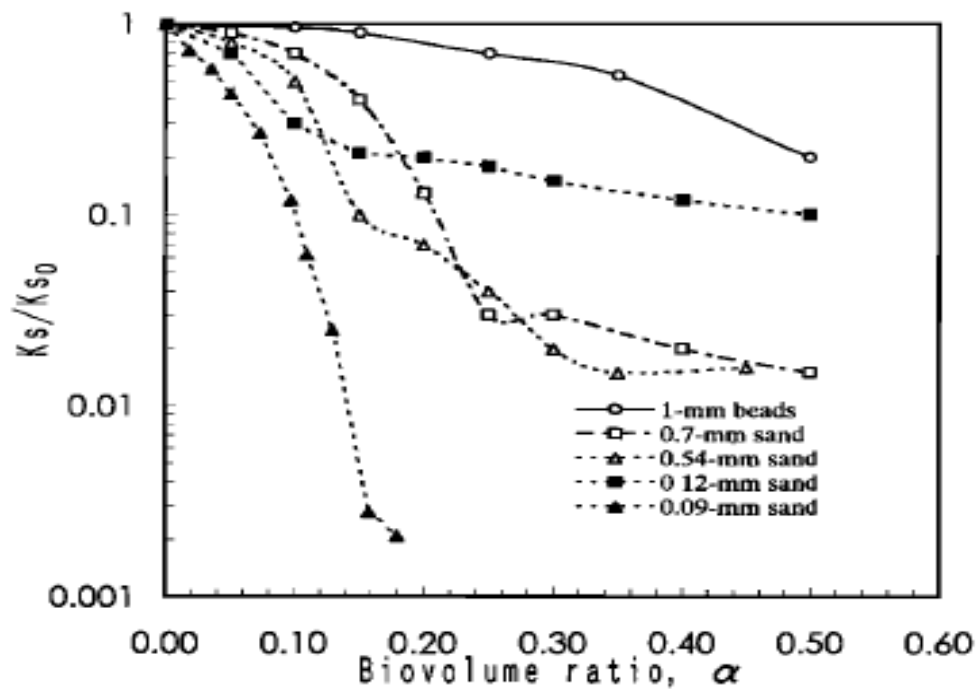


**Figure 2.10: Relationship between the saturated hydraulic conductivity ratio and the bio-volume ratio for different grain size (Vandevivere *et al.*, 1995).**

In addition to the effect of grain size on the bioclogging process, some studies investigated the effect of temperature on the bioclogging process. A sand column experiment was performed by Seki *et al.* (2005) who observed that the hydraulic conductivity did not change in columns held at 15°C column, while it decreased exponentially with time in columns held at 20, 25 and 30°C due to the increase of biomass production.

In addition to that, several studies indicated that the flow rate could be one of the important parameters that affect the bioclogging process in porous media (Bielefeldt *et al.*, 2002; Kim *et al.*, 2010). Bielefeldt *et al.* (2002) reported that bioclogging can be increased by reducing the flow rate, this also confirm by Kim *et al.* (2010) who stated that clogging at high flow rates can be accelerated due to the biofilms accumulation, but can be easily eliminated by high shear force.

#### 2.4.4 Bioclogging modelling approaches

The bioclogging modelling approaches describe the reduction of porosity and the associated reduction of hydraulic conductivity due to the biomass accumulation in porous media (Thullner, 2010). In general, bioclogging models can be classified into three categories: (1) macroscopic models which suggest that pore size distribution does not change due to biomass growth, but only the maximum pore radius reduces (Clement *et al.*, 1996), (2) micro-colonies models which suggest that biomass grows with a non-uniform distribution colony or aggregates, and the biomass does not cover the entire surfaces of soil particles (Vandevivere *et al.*, 1995; Vandevivere and Baveye, 1992; Thullner *et al.*, 2002; Seifert and Engesgaard, 2007), the micro-colonies can be modelled as cylindrical plates with constant radius and thickness (Seifert and Engesgaard, 2007) as shown in Figure 2.11, and (3) biofilm models assume that biomass grow distributed uniformly as continuous biofilm covering the surfaces of soil grains (Taylor *et al.*, 1990; Thullner *et al.*, 2002).

Vandevivere *et al.* (1995) assumed that porous media could be represented by a bundle of parallel pores all having the same radius and biomass growth as plugs or aggregates respectively. The relative hydraulic conductivity ( $k_{rel}$ ) was assumed to be given by the following equation.

$$k_{rel} = \phi_{(\eta_{rel})} \eta_{rel}^2 + (1 - \phi_{(\eta_{rel})}) \frac{k_c}{1 - \eta_{rel}(1 - k_c)} \quad 2.1$$

$\phi_{(\eta_{rel})}$  is defined as a distribution function describing how many pores show biofilm growth and plug growth, respectively. Vandevivere *et al.* (1995) proposed the equation below as an adequate expression for the distribution function  $\phi_{(\eta_{rel})}$ .

$$\phi_{(nrel)} = \frac{\exp(-0.5(1-\eta_{rel}))}{\eta_c} \quad 2.2$$

$\eta_c$  is introduced as a critical porosity change at which biofilm growth switches into plug growth and a value of  $\eta_c = 0.9$  was suggested after fitting to experimental data. On the other hand, Okubo and Matsumoto (1979) assumed that the porous medium to be represented by a bundle of straight capillary tubes with a fixed diameter embedded in a solid matrix and the biomass was considered to cover the pore walls with a continuous biofilm or plug which occupy a fraction of the volume of each pore. Following Okubo and Matsumoto (1979) approach the reduction of the saturated hydraulic conductivity was expressed as below:

$$k_{rel} = (\eta_{rel})^2 \quad 2.3$$

$k_{rel}$  and  $\eta_{rel}$  are the relative hydraulic conductivity and the relative porosity respectively (final values divided by initial values).

Nevertheless, Clement *et al.* (1996) introduced a macroscopic model for bioclogging, in this model; there is no any specific distribution of the biomass within the pores. Following Clement *et al.* (1996) approach the reduction of the saturated hydraulic conductivity was expressed as.

$$k_{rel} = (\eta_{rel})^{19/6} \quad 2.4$$

Once more  $k_{rel}$  is the relative hydraulic conductivity which can be defined as the hydraulic conductivity of the clogged porous media divided by the hydraulic conductivity of the clean porous media and  $\eta_{rel}$  is the relative porosity which can be defined as the porosity of the clogged porous media divided by the porosity of the clean porous media (Seki, 2013).

Moreover, Rittmann (1993) reported that growth pattern in porous media is more likely to be a combination of both biofilm and micro-colony models, where microorganisms initially grow in discrete colonies then gradually expand into a continuous biofilm.

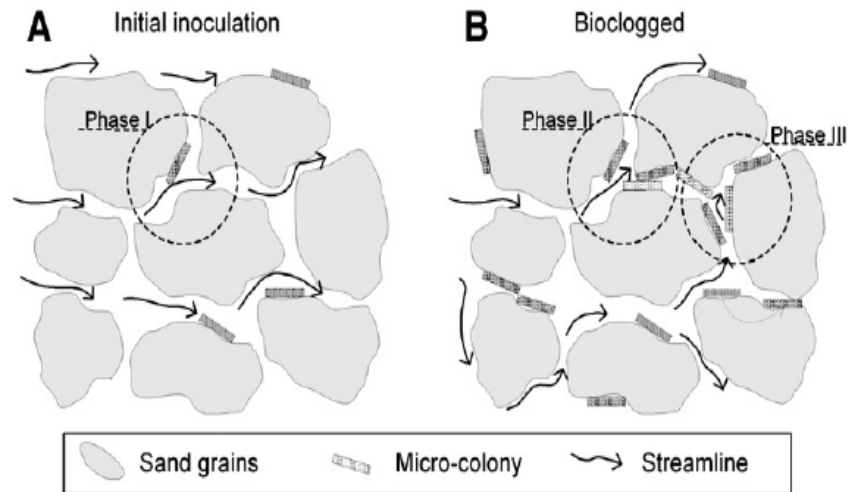


**Figure 2.11: Schematic diagram illustrating growth of micro-colonies. (A) A sparse distribution of micro-colonies after the initial inoculation of the porous medium. (B) A higher density of micro-colonies causing bioclogging of the pore throats (Seifert and Engesgaard, 2007).**

Consequently, some studies criticised the biofilm models based on the fact that biomass may not grow as a biofilm but it can grow as colonies or aggregates resulting in more reduction in hydraulic conductivity of porous media (Vandevivere *et al.*, 1995; Dupin *et al.*, 2001; Kim and Fogler, 2000; Thullner *et al.*, 2002). Vandevivere *et al.* (1995) assumed the porous medium to be represented by a bundle of parallel pores, all having the same radius, the biomass within a pore is present either as a biofilm or a colony causing a significant reduction in hydraulic conductivity of porous media. Dupin *et al.* (2001) also assumed that biomass grow as colonies or aggregate instead of biofilm.

Many models like the models that were suggested by Clement *et al.* (1996), Cunningham *et al.* (1991), and Suchomel *et al.* (1998) use porosity reduction as a critical parameter for assessing permeability reduction. While other models have focused on the relation between hydraulic conductivity and the distribution of biomass in soil such as the biofilm model that was suggested by Taylor *et al.* (1990).

The change in hydraulic properties due to biomass accumulation was investigated using two different methods. In the first method, the bioclogging process was investigated analytically through suggesting empirical relationships from the experiments results, while the second method included the use of network model or micro-models (Suchomel *et al.*, 1998; Kim and Fogler, 2002).

Thullner *et al.* (2002) used pore network models to link hydraulic conductivity with porosity by assuming that biomass grows either as biofilm or a colony. Thullner *et al.* (2002) concluded that the growth of biomass as a colony caused a higher reduction in hydraulic conductivity of the porous media. A similar study assumed that biomass grows as a colony or biofilm was presented by (Seki and Miyazaki 2001).

Macroscopic models based on developing analytical equations was suggested by Clement *et al.* (1996) to model change in porosity, permeability due to bacterial growth, and to study the bacterial interactions in porous media without suggesting any specific configuration for the microbial growth. These models assumed that the pore size distribution was not changed due to biomass growth, but only the maximum pore radius was reduced, also the model assumed that the larger pores of porous media clog first. The macroscopic models were criticized by other authors because it did not take into account plug formation (Thullner, 2010).

In addition to the previous models, Kim (2006) presented a mathematical model to describe bacterial transport in saturated porous media. The model indicated that the

permeability and porosity of porous media could be altered due to bacterial deposition and growth on the solid matrix, and the variation of permeability could reach three orders of magnitude compared with natural permeability variation. Brovelli *et al.* (2008) presented a numerical model to simulate the effect of biomass growth on the hydraulic properties of saturated porous media, the simulation results indicated that the common assumption of an initial uniform biomass distribution may not be appropriate and could cause a noticeable error because of the sensitivity of rates and patterns of bioclogging to initial biomass distribution.

Based on experimental data, Lappan and Fogler (1996) developed a model to describe the effect of exopolysaccharide production on the permeability of porous media. The model included two phases; the first phase known as the non-growth phase, including the occurrence of cell transport and retention and the growth phase in which porous media plug by the growing of retained cells.

Another mathematical model depended on macroscopic approach was developed by Ham *et al.* (2007) to identify the bioclogging process in saturated porous media. They performed numerical experiments to study the impact of biomass growth and attachment on the hydraulic properties of porous media, in addition to implement sensitivity analysis to examine the effect of key model parameters on the model behaviour. The model results indicated that variations in permeability and porosity of porous media occurred due to biomass growth and attachment on solid matrix. The results of sensitivity analysis gave an indication that hydraulic properties (permeability and porosity) were much more sensitive to the utilization rate of substrate.

A one-dimensional model was developed by Holm (2000) to study the bioclogging process, Holm (2000) reported that the detachment of bacteria close to the inlet and attachment further could interpret the reduction in the hydraulic conductivity. In

addition to that Thullner *et al.* (2004) indicated that the clogging process in two dimensions took place mainly in the vicinity of the glucose injection point for all models (macroscopic model, micro-colony model and biofilm model) and the general pattern of biomass distribution was similar, showing a V- to U-shaped structure starting close to the glucose injection port.

#### **2.4.5 The application of bioclogging in environmental biotechnology**

Information on bioclogging process has accumulated steadily in the last few decades; the vast majority of applications bioclogging in the field of environmental biotechnology, such as underground water biological treatment techniques, leakage dams and landfill, and microbial enhanced oil recovery is a research studies. Wastewater disposal, artificial groundwater recharge, in situ bioremediation of the contaminated aquifers, bio-barriers for sub-surface pollution, construction of water reservoirs, or secondary oil recovery are all affected by biological clogging process (Baveye *et al.*, 1998). For example, during artificial recharge of groundwater, excessive biomass growth can cause severe bioclogging that could change the flow pattern (Seifert and Engesgaard, 2007). Bioclogging of porous media could have beneficial consequences, for example, it will create a biofilm barrier which can control and minimize the transport of contaminants and promote the degradation of pollutants (Trefry and Johnston, 1998; Kao *et al.*, 2001; Komlos *et al.*, 2004; Kim *et al.*, 2006). In addition to that, contaminant mobility can be inhibited through plugging aquifer flow paths that can lead to the formation of bio-barriers (Vilcáez *et al.*, 2013). This technology involves using bacteria to remove or degrade groundwater pollution (Folch *et al.*, 2013), injection microorganisms and sufficient nutrient selectively into the subsurface stimulating microorganisms to grow and form thick biofilm (Komlos *et al.*, 2004; Kim *et al.*, 2006). This selective injection often causes early clogging near the

injection zone, limiting both bacterial and nutrient transportation lengths (Shaw *et al.*, 1985; Kim *et al.*, 2006), and thereby controlling the subsurface contamination plumes. Permeable reactive barrier or bio-barrier is a common solution for nitrate removal from groundwater and drinking water, barrier involves construction of a wall of porous material where the contaminants like nitrate will clean-up as it pass through these materials, usually soil bacteria used nitrate as a carbon source (Strietelmeier *et al.*, 2001), thereby reducing the hazard of nitrate by transforming it into less harmful material (Folch *et al.*, 2013). Figure 2.12 shows an example of PRB.

Bioclogging also can be used to seal a leaking construction pit, landfill or dike, reduce drain channel erosion, and form grout curtains to limit the migration of heavy metals and other organic contaminants (Ivanov and Chu, 2008). The porous media may be sealed and become more impermeable to water due to the accumulation of bacterial biomass, insoluble bacterial slime and soluble biogenic gas bubbles in soil (Vandevivere and Baveye, 1992; Bonala and Reddi, 1998).

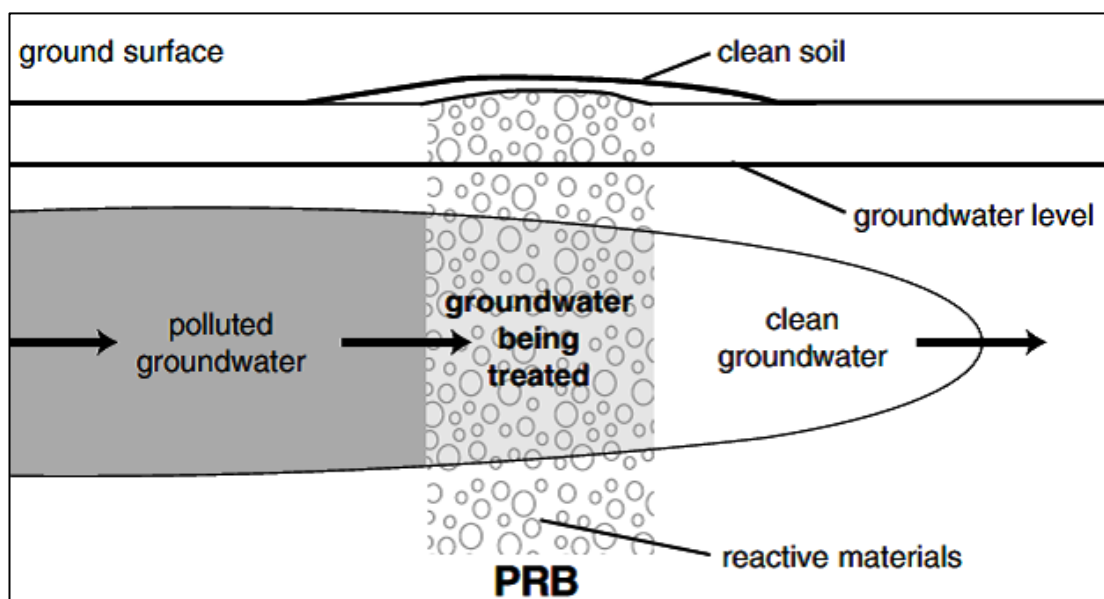


**Figure 2.12: Permeable Reactive Barrier Example (EPA, 2001)**

Soil properties can be modified and improved through filling the soil pores to reduce the hydraulic conductivity of porous media through using microorganisms (Soares *et al.*, 1991); Taylor and Jaffe, 1990; Vandevivere and Baveye, 1992; Kim and Fogler, 2000; Stewart and Fogler, 2000; Thullner, 2001; Ross *et al.*, 2001; Ivanov and Chu, 2008; Vilcaez *et al.*, 2013; Seki, 2013).

Even though bioclogging process has beneficial consequences in some cases (Zhang *et al.*, 1995), it has serious consequences in other cases (Baveye *et al.*, 1998; Sanin *et al.*, 2003). For instance, in water injection wells the injection capacity will be reduced due to the clogging of the well screen, where optimal conditions for microorganisms are available to grow and produce polysaccharides (Taylor and Jaffe, 1990; McCarty *et al.*, 1998). In Japan, bioclogging can cause plugging at producing water injection well, thereby reducing the well injection rate (Lim *et al.*, 2011).

The process of extracting crude oil entrapped in the capillary pores of underground reservoirs is one of the most important processes in the oil industry that need to be enhanced to keep pace with growing energy demand. In order to meet this target, several techniques were used including; thermal or heat, chemicals miscible gas injection, and microbial processes (Green and Willhite). Microbial enhanced oil recovery (MEOR) is an alternative method for EOR, where injected microorganisms grow and produce a variety of products like bio-surfactants, biopolymers, biomass, acids, gases and solvents, these products are able to improve unfavourable properties of heavy crude oil and increase oil recovery through mobilization oil trapped in the reservoir (Sen, 2008; Lazar *et al.*, 2007; Bryant *et al.*, 1990; Kowalewski *et al.*, 2006).

Microbial enhanced oil recovery technologies have progressed from laboratory-based studies in the early 1980s to field applications in the 1990s. In Canada, Stehmeir *et al.* (1990) carried out a field test of a *Leuconostoc* based on a plugging system and also a

new concept of selective plugging was reported by Cusack *et al.* (1992). During the last 15–20 years, China was very active in MEOR method and today is still active in this field and could be considered one of the leaders in this field (Lazar *et al.*, 2007). Biopolymers, for example, are one of bacterial products that added to the displacing water in order to increase both of the viscosity of water in water flooding to make the displacement process more effective and direct reservoir fluids to previously unswept areas of the reservoir and the sweep efficiency of water flood by plugging high permeability zones such as fractures that reduce the sweep efficiency of polymer flooding operation (Crespo *et al.*, 2014), in other words, the permeability of porous media can be modified by biopolymers and can be used in profile modification (Bryant *et al.*, 1990).

The early water breakthrough due to the heterogeneity of porous media are of the major challenges in water-flooded oil reservoirs, earlier reports on oil recovery studies have shown that the major factor limiting oil recovery is the variation of permeability (Suthar *et al.*, 2009).

The recovery fluid preferentially flows through high permeability zones, leaving the oil present in less permeable regions uncovered (Thullner *et al.*, 2002). Hence, MEOR is regarded as one of the efficient, applicable and cost effective methods for extracting crude oil from the oil reservoir through using microorganisms (Lazar *et al.*, 2007). Some advantages of using MEOR methods over other EOR methods are: (a) lower cost, (b) broader applicability, (c) the ability to produce in-situ the chemicals needed for the process, (d) required materials are widely available and economically (Crescente *et al.*, 2005).

A wide range of microorganisms is well-known in their capability of enhancing oil recovery through produce an extracellular enzyme called dextransucrase that widely

used in dextran production when sufficient sources of carbon are available (Vilcáez *et al.*, 2013). *Leuconostoc mesenteroides* is able to produce substantial amounts of dextran, an insoluble exopolymer, in the presence of sucrose (Lappan and Fogler, 1994; Stewart and Fogler, 2001), *Bacillus licheniformis* (Suthar *et al.*, 2009) and *Klebsiella pneumonia* are the most famous strains of bacteria that have the ability to plug the porous media selectively (MacLeod *et al.*, 1988).

#### **2.4.6 Heavy metal removal in the presence of bacteria**

Heavy metal is a general collective term, which applies to the group of metals and metalloids with atomic density greater than  $4000 \text{ kg m}^{-3}$ , or 5 times more than water Hutton and Symon (1986). In the environment, the heavy metals are generally more persistent than organic contaminants such as pesticides or petroleum products (Hashim *et al.*, 2011). Several technologies exist for the remediation of heavy metals contaminated groundwater and soil such as chemical treatment and biological treatment technologies (Hashim *et al.*, 2011). Chemical treatment technologies include the use of chemicals to decrease the toxicity or mobility of metals contaminants by converting them to inactive states (Evanko and Dzombak, 1997). Biological treatment technologies exploit natural biological process that allows certain plants and microorganisms to help in the remediation of metal in soil and groundwater. Bioremediation is an innovative and promising technology available for removal of heavy metals and recovery of the heavy metals in polluted water and lands. Since microorganisms have developed various strategies for their survival in heavy metal-polluted habitats, these organisms are known to develop and adopt different detoxifying mechanisms such as biosorption, bioaccumulation, biotransformation and biomineralization, which can be exploited for bioremediation either ex-situ or in-situ.

Biosorption can be defined as the selective sequestering of metal soluble species that result in the immobilization of the metals by microbial cells. However, bioaccumulation can occur only with living organisms through transport of contaminants to the cell and accumulation of metals inside the cell (Zabochnicka-Świątek *et al.*, 2014). Biotransformation refers to the process in which a substance is changed from one chemical form to another chemical form by chemical reactions; in the case of toxic metals, the oxidation state is changed by the addition or removal of electrons, thus their chemical properties are also changed, however, biomineralization describes the process in which toxic metal ions combine with anions or ligands produced from the microbes to form precipitation (Patel and Kasture, 2014).

---

## ***CHAPTER THREE***

### **MATERIALS AND METHODS**

#### **3.1 Introduction**

A series of experimental tests carried out to achieve the following targets;

- Evaluate the bioclogging process in porous media and the factors that could affect this process.
- Understand some aspects of flow, which could be influenced the clogging process in porous media.
- Explore how the potential of biological growth could control the direction and the location of the subsurface hydraulic flow thereby overcomes the problems of preferential flow.

The experimental work includes: Soil characteristics tests, the optimal growth condition of bacterial strains, and a series of bioclogging experiments in homogeneous and heterogeneous porous media.

In order to determine the characteristics of the soil several soil tests were carried out. These tests included, sieve analysis, hydraulic conductivity, and particle density and compaction tests. In addition to these soil tests, bacteria culturing methods, the optimal growth conditions and the ability to form biofilm were also implemented.

Furthermore, a series of sand column experiments using different sand fractions were carried out to investigate how the bacterial growth in homogenous and heterogeneous porous media will affect the hydraulic conductivity, and to study the effect of grain size on bioclogging process in homogenous and heterogeneous porous media, and finally to explore how the use of bioclogging may help the process of clean-up the contaminated porous media.

Analytical tests included a loss on ignition and total numbers of bacteria were implemented to analyse the soil samples which were taken from each sand column by the end of each experiment. Water samples were analysed for zinc concentrations using optical emission spectrometer.

## **3.2 Materials**

### **3.2.1 Sand**

Silica sand containing 98-100 % of silica ( $\text{SiO}_2$ ) was obtained from Hepworth Minerals and Chemicals Ltd. Prior to heating at  $550^\circ\text{C}$  to remove organic matter before sand packing; the sand was autoclaved for 20 minutes and dried at  $100^\circ\text{C}$ . Six sand fractions (A;  $>600\ \mu\text{m}$ , B;  $425 - 600\ \mu\text{m}$ , C:  $300 - 425\ \mu\text{m}$ , D:  $212 - 300\ \mu\text{m}$ , E:  $150 - 212\ \mu\text{m}$ , F:  $<63\ \mu\text{m}$ ) were used.

### **3.2.2 Bacterial strain**

#### **3.2.2.1 *Pseudomonas putida* mt-2**

*Pseudomonas putida* mt-2 (NCIMB10432/ATCC23973), aerobic or facultatively anaerobic bacterium was purchased from the National Collection of Industrial and Marine Bacteria (NCIMB). *P. putida* mt-2 carries the TOL plasmid which is responsible for further degradation of toluene (Tark *et al.*, 2005). *P. putida* biofilms exposed to toluene showed a significant increase in extracellular carbohydrate (Schmitt *et al.*, 1995).

#### **3.2.2.2 *Beijerinckia indica***

*Beijerinckia indica* (NCIMB8005/ATCC9540) was obtained from the National Collection of Industrial and Marine Bacteria (Aberdeen, UK); this strain is an aerobic soil bacterium that fixes nitrogen, this strain was selected because of its ability to produce a copious amount of toughness and adhesive exopolysaccharides material (EPS) (Dennis and Turner, 1998). The optimal temperature for the growth of *Beijerinckia* species is 20–30°C, and there is no growth occurs at 37°C (Kennedy, 2005).

#### **3.2.2.3 *Culturing techniques***

In this study, two strains of bacteria (*P. putida* mt-2 and *B. indica*) were cultured under aseptic techniques to reduce any probability of bacterial contamination. The strains were routinely sub-cultured, maintained in culture medium and stored at 4°C in 250 ml flask. For the first strain (*P. putida* mt-2), about 2.0 ml of cultured cells was sub-cultured in 250 ml flask containing 50.0 ml of sterilised nutrient broth solution as shown in Figure 3.1. The nutrient broth (CM001) was purchased from (OXOID LTD, UK) and contained the following ingredients in g<sup>l</sup><sup>-1</sup>: Lab-Lemco powder 1.0, Sodium

chloride 5.0, Peptone 5.0 and Yeast extract 2.0. This nutrient broth solution was prepared by adding 0.65 grams of nutrient broth to 50.0 ml of distilled water and sterilising the solution by autoclaving at 126°C for 15 minutes. The incubation period for this strain was 24 hours at 30°C.

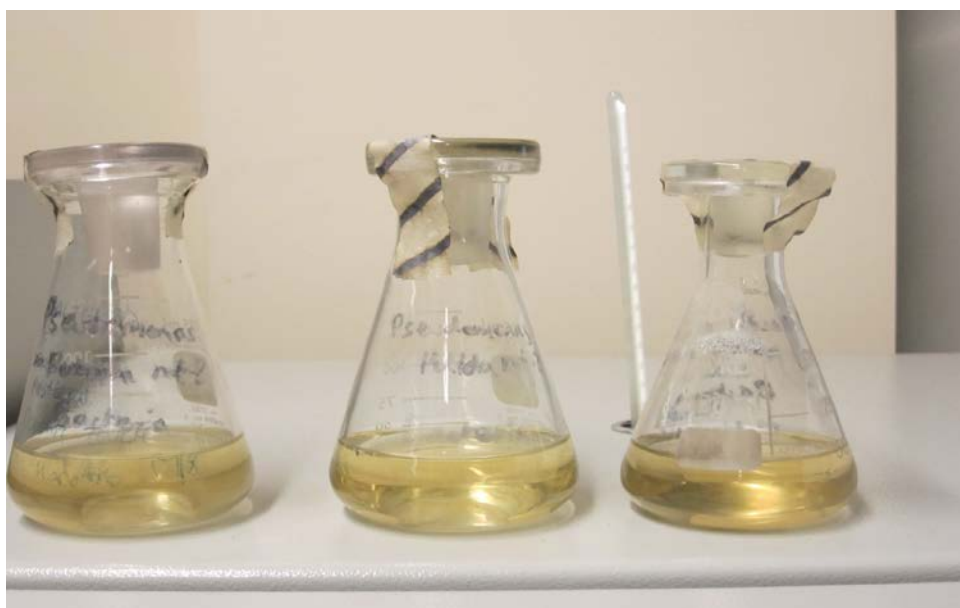


**Figure 3.1: Sub-culture the *P. putida* mt-2 in 50 ml of nutrient broth.**

For *B. indica*, cells were cultured in 250 ml flask containing 50 ml of nitrogen free medium containing ingredients in  $\text{g l}^{-1}$ :  $\text{K}_2\text{HPO}_4$  (1.0),  $\text{MgSO}_4 \cdot 7\text{H}_2\text{O}$  (0.2),  $\text{CaCO}_3$  (1.0),  $\text{NaCl}$  (0.2),  $\text{FeSO}_4 \cdot 7\text{H}_2\text{O}$  (0.1),  $\text{NaMoO}_4 \cdot 2\text{H}_2\text{O}$  (0.005), Glucose (10.0), the incubation period for this strain was 72 hours.

### **3.3 Analytical tests**

#### **3.3.1 Soil tests**

##### *3.3.1.1 Sieve analysis test*

A dry sieve analysis (or *gradation* test) is a procedure commonly used to assess the particle size distribution of a granular material. In this study the sand was sieved into six fractions for use in the remainder of the experiments according to British Standards BS1377: Part 2:1990. Typically, the sieve analysis test comprised of a set of sieves with screens, the top sieve which has the largest screen openings, and each lower sieve in the set has smaller openings than the one above, and a pan placed at the base of the set. The test can be started by pouring a weighed sample into the top sieve, and then the set placed on a shaker for a fixed amount of time. After the termination of the shaker, the retained soil weight was taken to estimate the finer passing percentage and draw the sieve analysis graph. In this test, the collected samples which ranging from 63 to 1180 $\mu$ m was selected to be used as a porous medium in the following experimental work. Figure 3.2 shows the graph of the sieve analysis test.

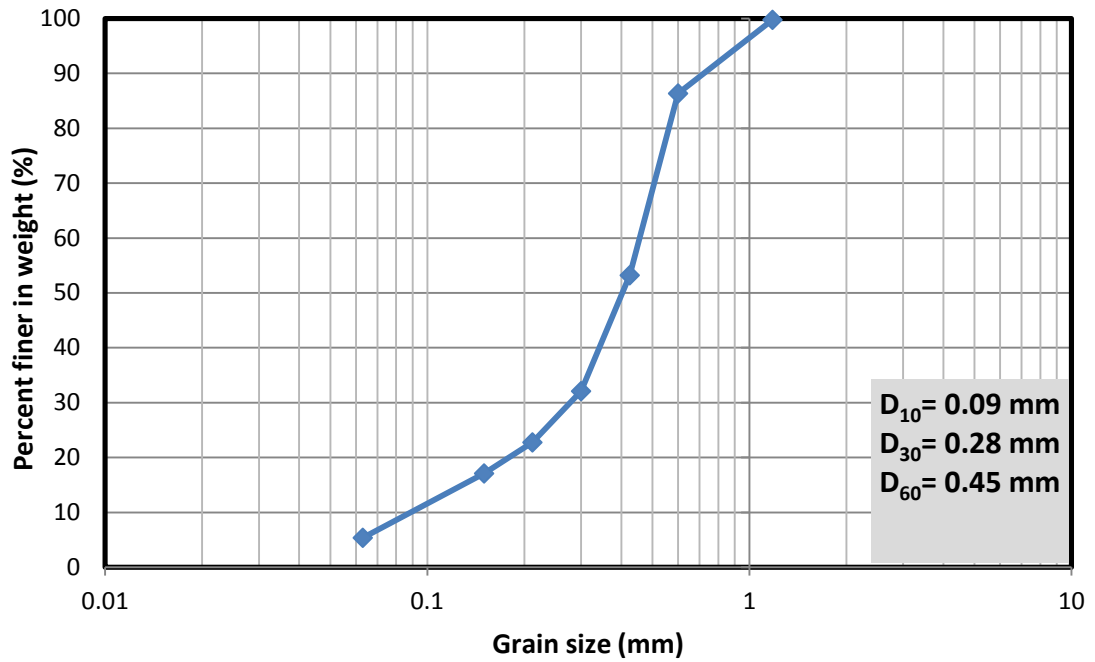


**Figure 3.2: Sieve analysis graph of soil.**

The coefficient of uniformity ( $C_u$ ) and coefficient of curvature ( $C_c$ ) were calculated using:

$$C_u = \frac{D_{60}}{D_{10}} \quad (1)$$

$$C_c = \frac{D_{30}^2}{D_{60} \cdot D_{10}} \quad (2)$$

$D_{10}$ , which is a diameter just larger than the diameters of 10% of the soil grains, in other words, it's the size of the sieve through which only 10% of the soil grains pass. Similarly,  $D_{60}$  means diameter of the soil particles for which 60 percent of the particles are finer. The value of  $C_u$  is equal to 5.0 which are greater than 4.0 and the value of  $C_c$  is equal to 1.935 which is less than 3, these two values are compatible with the

specifications of BS (British Standards BS1377: Part 2:1990), this indicates that the soil has a very narrow particle size range.

### ***3.3.1.2 Hydraulic conductivity test***

The aim of this test is to determine the hydraulic conductivity of sand by solving the following form of Darcy's law:

$$Q = -KA(dh/dl) \quad (3)$$

Where (Q) is the flow rate in  $m^3s^{-1}$ ,  $(dh/dl)$  represent the hydraulic gradient, (A) is the cross section area in  $m^2$ , and (K) denotes the hydraulic conductivity in  $ms^{-1}$ . There are two general types of hydraulic conductivity test methods that are routinely performed in the laboratory: (1) the constant head method, and (2) the falling head method. The hydraulic conductivity test on a clean and dry sand for six different size of sands ranging from 63-1180  $\mu m$  were carried out as specified by British Standards BS1377:Part 5:1990. Figure 3.3 shows the permeameter of the constant head and falling head method.

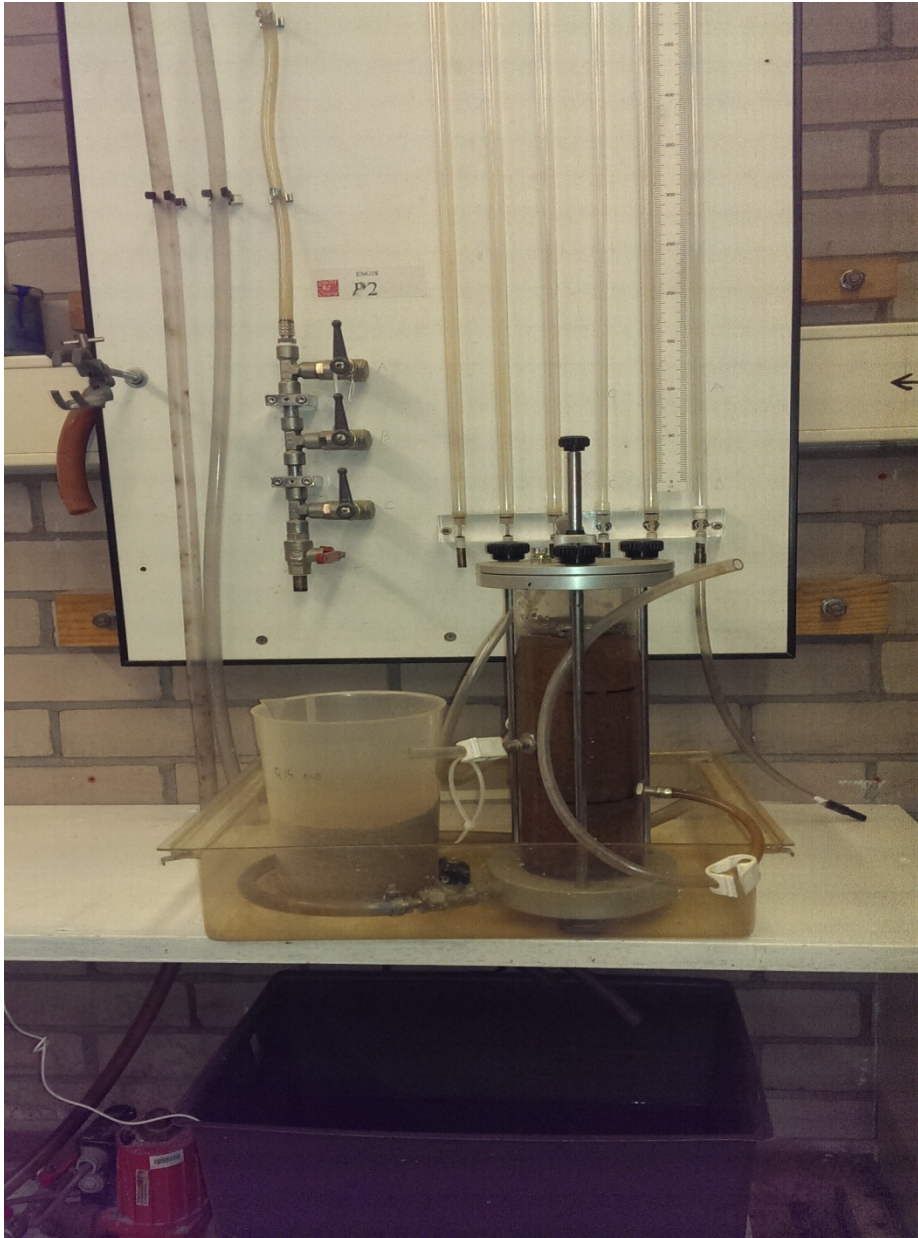


**Figure 3.3: Standard Permeameter of the constant and falling head method.**

This test was carried out to determine the initial hydraulic conductivity values for each sand fraction and also to compare them with the measured initial hydraulic conductivity values for each sand fraction during the bioclogging experiments.

The constant head method was used in the bioclogging experiment by using Mariotte bottle which provides a constant head; this method is slightly different from the standard hydraulic conductivity test which includes the use of manometers to provide

a constant head. The Mariotte bottle is sealed chamber containing a tube in the centre and when this bottle filled with water and connected to a tank through a port on the bottom, the water level kept in the tank is that at the base of the tube as this is the level at which atmospheric pressure is applied. This will hold true for as long as there is liquid in the reservoir above the level of the base of the central tube (Harbottle *et al.*, 2004).

Table 3.1 shows the results of the hydraulic conductivity tests for the six sand fractions, standard constant head method was used for the sand fractions ranging from 150-1180  $\mu\text{m}$ , whereas falling head method was used for the finer sand fractions 63-150  $\mu\text{m}$ . For each sand fraction the test was carried out in triplicate.

Table 3.1 Summary of hydraulic conductivity test for the six sand fractions

Size of the six sand fractions ( $\mu\text{m}$ )	Hydraulic conductivity $k$ ( $\text{ms}^{-1}$ )	Standard deviation
A (>600 $\mu\text{m}$ )	$3.46 \times 10^{-3}$	0.025
B (425-600 $\mu\text{m}$ )	$1.69 \times 10^{-3}$	0.006
C (300-425 $\mu\text{m}$ )	$9.51 \times 10^{-4}$	0.004
D (212-300 $\mu\text{m}$ )	$6.54 \times 10^{-4}$	0.002
E (150-212 $\mu\text{m}$ )	$1.67 \times 10^{-4}$	0.001
F (<63 $\mu\text{m}$ )	$9.80 \times 10^{-6}$	0.002

### 3.3.1.3 Particle density test

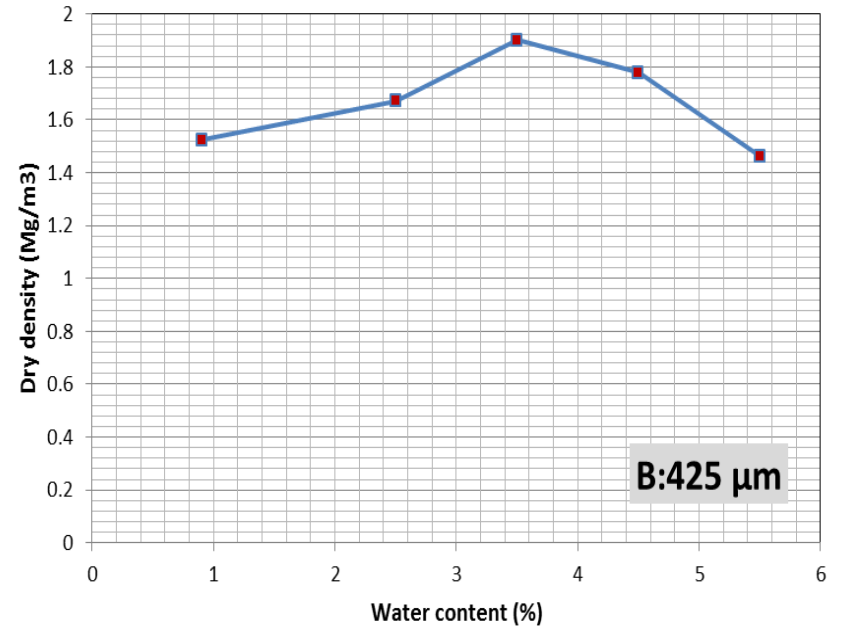
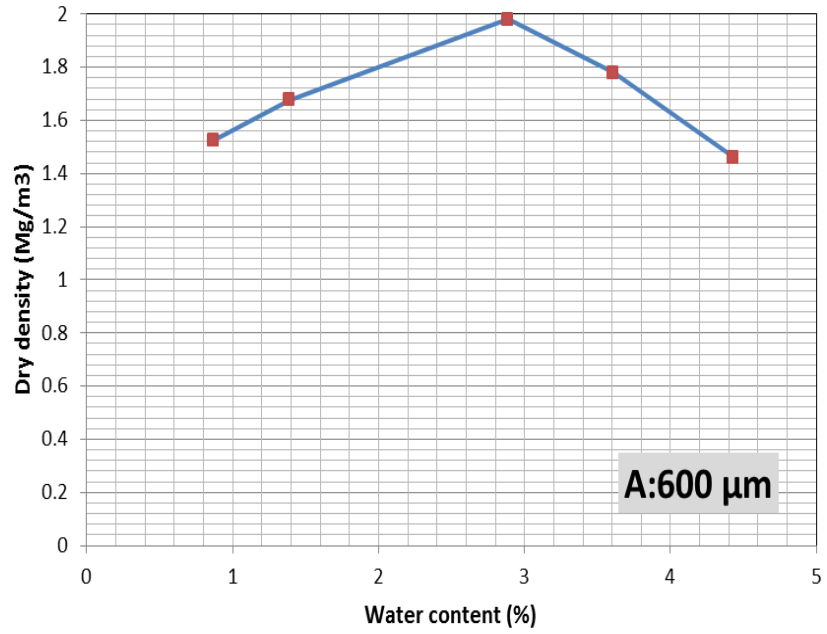
The specific gravity ( $G_s$ ) or particle density of different soil samples can be defined as the mass of a soil sample in a given volume of particles. This test was determined

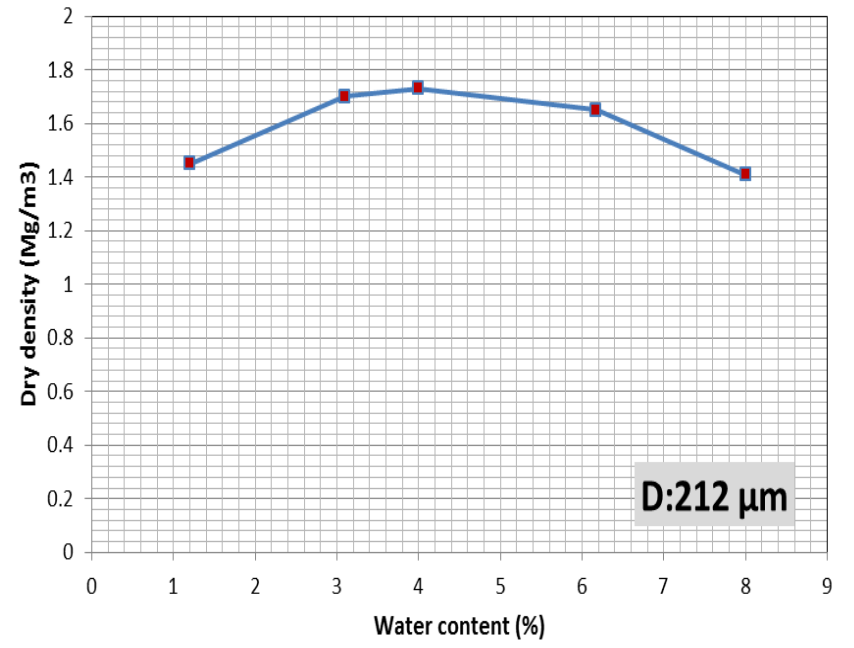
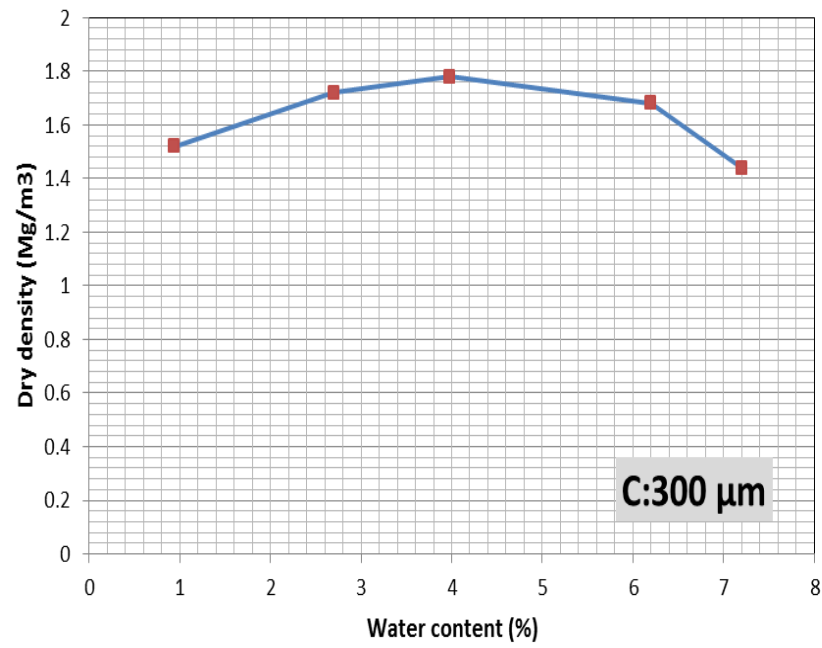
using pycnometer as specified by British Standards BS1377: Part 2:1990. The test results showed that the particle density of sand is  $2.650 \text{ Mgm}^{-3}$ , and the standard deviation is equal to 0.001.

#### ***3.3.1.4 Compaction test***

Compaction is the artificial improvement of the mechanical properties of the soil. Soil compaction is the process by which particle is forced to pack more closely together through a reduction in the air voids by using mechanical means (BS 1377: Part 4:1990). The compaction characteristics of six sand fractions 600, 425, 300, 212, 150, and 63  $\mu\text{m}$  were determined following the procedures described in the British Standard BS1377: Part 4:1990. Standard Proctor effort of (600 in  $\text{kN. m/m}^3$ ) was considered, in which 27.0 blows were applied from a 2.5 kg hammer falling through a height of 300 mm to compact the soil in three layers into a one litre compaction mould. A motorized apparatus was used with a metal rammer having 50.0 mm diameter circular faces.

The water content was estimated by following the British Standard (BS 1377:Part1:1990) with drying in a fan-assisted oven maintained at a temperature not exceeding  $105^\circ\text{C}$ . The compaction curves which represent the dry densities against the water contents for the six sand fractions were obtained from a compaction test are shown in Figure 3.4.





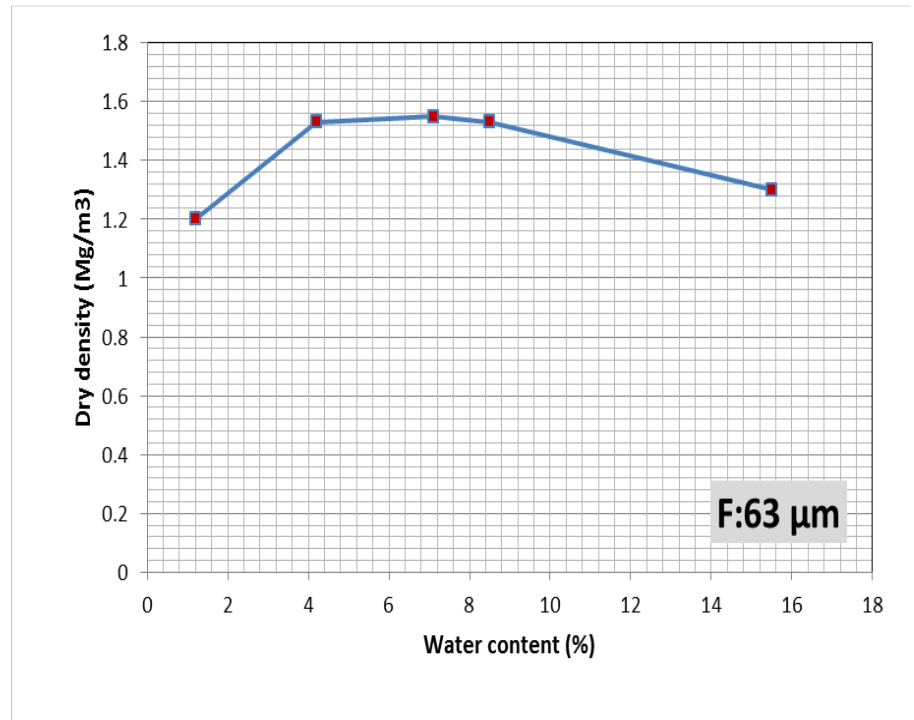
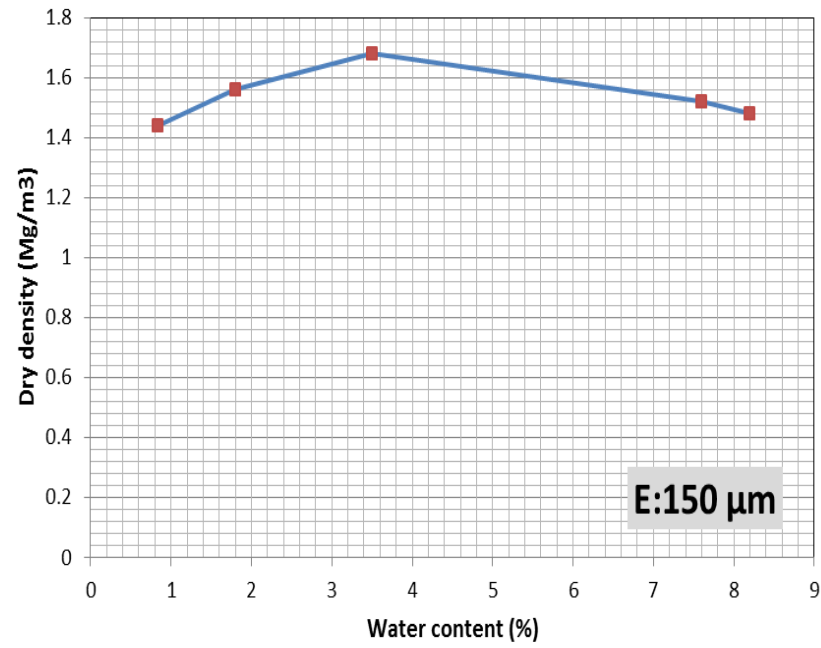


Figure 3.4: The relation between dry density and water content for six sand fractions: (A-F).

The minimum dry density for each sand fraction, which is obtained by pouring sand through a funnel into a cylinder to get the loosest arrangement of grains, was also measured following the same procedure specified by British Standards (BS1377: Part 2:1990). Afterwards, the relative density which is used to indicate the degree of packing of sand and mostly expressed in terms of void ratio was calculated for each sand fraction.

$$R_d (\%) = \frac{e_{max} - e_{measured}}{e_{max} - e_{min}} \cdot 100 \quad (4)$$

$$e = \frac{G_s \cdot \rho_w}{\gamma_{dry}} - 1 \quad (5)$$

$R_d$  is the relative density,  $e_{max}$  is the maximum void ratio,  $e_{min}$  is the minimum void ratio, and  $G_s$  the specific density, which is  $2.65 \text{ Mg m}^{-3}$  and  $\rho_w$  is the water density in  $\text{g/cm}^3$ . Sand porosity was calculated by subtracting the dry weight of sand from the saturated weight and dividing the results on the total. Table 3.2 shows the results of the compaction test for six sand fractions.

Table 3.2: Compaction test results for six sand fractions

Sand fraction ( $\mu\text{m}$ )	600	425	300	212	150	63
$\rho_{\text{dry max}}$ (Mg/m <sup>3</sup> )	1.95	1.90	1.78	1.73	1.68	1.55
$\rho_{\text{dry min}}$ (Mg/m <sup>3</sup> )	1.47	1.44	1.42	1.4	1.38	1.2

### 3.3.2 Loss on ignition

The total amount of biomass for each sand fraction was estimated by the end of each bioclogging experiment by collecting soil samples and analysing them using loss on ignition method. Loss on ignition is a commonly and widely used to estimate the

organic and carbonate content of sediments (Dean Jr, 1974). Because of the technical factors that could affect the results of this method such as sample size, exposure time, and the position of the sample in the furnace, the amount of organic matter determined by loss on ignition at 550°C.

This method simply compares the weight difference of soil samples before and after samples ignition using muffle furnace. After the termination of nutrient solution pumping by the end of each experiment, soil samples were collected from top, middle and bottom locations. Each soil sample is almost 16.0 cm<sup>3</sup> in volume, and the samples were left to dry at 105°C for 24 hours. After drying the samples, they were grinded using mill (LABTECH ESSA LM1-P, AUSTRALIA) to ensure homogeneity of the samples.

Before starting each test, ceramic crucible have been prepared in advance by placing them in an unheated carbolite furnace (HTC 1500), then heated up them to 550°C for 6 hours (Seki *et al.*, 2005). Then, the crucibles were removed from the furnace and allowed to cool at room temperature in a desiccator. Afterwards, the crucibles were weighed to the nearest fraction of 0.0001 grams, and then about 2.0 grams of each dried soil sample was transformed into each crucible and weighed again. Subsequently the crucibles were placed in a muffle furnace at 550°C to constant mass and weighed again after being left to cool down in a desiccator.

Loss on ignition as a percentage was calculated as the difference between the initial and final sample weights divided by the initial weight. The amount of biomass attached to the sand was measured as volatile solids (VS) per dry weight of sand (Bielefeldt *et al.*, 2002).

### **3.3.3 Separation of cells from soil sample method**

By the end of the bioclogging experiments, about 1.0 gram was taken from the collected soil samples to count the total number of cells. Then the 1.0 gram was diluted in a sterilized phosphate buffer solution with a ratio of (1:10, w/v) in a 20 ml tubes in order to separate cells from soil particles. (Amalfitano and Fazi, 2008) method was followed to separate cells from soil particles. This method is a combination of chemical and physical treatments.

The chemical treatments included the addition of  $0.266 \text{ g l}^{-1}$  of sodium pyrophosphate as a chelating agent to the diluted samples. In addition to the chemical treatment, physical treatment was conducted on samples through shaking and sonication. The samples were shaken for 30 minutes at 700 rpm using a shaker before sonicating them for one minute by using an ultrasonic bath. After sonication, the supernatant was collected using cellulose filter ( $0.2 \mu\text{m}$ ) and vacuum apparatus.

### **3.3.4 Bacteria counting using DAPI staining**

The total number of bacteria was counted using DAPI staining (4, 6-diamidino-2-phenylindole (Porter and Feig 1980). DAPI was purchased from (Sigma-Aldrich Ltd., UK). A concentrated DAPI stock solution of  $1.0 \text{ mg ml}^{-1}$  was diluted to  $0.1 \mu\text{g ml}^{-1}$  and stored at  $4^\circ\text{C}$ .

Samples were stained with  $0.01 \mu\text{g ml}^{-1}$  DAPI stock solution for 5 minutes at room temperature. Samples were filtered using cellulose nitrate filter 25.0 mm in diameter, with pore sizes of  $0.2 \mu\text{m}$ . The filtration process was carried out using vacuum filtration apparatus.

The stained filters were viewed via Nikon microscope Eclipse (LV 100) at a wavelength of 390 nm in order to count cell numbers. Typically 10 microscopic fields are counted with 25 to 300 cells per field.

Cell number (cells/ml) of the original sample was calculated by multiplying the mean of the counted cells per field by a conversion factor which is referring to the number of field areas on the whole filter and dividing by the volume filtered in ml. The conversion factor is the ratio of the area of the filter to the area of the microscopic field. Subsequently, the following equation (from Wetzeland Likens, 1991) was used to calculate final bacterial densities.

$$Bacteria\ ml^{-1} = membrane\ conversion\ factor \cdot ND \quad (6)$$

Membrane conversion factor = Filtration area/area of microscopic field

$N$  = Total number of bacteria counted/number of microscopic fields counted

$D$  = Dilution factor; volume of sample stained/total volume of sample available

### **3.3.5 Batch adsorption experiment**

In order to estimate the soil adsorption capacity, some parameters need to be determined first, such as the soil: solution ratio. An easy way to determine sorption behaviour of different sand fractions is via the use of the batch adsorption techniques (Shackelford and Daniel, 1991).

In order to represent how much solute can be adsorbed, an adsorption isotherm was used. Adsorption isotherm is an empirical equation that shows the relationship between the amounts of solute adsorbed by the adsorbent and the equilibrium concentration of the solute (Steve and Erika, 1998). The Freundlich and Langmuir isotherms used to describe the adsorption behaviour of zinc ions. The amount of metal adsorbed per unit mass ( $Q_e$ ) is calculated as:

$$Q_e = \frac{(C_1 - C_e) \cdot V}{M} \quad (7)$$

$C_1$  and  $C_e$  are the initial and equilibrium concentration (mg/L),  $M$  is the mass of the adsorbent (g) and  $V$  is the volume of the solution (mL).

The Freundlich isotherm is introduced as an empirical model, where  $Q_e$  represents the amount adsorbed per amount of adsorbent at the equilibrium (mg/g), and  $K_f$  and  $n$  are Freundlich constants which correspond to adsorption capacity and adsorption intensity, respectively.

$$Q_e = K_f \cdot C_e^{1/n} \quad (8)$$

The equation above can be linearized and the dependent constants  $K_f$  and  $1/n$  found by linear regression:

$$\ln(Q_e) = \ln(K_f) + \frac{1}{n} \ln(C_e) \quad (9)$$

The Langmuir equation is commonly written as shown in Eqn. 10., where  $q_e$  is the amount of solute adsorbed per unit mass of adsorbent in mg/g and  $C_e$  represent the equilibrium concentration of adsorbate in solution after adsorption in mg/l and  $q_{max}$  and  $b$  are Langmuir constants related to capacity and energy of adsorption respectively. Plot of  $C_e/q_e$  Vs  $C_e$  would give the value of constants

$$\frac{C_e}{q_e} = \frac{1}{b q_{max}} + \frac{C_e}{q_{max}} \quad (10)$$

Percent zinc ion removal (%R) was calculated using the equation below:

$$R = \frac{C_1 - C_e}{C_1} \cdot 100 \quad (11)$$

Regarding the bioclogging experiment in the contaminated heterogeneous porous media, only one set of sand fractions 600, 300, and 150  $\mu\text{m}$  was chosen. These sand fractions were selected depending on the wide difference of permeability between them as this might help in the detection the changes in hydraulic conductivity for the heterogeneous bioclogging experiments in contaminated porous media. The standard method of adsorption test included the use of a given amount of the zinc solution in this case (76 ml of zinc stock solution at 1.0 mM) was added to the solution (nitrogen free medium) to get a total of 380 ml with a final concentration of zinc of 0.2 mM. The zinc solution was autoclaved for 20 minutes, then mixed in a centrifuge tubes with three sand fractions 600, 300, and 150  $\mu\text{m}$  at different soil: solution ratio of (1:4, 1:5: 1:10: 1:20, and 1:40). Centrifuge tubes then were shaking for 24 hours at 180 rpm (Chen *et al.*, 2011). By the end of the shaking period, the solutes were separated from soil by centrifuging the tubes for 20 minutes at 3200 rpm. Subsequently, the effluent was filtered and analysed using optical emission spectrometer.

### **3.3.6 Inductively Coupled Plasma-Optical emission spectrometers ICP-OES method**

Inductively coupled plasma optical emission spectrometry (ICP-OES) is an analytical technique used for the detection of trace metals found in aqueous samples, soils, industrial and organic wastes, sediments, and other solid wastes. Zinc concentration was determined by Inducting Coupled Plasma (ICP-OES, Perkin Elmer Optima 2100 DV). 5-10 ml of samples was collected in 40 ml plastic container. The samples were then filtered using filter paper (0.45  $\mu\text{m}$ ). To prevent any precipitation of zinc about 0.1 % of  $\text{HNO}_3$  was added to the samples.

### **3.4 Experimental methods**

The experimental work include preliminary experiments and different experiments in both homogenous and heterogeneous porous media, Table 3.3 shows the details of the main experiments.

#### **3.4.1 Preliminary experiments**

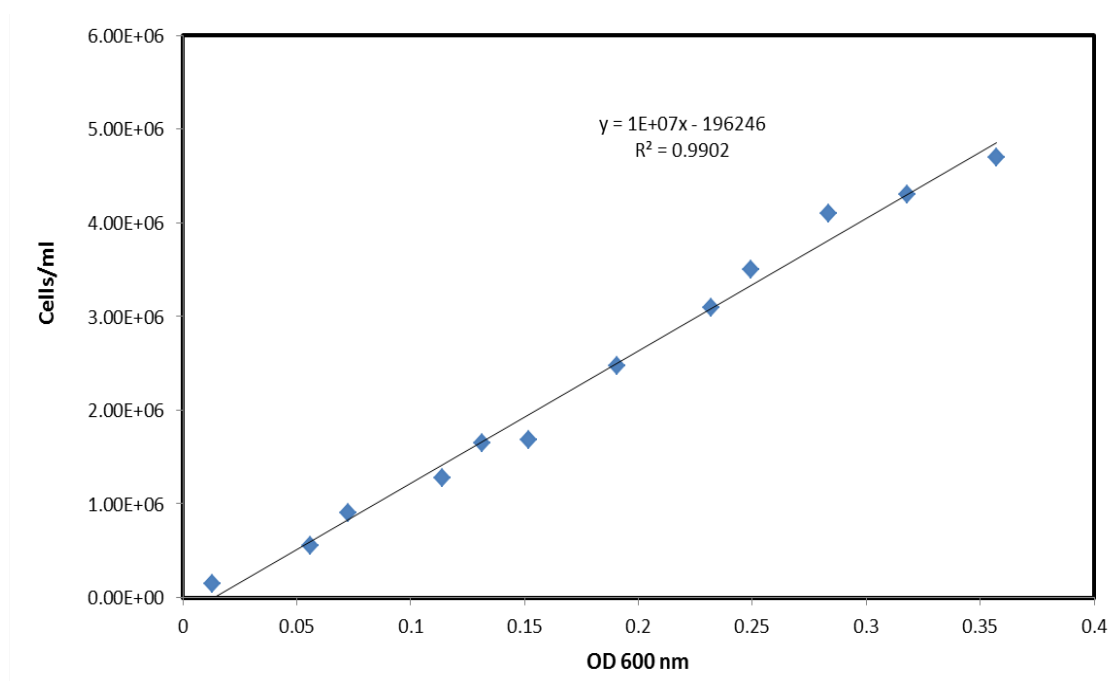
The purpose of these experiments is to examine the ability of bacterial strains to form biofilm under batch and continuous flow conditions. *B. indica* has already been reported to form a huge amount of biofilm using nitrogen free medium. However, the ability of *P. putida* to form biofilm under different nutrient media was unknown, so that the ability of this strain to form biofilm was investigated under batch and continuous flow conditions by using different nutrient media.

Table 3.3: The main Experiments in both homogenous and heterogeneous porous media

Experiment code	Description	Bacteria strain	Number of repeat	Sand fractions ( $\mu\text{m}$ )
EXP-P-S-FR	Flow rate effect on hydraulic conductivity	<i>P. putida</i> mt-2	Duplicate	A
EXP-B-S-FR	Flow rate effect on hydraulic conductivity	<i>B. indica</i>	Duplicate	A
EXP-P-T-FGV	Grain size effect on hydraulic conductivity	<i>P. putida</i> mt-2	Triplicate	A, D, and E
EXP-B-T-FGV	Grain size effect on hydraulic conductivity at laboratory temperature	<i>B. indica</i>	Triplicate	A, B, C, D, and E
EXP-B-T-FGC	Grain size effect on hydraulic conductivity at 25°C	<i>B. indica</i>	Triplicate	A, B, C, D, E, and F
EXP.(1)	Narrow ranges of permeability	<i>B. indica</i>	Triplicate	A, B, and C
EXP.(2)	Two high permeable sand fractions	<i>B. indica</i>	Triplicate	A, B, and E
EXP.(3)	Wide range of permeability	<i>B. indica</i>	Triplicate	A, C, and E
EXP.(4)	One high permeable sand fraction with two low permeable sand fractions.	<i>B. indica</i>	Triplicate	A, D, and E
EXP.(5)	Narrow range in permeability for fine sand	<i>B. indica</i>	Triplicate	D, E, and F

### 3.4.1.1 Cells preparation

By the end of the incubation period, cells were prepared for experimental work. 1.0 ml of bacterial solution was transferred into 1.2 ml cuvette to measure the optical density ( $OD_{600}$ ) which gives an indication of the cell concentrations. A standard curve correlating the total number of cells with the corresponding optical density ( $OD_{600}$ ) was drawn as shown in Figure 3.5. The total number of cells was counted using DAPI staining method, whereas the corresponding optical density values  $OD_{600}$  were determined using the spectrophotometer.



**Figure 3.5: The relation between number of cells and optical density of *B. indica***

After the estimation of the initial number of cells, the cells suspension was transferred from the 250 ml flasks into centrifuge tubes to centrifuge them at 3200 rpm for 20.0 minutes, after that the supernatant was discarded.

Cells then were re-suspended in phosphate buffer solution (PBS; 40 ml in total) prior to more centrifugation to remove the culture medium. The supernatant was again discarded before cells were re-suspended in 40 ml phosphate buffer solution (PBS)

which contained the following components in  $\text{gl}^{-1}$ : NaCl(8.01),  $\text{Na}_2\text{HPO}_4 \cdot 2\text{H}_2\text{O}$  (1.78),  $\text{KH}_2\text{PO}_4$  (0.27), KCl (0.2).

#### **3.4.1.2 *P. putida* mt-2 biofilm formation in batch experiment**

A batch experiment was carried out to study the effect of the varying nutrient conditions on biofilm formation of *P. putida* mt-2. Six different culture media were chosen with different concentrations of glucose and ammonium sulphate.

The first three media contained (0.3, 3.0, and 30)  $\text{gl}^{-1}$  of glucose, respectively and same concentrations of ammonium sulphate of 0.2  $\text{gl}^{-1}$  in each. The second three media contained (0.3, 3.0, and 30)  $\text{gl}^{-1}$  of glucose, respectively and same concentrations of ammonium sulphate of 2.0  $\text{gl}^{-1}$  in each, as well as constant concentrations of the following:  $\text{K}_2\text{HPO}_4$  (6.0),  $\text{KH}_2\text{PO}_4$  (3.0), NaCl (3.0),  $\text{MgCl}_2$  (0.0093),  $\text{CaCl}_2$  (0.0011), and 1 ml of trace element solution which included the following:  $\text{CaSO}_4 \cdot 2\text{H}_2\text{O}$  (0.2),  $\text{FeSO}_4 \cdot 7\text{H}_2\text{O}$  (0.2),  $\text{ZnSO}_4 \cdot 7\text{H}_2\text{O}$  (0.02),  $\text{MnSO}_4 \cdot \text{H}_2\text{O}$  (0.02),  $\text{CuSO}_4 \cdot 5\text{H}_2\text{O}$  (0.02),  $\text{CO}_2\text{SO}_4 \cdot 7\text{H}_2\text{O}$  (0.01),  $(\text{NH}_4)_6\text{Mo}_7\text{O}_{24} \cdot 4\text{H}_2\text{O}$  (0.005),  $\text{Na}_2\text{B}_4\text{O}_7$  (0.005). The culture medium for bacterial growth was adjusted at pH 7.0 with HCl.

Glucose was prepared by autoclaving the concentrations separately, to avoid any chemical reaction with other materials, unlike the ammonium sulphate which could be overflowed during autoclaving. In order to overcome this problem, a 0.2  $\mu\text{m}$  syringe filter purchased from (Fisher scientific Ltd., UK) was used under aseptic technique to sterile the ammonium sulphate.

Subsequently, eighteen glass test tubes of a volume of 13 ml, all equipped with caps to avoid contents from pouring while being autoclaved. Each three test tubes were filled with 9 ml of the sterilized culture media, all of the same type and 1 ml of bacterial suspension. All the tubes were left at 30°C to give cells more time to grow, multiply

and form biofilm. When biofilm was formed in these tubes after five days of nutrient supply, the experiment was ceased to estimate the EPS weight.

EPS was precipitated following the method of (Lembre *et al.*, 2012). This method involved the use of the solution made up from 0.5 M of Ethylenediaminetetraacetic acid (EDTA) and 5.0 M of sodium chloride.

After shaking the flask containing the solution, about of 0.2 ml of this solution was added to each test tube to separate the bacterial strain from the EPS. All tubes were shaken using a vortex mixer before centrifuging them at a speed of 3200 rpm for 30 min to separate EPS from cells.

Then the supernatant was transferred into 50 ml centrifuge tubes and propanol was added to each centrifuge tube at 3:1 ratio to precipitate the EPS, then the solution was centrifuged again at 3200 rpm for 20 min.

Subsequently, the supernatant was poured in the sink and the weight of each centrifuge tube was taken. The weight of the empty centrifuge tubes was measured before and after the formation of EPS and the difference in measurements represented the weight of the EPS. The eighteen test tubes that contained the cells were dried at 30°C using the incubator to take the dry weights of the cells later.

#### ***3.4.1.3 P. putida biofilm formation under continuous flow***

This experiment was performed to examine the ability of *P. putida* mt-2 to form biofilm under continuous feeding of nutrient solution to compare the amount of EPS that was produced by *P. putida* mt-2 in the batch experiment using three culture media with different concentrations of glucose and ammonium sulphate. Three pairs of microscopic glass slides were used. Each pair of slides was structured as a channel with a gap of approximately 1.0 mm between the slides allow the nutrient solution pass through using peristaltic pumps at 5.0 ml min<sup>-1</sup> flow rate.

Two experiments using three different nutrients media were carried out simultaneously and under the same conditions, during which the first medium containing 30  $\text{gl}^{-1}$  glucose and 0.02 $\text{gl}^{-1}$  ammonium sulphate was injected to the first pair, the second medium containing 0.3 $\text{gl}^{-1}$  glucose and 2.0  $\text{gl}^{-1}$  ammonium sulphate was injected into the second pair and the third medium containing 30  $\text{gl}^{-1}$  glucose, and 2.0  $\text{gl}^{-1}$  ammonium sulphate was injected to the third pair, in order to obtain an average of the required EPS.

The injection of nutrients was terminated at the same time for all pairs soon after the formation of biofilm in each pair of the glass slides, which were dried at lab temperature to estimate the dry weight of EPS.

### **3.5 Experimental work in homogeneous porous media**

Many sand column experiments were performed using two bacteria strains *P. putida* mt-2 and *B. indica*. The first experiment was performed to investigate the effect of different culture media (six culture media were used) on hydraulic conductivity of sand due to the growth of *P. putida* mt-2. Because the second strain (*B. indica*) is known by its ability to form a large amount of EPS for that first experiment was performed using only the first strain (*P. putida* mt-2).

The next experiments were conducted to investigate the effect of nutrient flow rate on hydraulic conductivity of sand due to the growth of *P. putida* mt-2 and *B. indica*. Subsequently, the final experiments were allocated to study the effect of grain size on the bioclogging due to the growth of bacteria in media porous homogeneous.

### **3.5.1 Set-up the bioclogging experiments in homogenous porous media**

The structure of the bioclogging experiments in homogenous porous media as shown in Figure 3.6 included the use of clear acrylic identical columns 20.0 cm long with an inner diameter of 2.6 cm.

Each column was connected to a single pump to deliver nutrient solution from sterilised flasks into the system, and Mariotte bottle which is only getting connected to the system when hydraulic conductivity is being measured to provide constant head. The sand columns were connected to the Mariotte bottle and the peristaltic pumps via flexible, clear tubing 6 mm in diameter. An autoclaved glass wool was used as a filter to prevent the sand from washing out was placed above the rubber stoppers which were fitted on both ends of each column. A waste tank was used to collect the waste.

The system was operated at 25°C and upward flow mode to get rid of all the air bubbles under water saturated conditions during the experiment. All the system components were soaked in Virkon for 2 hours to be sterilized, and then washed with distilled water.





**Figure 3.6: Schematic diagrams for bioclogging experiment in homogeneous soil**

### ***3.5.1.1 Sand preparing and packing***

A wet pluviation method (Vaid and Negussey, 1988) was followed for sand packing. The porosity of each sand fraction (0.38-0.47) was measured during the sand packing by subtracting the dry weight from the saturated weight divided by the total volume of the saturated sand column.

The sand packing method includes, filling up each sand column with bacterial suspension, and the amount of the bacteria suspension depends on the porosity of each sand fraction. Then, sand was poured into the column as layers from a distance of 20.0 mm above the top of the column; each layer of sand about 3.4 cm in height was compacted by shaking the sand column with vortex mixer to achieve a final bulk density ranging from (1.38-1.62 Mg/m<sup>3</sup>) which is corresponding to a relative density ranging from (42.0-64.0%). By completing the sand packing all columns were left for

2 hours before measuring the initial values of hydraulic conductivity to allow the bacteria attaching to the soil particles (Vandevivere and Baveye 1992). Table 3.4 shows the parameters of the bioclogging experiments.

Table 3.4: Parameters of the bioclogging experiments in homogenous and heterogeneous porous media

<b>Sand fractions(<math>\mu\text{m}</math>)</b>	A	B	C	D	E	F
<b>Porosity</b>	0.38	0.39	0.408	0.41	0.42	0.47
<b>Standard deviation of porosity</b>	0.003	0.001	0.002	0.001	0.002	0.003
<b>Relative density (%)</b>	0.42	0.45	0.45	0.52	0.56	0.64
<b>Volume of bacterial suspension(<math>\text{cm}^3</math>)</b>	34.9	35.9	36.9	37.4	37.9	42.4
<b>Mass of soil (g)</b>	150	148	145	140.5	140	125
<b>Dry density (<math>\text{g}/\text{cm}^3</math>)</b>	1.66	1.64	1.6	1.55	1.55	1.38
<b>Standard deviation of dry density</b>	0.02	0.01	0.02	0.03	0.01	0.02

### 3.5.2 Different culture medium effect on bacterial growth in homogeneous soil

The targets of this experiment are to investigate the growth of *P. putida* mt-2 in homogeneous soil, and to investigate the effect of different culture media on bacterial growth. Six identical acrylic columns were filled with sand 600-1180  $\mu\text{m}$  and bacterial suspension.

Six different sterilized nutrient media contained different concentrations of glucose in  $\text{g}/\text{l}$  0.3, 3.0, and 30 and different concentrations of ammonium sulphate in  $\text{g}/\text{l}$  0.2 and 2.0 were used in each experiment.

The pump is applying a constant head and the feeding period was adjusted to 8 minutes per day using a timer with an initial flow rate of  $5 \text{ ml min}^{-1}$ . The nutrient feeding rate

was almost 1.0 pore volumes of a solution because it is expected that the pore volume will be decreased due to bacterial growth. The hydraulic conductivity reading was taken three times weekly, and this experiment was performed in duplicate.

### **3.5.3 Flow rate effect on bacterial growth in homogeneous soil**

Sand column experiments were conducted to investigate the effect of flow rate on bioclogging in homogeneous porous media due to the growth of two bacterial strains (*P. putida* mt-2 and *B. indica*). Bacterial cells were prepared by following the way that is mentioned in Section 3.5.11 as well as the sand packing. In these experiments, six identical sand columns were operated on under biological conditions.

The nutrient solutions were delivered at three initial flow rates 5.0, 2.5 and 1.5 ml min<sup>-1</sup> with 30.0 g l<sup>-1</sup> of glucose and 2.0 g l<sup>-1</sup> of ammonium sulphate for the *P. putida* mt-2 and nitrogen free medium for the *B. indica*. The pump is applying a constant head and the nutrient feeding for each experiment was adjusted to provide a volume of 40 ml into each column.

For the experiment, the pump was adjusted at 5.0 ml min<sup>-1</sup> pumping rate, the feeding period was 8 min per day, when the feeding rate was reduced to 2.5 ml min<sup>-1</sup>, the feeding time increased to 16 minutes and again this period was increased to 27 minutes when the flow rate was adjusted at 1.5 ml min<sup>-1</sup>. The hydraulic conductivity readings were measured three times weekly, and these experiments were performed in duplicate.

### **3.5.4 Experiments of grain size effect on bioclogging in homogeneous porous media**

The main purposes behind conducting these experiments are to study the effect of grain size on the hydraulic conductivity due to the bacterial growth in homogeneous

porous media, and to investigate the spatial distribution of bacteria in a homogeneous porous medium. In these experiments and for each sand fraction experiment six identical acrylic columns were used.

Three of them under controlled conditions, where dead cells (killed by autoclaving) were mixed with sand using the wet pluviation method, whereas the other columns were operated on under biological conditions (live cells). Six different fractions of sand (600-1180, 425-600, 300-425, 212-300, 150-212, and 63-150  $\mu\text{m}$ ) were selected to achieve the targets of these experiments with *B. indica*. However, only three sizes of sand (600-1180, 212-300, and 150-212 $\mu\text{m}$ ) were chosen when *P. putida* mt-2 was used as a bacterial strain, this selection is just a first trial to assess the ability of this strain on hydraulic conductivity for different sizes of sand (course, medium, and fine). For *P. putida* mt-2, the nutrient solution that was delivered by the peristaltic pumps contained 30.0  $\text{g l}^{-1}$  of glucose and 2.0  $\text{g l}^{-1}$  of ammonium sulphate, while nitrogen free media was used as a nutrient solution for *B. indica*. The peristaltic pump is supposed to apply a constant flow rate during the experiment but during the experiment and regarding to the measured flow rates, this pump failed to apply a constant flow rate and it applied a constant head instead. The nutrient solution was delivered at an initial flow rate 2.5  $\text{ml min}^{-1}$ . The nutrient feeding rate was set at 16 min per day using a timer. This flow rate was selected to provide a total flow of 40 ml for each sand fraction. For the experiments with *B. indica* the initial number of cells was ranging from  $1.53 \times 10^6$  to  $1.66 \times 10^6$  cells/gram.

The hydraulic conductivity was measured 3 times weekly using Mariotte bottle which provides a constant head. The duration of the all experiments were of the same time period, and they were dismantled when equilibrium values was reached.

### **3.6 Experimental work in heterogeneous porous media**

Bioclogging experiments in heterogeneous porous media were performed to investigate the potential of biological growth to control direction and location of subsurface hydraulic flow to overcome the problems of preferential flow using a different range of sand fractions, and also to investigate the spatial distribution of bacterial growth and bioclogging in heterogeneous porous media. Moreover, to ensure the applicability of bioclogging in the process of clean-up the contaminated porous media.

#### **3.6.1 Set-up the bioclogging experiments in heterogeneous porous media**

In order to achieve the aim of the experimental work in heterogeneous porous media, the experiment design almost mimics the natural behaviour in heterogeneous porous media. In this design, the porous media were assumed to be stratified and the flow is parallel to the soil layers. Three sand columns were selected to mimic three soil layers with different permeability. The potential flow between these three layers was neglected, and this is the only disadvantage in this design as shown in Figure 3.7.



**Figure 3.7: Photo of heterogeneous experiment structure**

The structure of each bioclogging experiment as shown in Figure 3.8 included the use of six identical columns with 20 cm long and 2.6 cm inner diameter. Three of them

were tested under controlled conditions (dead cells) and the other columns were tested under biological conditions (live cells). Each three columns were connected to a single pump to deliver the nutrient solution into the columns via small tanks to ensure a constant head was applied across all columns equally. The dimensions of the small container that distributes the nutrients into the sand columns are 5.7 cm depth and 6.2 cm inner diameter.

Outflow tanks were also connected to the outlet of each three sand columns via one way valves or check valves to ensure a one directional flow. Mariotte bottle was used to provide a constant head was connected to the system only when the hydraulic conductivity values were being measured. A waste tank was placed at the bottom of the system to collect the waste solution that could overflow from the outflow tanks. All parts of the system were sterilised with Virkon and then washed with distilled water before sand packing.

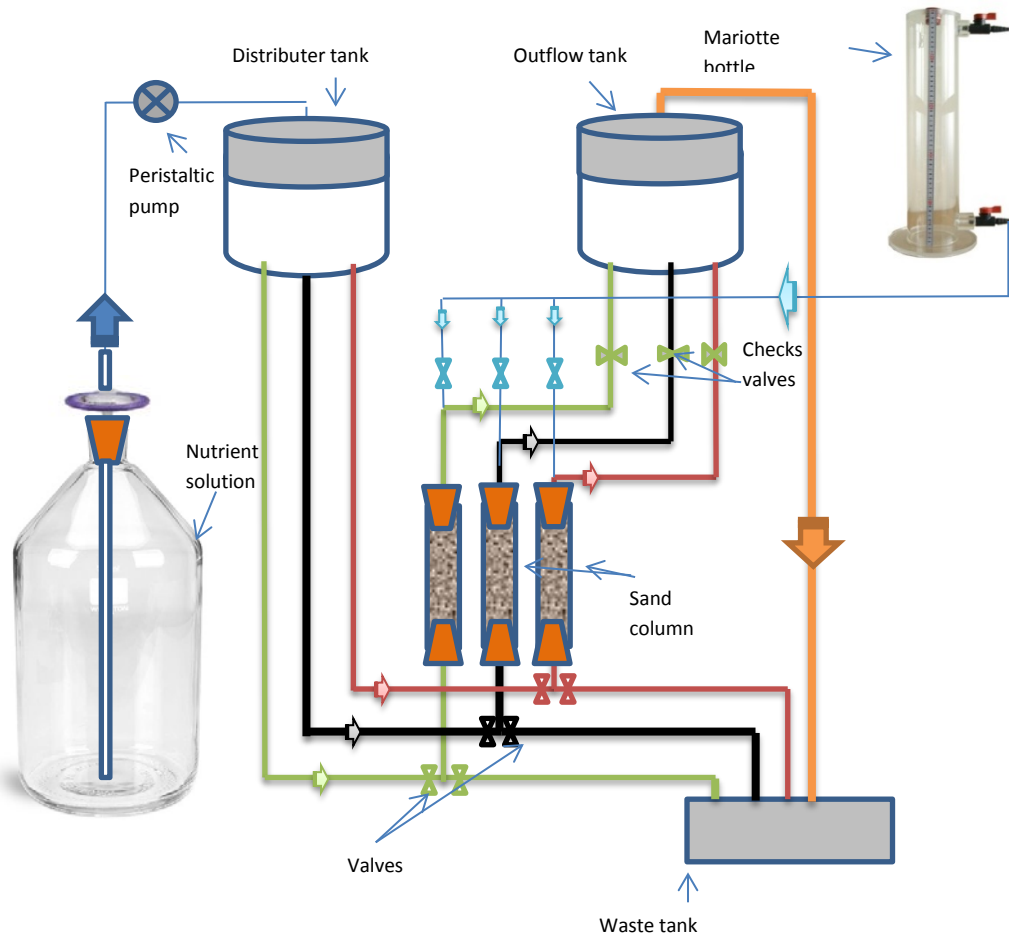


**Figure 3.8: Schematic diagrams for the bioclogging experiment in heterogeneous porous media.**

### 3.6.2 Grain size effect on bioclogging in heterogeneous porous media

Five heterogeneous experiments were carried out to study the changes in hydraulic conductivity due to bacterial growth, and to understand the effect of biological clogging on preferential flow in heterogeneous porous media using different sand fractions.

Each experiment included the use of 18 identical columns, every nine columns were grouped into three sets, nine columns were under biological conditions (live cells) and the other nine were under control conditions (dead cells). Table 3.3 shows the five sets

of the heterogeneous experiments which included the use of six sand fractions ranging from 63-1180  $\mu\text{m}$ . Each experiment experienced the use of three different sand fractions. In other word, each group of three columns contains three different sand types.

The bacterial suspension was mixed with sand using sand packing method which was explained in section (3.5.1.1). Each experiment was conducted under constant head and the nitrogen free medium was being delivered at an initial pumping rate of 5.0 ml  $\text{min}^{-1}$  for 24 minutes each day, providing a volume of 40 ml for each sand column. The initial number of cells was ranging from  $1.19 \times 10^6$  to  $1.6 \times 10^6$  cells/gram. The columns under control conditions (dead cells) were fed with nitrogen free medium solution without glucose to prevent any potential contamination of other microorganisms. All the experiments were running under constant temperature of 25°C which is the optimal growth temperature for *B. indica* and upward flow to prevent the effect of air bubble. The hydraulic conductivity was measured 3 days weekly using the Mariotte bottle technique, and each experiment was dismantled when the hydraulic conductivity readings remained constant in values. These experiments were performed in triplicate.

Subsequently, a volume of 16.0  $\text{cm}^3$  of soil samples was collected from top, middle, and bottom of each column by the end of each experiment. The collected soil samples were promptly stored in sealed polythene bags for no more than 4 days at 4.0°C to analyse them for the total number of bacteria and the loss on ignition (Boone, 1999).

The possible combination of sets of three out of the six sand fractions would results in nineteen experiments that can be carried out, and due to time limitations, only five experiments were carried out. The selection of these five sets of experiments was based on sand fractions that have the most significant range of permeability. Three relatively

high permeable sand fractions 600, 425, and 300  $\mu\text{m}$  with small differences in permeability between them were used in EXP.(1) to study the effect of the bacterial on the flow direction.

In order to study how the bacterial growth would affect the flow direction from two high permeable sand fractions into one low permeable sand fraction, an experiment EXP.(2) was performed using these three sand fractions; 600, 425, and 150  $\mu\text{m}$ .

The third experiment EXP.(3) was carried out to study how the bacterial growth would affect the flow direction when three sand fractions 600, 300, and 150  $\mu\text{m}$  with a wide range of permeability were used.

The fourth experiment EXP.(4) was performed to study how the bacterial growth would affect the flow direction from high permeable sand fraction 600  $\mu\text{m}$  into two low permeable sand fractions 212 and 150  $\mu\text{m}$ .

To investigate the bioclogging process in heterogeneous porous media with a narrow range in permeability with relatively low permeable sand fractions, three sand fractions 212, 150, and 63  $\mu\text{m}$  were chosen to use in the last experiment EXP.(5).

### **3.6.2 The effect of different zinc concentrations on bacterial growth**

The bioclogging experiments were carried out to understand the effect of biological clogging on preferential flow in heterogeneous sand deposits. Therefore, extra heterogeneous experiments were needed to investigate how the control of groundwater flows biologically could be of use in the treatment of contaminated land. Before these experiments, the effect of zinc on the bacterial growth was performed as a preliminary test.

Four concentrations of zinc ranging from 0.1 to 0.5 mM were selected based on the study of (Nasrazadani *et al.*, 2011) who used different concentrations of zinc around the four concentrations mentioned above. The influence of zinc was determined on the basis of the optical density method (OD<sub>600</sub>) using a spectrophotometer (Hitachi U-1900).

The zinc concentrations were determined following Mittal and Goel (2010) method which provides the estimation of OD<sub>600</sub> for the three day incubated cells in the absence and presence of different concentrations of zinc.

To prepare 50 ml of zinc as a stock solution, 0.0068 g of ZnCl<sub>2</sub> was added to 50 ml of distilled water to get a final concentration of 1.0 mM.

After that 2.4 ml of sterilized standard zinc solution was individually added to the bacterial suspension to get a total of 24 ml with final concentration of zinc 0.1 mM.

Three autoclaved capped glass test tubes were filled with 8.0 ml of the solution, and then incubated for 3 days at 30°C.

A further three test tubes were filled with bacterial suspension alone for control conditions which were also incubated for 3 days at 30°C. 1.0 ml was taken from each test tube to estimate the corresponding initial optical density values. The final optical density was estimated after 3 days of incubation period. The same procedure was used for the other concentrations of zinc 0.2, 0.3, and 0.5 mM.

### **3.6.3 The heavy metals removal in the presence and absence of *B. indica***

#### ***3.6.3.1 Zinc effect on bacterial growth in porous media***

Column experiments in heterogeneous porous media were performed to investigate how bioclogging could enhance the remediation of soil from heavy metal contaminants, and also to investigate the effect of heavy metals (zinc in this case) on bacterial growth in heterogeneous porous media.

In these experiments three sand fractions acting as a porous medium of (600, 300, 150  $\mu\text{m}$ ) were chosen on the basis of the wide range in permeability between them. The reason behind choosing three sand fractions with a wide range of permeability rather than a narrow range of permeability was to observe the changes in hydraulic conductivity between the three sand fractions evidently.

The structure of these experiments was completed in the same way as in the previous sections as shown in Figure 3.4, the only difference was the addition of zinc at 0.2 mM.

Before sand packing, 80 ml of stock zinc solution at 1.0 mM concentration was prepared. This stock solution was added into the bacterial suspension to get a total of 400 ml at 0.2 mM of zinc as a final concentration.

Nine acrylic, sand columns were used to accommodate the live cells (*B. indica*). The nine sand columns were left for two hours to allow the cells to be attached to the soil particles. Then, the initial readings of hydraulic permeability were recorded by using Mariotte bottle.

The nutrient solution (nitrogen free medium) was pumped through peristaltic pumps at  $5.0 \text{ ml min}^{-1}$  pumping rate, and the feeding period was adjusted at 24 min per day. During the experiment, the hydraulic conductivity readings were recorded every three days a week, and the outflow samples were collected accordingly to test the amount of zinc that was left in the soil columns.

Zinc concentrations were measured by using optical emission spectrometer. By the end of this experiment, soil samples were collected from each sand column from three locations (upper, middle, and bottom) to analyse the loss on ignition and the total number of cells. The soil samples were left without analysing the zinc concentrations as it is beyond the aim of this experiment.

Control experiment was carried out by adding 0.2 mM of the zinc solution to the same medium (nitrogen free medium) and mixing the solution with the soil but without bacterial inoculum. In addition to the system sterilization with Virkon, glucose was excluded from the nitrogen free medium again to prevent any types of contamination which might occur due to the growth of other types of microorganisms.

---

## ***CHAPTER FOUR***

### **RESULTS AND DISCUSSION OF BIOLOGGING EXPERIMENTS IN HOMOGENEOUS POROUS MEDIA**

#### **4.1 Experimental results**

Although, biological clogging of porous media is often considered to be a problem (e.g. in nutrient delivery for in-situ contaminated land remediation), it can be exploited for hydraulic control, such as through the formation of in-ground barriers. In this study, the potential of bioclogging to control fluid flow in range of porous medium size fractions was considered. This can be achieved through investigating the changes in the flow pattern which can be caused by bacterial clogging of the pore volume, and address the factors that have a direct influence on this clogging of pore volume such as the effect of grain size and the bacterial growth conditions.

Sand column experiments were conducted to study the extent of biological clogging in homogeneous porous media. Section 3.5.1 shows the set-up of the homogenous experiments. The effect of grain size on bacterial growth, extracellular polymeric substance (EPS) production and the subsequent reduction of hydraulic conductivity were explored. The experimental work in homogeneous porous media was performed through using two bacterial strains (*Pseudomonas putida* mt-2 and *Beijerinckia indica*). The details of these strains and the six sand fractions are presented in section 3.2.2., and section 3.2.1. Moreover, the analytical methods were described in section 3.3.

#### **4.1.1 Optimization of biofilm production**

As mentioned in the previous paragraph, two bacterial strains were used in this study. *B. indica* was already known to produce a large amount of EPS using nitrogen free medium (Kennedy, 2005), but regarding *P. putida* mt-2 it was important to establish the optimum growth conditions that lead to form biofilm.

In order to achieve this target, two experiments were performed. In the first experiment, the ability of *P. putida* mt-2 to form biofilm by using different

concentrations of glucose and ammonium sulphate was estimated in static conditions, while the second experiment was carried out under flow to estimate the ability of this strain to form biofilm.

The results of the batch experiment showed that the maximum amount of EPS was 11.033 g l<sup>-1</sup> and the highest weights of cells were observed when 30.0 g l<sup>-1</sup> of glucose and 2.0 g l<sup>-1</sup> of ammonium sulphate were used as shown in Table 4.1. C:N:P represent the ratio of carbon to nitrogen and phosphor.

Table 4.1: Comparisons between cell and EPS weights in batch experiment using six culture media with different concentrations of glucose (G) and ammonium sulphate (A).

Concentrations of (G, A) in g l <sup>-1</sup>	C:N:P ratio	Average cell weight (g l <sup>-1</sup> )	Standard deviation	Average EPS weight (g l <sup>-1</sup> )	Standard deviation
(0.3, 0.02)	15: 1: 0.05	0.933	0.25	7.10	1.248
(3.0, 0.02)	150: 1: 0.5	1.100	0.00	6.10	0.458
(30.0, 0.02)	1500: 1: 5	1.960	0.25	7.06	1.504
(0.3, 2.0)	0.15: 1: 0.05	1.060	0.21	6.10	0.458
(3.0, 2.0)	1.5: 1: 0.5	1.266	0.06	8.53	0.014
(30.0, 2.0)	15: 1: 5	2.200	0.00	11.03	0.432

This finding was confirmed when the ability of *P. Putida* to form biofilm was investigated under continuous flow conditions. The results of the second experiment indicated that the highest concentration of glucose 30.0 g l<sup>-1</sup> and ammonium sulphate 2.0 g l<sup>-1</sup> led to produce the highest amount of EPS 0.00132 g cm<sup>-2</sup>. Table 4.2 shows the average amount of EPS, which was produced under flow using three different culture media with different C: N: P ratios.

Table 4.2: The average of EPS weight under continuous nutrient feeding using three different culture media with different concentrations of glucose (G) and ammonium sulphate (A).

Concentrations of (G, A) in g l <sup>-1</sup>	C:N:P ratio	Average of EPS weight (g cm <sup>-2</sup> )	Standard deviation
30.0, 2.0	15:1: 5	0.00132	0.0002
3.0, 2.0	1.5: 1: 0.5	0.00038	0.0002
30.0, 0.02	1500: 1: 5	0.0008	0.0006

The results of both batch and continuous flow experiments indicated that the concentrations of nutrients have a greater effect on EPS production and the highest amount of EPS was detected at 30.0 g l<sup>-1</sup> and 2.0 g l<sup>-1</sup> of glucose and ammonium sulphate respectively.

This outcome coincided with the results of (Characklis and Marshall, 1990) who both correlated the biofilm accumulation with the concentration of carbon source and reported that biofilm accumulation increases with the increase in glucose concentration. Also the results agree with the results of (Pal and Paul, 2013) who both suggested that EPS production increases with the increase of nitrogen content in the medium.

The reasons behind that providing more glucose (to a certain extent) increases the activity of the bacteria, and leading to more EPS production biofilm. These results agree to some extent with the study of Rochex and Lebeault (2007) who investigated the effect of varying nutrient conditions on biofilm formation of a *Pseudomonas putida* strain isolated from a paper machine under controlled conditions. Rochex and Lebeault (2007) found that high erosion rates were observed both at higher (1.0 g/ l glucose) and lowest (0.1 g/ l glucose) nutrient concentrations and sloughing was

observed in highest nitrogen concentration. The findings of Rochex and Lebeault (2007) refer to the fact that biofilm accumulation is the result of biofilm production and biofilm detachment (Bryers and Characklis, 1982).

After studying the ability of *P. putida* mt-2 to form biofilm in static and continuous flow conditions, this strain was used to investigate its growth in soil and how it could affect the hydraulic properties of soil using different concentrations of glucose and ammonium sulphate. Three concentrations of glucose in  $\text{g l}^{-1}$  of (0.3, 3.0, and 30.0) and two concentrations of ammonium sulphate in  $\text{g l}^{-1}$  of 0.02 and 2.0 were used. The results of this experiment as shown in Figure 4.1 reveals the effect of different culture media, including different concentrations of glucose (G) and ammonium sulphate (A) on the growth of *P. putida* mt-2 and the subsequent changes in hydraulic conductivity with time. In this figure, the greatest reduction in hydraulic conductivity was 26.0 %, which occurred due to the growth of *P. putida* mt-2 using a culture medium contained 30.0  $\text{g l}^{-1}$  of glucose (G) and 2.0  $\text{g l}^{-1}$  of ammonium sulphate (A).

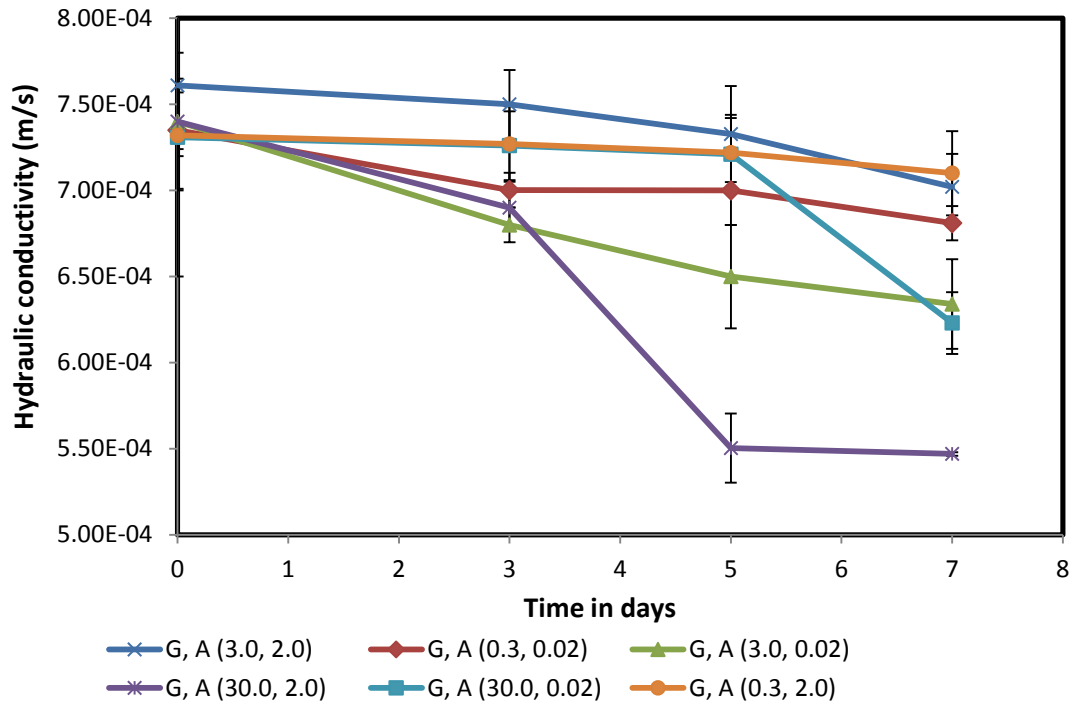


**Figure 4.1: Effect of different culture medium on the growth of *P. putida* mt-2, error bars represent standard deviation of measured hydraulic conductivity values, G and A refer to glucose and ammonium sulphate respectively.**

#### 4.1.2 Flow rate effect (EXP-P-S-FR and EXP-B-S-FR)

Sand column experiments were carried out to inspect the effect of nutrient flow rate on the bacterial growth and the subsequent reduction of the hydraulic conductivity in homogeneous porous media. In these experiments, 600  $\mu\text{m}$  sand fraction was selected to represent the porous media and three different flow rates 5.0, 2.5, and 1.5  $\text{ml min}^{-1}$  were used to determine the optimal flow rate that would reduce the hydraulic conductivity significantly. The results of these experiments indicated that bacterial growth of both bacterial strains *P. putida* mt-2 and *B. indica* were highly affected by the nutrient flow rate as shown in Figures 4.2 and 4.3.

With regard to experiments with *P. putida* it was observed that the hydraulic conductivity decreases significantly by 80 % of the initial value when using 1.5  $\text{ml min}^{-1}$

min<sup>-1</sup> the initial value. Whilst, the hydraulic conductivity decreased by 43.0 % for the 2.5 ml min<sup>-1</sup> flow rate and 37.0 % for the 5.0 ml min<sup>-1</sup> as shown in Figure 4.2.

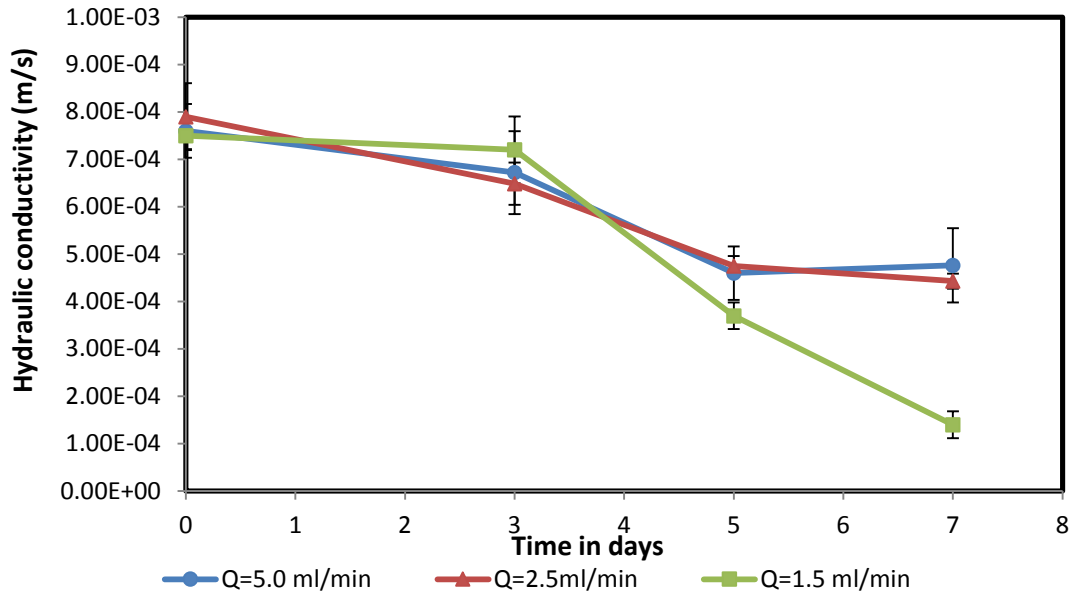


**Figure 4.2: Effect of flow rate on hydraulic conductivity due to growth of *P. putida* mt-2, error bar represent standard deviation of measured hydraulic conductivity values.**

By comparing the reduction in hydraulic conductivity of this experiment with the previous experiment which included the use of 30 g l<sup>-1</sup> of glucose and 2.0 g l<sup>-1</sup> of ammonium phosphate for the same flow rate 5.0 ml min<sup>-1</sup>, it can be noticed that the reduction of hydraulic conductivity is about only 26.0 % which is slightly less than 37.0 %.

According to Figure 4.3 it can be noticed that the flow rate affects the *rate* at which the hydraulic conductivity decreases with *B. indica*. It decreases fastest with the highest flow rate during the first 3 days of the experiment. This rapid reduction of the hydraulic conductivity with the high flow rate could be resulted from the large amount of nutrients which enhanced the bacterial growth.

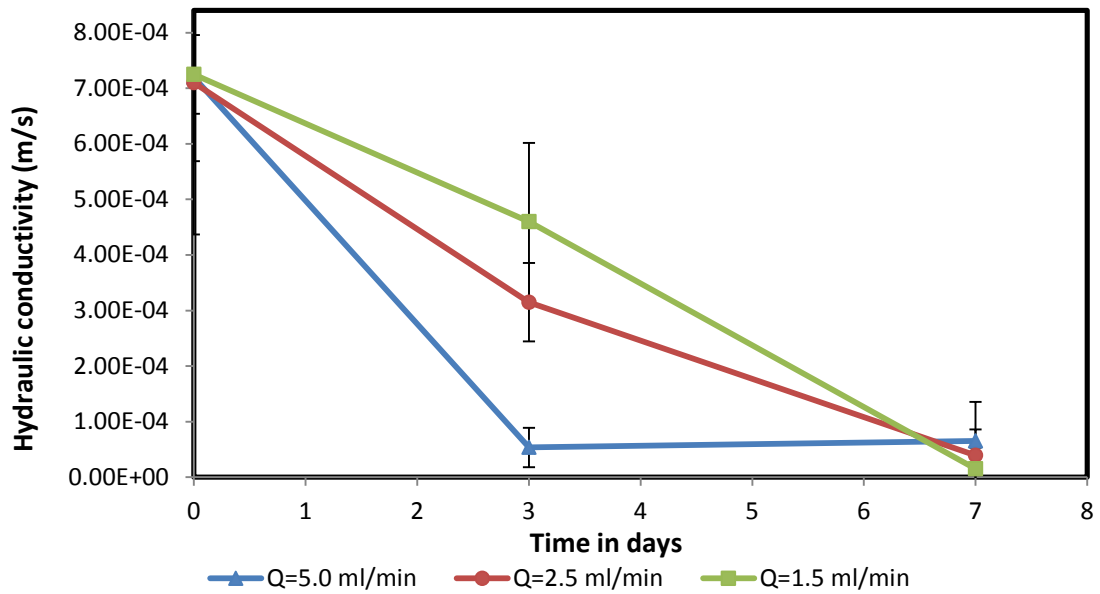


**Figure 4.3: Flow rate effect on hydraulic conductivity due to the growth of *B. indica*, error bars represent standard deviation of measured hydraulic conductivity values.**

By the end of the experiment the hydraulic conductivity values went down by (90.0%, 93.0 % and 97.0 %) for the following flow rates 5.0, 2.5, and 1.5 ml min<sup>-1</sup>. By comparing the results of this experiment with the results of the experiment that included the use of *P. putida* mt-2, it can be noticed that the reduction of hydraulic conductivity using *P. putida* mt-2 is much less than the detected values when *B. indica* was used for the same flow rates. This different behaviour could be attributed to the fact that *B. indica* produces a large amount of EPS.

Moreover, the results of the experiment with *P. putida* came similar to the results of (Peyton and Characklis (1993), Bielefeldt *et al.* (2002), and Manuel *et al.* (2007) who reported that the higher the flow rates are the thinner the biofilm thickness would be. Also, Choi and Morgenroth (2003) concluded that the increase in the shear stress can

lead to an increase in the rate of biofilm detachment. Whilst, the hydraulic conductivity values with the use of *B. indica* shows different respond to the flow rates.

#### **4.1.3 Grain size effect**

In order to study the grain size effect on bioclogging process three sand fractions ranging from 150 to 1180  $\mu\text{m}$  were chosen as a porous media using *P. putida* mt-2. The results of these experiments as presented in Figure 4.4 showed that the hydraulic conductivity values remained stable for the three control columns, whereas the hydraulic conductivity of the columns in which live cells were operated on decreased dropped to some extent in the 600 and 300 $\mu\text{m}$  sand fractions.

On the contrary, a limited change in hydraulic conductivity was observed in the 212  $\mu\text{m}$  sand fraction as shown in Figure 4.4. In this figure, the hydraulic conductivity decreased by 34.0, 56.0 %, and 24.0 % for the 600, 300, and 212  $\mu\text{m}$  sand fractions. These different behaviours of each sand fraction indicated that the grain size has a great effect on the bacterial growth in porous media, and the reduction could be attributed to the amount of EPS produced by the this bacterial strain with the availability of nutrient solution. Nevertheless, the results showed that *P. putida* mt-2 has the ability to reduce the hydraulic conductivity of the porous media to some extent.

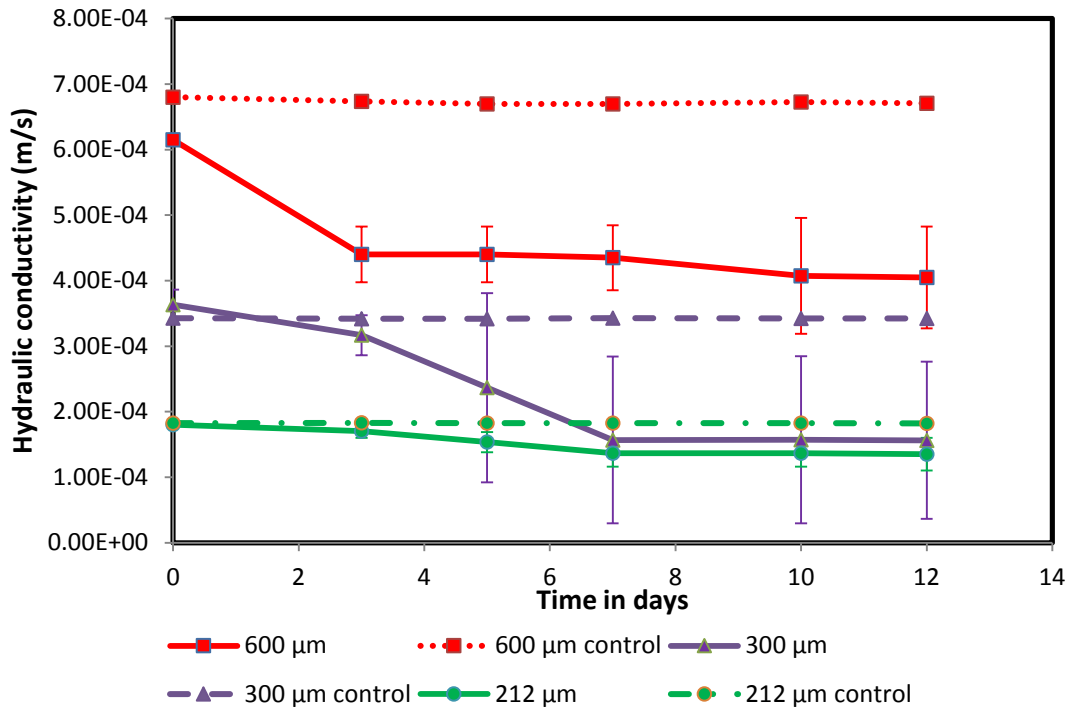


**Figure 4.4: Change in hydraulic conductivity for three different sand fractions 600, 300, and 212 μm in homogeneous soil due to the growth of *P. putida* mt-2, error bars represent standard deviation of measured hydraulic conductivity values.**

Because *P. putida* has a limited effect in reducing the hydraulic conductivity of the soil, *B. indica* was chosen as an alternative bacterial strain due to the ability of this strain to secrete large amounts of EPS. This strain was used to investigate the grain size effect on the bioclogging process at room temperature, which ranged from 12-22°C, only five sand fractions ranging from 150 to 1180 μm were used the reason behind that, this experiment is a preliminary one.

The results of the experiments which carried out with *B. indica* and under lab temperature as in Figure 4.5 indicate that the hydraulic conductivity decreases with a significant percentage of 95.0-98.0 % in the columns that were operated with live cells. This significant reduction of hydraulic conductivity under biological conditions (live cells) might be attributed to the large amount of biomass accumulation. Nevertheless, the hydraulic conductivity remained constant or unchanged compared

to the initial values in the control columns for all sand factions except for the 212  $\mu\text{m}$  sand fraction where the hydraulic conductivity decreased slightly compared to the initial value. This drop in the control columns could be attributed to the increase of temperature during the conducting of the experiment. The data presented in normal and logarithmic based as shown in Figure 4.5 and Figure 4.6.

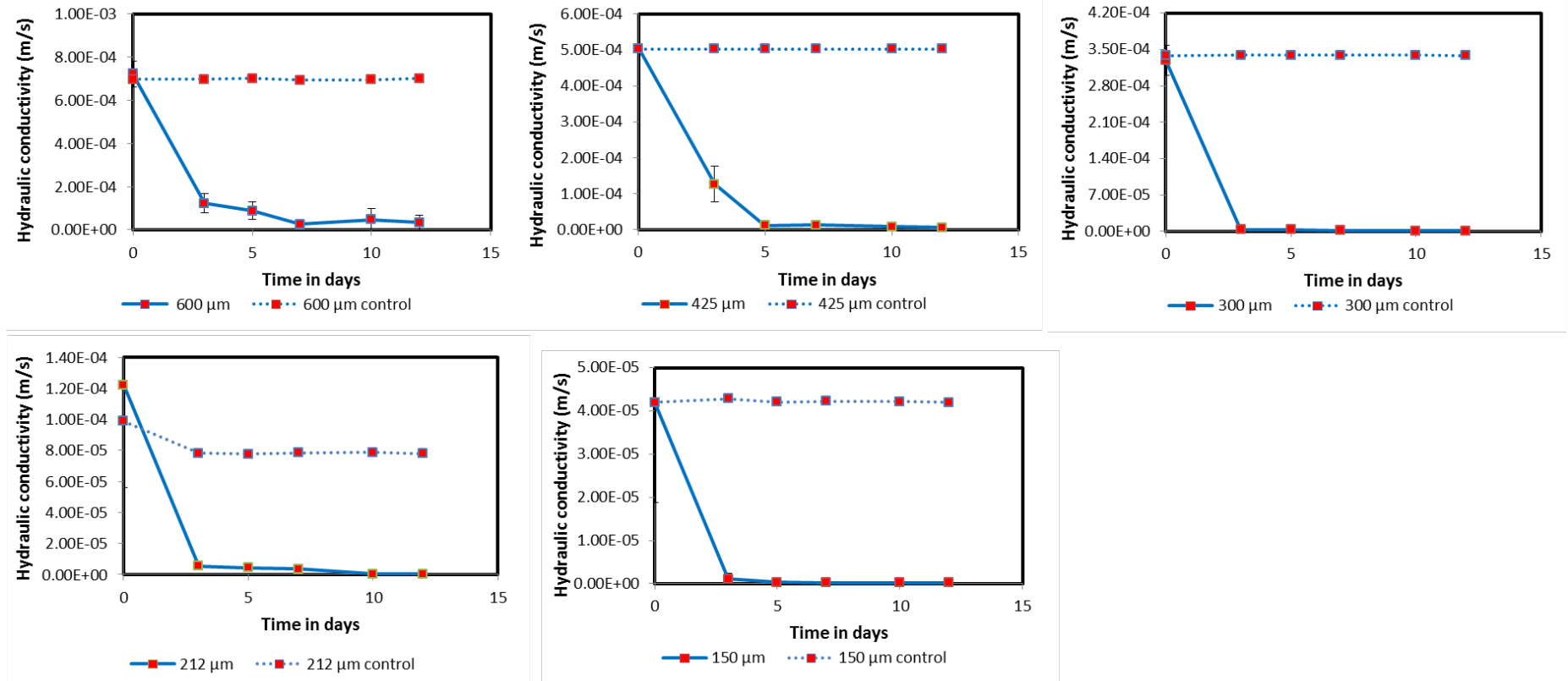


**Figure 4.5: The changes of hydraulic conductivity with time due to the growth of *B. indica* for five sand fractions ranging from 150-1180 μm in normal scale at laboratory temperature.**

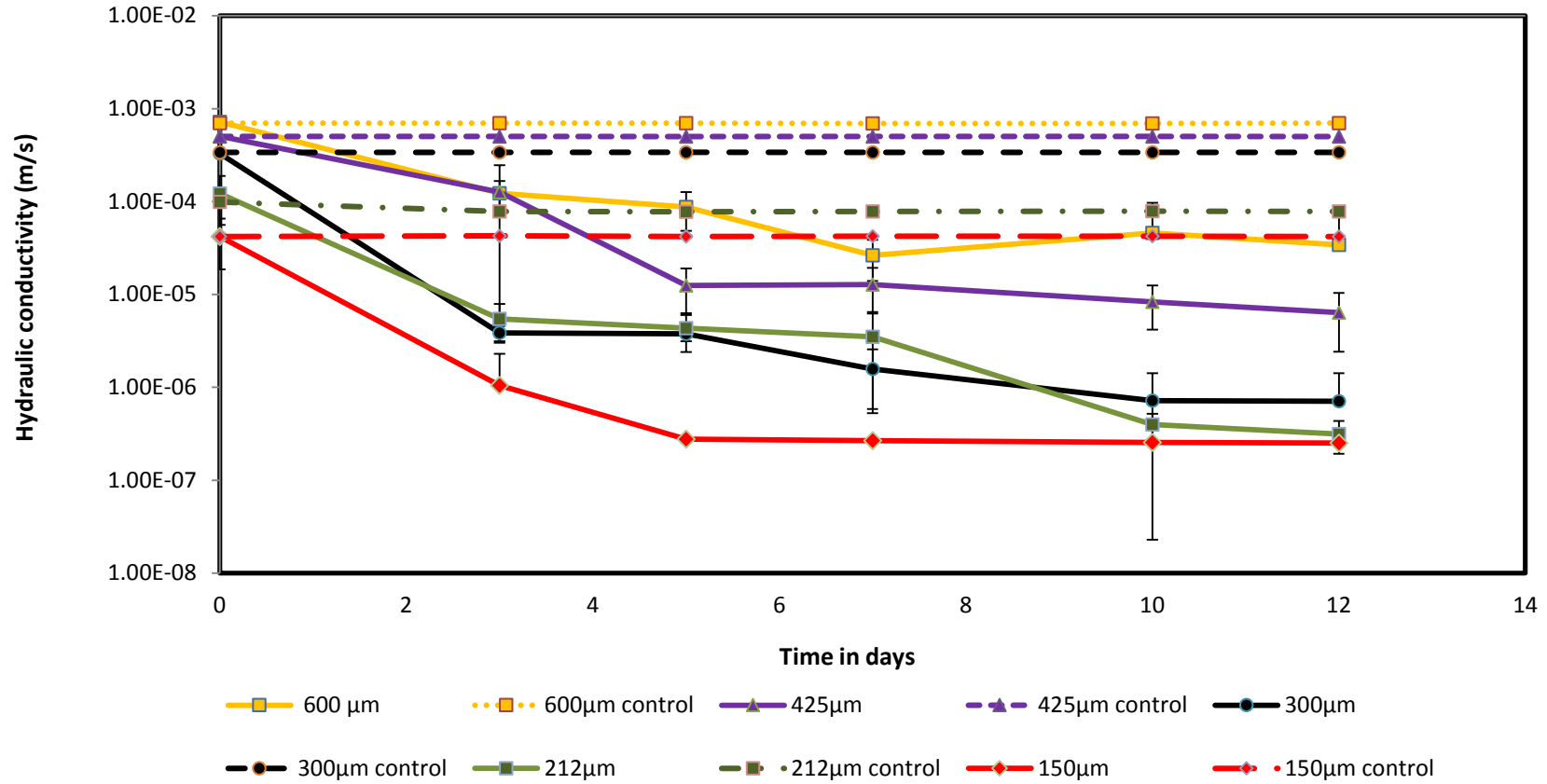
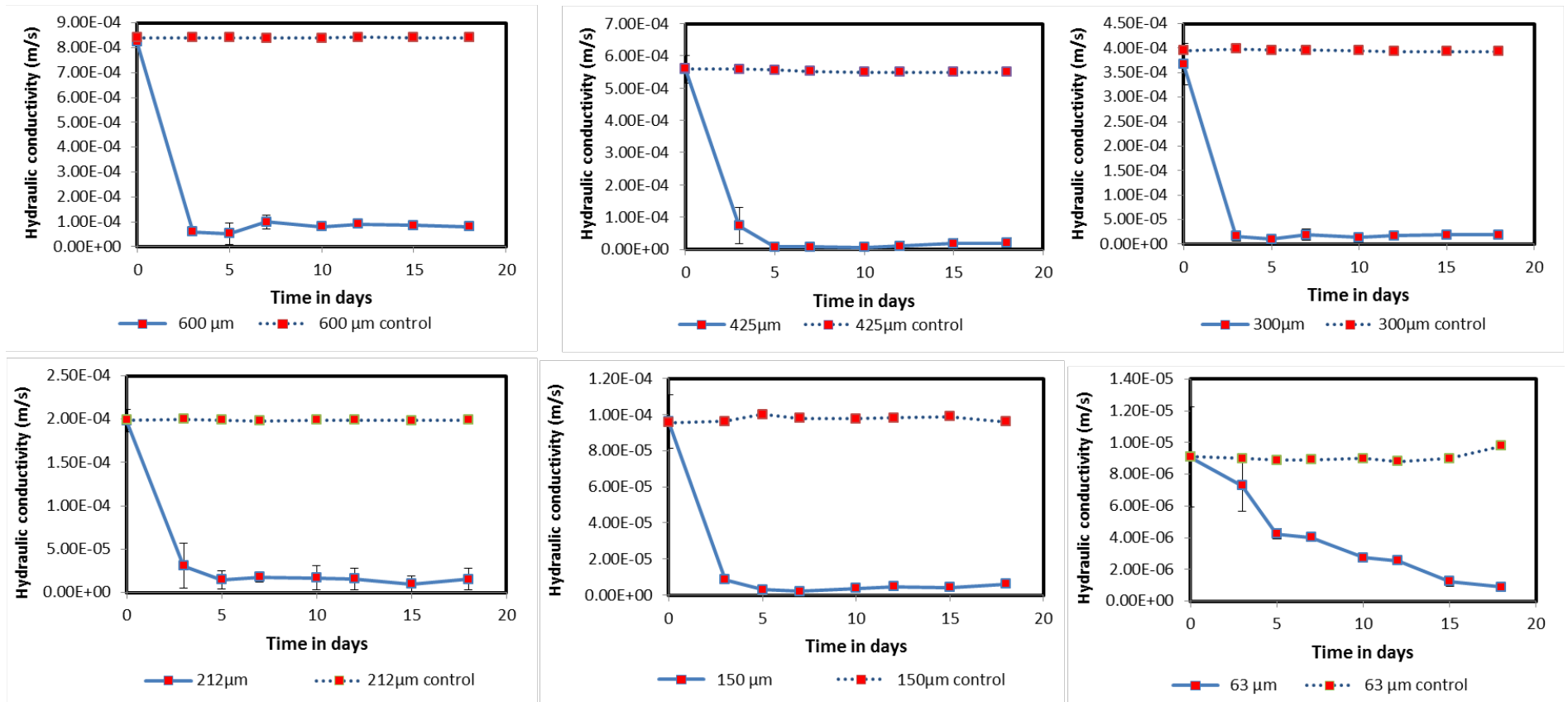


Figure 4.6: Changes of hydraulic conductivity with time due to growth of *B. indica* at 12-22°C for five sand fractions ranging from 150-1180 μm in logarithmic scale, error bars represent standard deviation of the measured hydraulic conductivity values.

In order to eliminate the potential temperature effects, sand column experiments for six sand fractions ranging from 63 to 1180  $\mu\text{m}$  were performed at constant temperature of 25°C.

During the first five days of the first four experiments, the results showed that the hydraulic conductivity decreased sharply by 92.0-98.0 % for the 150-600  $\mu\text{m}$  sand fractions, then continued to go down steadily until the end of the experiment. Whereas, for the 63  $\mu\text{m}$  sand fraction, the hydraulic conductivity continues to decrease gradually throughout the last experiment by 90.0 % as shown in logarithmic based Figures 4.7 and linear based Figure 4.8.

This different trend in the last experiment may have occurred because of the small pore volume of the fine grain size of sand 63  $\mu\text{m}$  which could be the reason behind the bacterial growth. These results agree with the results of Jenneman *et al.* (1984), Torbati *et al.* (1986), and Cunningham *et al.* (1991) who all reported that microorganisms prefer to plug large pores first.



**Figure 4.7: Changes of hydraulic conductivity with time due to the growth of *B. indica* for six sand fractions ranging from 63-1180 μm in normal scale at 25°C.**

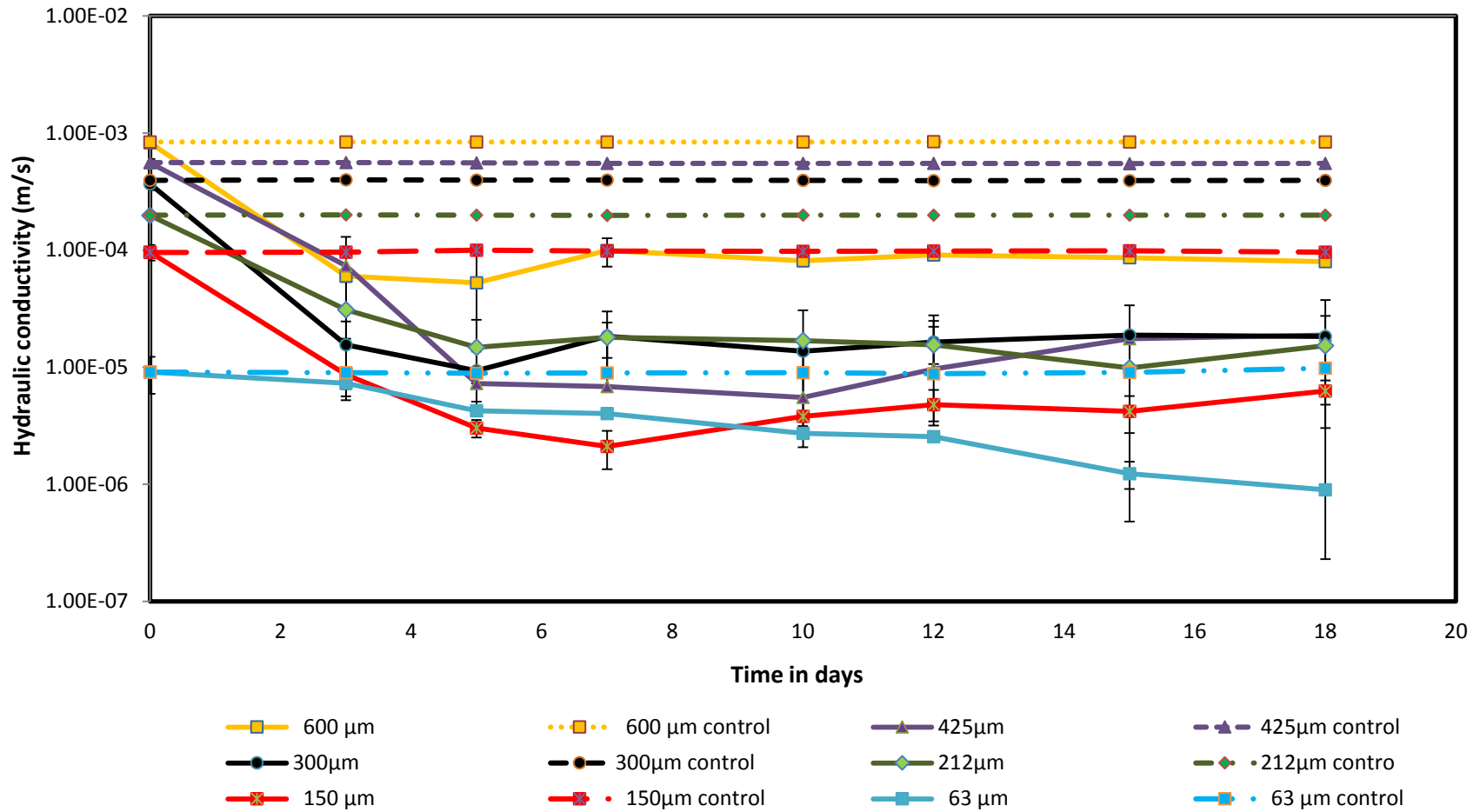
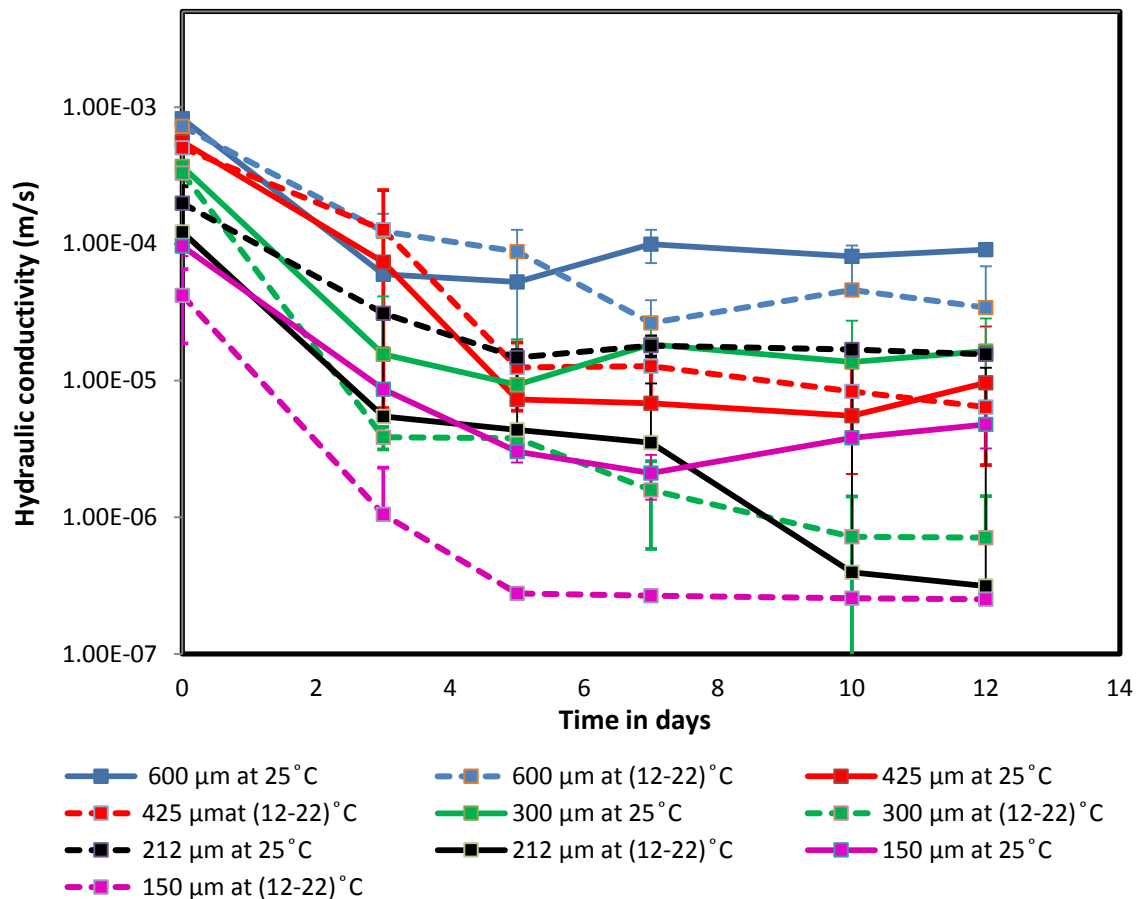


Figure 4.8: Changes of hydraulic conductivity with time due to growth of *B. indica* at 25°C for six sand fractions ranging from 63-1180 μm at logarithmic scale, error bars represent standard deviation of the measured hydraulic conductivity values.

By comparing the experiments conducted under laboratory temperature 12-22°C for five sand fractions with those conducted under the constant temperature 25°C for six sand fractions as shown in Figure 4.9, it can be noticed that after three days of the nutrients feeding the hydraulic conductivity in both experiments was decreased significantly up to 74.0 % for all sand fractions.



**Figure 4.9: Change in the hydraulic conductivity values with time at 25°C and 12-22°C.**

Also by comparing the hydraulic conductivity values of the standard hydraulic test with the initial values which were measured with by using *B. indica* and *P. putida*, it can be detected that the measured values of the hydraulic conductivity are smaller than the measured values with the standard test. The reason for the differing hydraulic conductivity values in the soil tests than those recorded in the sand column experiments may be due to the different flow values, cross sectional area in both cases

## **4.2 Chemical and biological tests**

As mentioned in the previous chapter that the hydraulic conductivity reduction is not enough to prove that the decline has occurred due to the accumulation of biomass so more chemical and biological tests need to be performed to confirm this.

The analysis included loss on ignition which can generally be regarded as an accurate measure of the organic matter content of a sediment (Dean Jr, 1974), and the DAPI staining method which used to estimate the total number of bacteria.

### **4.2.1 Total number of cells**

Figure 4.10 shows the distribution of the total number of bacteria throughout each sand column for the experiments performed at 25°C. By the end of each sand column experiment soil samples were collected from three locations (top, middle, and bottom) of each column, where the top layer is the nearest to the inlet. Figure 4.11 shows the average of the total number of cells for each sand fraction of the experiment running under constant temperature. The initial number of bacteria, which was mixed with sand, was ranging from  $1.53 \times 10^6$  to  $1.66 \times 10^6$  cells/gram of soil. By the end of the experiment these figures increased in all the sand fractions to an average, ranging from  $1.09 \times 10^7$  to  $1.68 \times 10^7$  cells/ gram of soil for all sand fractions.

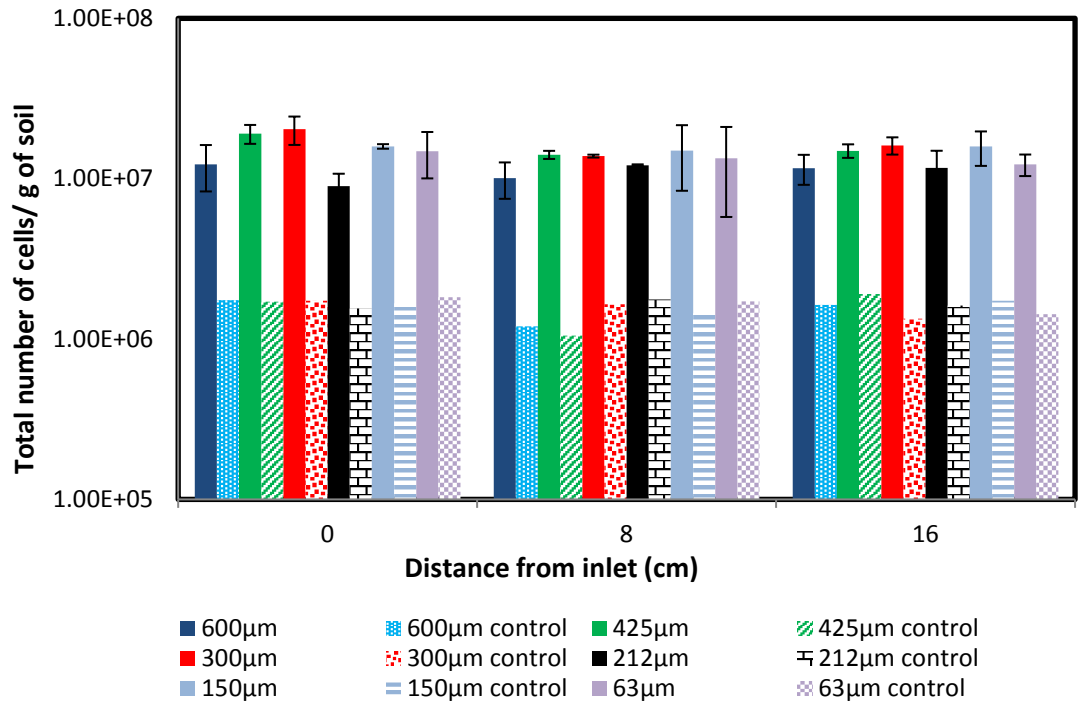


**Figure 4.10: Comparison between total numbers of cells per gram of soil in control and biological conditions for six sand fractions at 25°C at logarithmic scale, error bars represent standard deviation of the total number of cells, data collected by the end of the each sand column experiment.**

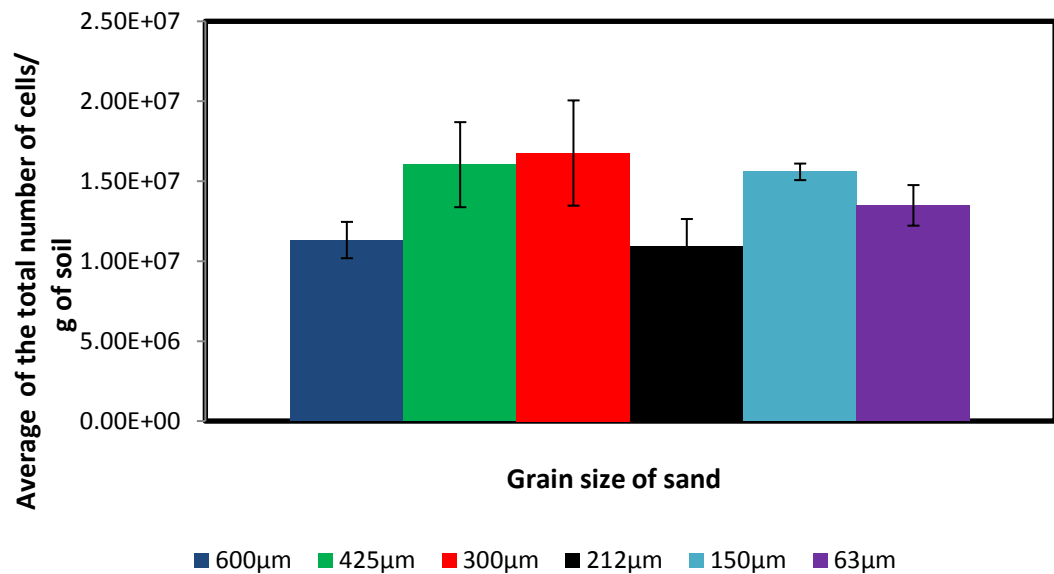
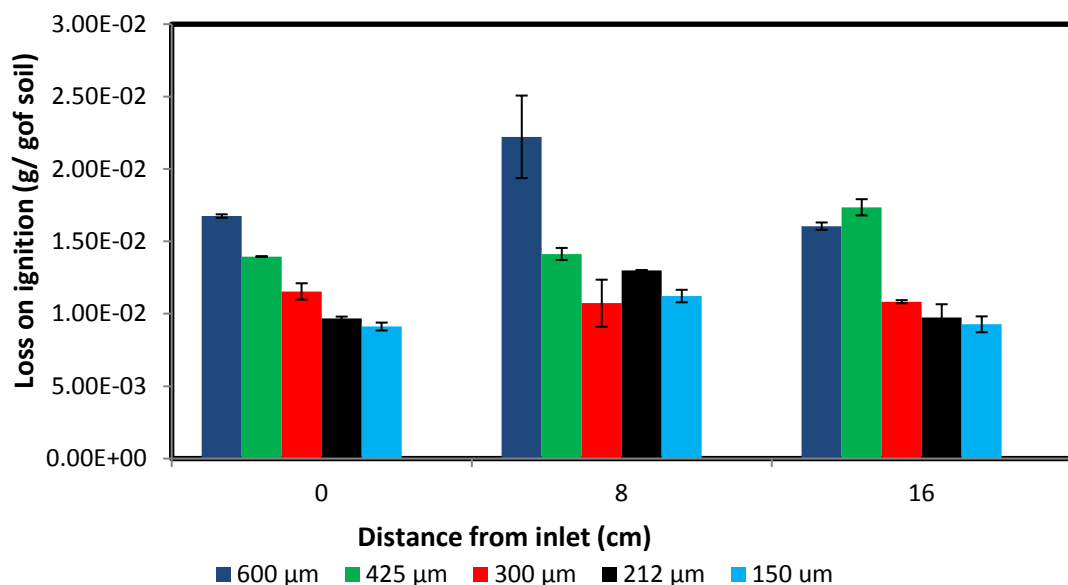


**Figure 4.11: The average of the total numbers of cells per gram under the biological conditions (live *B. indica*) for six different sand fractions at 25°C, error bars represent standard deviation of the average of the total cells numbers, the data collected the end of sand column experiment.**

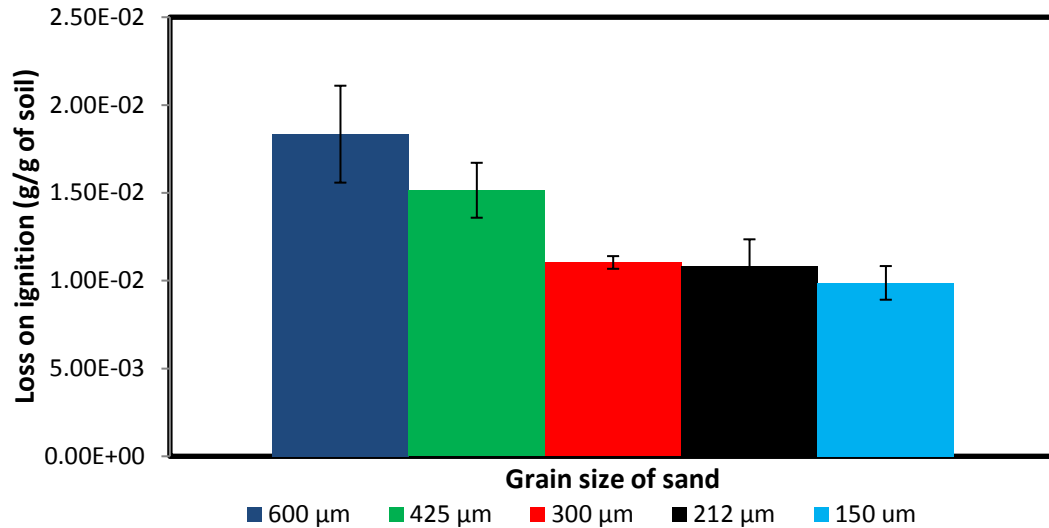
#### 4.2.2 Loss on ignition analysis

Figure 4.12 shows the biomass distribution in each sand fraction after running the experiment for 12 days. In this figure it can be detected that the biomass amount distributed uniformly through each sand column. Also Figure 4.13 shows that the largest sand fraction has the greater amount of biomass.

By comparing the average amount of volatile solid concentrations in each sand fraction, it can be shown that the biomass amount changes directly with the sand fractions, and the greatest loss on ignition of 1.83 % of the total soil dry mass was obtained with the largest sand fraction of 600  $\mu\text{m}$ , whereas loss on ignition of 0.98 % of the total soil dry mass was obtained with the finest sand fraction of 150  $\mu\text{m}$  as shown in Figure 4.13.



**Figure 4.12: Loss on ignition due to *B. indica* growth at 12-22°C for five sand fractions, error bars represent standard deviation of the measured loss on ignition values at the end of sand column experiment.**



**Figure 4.13: Relation between the average loss on ignition due to *B. indica* growth and grain size, error bars represent the standard deviation of the measured loss on ignition values at the end of sand column experiment which carried out at 12-22°C.**

The same trend was identified in the sand column experiment which performed at 25°C as seen in Figures 4.14, 4.15 and 4.16. These results showed that the largest grain size had the greatest amount of biomass, and this matches with the results of Cunningham *et al.* (1991), who related the biofilm thickness with the porous media pore space confirmed that the biofilm thickness increases with the increase of porous media pore space, and also with the results of Bielefeldt *et al.* (2002), who observed that more biomass accumulated in the pores of the larger grain sand.

Regarding the biomass distribution, the results show that the biomass distributed uniformly which agree with the results of Cunningham *et al.* (1991) who reported that the biomass was distributed homogeneously throughout each sand column. Whereas, Thullner *et al.* (2002) reported that the biomass was mainly located in a growth zone. The differences between the results of the current study and the study of Thullner *et al.* (2002) could be attributed to the experimental set-up.

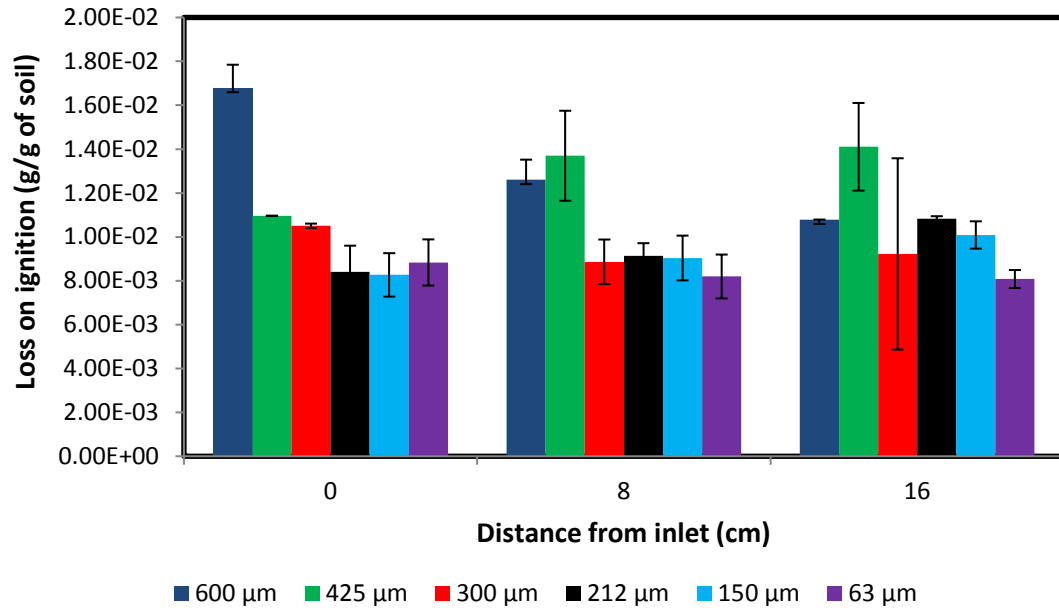


**Figure 4.14:** Loss on ignition due to *B. indica* growth at 25°C for six sand fractions ranging from 63 to 1180 μm, error bars represent standard deviation of the measured loss on ignition values at the end of sand column experiment.

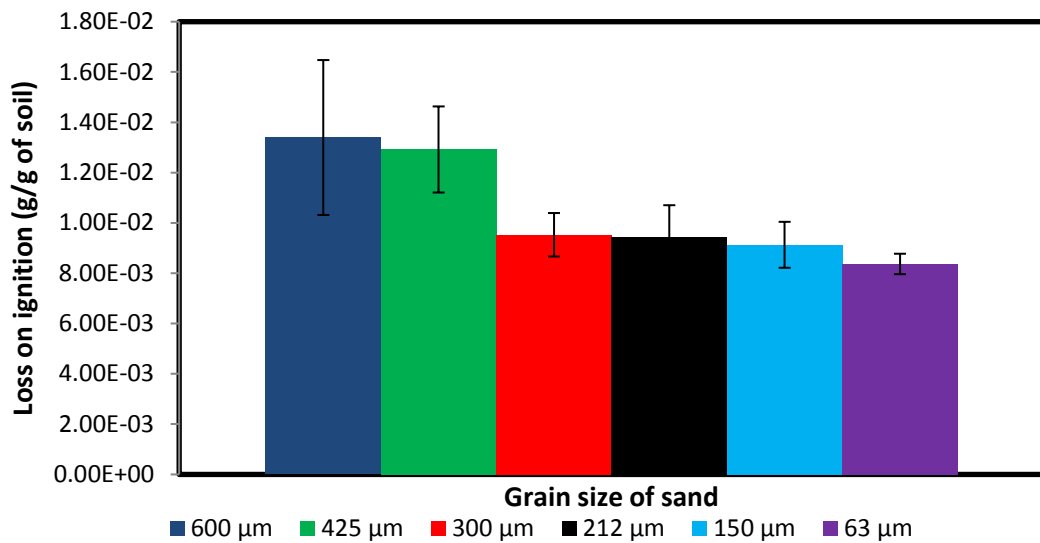


**Figure 4.15:** Relation between the average loss on ignition due to *B. indica* growth and grain size, error bars represent the standard deviation of the measured loss on ignition values at the end of sand column experiment which carried out at 25°C.

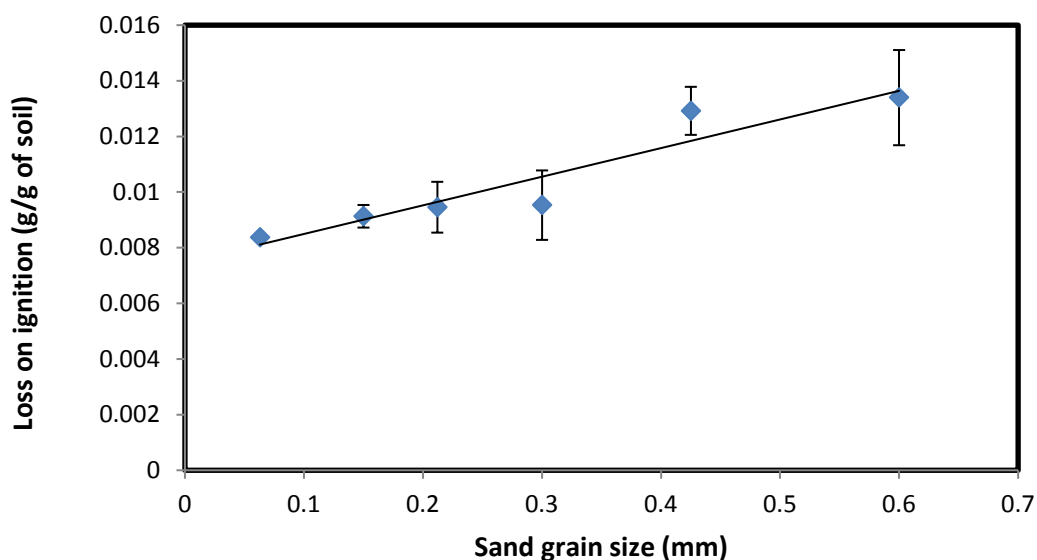


**Figure 4.16:** The relation between the average loss on ignition and sand grain size on the actual x-axis, error bars represent the standard deviation of the measured loss on ignition values at the end of sand column experiment which carried out at 25°C.

### 4.3 Overall discussion

The results of both batch and continuous flow experiments using *P. putida* mt-2, showed that the concentrations of nutrients had a great effect on EPS production and the highest amount of EPS was observed at 30.0 g l<sup>-1</sup> and 2.0 g l<sup>-1</sup> of glucose and ammonium sulphate respectively. The results were confirmed when *P. putida* mt-2 was mixed with porous media to investigate the ability of this strain to form biofilm using different culture media.

The results of the sand column experiment as presented in Figure 4.1 indicate that the most significant reduction of hydraulic conductivity of porous media due to the growth of *P. putida* mt-2 was observed when 30.0 g l<sup>-1</sup> of glucose and 2.0 g l<sup>-1</sup> of ammonium sulphate concentrations were used as carbon and nitrogen sources, whereas less

reduction in hydraulic conductivity of porous media was detected when lower concentrations of glucose and ammonium sulphate were used.

This reduction of hydraulic conductivity could be attributed to the accumulation of biomass, which increased by increasing nutrient concentrations. These results correspond with the results of Characklis and Marshall (1990) and Stoodley *et al.* (1999) who all concluded that the biofilm accumulation increases with the increase of carbon concentration, and also agree with the results of Rochex and Lebeault (2007) who correlated maximum biofilm production rate with nitrogen and glucose concentrations.

The optimum culture medium for *P. putida* mt-2 was chosen to use in the sand column experiment which were performed to examine the effect of flow rate on the growth of this strain. The results shown in Figure 4.2 indicate that the growth of *P. putida* mt-2 reduce the hydraulic conductivity significantly at the low flow rate 1.5 ml min<sup>-1</sup>, whereas no significant reduction was detected at the higher flow rates 2.5 and 5.0 ml min<sup>-1</sup>. In contrast, the same experiment which performed using *B. indica* detected much more reduction of hydraulic conductivity exceeded 90.0 % at all flow rates.

By comparing the results from different culture media experiment as presented in Figure 4.1 and that from the flow rate experiment as shown in Figure 4.2, it can be noticed that the hydraulic conductivity almost decreased by a similar rate due to the growth of *P. putida* mt-2 in the 600 µm sand fraction with a flow rate of 5.0 ml min<sup>-1</sup>. The data from the flow rate experiments also indicate that the effect of flow rate on bacterial growth is a very complicated process as shown in Figure 4.16 which represents the changes in the hydraulic conductivity of porous media with time using three different flow rates and two bacterial strains. The key points that can be observed in Figure 4.17 is a significant decrease in hydraulic conductivity of all flow rates as a

result of the growth of *B. indica*, in contrast a different trend was detected with *P. putida* mt-2. The high flow rate of  $5.0 \text{ ml min}^{-1}$  reduced the hydraulic conductivity by only 37.0%, whereas a significant reduction of hydraulic conductivity of 80.0 % was detected at the low flow rate of  $1.5 \text{ ml min}^{-1}$ , by the end of the experiment. This different trend for both bacterial strains could be attributed to the ability of each strain to form biofilm at different flow rates.

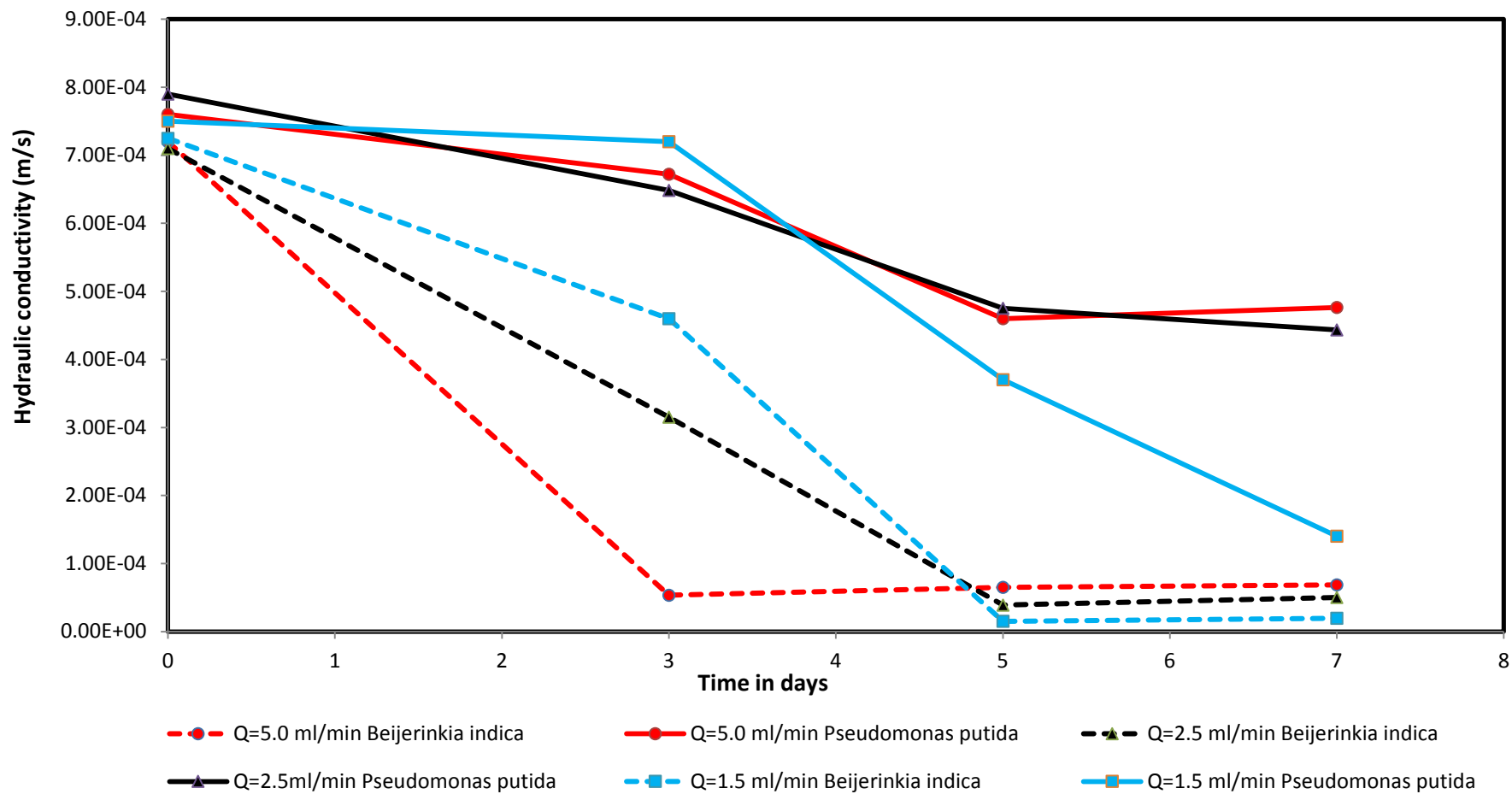


Figure 4.17: The flow rate effect on the growth of *P. putida* mt-2 and *B. indica*.

The grain size effect on bioclogging was studied using three different sand fractions ranging from 212  $\mu\text{m}$  to 1180  $\mu\text{m}$  in the sand column experiment. The results of this experiment as displayed in Figure 4.4 denoted that the reduction of the hydraulic conductivity with *P. putida* was maximised at the highest levels of glucose and ammonium phosphate tested, but was still at a much lower level than that produced by *B. indica*. The latter was therefore used for subsequent experiments.

As for the sand column experiments which were performed with the use of *B. indica* under a varied range of temperature 12-22°C, five sand fractions ranging from 150-1180 microns in size were selected as a porous medium to study the potential effect of temperature on the biological growth with using different sand fractions.

The results shown in Figure 4.6 depicts that a significant reduction of hydraulic conductivity occurred by the end of the experiments due to the growth of *B. indica* in all five sand fractions. The results gave an indication that the temperature between 12-25°C has no important effect on the growth of *B. indica*, and this outcome coincides with the results of Kennedy (2005) who reported that the temperature range for the growth of *Beijerinckia* species from 10 to 35°C and the optimum growth temperature is 25°C.

In order to eliminate any potential temperature effect on the growth of *B. indica* in porous media and to cover a wide range of sand fractions, sand column experiments were performed at constant temperature 25°C using six sand fractions ranging from 63-1180 $\mu\text{m}$ .

The results in Figure 4.8 show that the hydraulic conductivity dropped significantly by 90.0 % for all sand fractions at the end of the experiments. That could be attributed to the ability of *B. indica* to produce a large amount of EPS. Nevertheless, the

hydraulic conductivity values remained constant or unchanged compared to the initial values for the control columns (dead cells).

In order to compare the effect of grain size on the hydraulic conductivity through using *P. putida* mt-2 and *B. indica*, three sand fractions 600, 300, and 212  $\mu\text{m}$  were chosen. Figure 4.18 illustrates the changes of the hydraulic conductivity for these sand fractions due to the growth of both bacterial strains in lab temperature. This figure shows that after 12 days of the growth of *B. indica*, the hydraulic conductivity values dropped significantly by 88.0-95.0 % for all the three sand fractions, but less figures was recorded with *P. putida* mt-2. This different behaviour could be attributed to the accumulation of the large amount of biomass due to the growth of *B. indica* compared to *P. putida* mt-2.

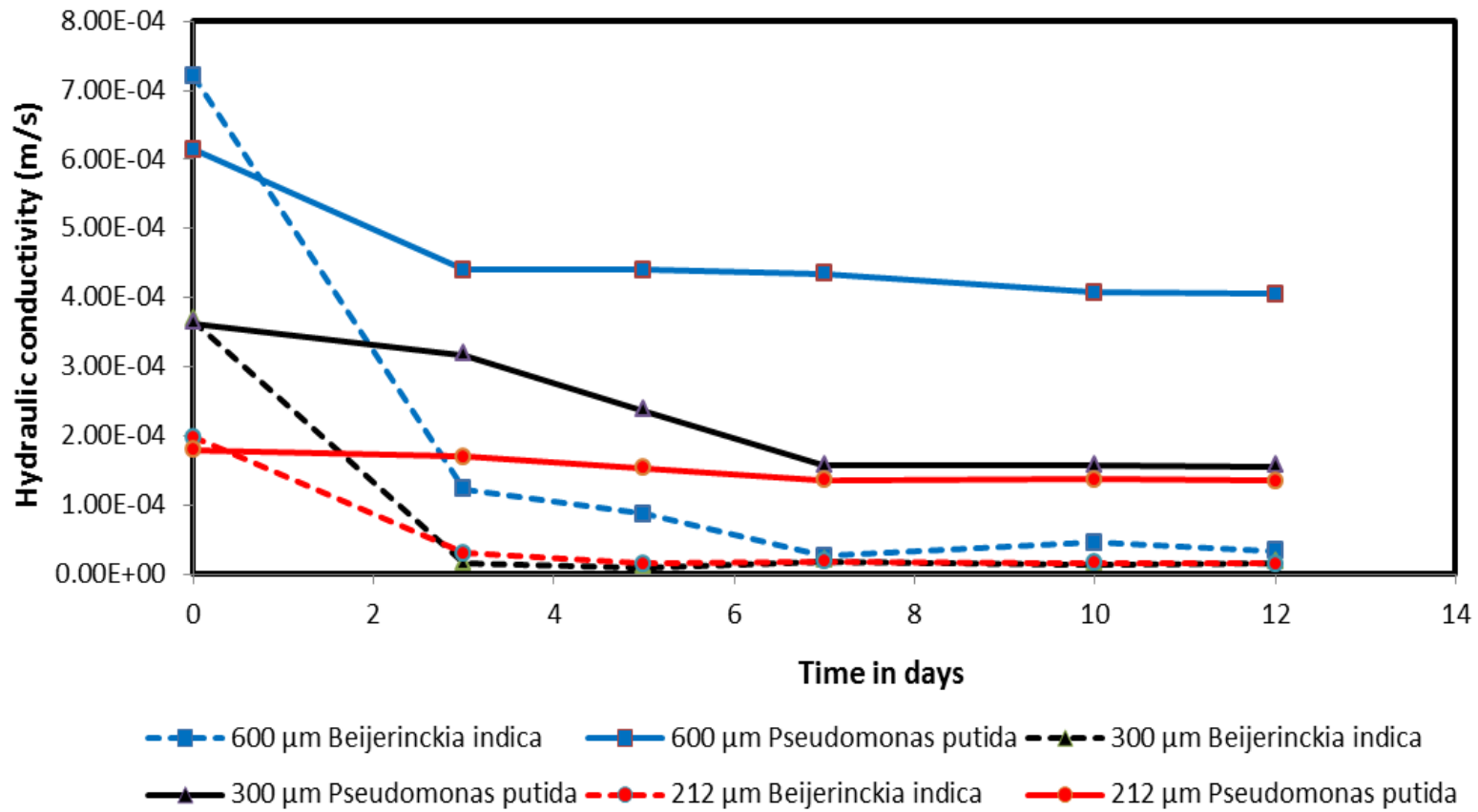


Figure 4.18: The effect of grain size on hydraulic permeability due to the growth of *P. putida* mt-2 and *B. indica* for three sand fractions.

In order to make sure that the reduction of hydraulic conductivity was caused by the accumulation of biomass, loss on ignition and total numbers of bacteria were estimated by the end of each sand column homogenous experiment.

The results of the loss on ignition for the sand column experiments indicated that the large sand fraction has the great amount of biomass (Figure 4.15); this could be attributed to the preferential growth of bacteria in the large pore. Also, the large pore was conduct larger quantities of nutrients due to lower resistance of flow (Torbaty *et al.*, 1986). Whilst, the average of the total cells number has no correlation with the grain size (Figure 4.11), which suggest that the reduction of the hydraulic conductivity occurs due to the biomass accumulation.

In terms the reduction of hydraulic conductivity with time for the six sand fractions, it can be observed that after only three days, the hydraulic conductivity decreased significantly by 85.0-95.0 % for all sand fractions, but for the 63  $\mu\text{m}$  sand fraction the hydraulic conductivity decreased by 19.0 % of the initial values. This lag in reduction of the hydraulic conductivity could be attributed to the large surface area of this fine sand fraction (63  $\mu\text{m}$ ) which needs more biofilm to form and clog the pore volume. Another potential reason is the less amount of biomass in this sand fraction compared to other sand fractions, as suggested in the previously it may be the presence of more preferential flow paths in the fine sand fraction could led to a lower chance of bacteria growth, and thus less biomass production. Nevertheless, the reduction of the hydraulic conductivity of all sand fractions went down by more than 90.0 % by the end of the experiment due to the accumulation of biomass. Despite the fact that the largest sand fraction has the greater amount of biomass, but there was no big difference in the relative hydraulic conductivity for all sand fractions by the end of the experiment. The relative

hydraulic conductivity can be defined as the final hydraulic conductivity value divided by the initial of the hydraulic conductivity value.

In a similar study, Taylor and Jaffe (1990) reported that the relative hydraulic conductivity is correlated with biomass amount of less than  $0.4 \text{ mg cm}^{-3}$ , and for more than  $0.4 \text{ mg cm}^{-3}$ , the relative hydraulic conductivity became independent. The results of this study are slightly different to the above study as shown in Figure 4.19 that correlated the relative hydraulic conductivity as a function of loss on ignition. In this figure it can be noticed that the relative hydraulic conductivity decreased with the loss on ignition increasing for five sand fractions (B-F).

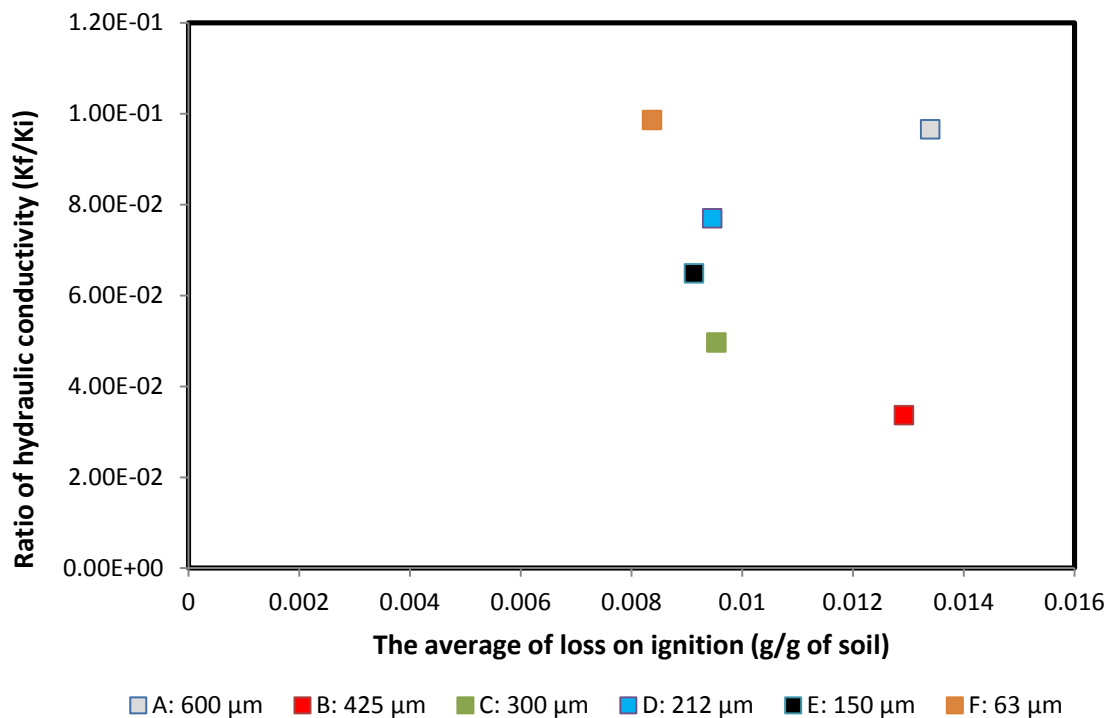


**Figure 4.19:** The relation between the average of the loss on ignition and relative hydraulic conductivity due to the growth of *B. indica* at  $25^\circ\text{C}$  for five sand fractions.

## **RESULTS AND DISCUSSION OF BIOLOGGING EXPERIMENTS IN HETEROGENEOUS POROUS MEDIA**

### **5.1 Experimental results**

In this chapter, *B. indica* was selected to study the effect of bacterial growth on the hydraulic conductivity of heterogeneous porous media. For the heterogeneous porous media six sand fractions ranging from 63 to 1180  $\mu\text{m}$  were chosen as described in section 3.2. From these six sand fractions, five sets of experiments were performed. The way these five experiments were selected is discussed in chapter three. The experiment set-up is described in section 3.6.1. The same experiments were repeated in the presence and absence of *B. indica* 3.6.3 to investigate the heavy metals removal with the use of one set of sand fraction as presented in section 3.6.3.1.

### **5.2 Grain size effect**

In general, the results of five experiments that were running for seventeen days showed that the hydraulic conductivity values decreased considerably in the more permeable sand fractions, there appears to be an increased lag with smaller grain sizes, then the final values end up being quite similar.

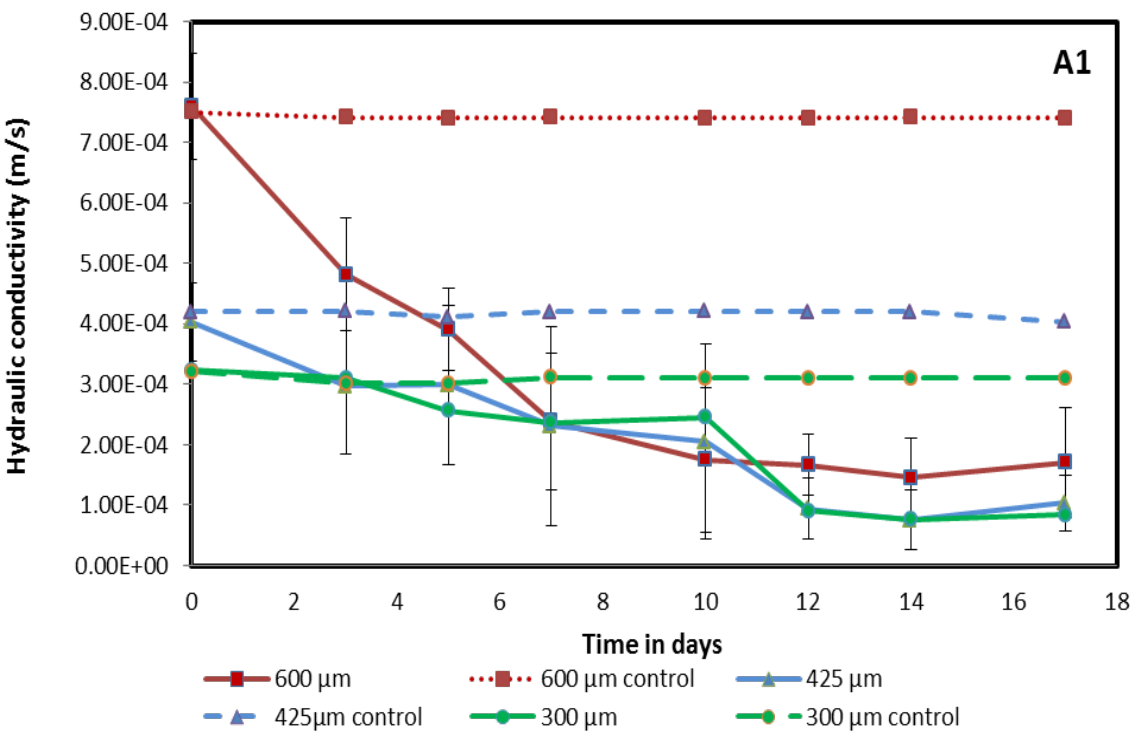
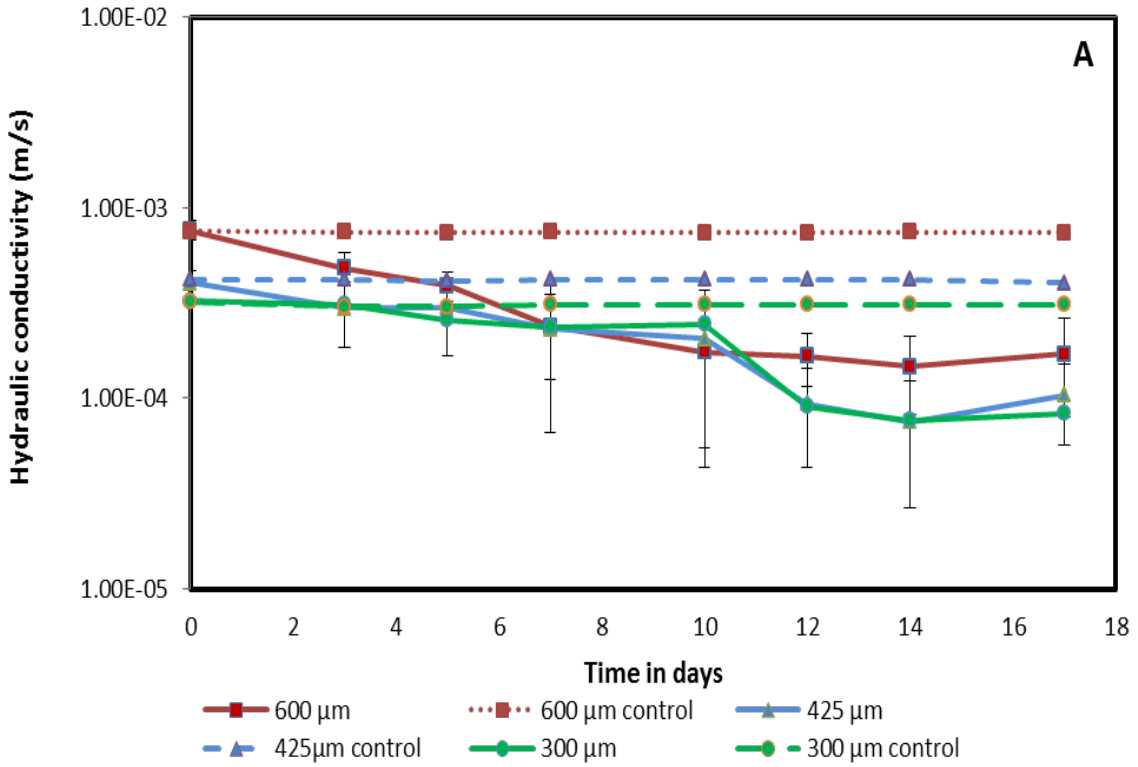
Figures 5.1A and 5.1A1 show the changes in hydraulic conductivity with time due to the growth of *B. indica* at 25°C in logarithmic and normal scales for the first experiment EXP.(1).

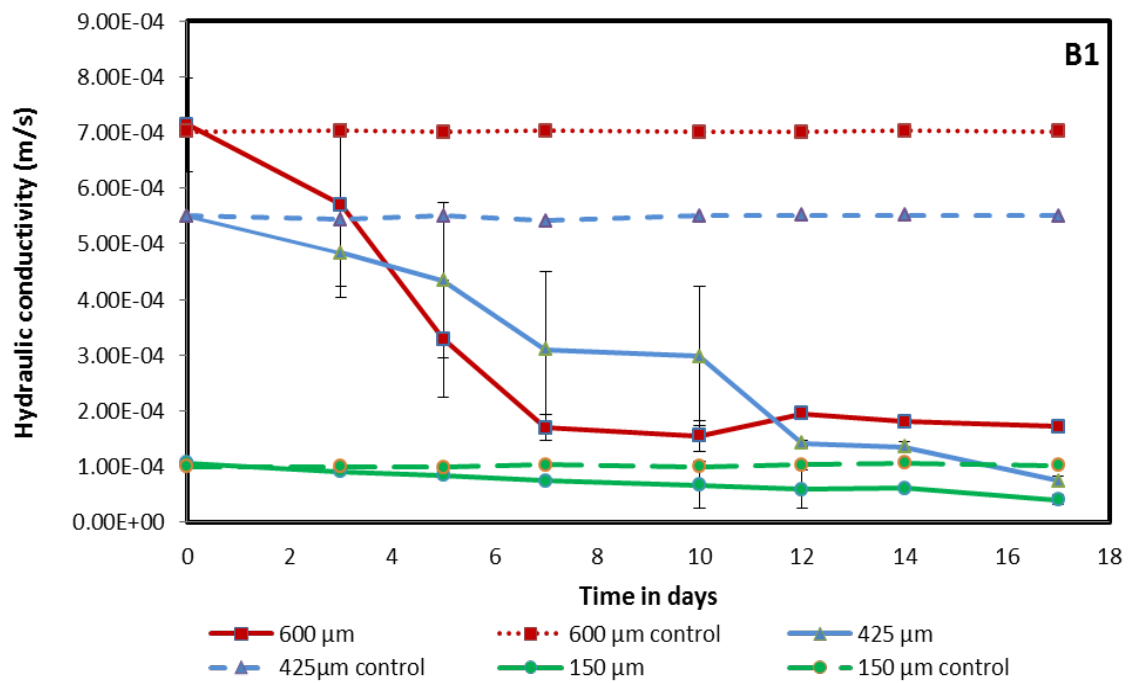
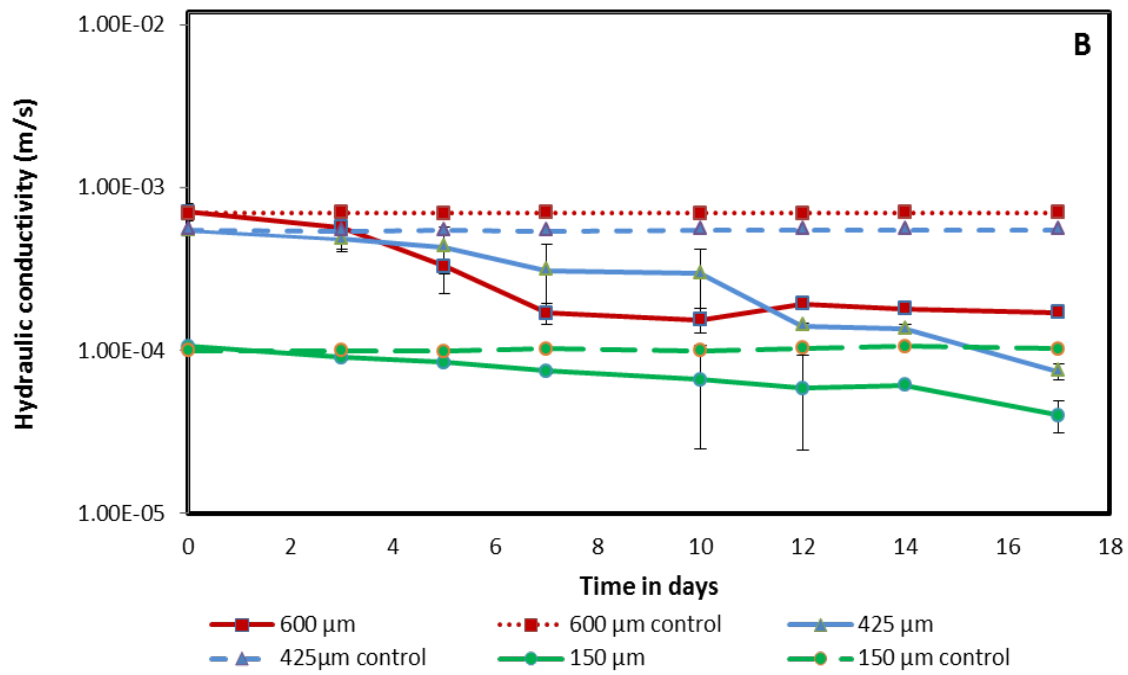
The important points to make are that the initial rate of permeability reduction decreases significantly with grain size for all sand fractions, there appears to be an increased lag with smaller grain sizes (425 and 300  $\mu\text{m}$ ), and the three curves end up being quite similar,

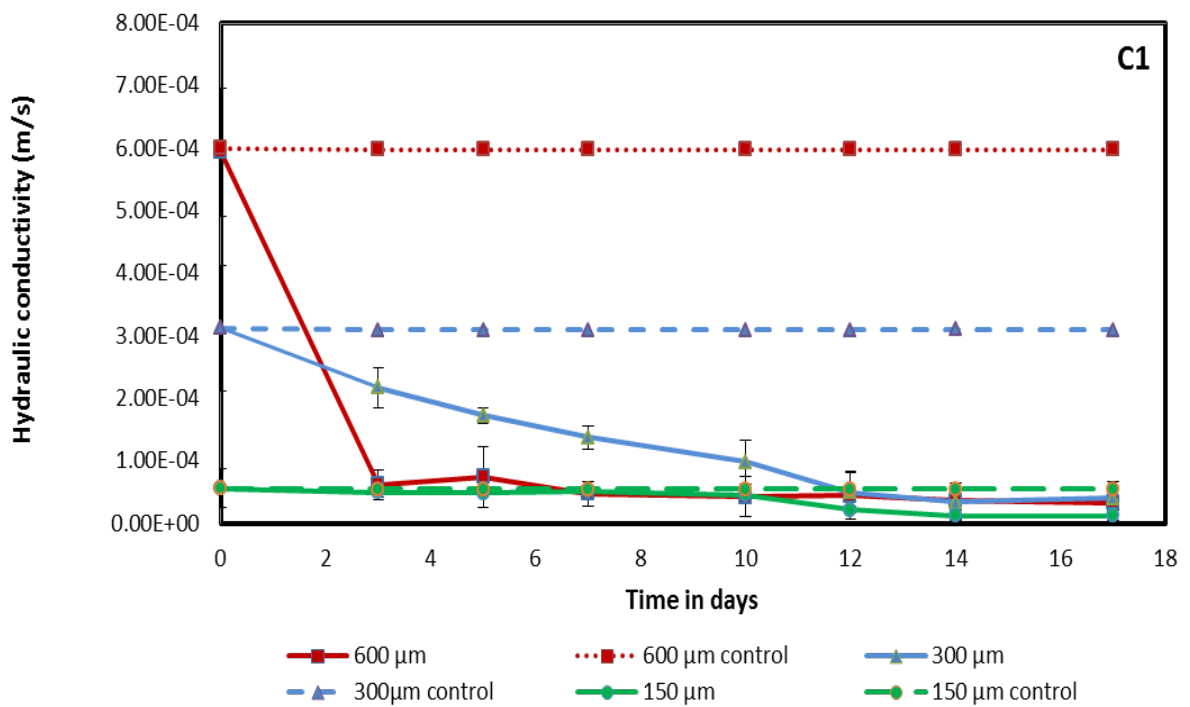
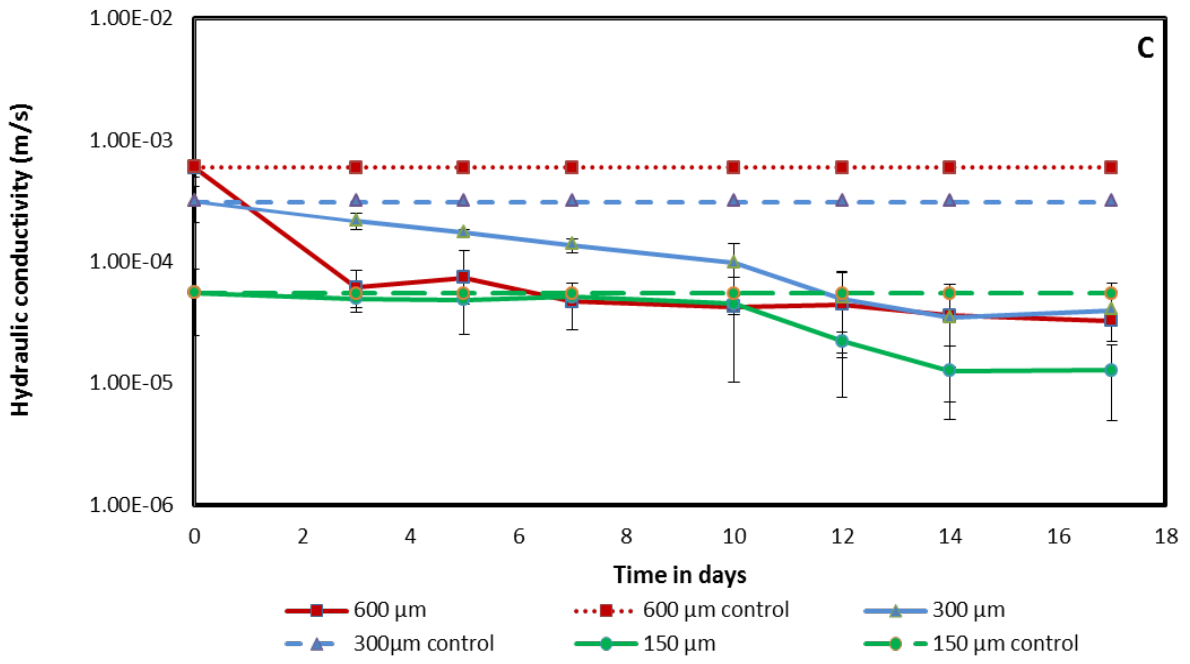
suggesting that there has been a degree of equilibration between the three fractions. As for the control columns, there were no detectable changes in the hydraulic conductivity values with time for all sand fractions. By comparing the results of the EXP.(1) to the second experiment EXP.(2), the results as shown in Figures 5.1B and 5.1B1 indicate that the rate of the hydraulic conductivity reduction also decrease with the grain size, and with the continued nutrients feeding the three sand fractions reached the equilibrium state to end with quite similar values. Regarding the third experiment EXP.(3), the results as presented in Figures 5.1C and 5.1C1 showed that there was an early clogging in the large sand fraction compared to the previous experiments, whereas the other less permeable sand fractions 300 and 150 microns experienced a less rate of reduction than the large sand fractions 600 microns. However, the three curves also end with quite similar values. The results of the fourth experiment EXP.(4) as shown in Figures 5.1D and 5.1D1 showed that the hydraulic conductivity of the 600 and 212 microns decreased by a similar rate, whereas there was there was no significant reduction of hydraulic conductivity in the least permeable sand fraction 150  $\mu\text{m}$  in the first 3 days, however with continuous feeding the three sand fractions achieved relatively similar values by the end of the experiment. Once more, for the control sand columns there was no change in the hydraulic conductivity values with time. Finally, the results of the last experiment EXP.(5) as shown in Figure 5.1E and 5.1E1 slightly revealed different trend for experiments that preceded it. In this experiment, and after three days of nutrients delivery the hydraulic conductivity of the 212  $\mu\text{m}$  sand fraction decreased by 0.16 % of its initial value, while there was no substantial change for the 150 and 63 $\mu\text{m}$  sand fractions.

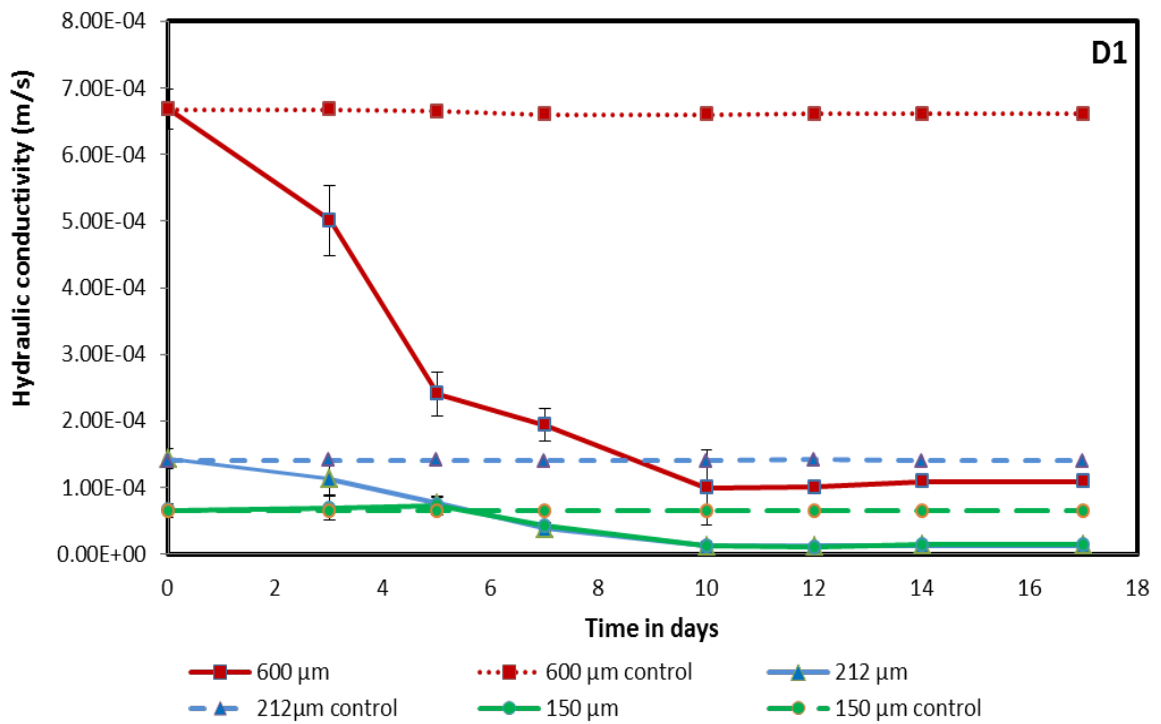
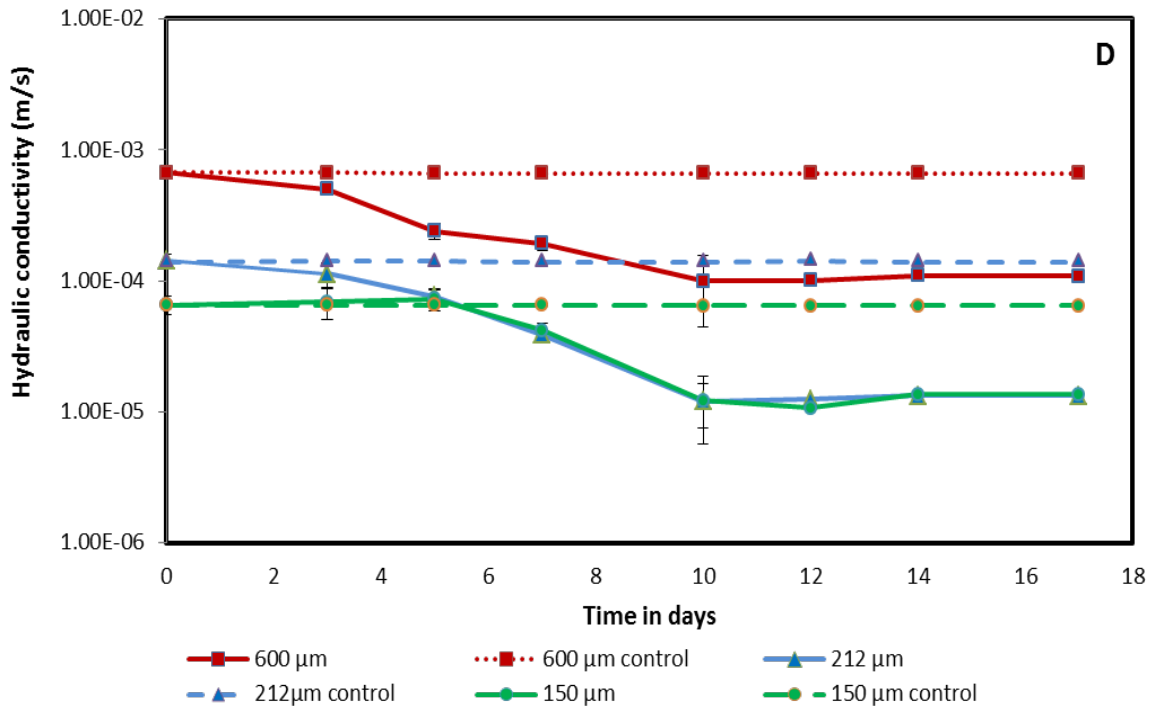
The reduction of the hydraulic conductivity for the 212  $\mu\text{m}$  after three days is very small comparing to the previous experiments that achieved a reduction of hydraulic conductivity up to 90.0 % of the initial value.

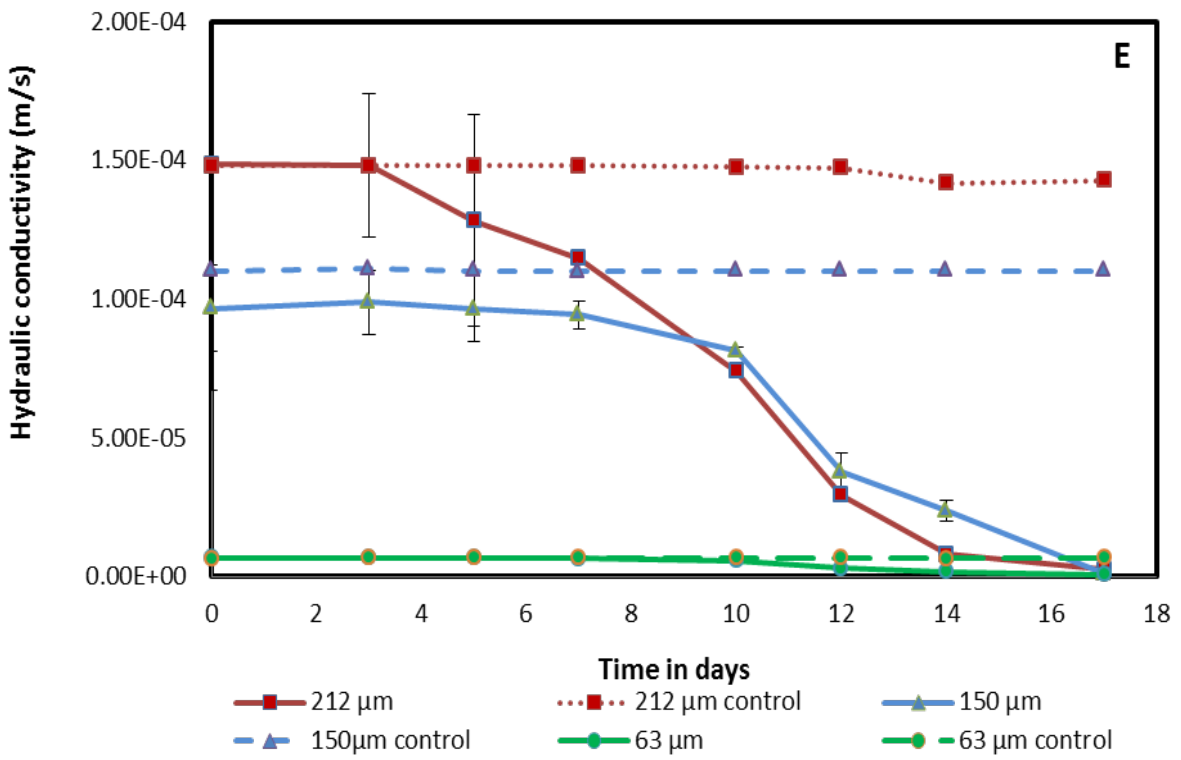
By the tenth day, the hydraulic conductivity dropped by half in the 212  $\mu\text{m}$ , whereas it decreased by only 14.0% of its initial values in the other sand fractions 150 and 63  $\mu\text{m}$ . By the end of this experiment, the reduction in the hydraulic conductivity was 98.0 % in the 212 and 150  $\mu\text{m}$ , and 88.0 % in the 63  $\mu\text{m}$ . Again, the control columns did not reveal any significant changes in the hydraulic conductivity.











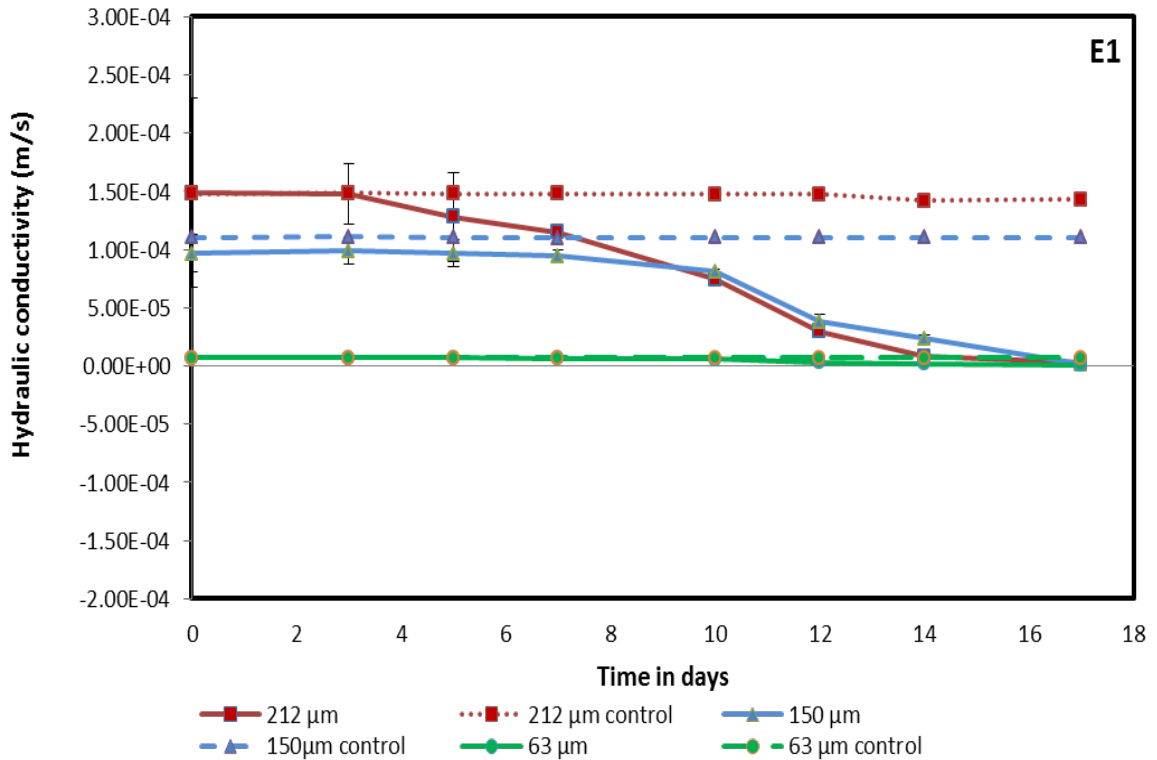


**Figure 5.1: Changes in the hydraulic conductivity with time due to the growth of *B. indica* for five experiments using different sand fractions, A and A1 logarithmic and normal scale for EXP.(1), 5.1B and 5.1B1 for EXP.(2), C and C1 for EXP.(3), D and D1 for EXP.(4), and E and E1 for EXP.(5), error bars represent the standard deviation of the measured hydraulic conductivity value.**

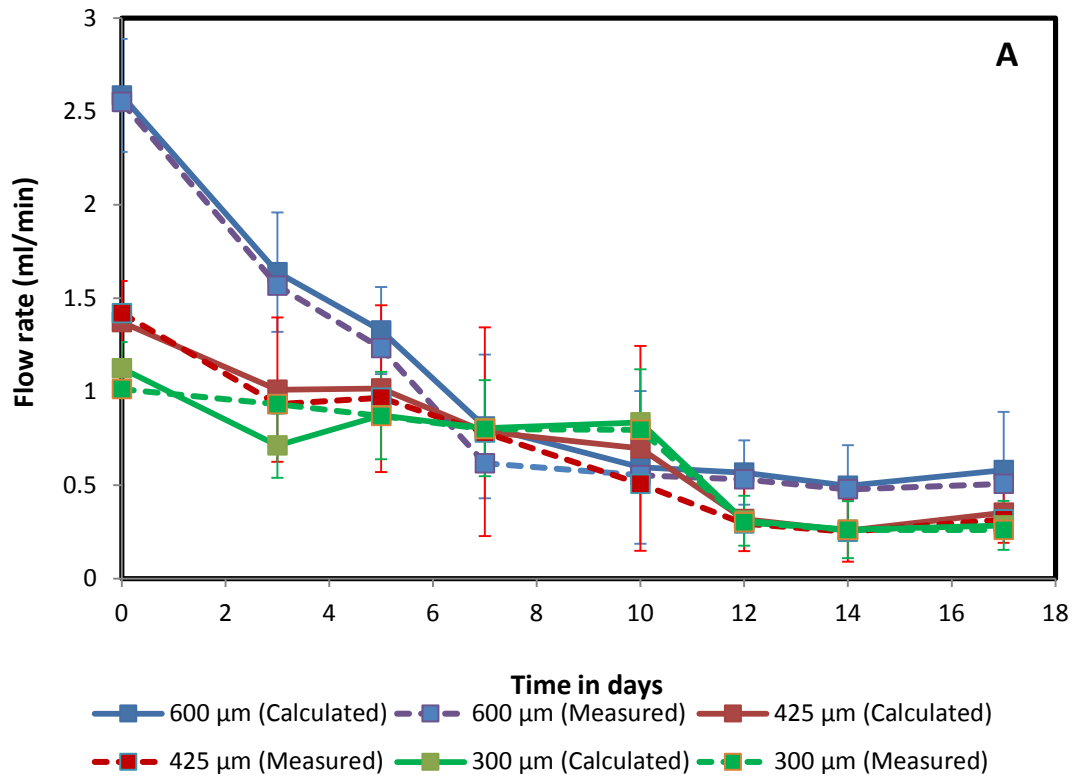
In order to understand the bioclogging process in heterogeneous porous media, and to investigate how the bioclogging process affect the flow rate in each set of experiment, the flow rate was calculated then compared with the measured flow rate as shown in Figure 5.2A-E. The flow rate for each sand fraction was calculated by assuming that the peristaltic pump applies a constant head. Based on the initial hydraulic conductivity reading and the initial measured flow rates for each sand fraction, the hydraulic gradient was calculated. Subsequently, by applying Darcy's law, the hydraulic gradient value for

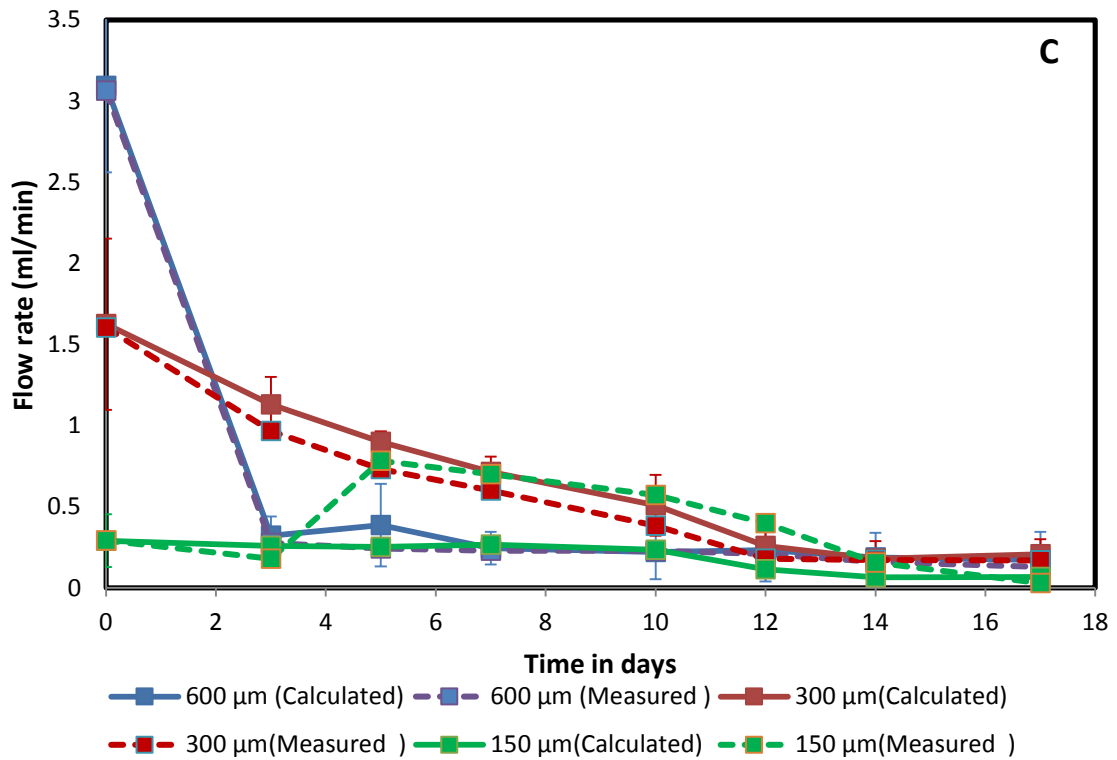
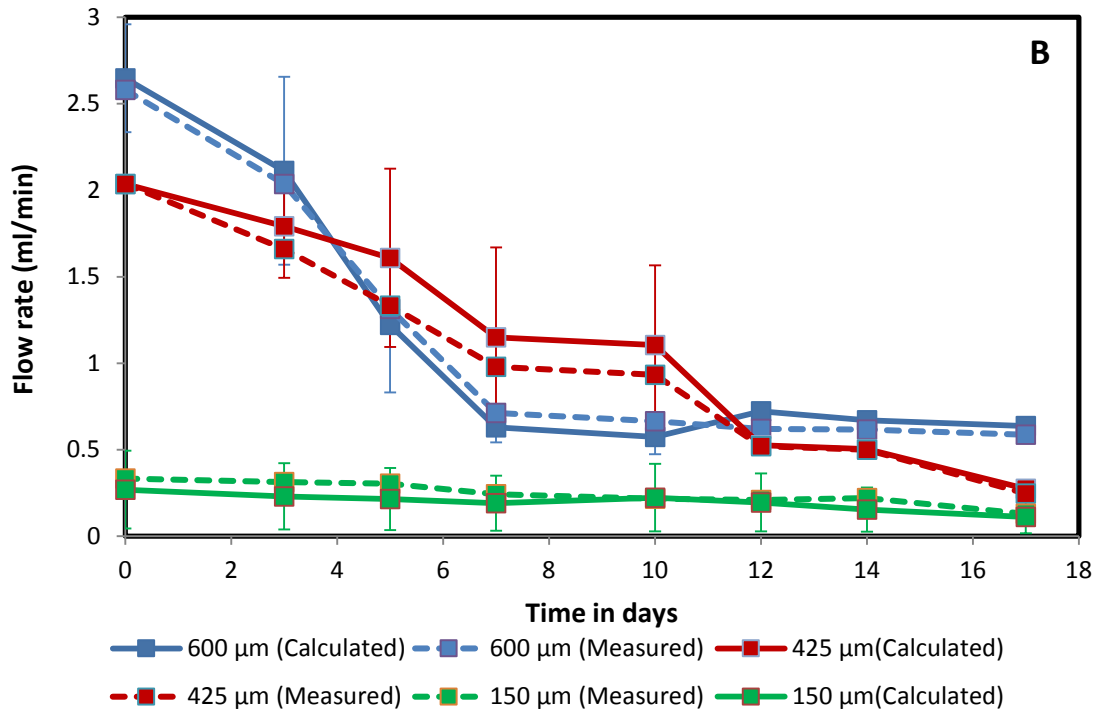
each set of the experiment was used to calculate the flow rate by using the measured hydraulic conductivity values.

Overall the first four figures (Figure 5.2A-D) depict a relatively similar pattern showing a significant decrease of the flow rate with time compared to the initial values with the exception of the latter figure (Figure 5.2E) which shows a delay of the flow rate decrease. Moreover, the measured flow rate values for the five experiments are consistent with the calculated values which are calculated by assuming a constant head.

Regarding the first heterogeneous experiment EXP. (1), almost 51.0 % of the initial total flow rates were delivered into the 600  $\mu\text{m}$  sand fraction, and 28.0 % of the total initial flows were delivered into the 425  $\mu\text{m}$  sand fractions, whereas only 20.0 % went to the 300  $\mu\text{m}$  sand fraction. Figure 5.2A reveals that the total flow rate decreases significantly up to 76.0 % by the end of the experiment. This reduction in flow rate could be attributed to the bacterial growth and the relevant accumulation of biomass in the pore volumes in each sand fraction. The same trend was detected in the second experiment which included the use of three sand fractions 600, 425, and 150  $\mu\text{m}$ ; 52.0 % of the total flow rate were delivered to the large grain size 600  $\mu\text{m}$  and 40.0 % of total flow rate were delivered to the 425  $\mu\text{m}$ , while the 150  $\mu\text{m}$  received only 8.0 % of the total flow rate as presented in Figure 5.2B. Subsequently, the total flow rate profile for the third experiment shows a slightly sharp decrease as shown in Figure 5.2C compared to the previous experiments. Moreover, the fourth heterogeneous experiment once again shows that the total flow rate decrease by the same rate of the former two experiments EXP.(1) and EXP.(2) as presented in Figure 5.2D. On the contrary, the total flow rate of the last experiment as

shown in Figure 5.2E experienced a delay during the first 3 days, but the final values decreased significantly.





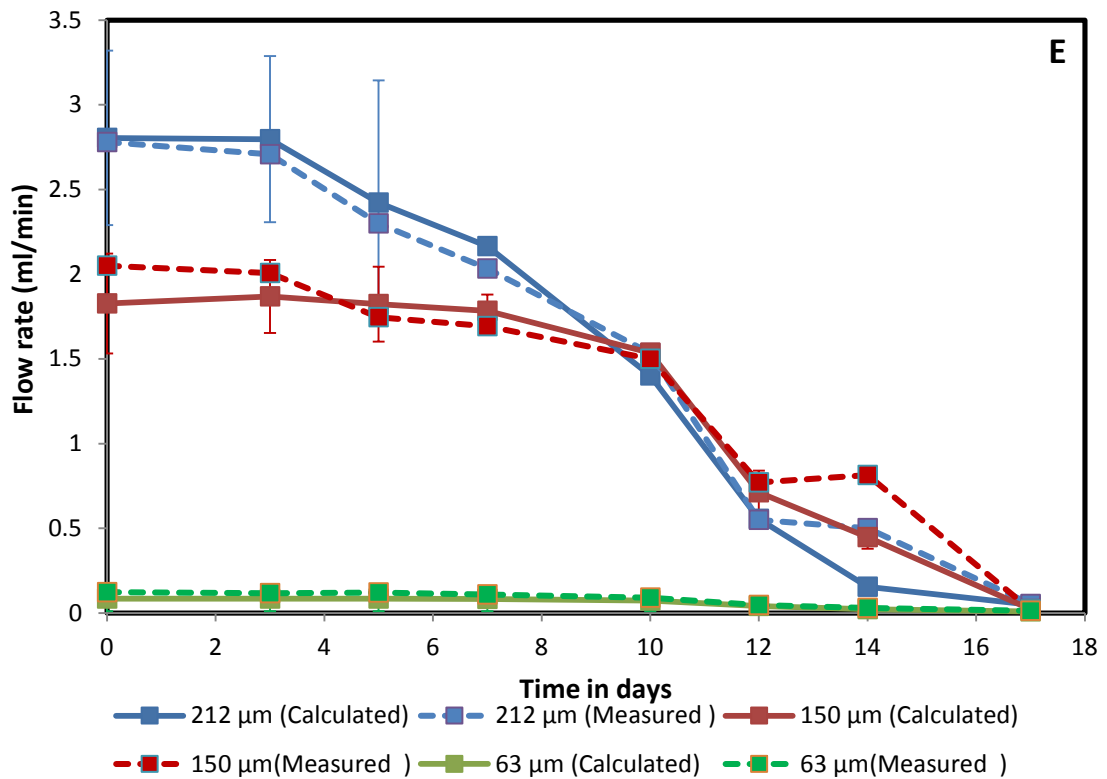
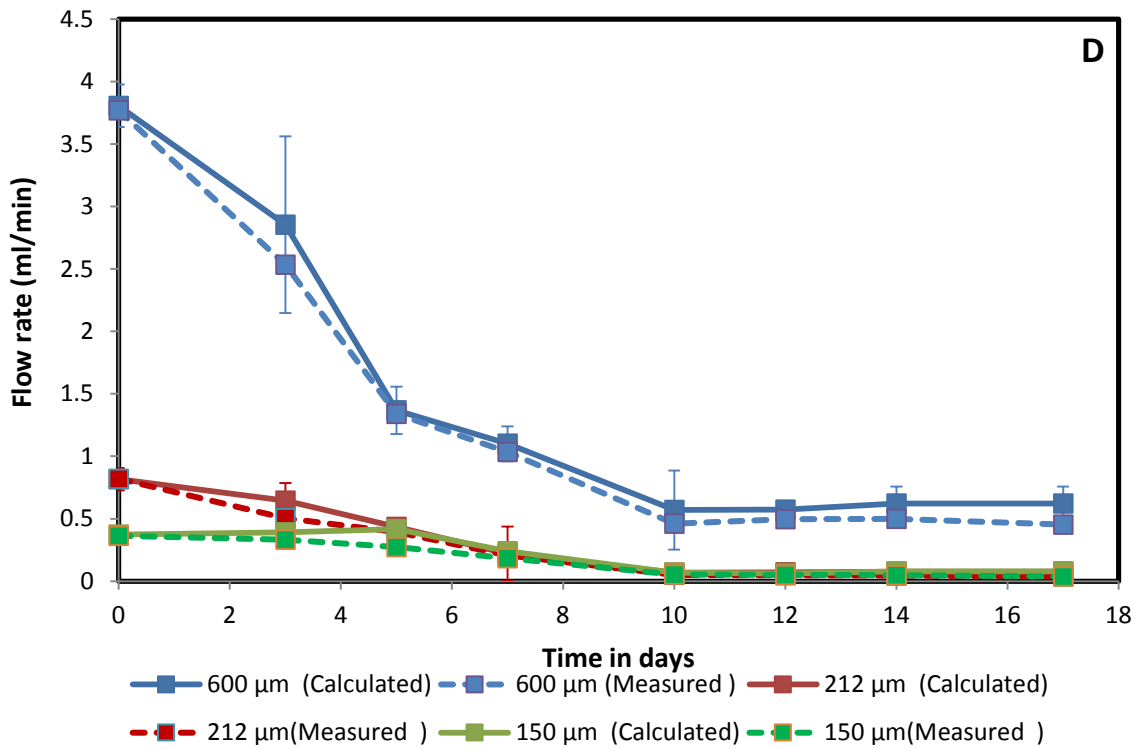


**Figure 5.2: Flow rate profile for all heterogeneous experiments(A:EXP(1), B:EXP(2), C:EXP(3), D:EXP(4), and E:EXP(5), error bars represent the standard deviation of the measured and calculated flow rates for different sand fractions.**

### **5.3 Loss on ignition analysis**

After dismantling the heterogeneous bioclogging experiments, soil samples were collected from three locations of each sand column (top, medium and bottom); each sample was about 16.0 cm<sup>3</sup> in volume to estimate the loss on ignition for each sand column. Figures 5.3A-E shows the loss on ignition for the three sand fractions in each heterogeneous experiment.

In general, the results of this test as shown in Figures 5.3A-E and 5.4A-E indicate that the larger grain sand has the greatest amount of biomass, whereas the small sand fraction has the least amount of biomass, and the loss on ignition values distributed in a homogeneous way through each sand column.

For the first experiment EXP.(1), however the homogeneous distribution of biomass amount through each sand column as shown in Figure 5.3A, it can be observed that the amount of biomass varies with the grain size of sand. The 600 µm sand fraction has the greater amount of biomass (1.19 % of the soil dry mass), and the 300 µm fraction has the least amount of biomass (0.65 % of the soil dry mass) as shown in Figure 5.4A.

For the second experiment EXP.(2), the results as shown in Figures 5.3B and 5.4B show that the 600 µm fractions have the greater amount of biomass about (1.19 % of the soil dry mass), whereas the 150 µm fraction has the least amount of biomass about (0.69 % of the soil dry mass).

The calculated loss on ignition values for the third heterogeneous experiment EXP.(3) as shown in Figure 5.4C indicate that the biomass amount for the 600 µm is (1.64 %

of the soil dry mass); this value is greater than the corresponding loss on ignition values for the 300 and 150  $\mu\text{m}$  sand fractions.

For the fourth heterogeneous experiment EXP.(4), the loss on ignition values indicate that the 600  $\mu\text{m}$  sand fraction has about 1.3 % of the soil dry mass, whereas only 0.8 % of the soil dry mass was detected in the 150  $\mu\text{m}$  sand fraction as seen in Figure 5.4D. Finally, the results of the last heterogeneous experiment EXP.(5) as shown in Figure 5.4E reveal that the 212 $\mu\text{m}$  has a biomass amount about 1.43 % of soil dry mass; whereas the least amount of biomass 1.0 % are detected in the 63  $\mu\text{m}$ .

The overall all results of loss on ignition of the five heterogeneous experiments agree with the results of Cunningham *et al.* (1991) and Bielefeldt *et al.* (2002). Cunningham *et al.* (1991) observed that more biomass grew in columns packed with larger size media, with 10  $\mu\text{m}$  biofilm thicknesses on 0.12 mm diameter glass beads versus 37  $\mu\text{m}$  biofilm thickness on 0.5 mm sand or glass beads. Bielefeldt *et al.* (2002) found that when sand grains from the columns were viewed under a microscope, a large variability in the biofilm thickness was evident on the individual sand grains at the microscale. Some areas contained thick biomass while other areas were virtually free of biomass and the largest grain size has the greater amount of biomass.

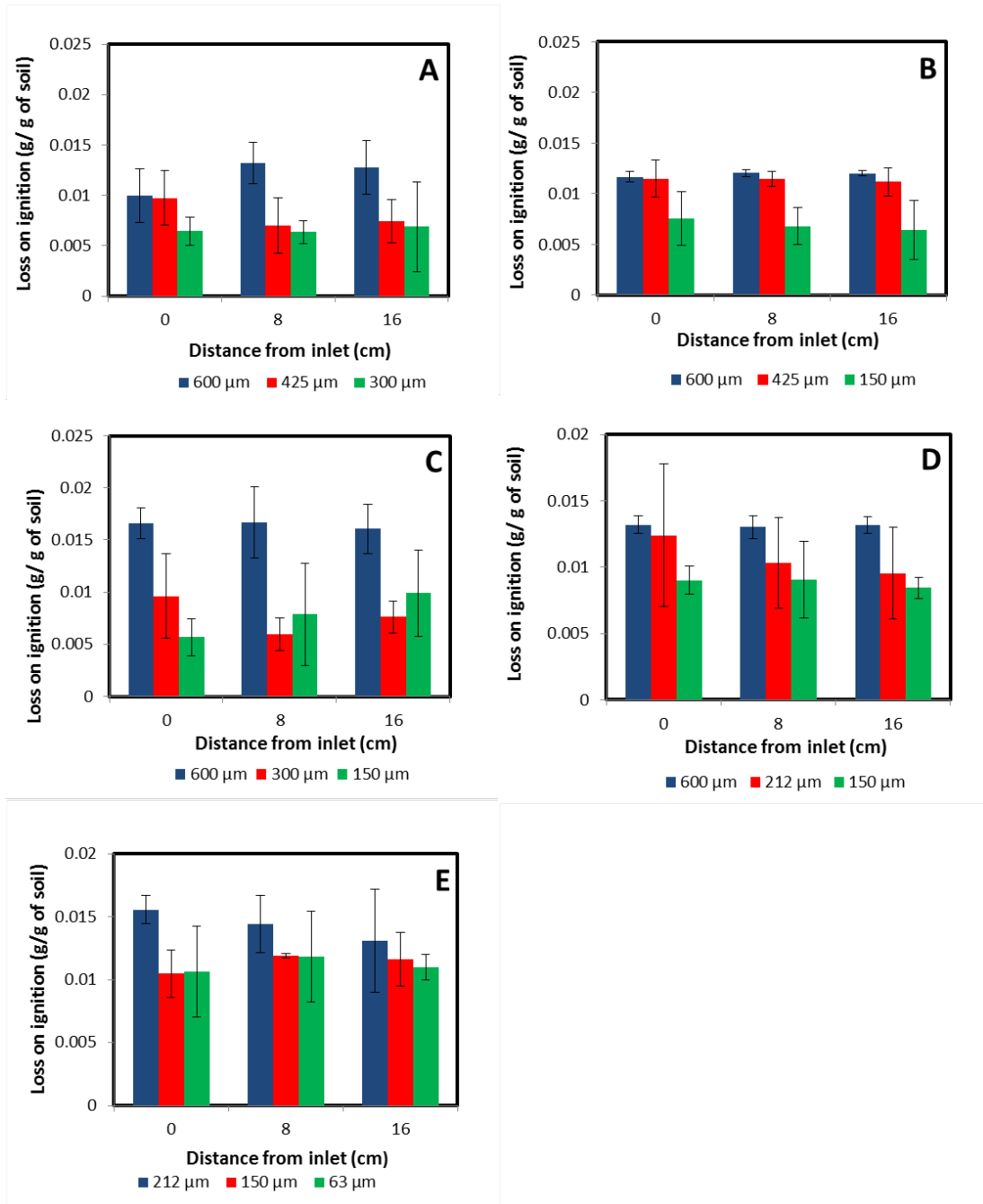


**Figure 5.3:** Loss on ignition values for all heterogeneous experiments, error bars represent the standard deviation of loss on ignition values.

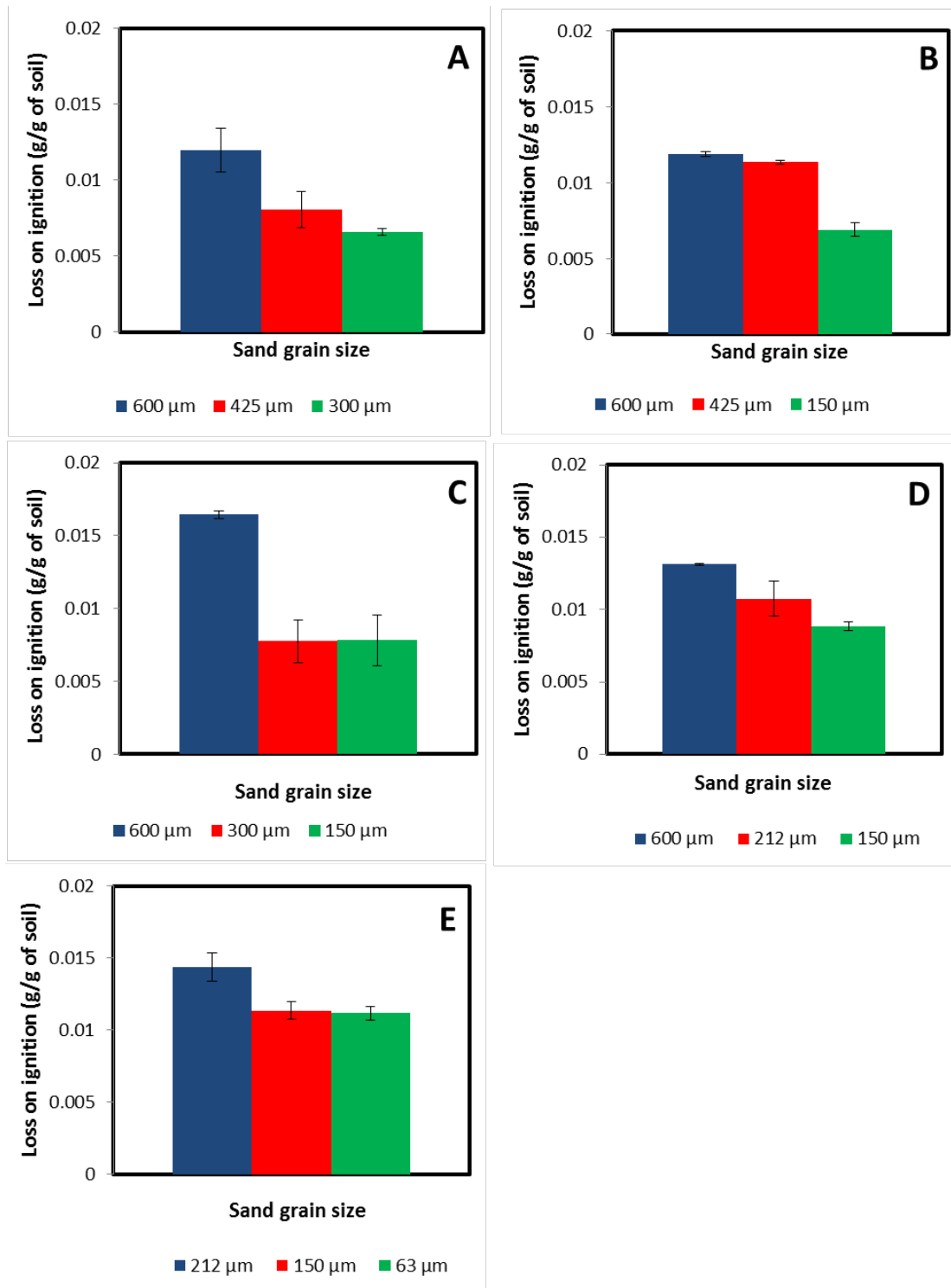


**Figure 5.4: Relation between loss on ignition due to *B. indica* growth and grain size of sand for all heterogeneous experiments, error bars represent the standard deviation for loss on ignition values.**

#### 5.4 Total number of cells

The initial and final numbers of cells were calculated using DAPI staining method and the initial number of cells which were mixed with the sand for all heterogeneous experiments were ranging from  $1.19 \times 10^6$  to  $1.16 \times 10^6$  cells  $g^{-1}$  of soil.

Figures 5.5A-E shows a comparison between the initial and final number of cells for the five heterogeneous experiments. These figures show clearly that the total number of cells increased considerably in proportion to the initial values in all sand column experiments.

This trend can be detected clearly in the first experiment as presents in Figure 5.5A. For the 600  $\mu m$  sand fractions and for the inlet location, the average of the total number of cells per gram of soil increased from  $1.19 \times 10^6$  to  $1.23 \times 10^7$ , then this figure dropped to  $6.02 \times 10^6$  cells  $g^{-1}$  of soil in the bottom location. As for 425  $\mu m$  sand fraction, a similar trend has been observed, where the average of the total number of cells per gram of soil increased from  $1.19 \times 10^6$  to  $8.86 \times 10^6$  at the top layer, and from  $1.19 \times 10^6$  to  $6.22 \times 10^6$  at the bottom one. Whilst, the average of the total number of cells for the 300  $\mu m$  exhibited a distribution of cells differed from the previous sand fractions, where it increased from  $1.19 \times 10^6$  to  $5.43 \times 10^6$  cells  $g^{-1}$  in the top layer, and from  $1.19 \times 10^6$  to  $8.57 \times 10^6$  cells  $g^{-1}$  in the bottom one as shown in Figure 5.5A.

For experiments EXP.(2)-EXP(3), as shown in Figures 5.5B-C, the average of the total number of bacteria is increased significantly by the end of each experiment in each sand location through each sand column. This increase in cell numbers could be occurred due to the nutrient availability which enhanced the growth of bacteria in each sand column. On the contrary, the control columns did not exhibit any substantial changes of cell numbers.

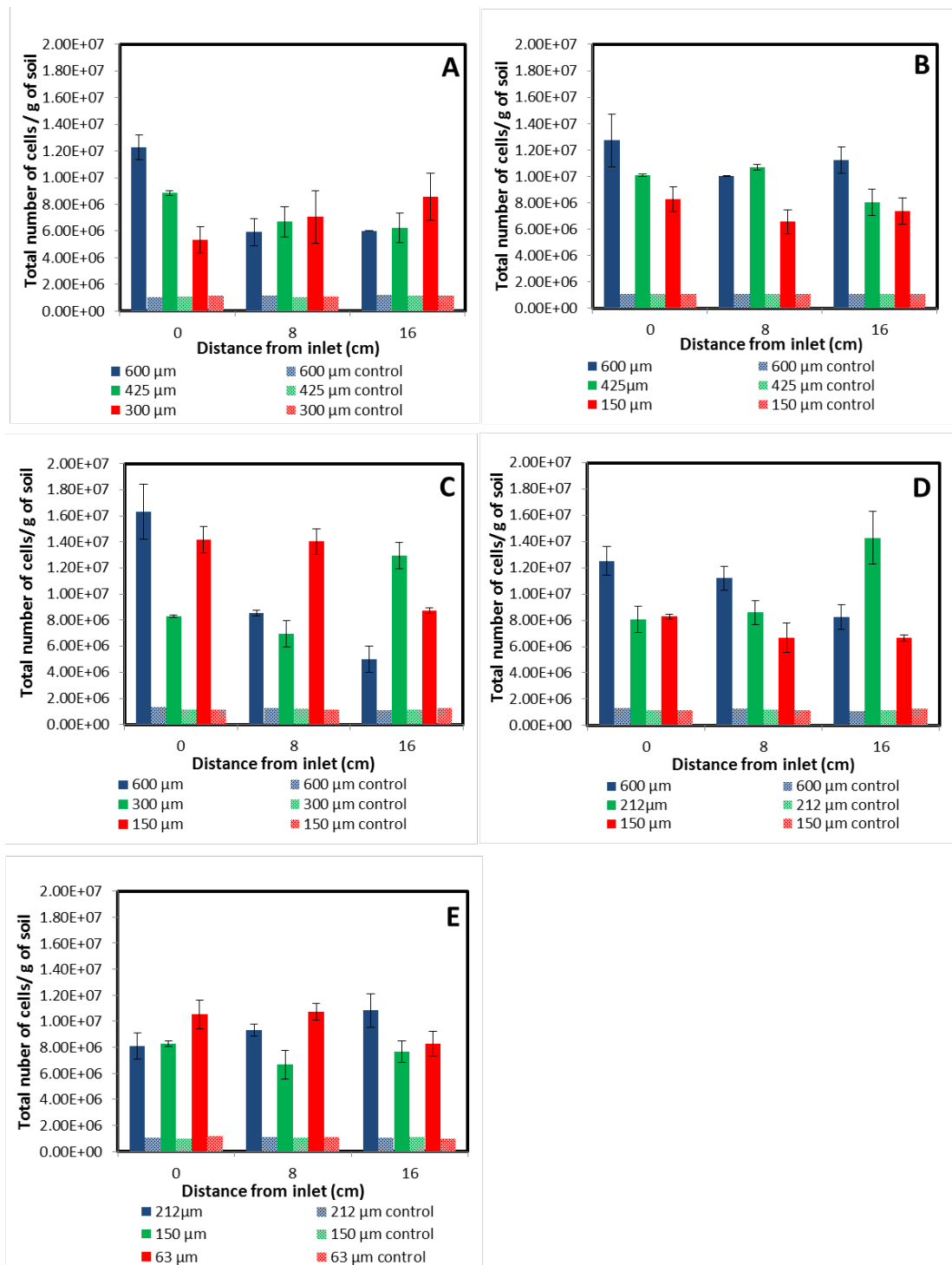


**Figure 5.5: Average of the total number of bacteria for all heterogeneous experiments, error bars represent the standard deviation for the total number of bacteria.**

Both loss on ignition and total number of cell analysis confirmed that the reduction of hydraulic conductivity could be attributed to the biomass accumulation in the sand

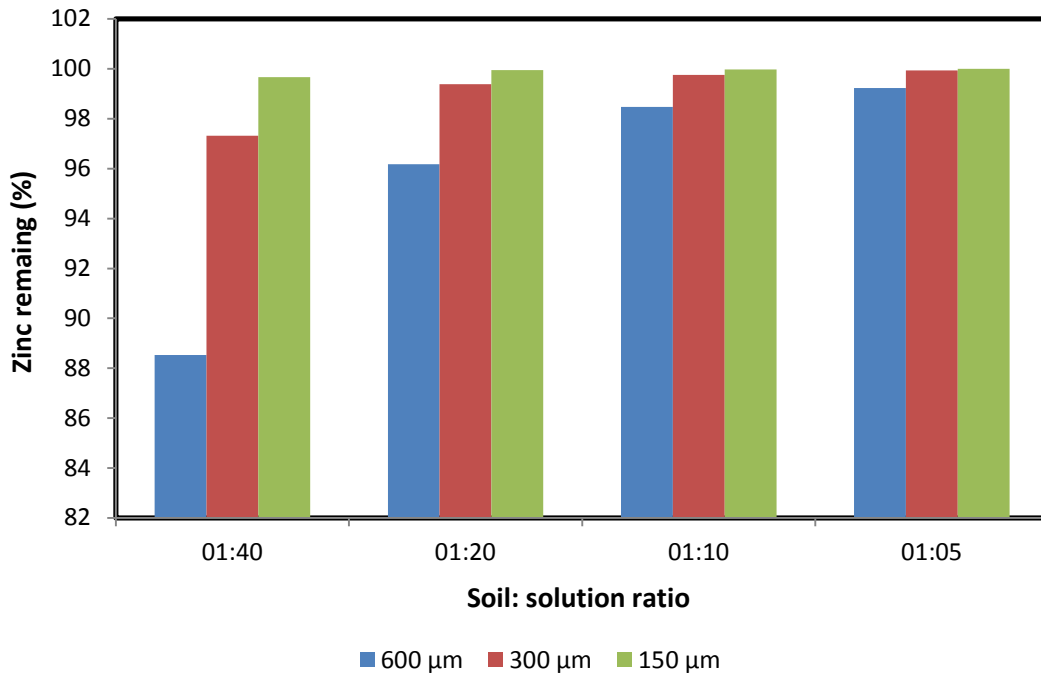
pore space. The greater amount of biomass accumulated in the large grain size, whilst the least amount of biomass accumulated at the fine sand fractions as shown in Figures 5.3A-E and 5.4A-E.

As for the total number of cells, the cell numbers have increased dramatically compared to the initial numbers, and this increase in the number of cells is possible that they may have occurred as a result to the nutrient availability which enhanced bacterial growth and production of biomass that caused bioclogging.

### **5.5 Batch adsorption experiment**

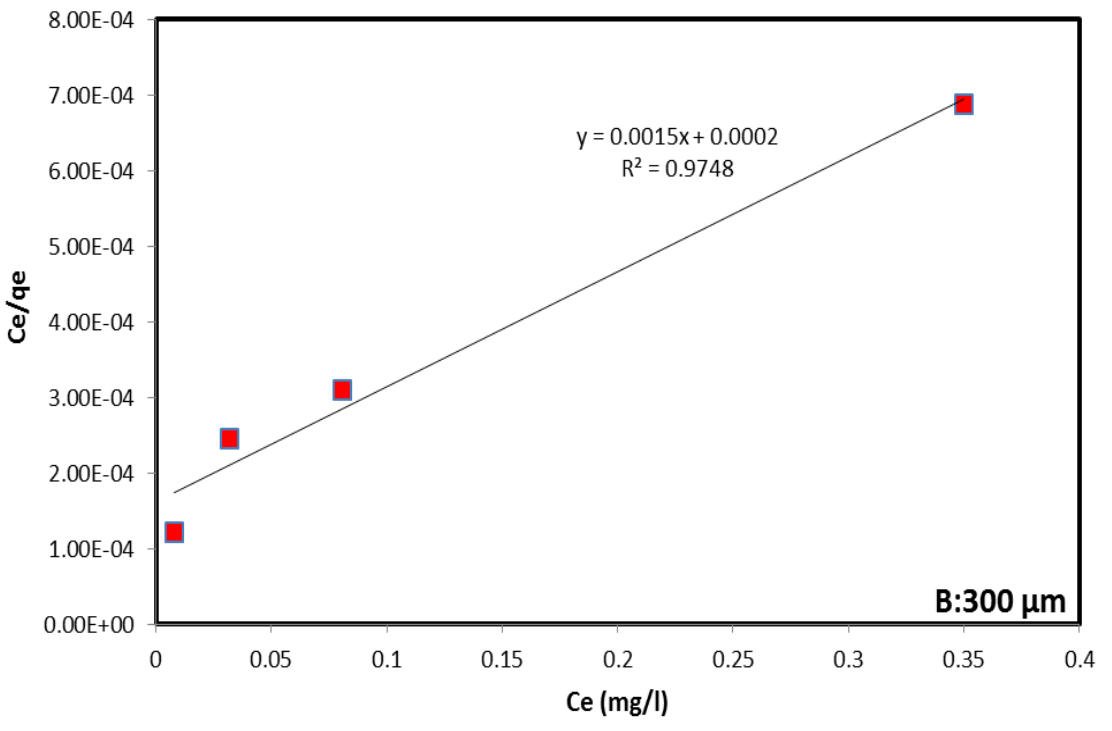
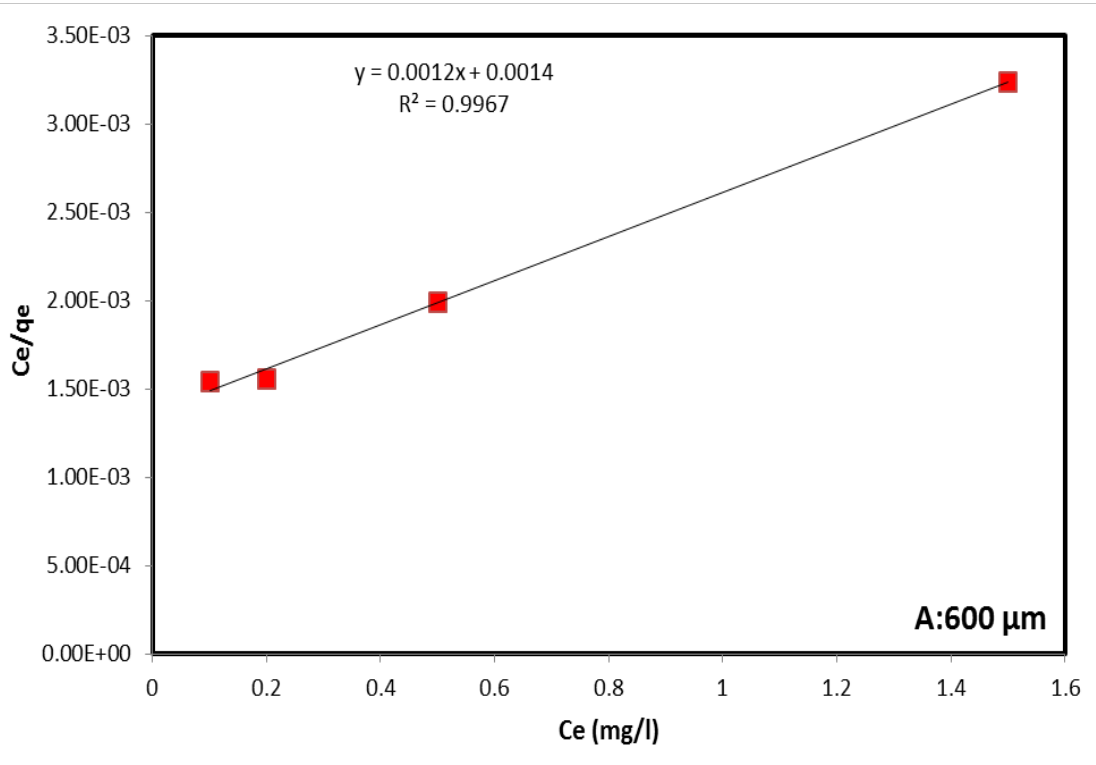
A batch adsorption test was performed to determine the soil capacity adsorption for each sand fraction. Four different soils: solution ratios were used to determine the optimal soil: solution ratio for each sand fraction, in this experiment the contact time was chosen to be 24 hours.

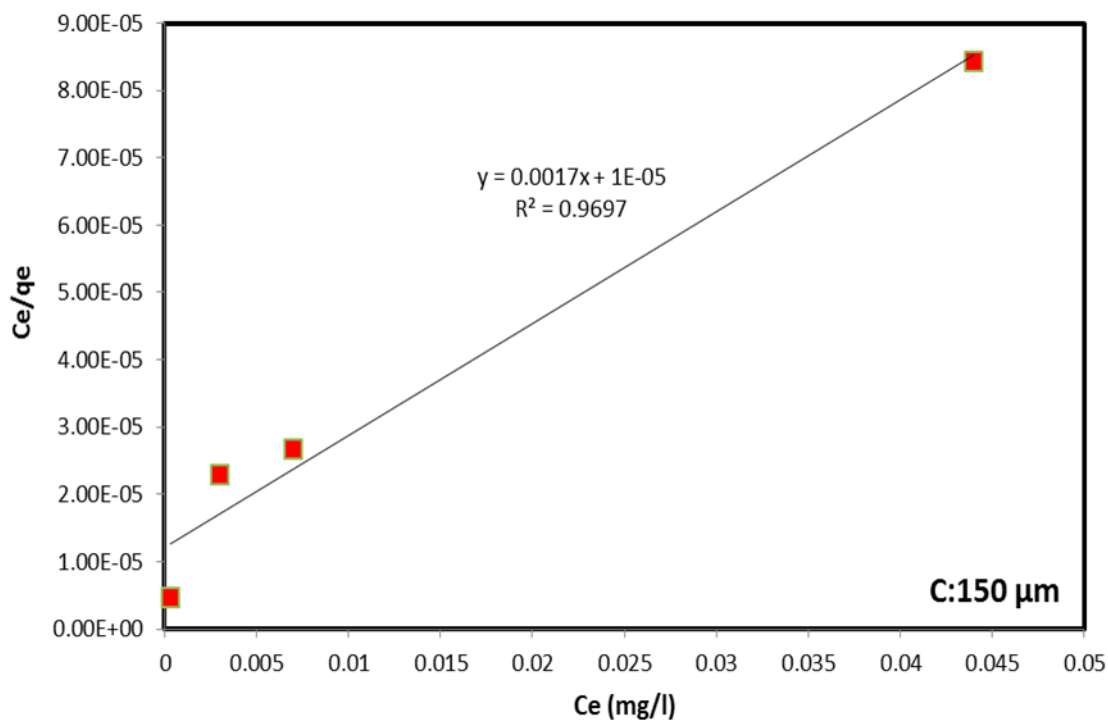
Figure 5.6 shows the percentage of zinc removal for three sand fractions and four soils: solution ratios. The figure shows that the higher adsorption of zinc is detected in the 600  $\mu\text{m}$  sand fraction for 4 soil: solution ratios. This variation could be attributed to the large surface area of small particle grain size that adsorbs metal ions. The results of this test coincide with the results of Chen *et al.* (2011) who reported that the adsorption rate of heavy metals increased as the grain size decrease. In this test zinc chloride was used to estimate the adsorption capacity of sand for zinc, in case of using zinc sulphate instead of zinc chloride, it is expected more amount of zinc will be adsorbed by sand due to the different molar weight of the zinc sulphate which is higher than of zinc chloride.



**Figure 5.6: The change of zinc after 24 hours of contact with four different soils: solution ratio for three sand fractions 600, 300, and 150 μm.**

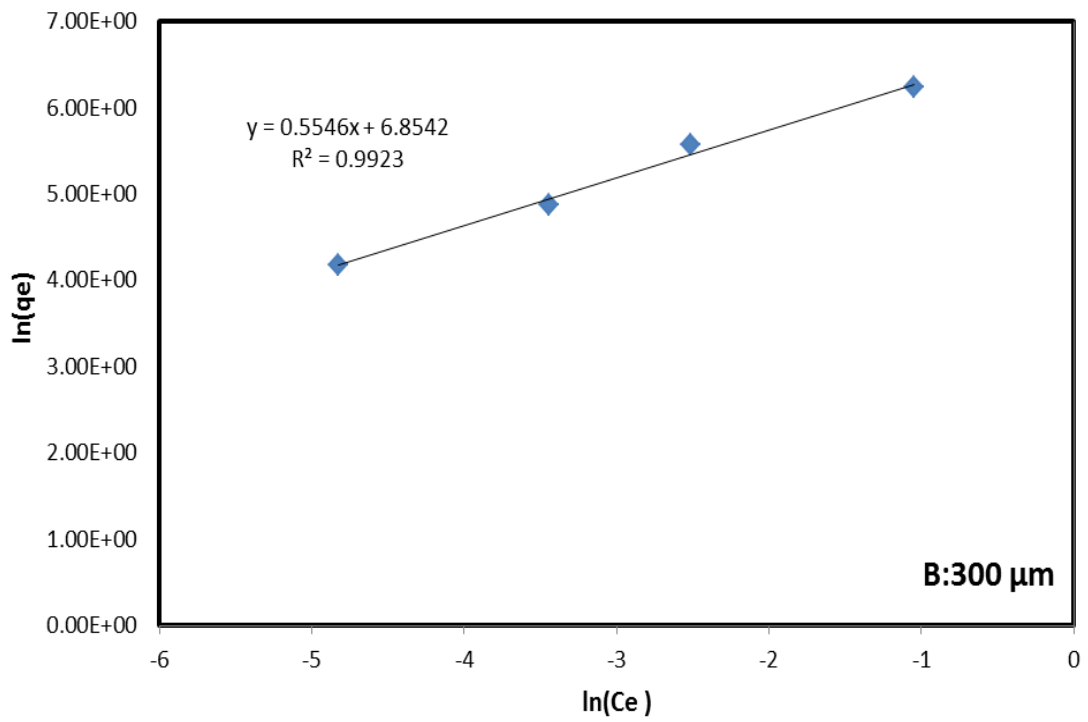
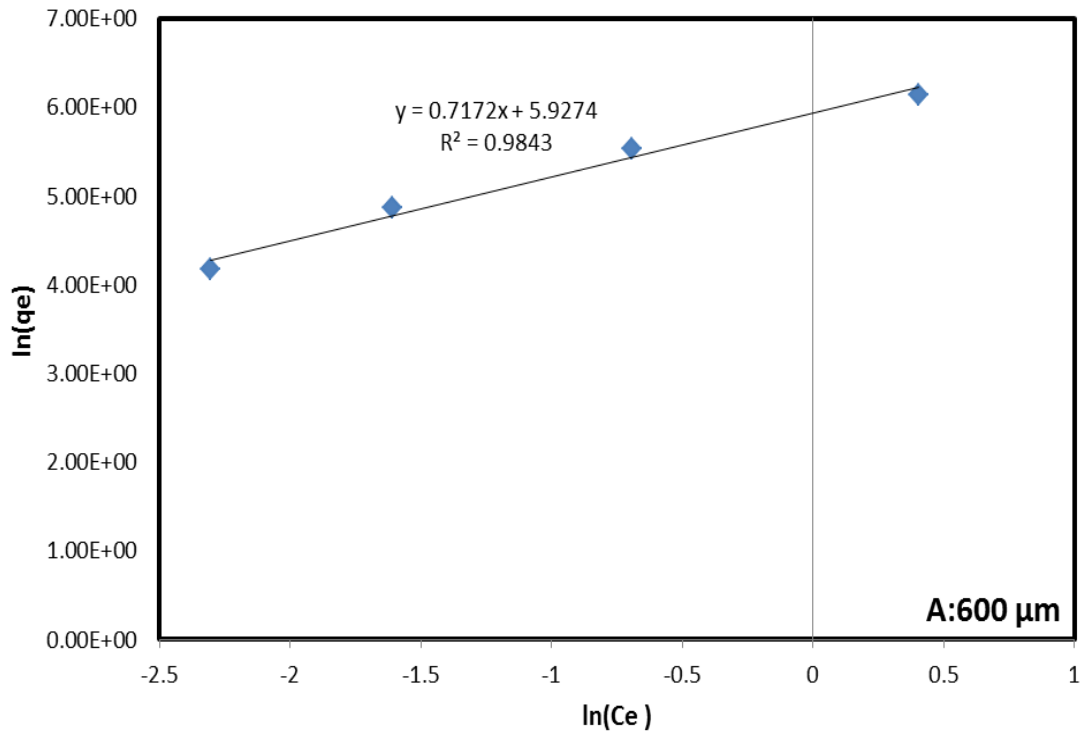
Data were fitted to Langmuir and Freundlich isotherm models to find the most appropriate model for the zinc ions adsorption behaviour. Figure 5.7 shows the variation of adsorption ( $C_e/q_e$ ) against the equilibrium concentration ( $C_e$ ) for adsorption of zinc ions onto 600 μm, 300 μm and 150 μm sand fractions using the Langmuir isotherm.





**Figure 5.7: Langmuir isotherm links adsorption ( $Ce/qe$ ) against the equilibrium concentration ( $Ce$ ) for adsorption of zinc ions onto soil particle: A for 600  $\mu\text{m}$ , B for 300  $\mu\text{m}$  and C for 150  $\mu\text{m}$  sand fractions.**

Figure 5.8 shows the variation of adsorption  $\ln(qe)$  against the equilibrium concentration  $\ln(Ce)$  for adsorption of zinc ions onto 600  $\mu\text{m}$ , 300  $\mu\text{m}$  and 150  $\mu\text{m}$  sand fractions using the Freundlich isotherm. The results revealed that Freundlich adsorption isotherm was the best model for the zinc ions adsorption and adsorption of zinc onto soil particle increases with the amount of adsorbent. Similar results reported by (Mittal *et al.* 2007).



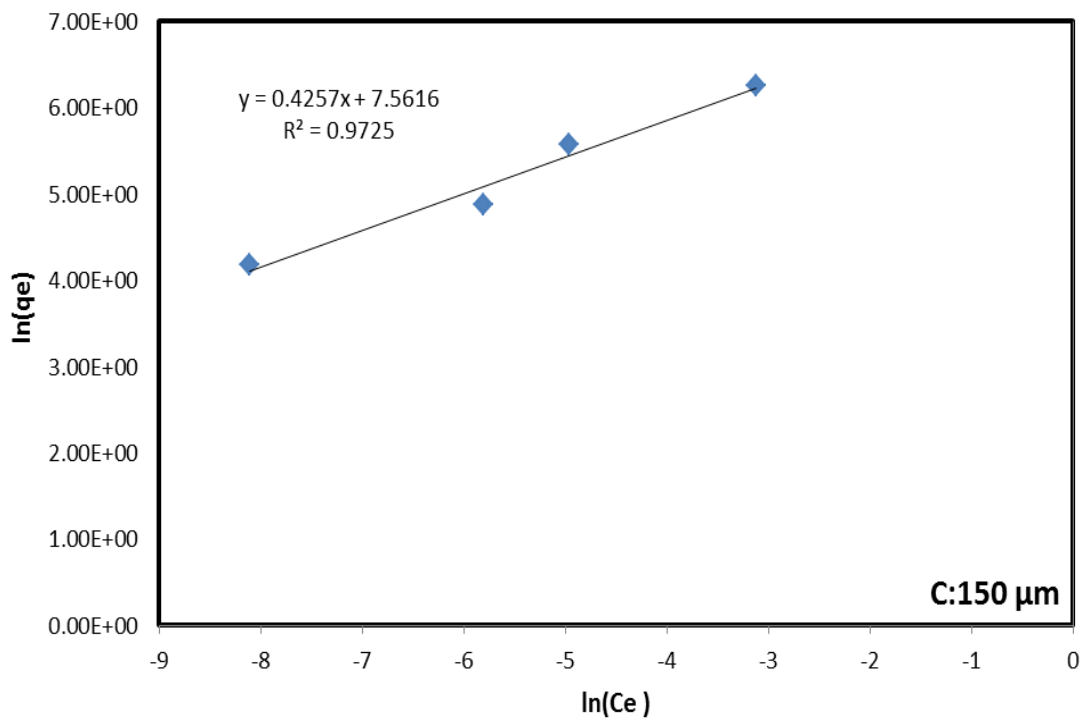


**Figure 5.8: Freundlich isotherm links the adsorption  $\ln (q_e)$  against the equilibrium concentration  $\ln (C_e)$  for adsorption of zinc ions onto soil particle: A for 600  $\mu\text{m}$ , B for 300  $\mu\text{m}$  and C for 150  $\mu\text{m}$  sand fractions.**

## **5.6 The effect of different zinc concentrations on bacterial growth in batch experiment**

A batch experiment was conducted to investigate the effect of different concentrations of zinc on microbial growth by measuring the optical density of different microbial suspension that containing different concentrations of zinc ranging from 0.1 to 0.5 mM. The optical density (absorbance) of the solutions was measured at  $\text{OD}_{600}$  using a spectrophotometer.

The results of this experiment showed that after 3 days of incubation period the bacterial suspension showed greater optical density in the absence of zinc than the presence of zinc in it, except for the use of 0.1 mM of zinc where the final optical density experienced an increase compared with the initial value.

Figure 5.9 illustrates the initial and final measured optical density values for different concentrations of zinc after 3 days incubation period. In this figure the OD<sub>600</sub> of the microbial suspension, increased at low concentration of zinc 0.1 mM which could be attributed to the cell resistance to zinc. Whilst by increasing zinc concentration from 0.1 to 0.5 mM, the OD<sub>600</sub> of the microbial suspension, decreased compared to the control condition (cells without zinc) which also presents an increase in the optical density values by the end of the incubation period. The drop of OD<sub>600</sub> values by increasing zinc concentrations indicated that the increase of zinc concentrations could be resulted in an inhibition of the bacterial growth.

The results of this experiment agree with the results of Mittal and Goel (2010) who reported that the optical density values of the bacterial suspension, increased with using 0.2 mM of zinc but by increasing the concentrations of zinc the optical density values dropped. Mittal and Goel (2010) reported that the drop of the optical density values of the bacterial suspension is due to the decay of cells.

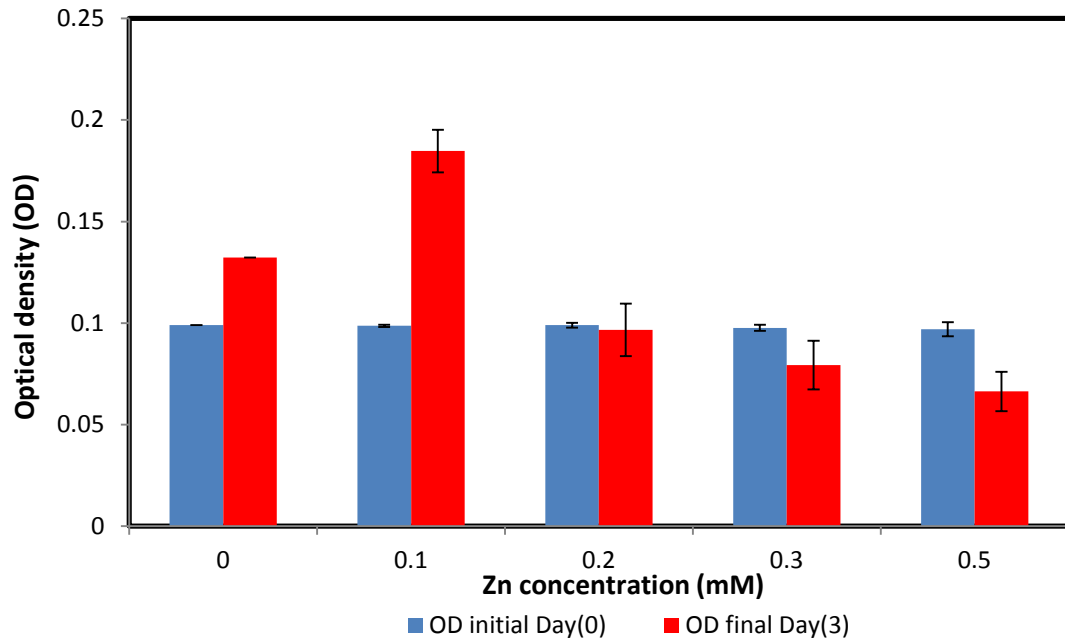


**Figure 5.9: The effects of different concentrations of zinc on the growth of *B. indica* in batch experiment, error bars represent the standard deviation of the optical density values.**

### **5.7 Zinc effect on bacterial growth in heterogeneous porous media**

In order to investigate how bioclogging could enhance heavy metal removal from heterogeneous porous media, parallel sand column experiment with the presence of zinc and *B. indica* was performed. Three sand fractions 600, 300, and 150  $\mu\text{m}$  were chosen due to the wide range in permeability. In other word, using these sand fractions will make it easier to notice any changes in hydraulic conductivity due to the wide range of permeability between these sand fractions. In addition to that, the selection of these sand fractions will help for in identifying the difference of zinc removal in each sand fraction which expected to be variable depending on particle size.

Figures 5.10 and 5.11 show the change of hydraulic conductivity in contaminated heterogeneous porous media with time due to the growth of *B. indica* in normal and logarithmic scale. These figures exhibit that the initial rate of hydraulic conductivity reduction decreases with grain size, there appears to be an increased lag with smaller

grain sizes, and the three curves end up being quite similar, suggesting that there has been a degree of equilibration between the three fractions. The other interesting point in these figures is the crossing of the hydraulic conductivity values, which refers to the occurrence of flow diversion.

By comparing the outcome of this experiment with the previous heterogeneous experiment EXP.(3), it could observe that both experiments have similar trend.

On the other hand, the hydraulic conductivity values remained constant over time when the bacteria and glucose were excluded for all the three sand fractions as shown in Figure 5.12.

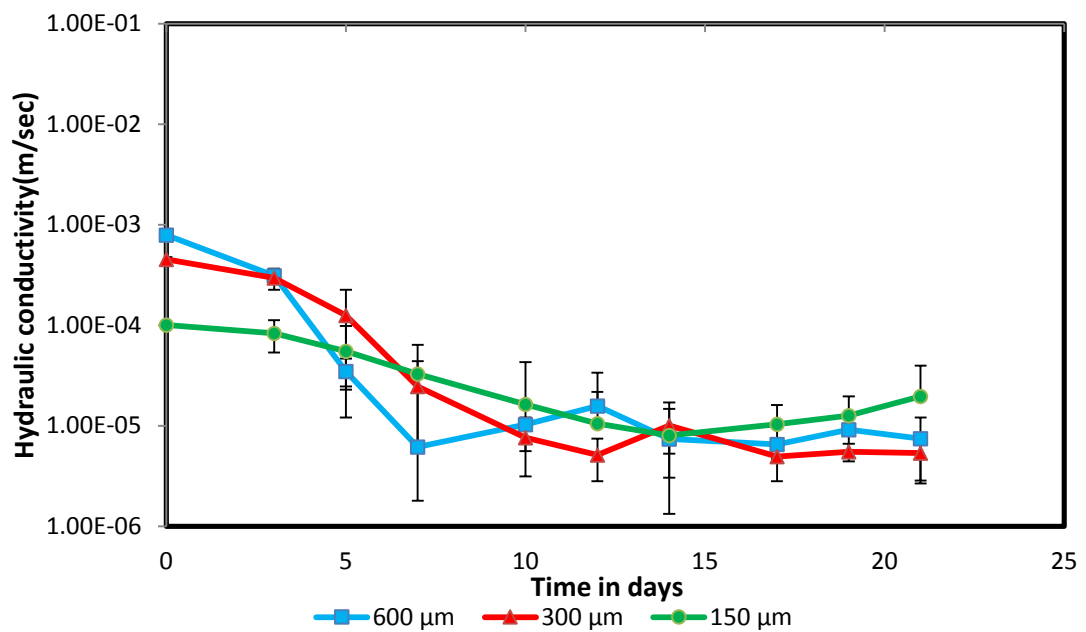


**Figure 5.10: The effect of zinc concentration on hydraulic conductivity of porous media due to *B. indica* growth in three different sizes of sand 600, 300 and 150  $\mu\text{m}$  in logarithmic scale, error bars represent the standard deviation of the hydraulic conductivity readings.**

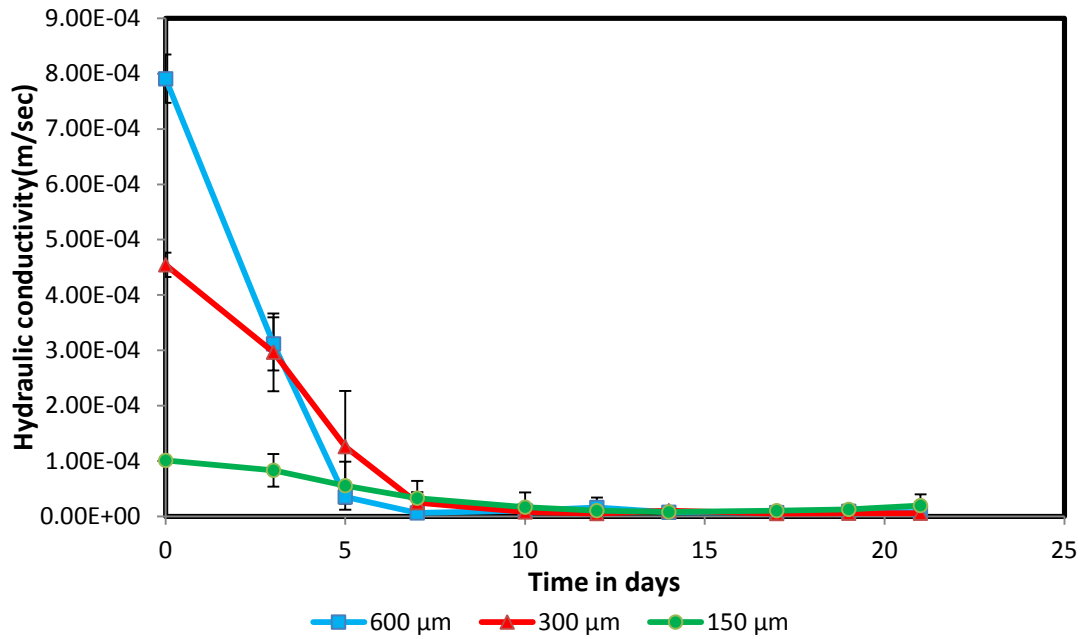


**Figure 5.11:** The effect of zinc concentration on hydraulic conductivity of porous media due to *B. indica* growth in three different sizes of sand 600, 300 and 150 μm in normal scale, error bars represent the standard deviation of the hydraulic conductivity readings.

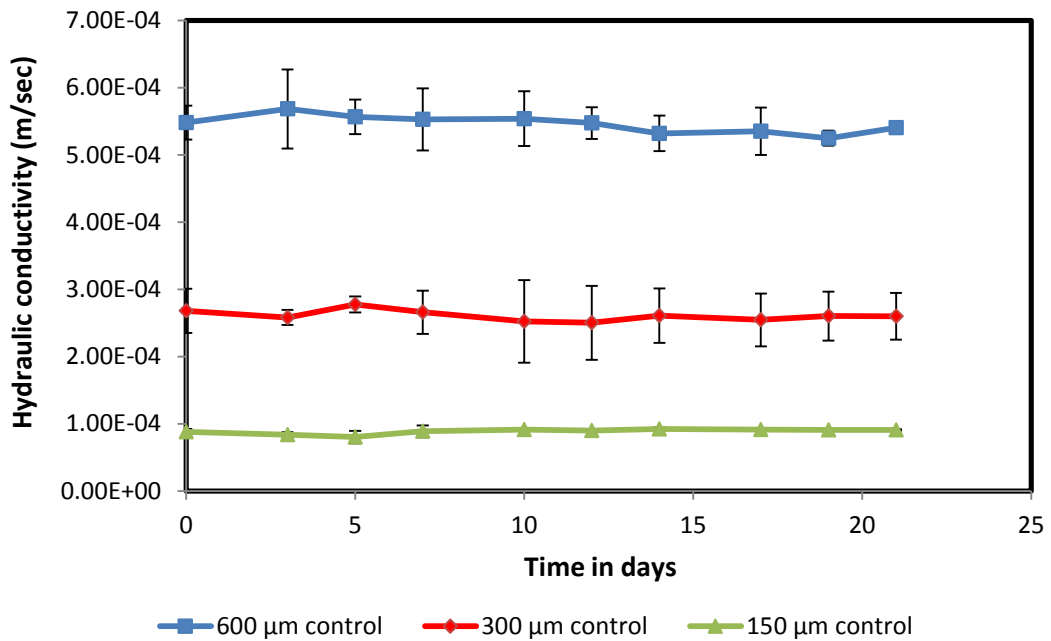


**Figure 5.12:** The effect of zinc concentration on hydraulic conductivity of porous media under control conditions (dead cells) in three different sizes of sand 600, 300 and 150 μm, error bars represent the standard deviation of the measured hydraulic conductivity values.

### **5.7.1 Loss on ignition analysis**

The loss on ignition results suggested that the significant reduction of hydraulic conductivity occurred due to the growth of bacteria that led to produce more amount of biomass 1.1 % in the 600  $\mu\text{m}$  sand fraction, and less amount of biomass 0.9 % was detected in the 300  $\mu\text{m}$  sand fraction, and the least biomass amount 0.8 % was detected the 150  $\mu\text{m}$  sand fraction as shown in Figures 5.13 and 5.14.

This trend is the same for the previous heterogeneous experiments where the large grain sand has the largest amount of biomass, and the least amount of biomass accumulated was detected in the small sand fraction. Again the results of the loss on ignition of this experiment agree with the results of Cunningham *et al.* (1991) who observed that the thickness of biofilm increase with increasing the media pore space, and with Bielefeldt *et al.* (2002) who also reported that more biomass accumulate in the large sand fraction. The explanation of this trend could be attributed to the fact that the large surface areas need more biofilm to form.

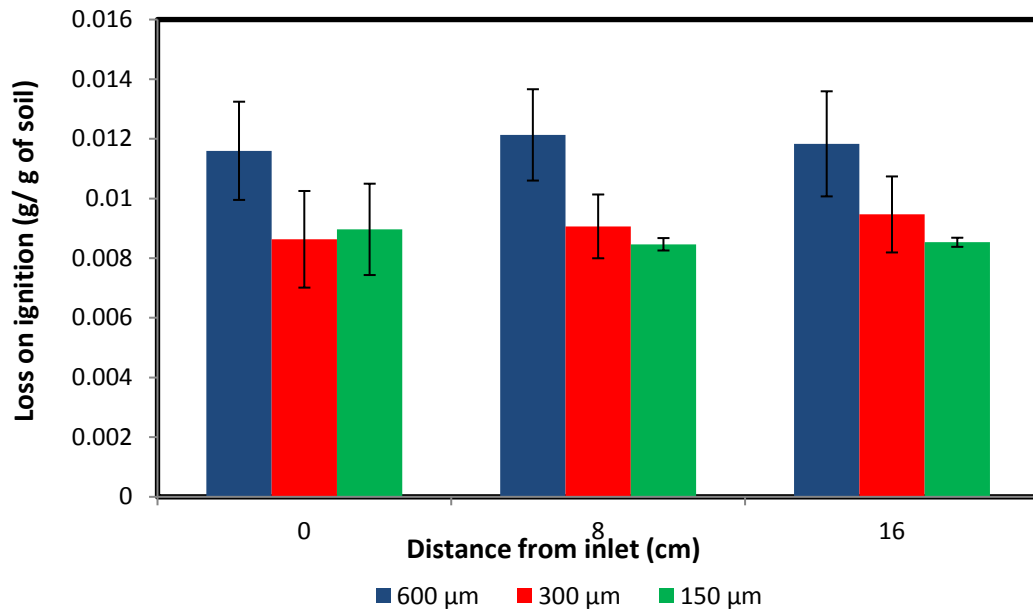


**Figure 5.13:** Loss on ignition due to *B. indica* growth in three different sizes of sand 600, 300 and 150 μm contaminated with zinc, error bars represent the standard deviation of the loss on ignition values.

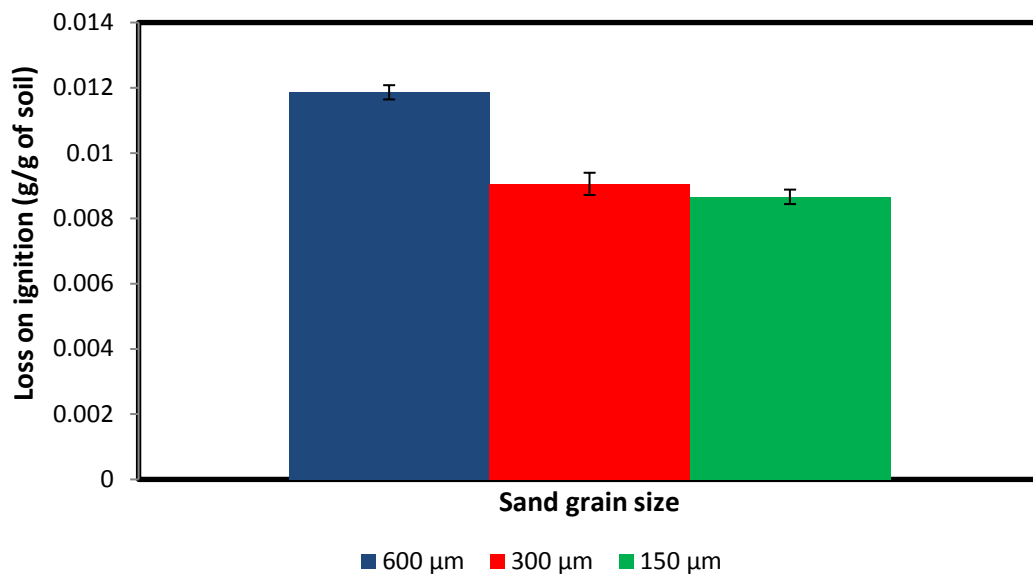


**Figure 5.14:** Relation between losses on ignition due to *B. indica* growth and grain size of sand 600, 300 and 150 μm, error bars represent the standard deviation of the loss on ignition values.

### 5.7.2 Zinc concentrations analysis

Effluent water samples were collected regularly to estimate zinc concentrations by using ICP-OES. Figure 5.15 reveals the changes in zinc concentrations with time for the 600, 300 and 150  $\mu\text{m}$  sand fractions. The results indicate that flow diversion can work in heterogeneous soils. Figure 5.16 shows that zinc is initially only removed from the 600 micron fraction, but then starts to be removed from the other fractions too, suggesting that flow must be occurring in these columns too, but that it requires a certain amount of biofilm growth before it happens.

The adsorption capacity for each sand fraction was calculated by using the equation of Freundlich isotherm which was shown Figure 5.8A, B, and C. The outcome of these equations showed that the large sand fraction (600  $\mu\text{m}$ ) has the lowest adsorption capacity 1.34 mg/g of zinc, whereas about 5.25 mg/g of zinc was adsorbed by the 150  $\mu\text{m}$ .

This outcome agrees with the results of Kumar *et al.* (2011) who reported that the particle size of adsorbents is one of important factors affecting the adsorption capacity as it influences the surface area of adsorbent. The lower the particle size higher the surface area hence it absorbs more metal ions.

In contrast, the results of the control experiment as shown in Figure 5.16 revealed that control columns did not show any significant changes of zinc concentration with time. This could be attributed to the high adsorption capacity of sand in the absence of bacteria.

By comparing the biological and control experiments, it could observe that the presence of *B. indica* increases the percentages of zinc removal. This could be occurred because of the cell attachment to the soil particle during sand packing. The cell attachment occurred because the bacterial suspension was added to each sand

fraction before the addition of zinc solution. This could be the reason that affected on the sand adsorption capacity and caused a removal of less percentages of zinc from the sand columns that were operated without bacteria.

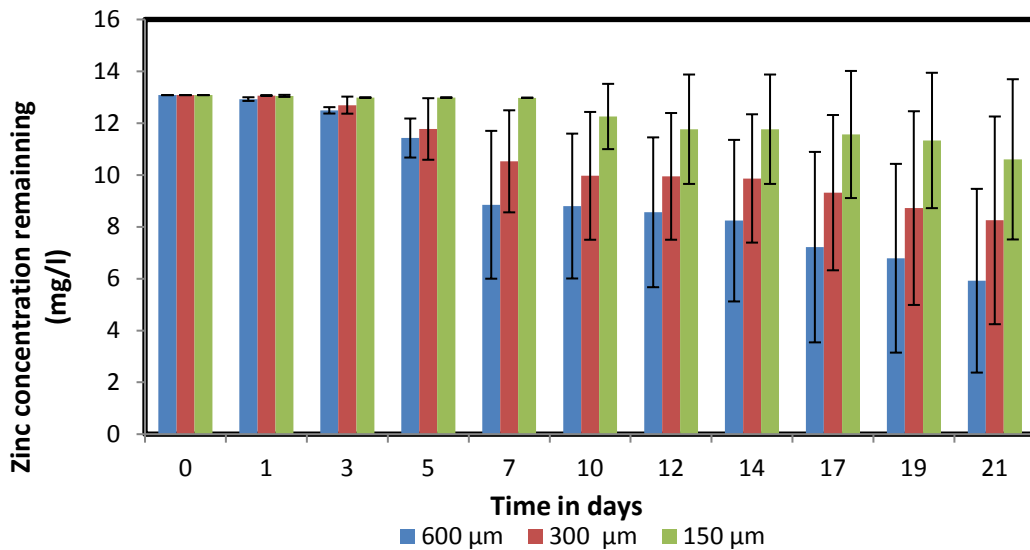


**Figure 5.15: Changes in zinc concentration in three sand fractions 600, 300 and 150 μm for the biological conditions (live cells), error bars represent the standard deviation of the zinc concentrations.**

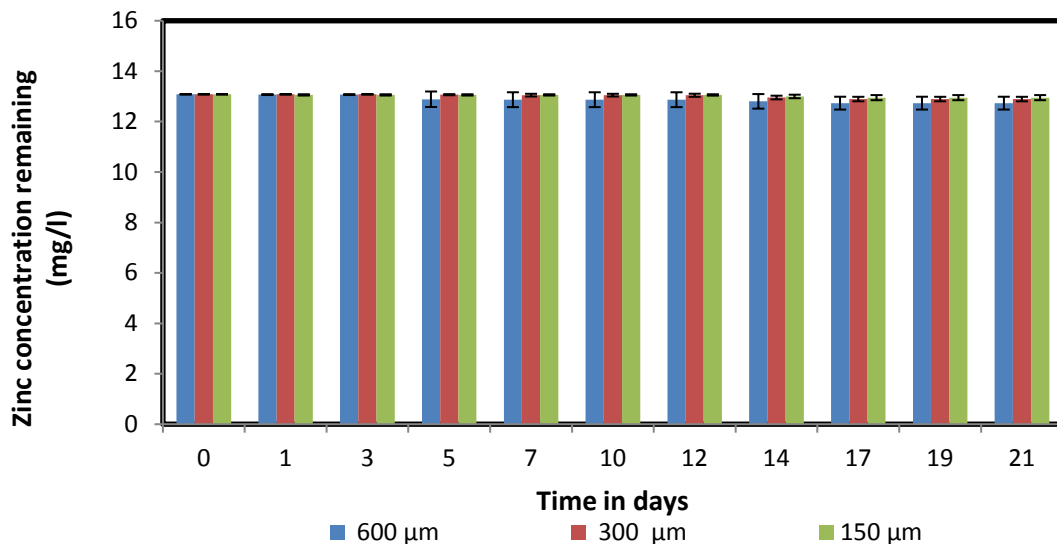


**Figure 5.16: Changes in zinc concentration in three sand fractions 600, 300 and 150 μm for the control conditions, error bars represent the standard deviation of the zinc concentrations.**

## 5.8 Overall discussion

The results of the all sand column experiments clearly showed that the hydraulic conductivity decreases significantly in the columns that were injected with live cells. In contrast, there were no signs of any significant changes in hydraulic conductivity in the control columns. In general, the reduction in hydraulic conductivity took nearly a similar trend for the five experiments, and can be summarized as follows:

In regards to the four bioclogging heterogeneous experiments and after three days of nutrients pumping, the hydraulic conductivity of the 600  $\mu\text{m}$  (the most permeable sand fraction) decreased by 21.0-36.0 % due to the large amount of nutrient solution that was delivered to this sand fraction except for the third experiment EXP.(3) where a massive reduction of the hydraulic conductivity up to 89.0 % occurred on by the third day as shown in Figures 5.1A-5.1D. By the 7th day the reduction in hydraulic conductivity for the 600  $\mu\text{m}$  was ranging from 68 % to 76 % causing clogging of this sand fraction and thus resulted in change the of paths nutrient solutions to the less permeable sand fraction.

This flow diversion led to more growth of *B. indica* in pore volume and subsequently more production of EPS that caused a significant reduction in the permeability of these sand fractions. The same process continued for the third sand fraction (the least permeable sand fraction) which was clogged when the flow was diverted from the most permeable sand fraction due to the accumulation of biomass.

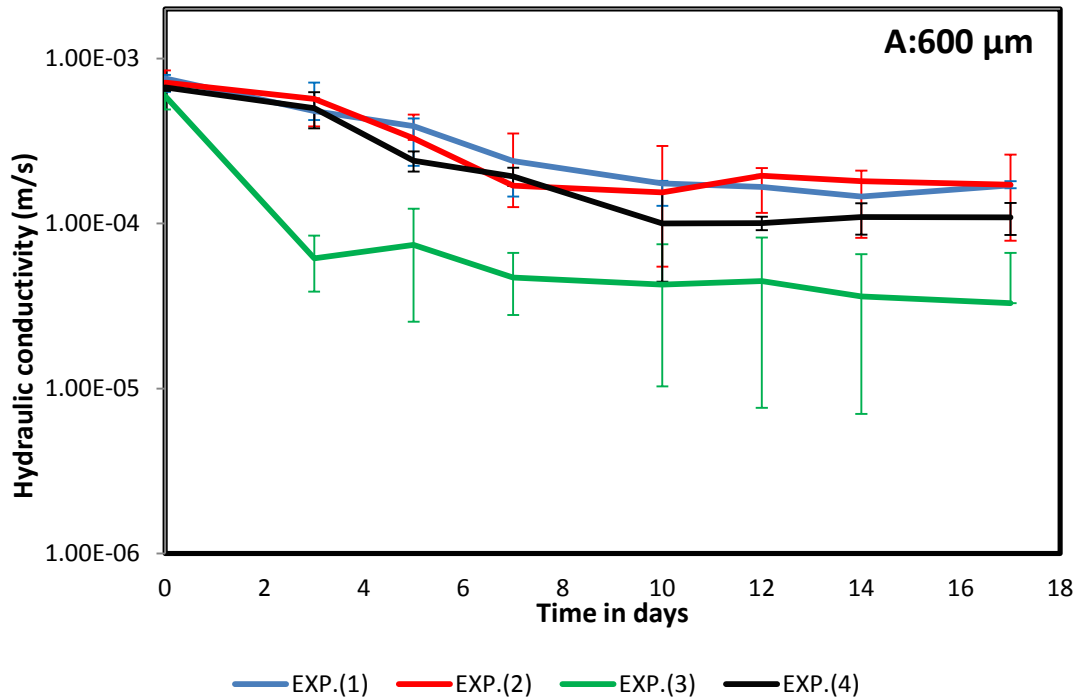
Different trend can be spotted in the last heterogeneous experiment EXP.(5); where the 212  $\mu\text{m}$  and the 150  $\mu\text{m}$  sand fractions were clogged first on the 5th day of the experiment, but the reduction in hydraulic conductivity was very low compared with the previous experiments that showed significant reduction in hydraulic conductivity

up to 90 % after three days only of nutrient delivery as seen in Figure 5.1E. The reasons behind that could be ascribed to the small pore volumes of these sand fractions which could affect the bacterial growth. The large pores offer the least resistance to fluid through the porous media (Torbati *et al.*, 1986) and so bacteria could have access to large amounts of nutrients and this is consistent with the results of Cunningham *et al.* (1991) who reported that bacteria clog large pores first. By the 10th day, the 63  $\mu\text{m}$  sand fraction began to gradually clog as well, where the hydraulic conductivity decreased by 15.0 % of the initial value, then it started to rise up to 90.0 % by the end of this experiment.

By the end of these experiments, the difference in hydraulic conductivity for each sand fraction set decreased significantly compared to the initial values due to the biomass accumulation.

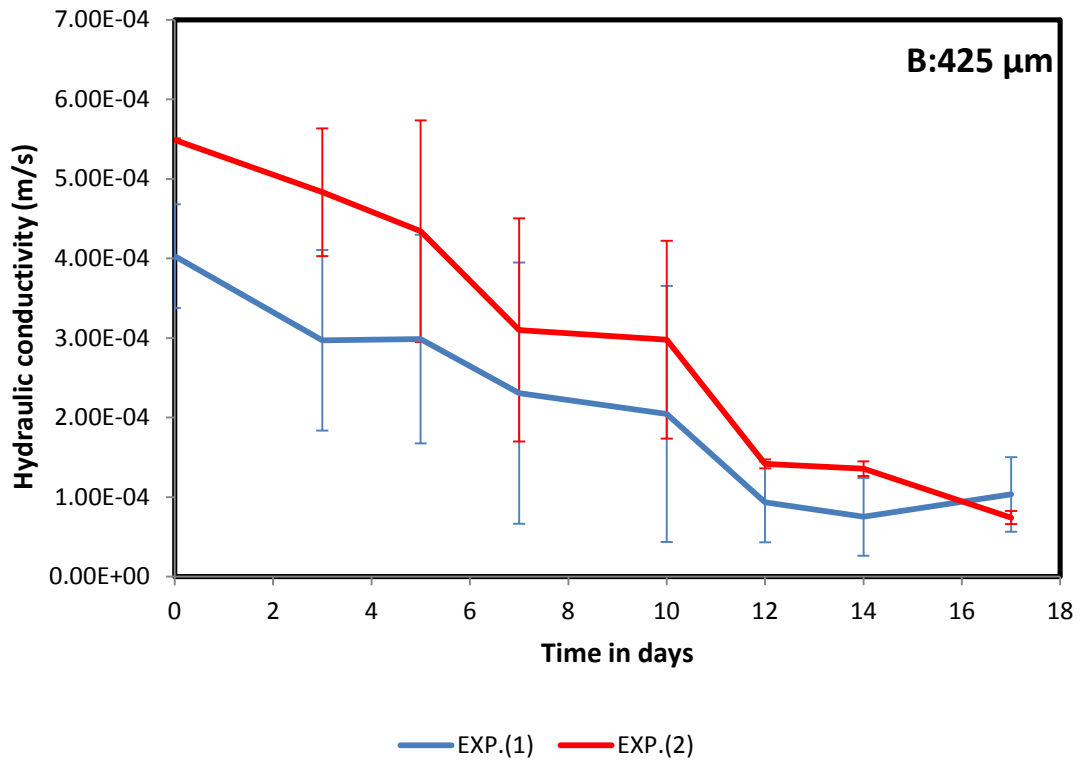
For more explanation of the results of the five heterogeneous experiments and to understand more about how the flow is diverted from the high permeable sand fraction to the least permeable one, the change of the hydraulic conductivity with time for each sand fraction was displayed as shown in Figure 5.17A-F.

In general the results as shown in Figure 5.17A are very similar for three of the experiments, but they are very different for another. In the first, second and fourth experiments, it can observe that the hydraulic conductivity decreased significantly, then remained constant by the end of the experiment which means that there is no flow diverted from the 425 $\mu\text{m}$  into the 600  $\mu\text{m}$  sand fractions. While the hydraulic conductivity for the 600  $\mu\text{m}$  in the third experiment decreased more sharply than other experiments and then remained constant until the end of the experiment.



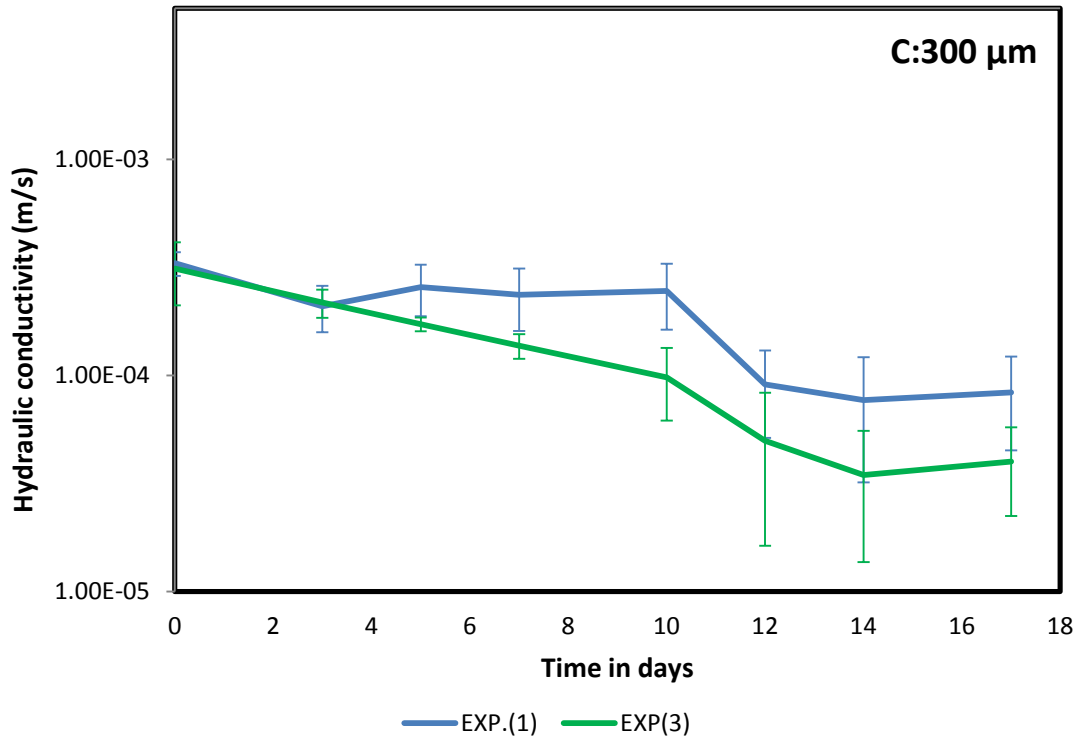
**Figure 5.17A: The changes of hydraulic conductivity via time in the 600 μm in four heterogeneous experiments, error bars represent standard deviation of the average values of the hydraulic conductivity.**

As for the 425 μm and by comparing the results from the first EXP.(1) and EXP.(2), it can be noticed that there is no big difference of the reduction of the hydraulic conductivity for both experiments as shown in Figure 5.17B. In the first and the second experiments, the flow in the 425 μm continued with decreasing until the last day.



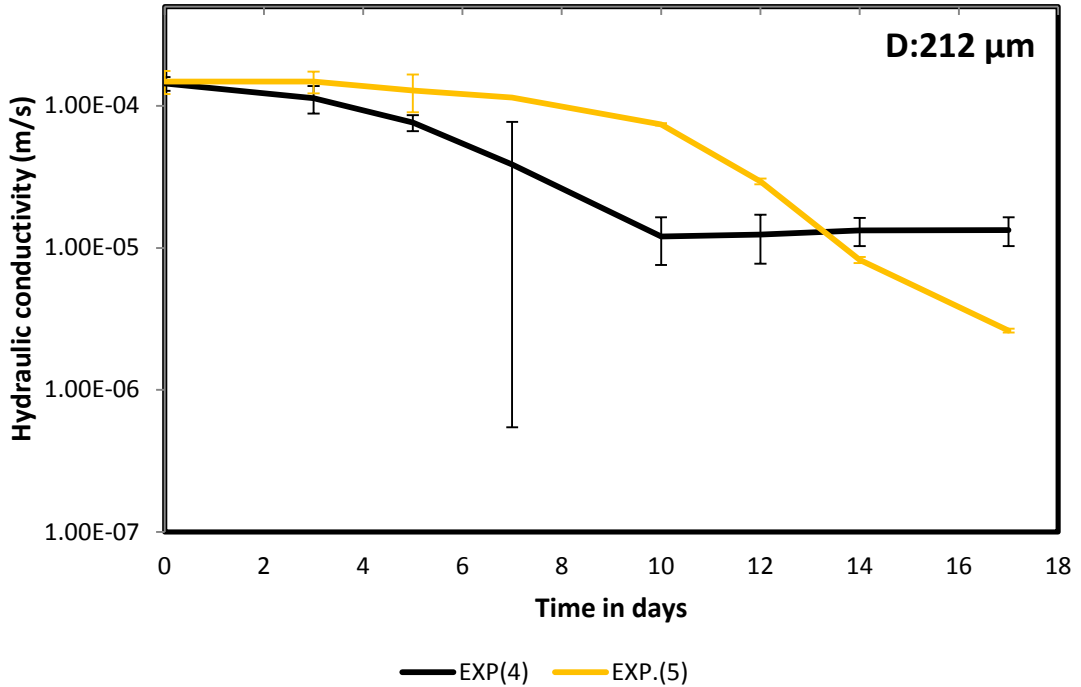
**Figure 5.17B: The changes of the hydraulic conductivity via time in the 425 μm in two heterogeneous experiments, error bars represent standard deviation of the average values of the hydraulic conductivity.**

For the 300 μm, it can be remarked that the hydraulic conductivity in EXP.(3) decreased more than in EXP.(1). The reason behind that could be because of the 300 micron in EXP.1 is the third column and the flow has to be diverted through two columns first. In addition to that, the flow diversion from the 600 μm into the 300 μm sand fractions could be the reason behind the more biomass accumulation in the 300 μm sand fractions which caused more reduction of the hydraulic conductivity in EXP.(3) than in EXP.(1) as shown in Figure5.17C.



**Figure 5.17C: The changes of the hydraulic conductivity via time in the 300 μm in two heterogeneous experiments, error bars represent standard deviation of the average values of the hydraulic conductivity.**

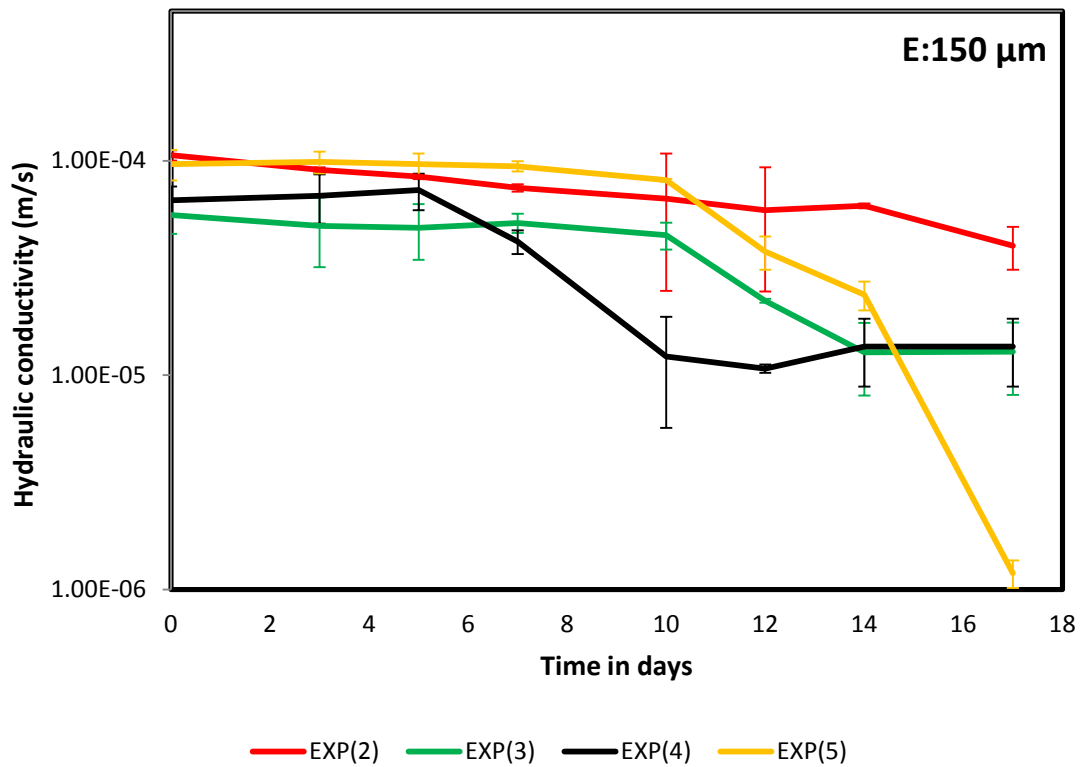
By comparing the behaviour of the 212 μm in two experiments, it had been expected that the hydraulic conductivity will be decreased greatly in EXP.(5) than in EXP.(4) because the amount of flow which was delivered to this sand fraction in EXP. (5) is greater than in EXP. (4). However, the results of these experiments show slightly different bioclogging behaviour as shown in Figure 5.17D where the hydraulic conductivity of this sand fraction in EXP.(4) decreased greatly than EXP.(5) in the first 5 days of the experiment. Although this contrary is hard to explain, but the reasons behind that might be related to the small amount of biomass that accumulated in this sand fraction in EXP.(5). In general both of the two experiments did not experience any flow diversion from the other sand fractions.



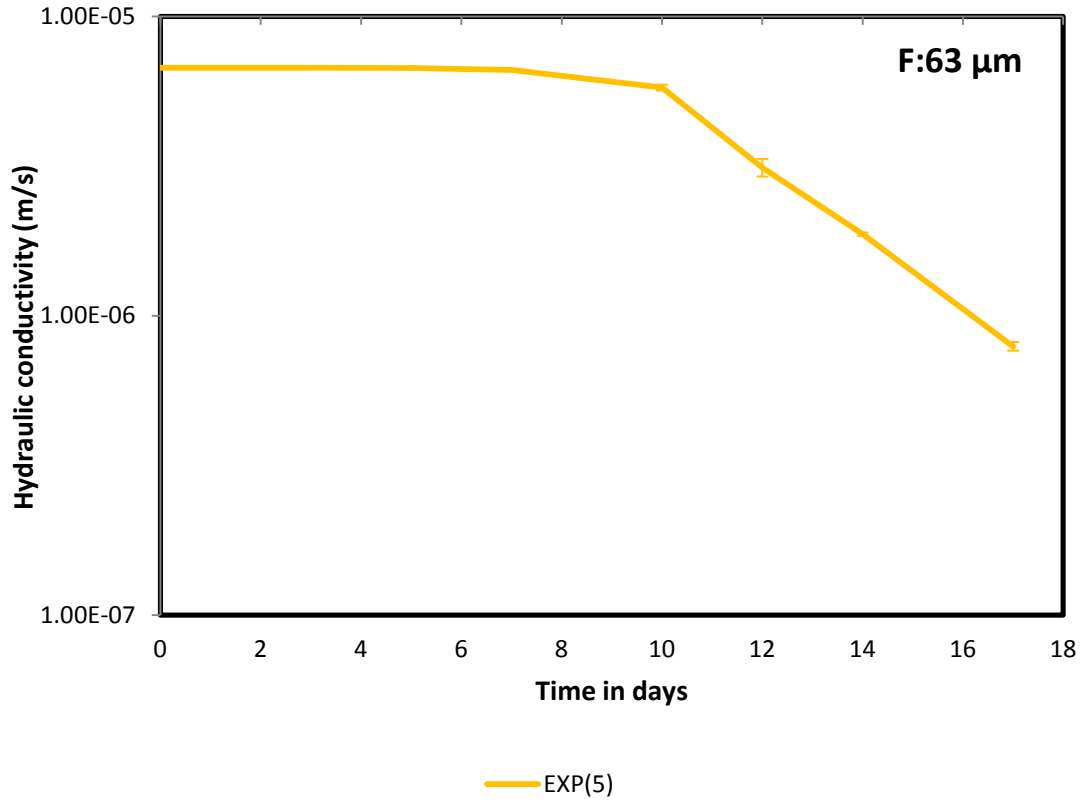
**Figure 5.17D: The changes of the hydraulic conductivity via time in the 212  $\mu\text{m}$  in two heterogeneous experiments, error bars represent standard deviation of the average values of the hydraulic conductivity.**

Figure 5.17 E shows the reduction of the hydraulic conductivity for the 150  $\mu\text{m}$  sand fraction when this sand fraction used as a porous media in four experiments. Figure 5.17 E shows the reduction of the hydraulic conductivity for the 150  $\mu\text{m}$  sand fraction when this sand fraction used as a porous media in four experiments. At first glance different bioclogging behaviour can be noted for this sand fraction in the four experiments, but in fact it is the opposite. This sand fraction clogged at the same rate in the four experiments and the variation in this figure only attributed to the initial values of the hydraulic conductivity which differ from one experiment to another. The presence of air bubbles in the beginning of each experiment is probably the reason behind the variance of the initial hydraulic conductivity readings for the same sand fraction in the four experiments.

As for the 63 $\mu\text{m}$  sand fraction which was used only in one experiment, it can be seen that the three sand columns have a very similar trend. This is shown in Figure 5.17F. Furthermore this sand fraction took additional time to clog than other sand fractions and due to that fact, no flow diversions can be observed during this experiment.

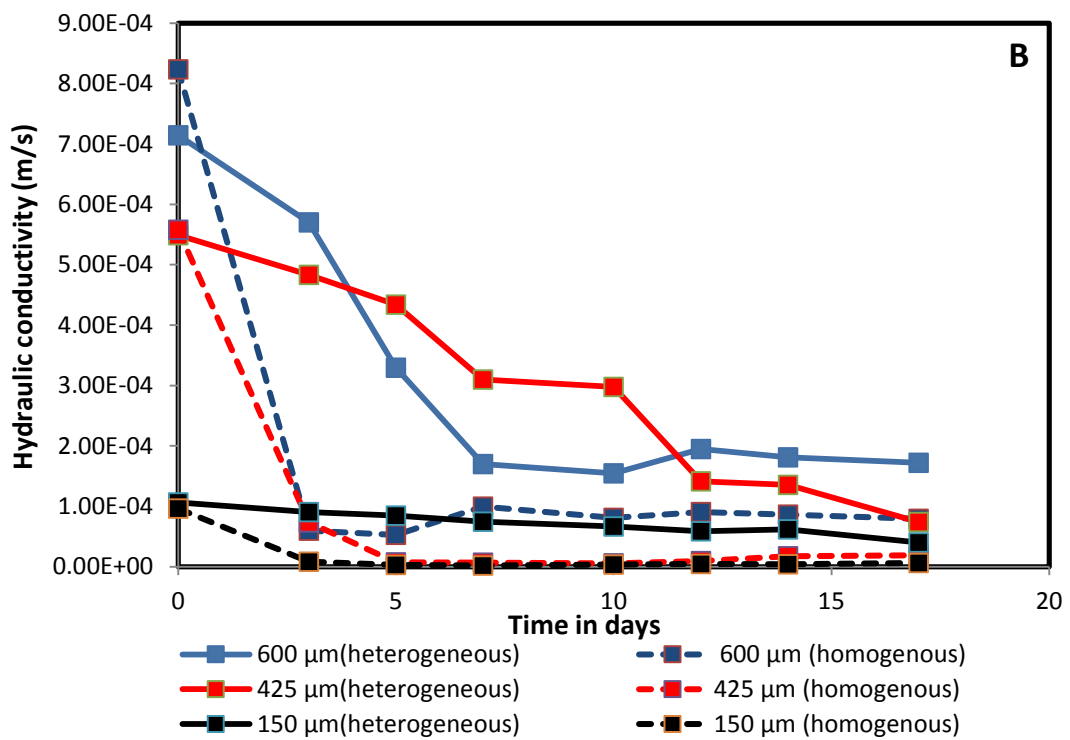
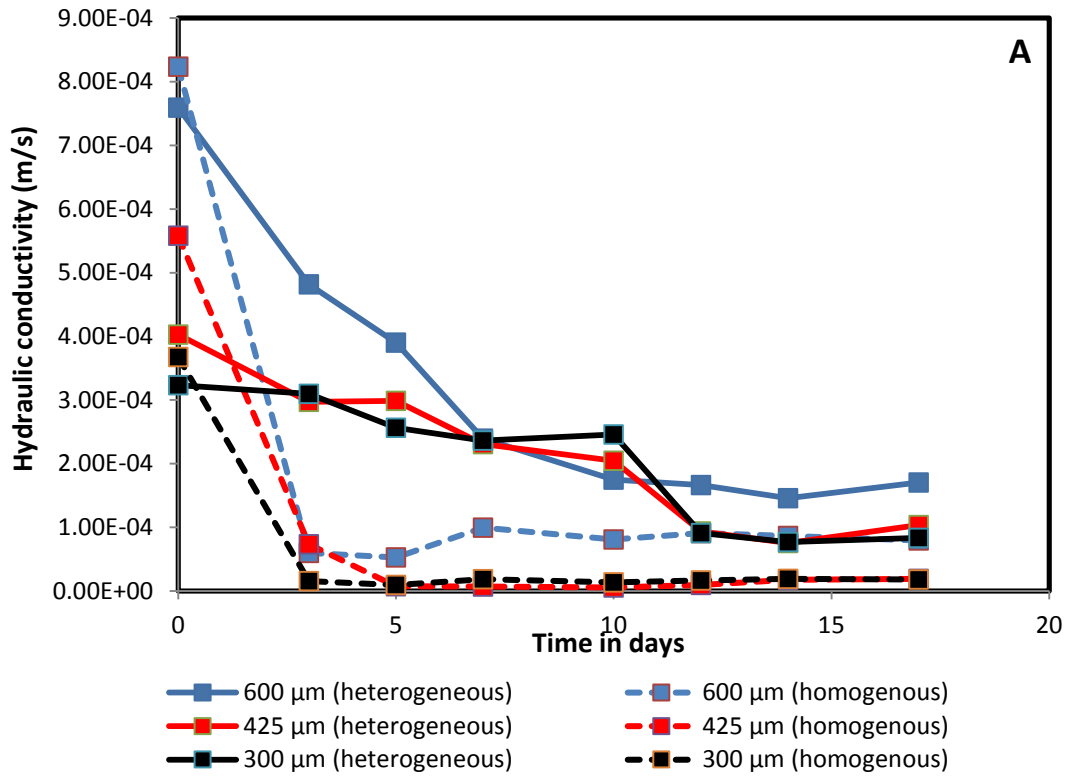


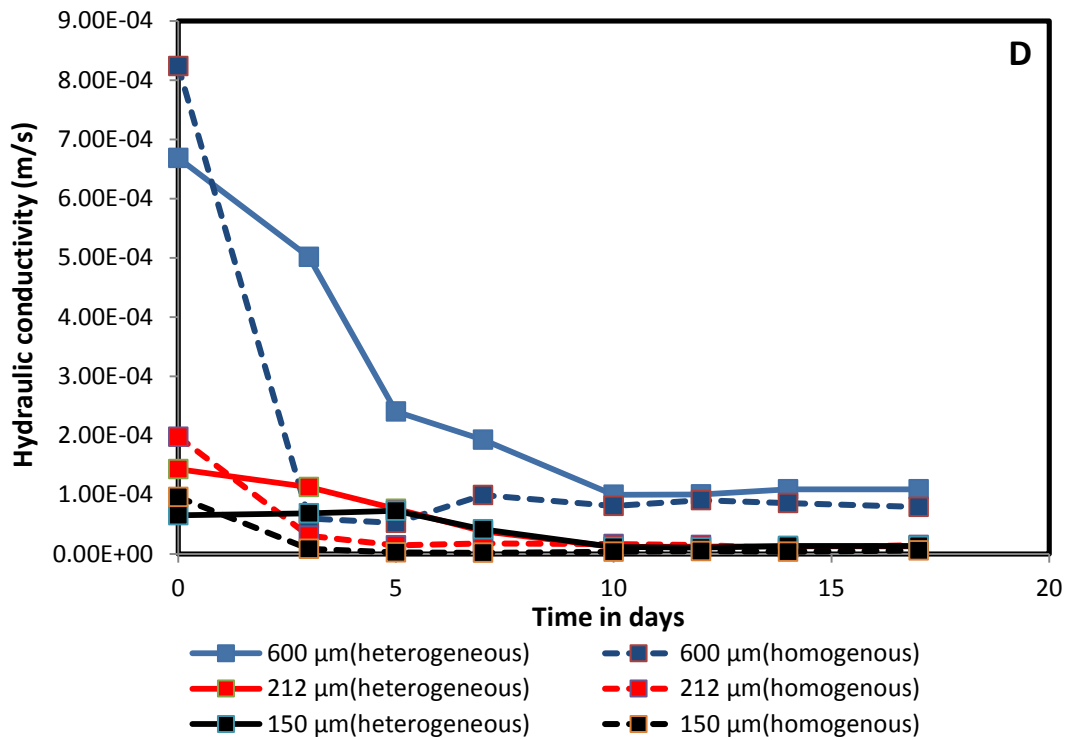
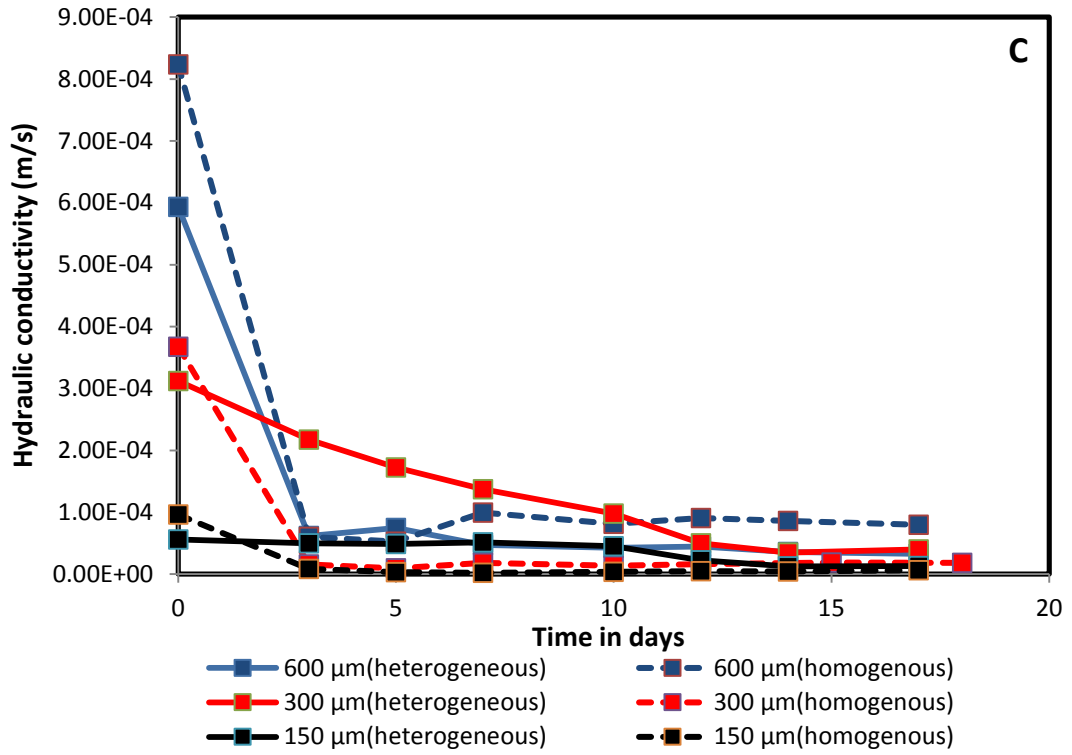
**Figure 5.17E: The changes of the hydraulic conductivity via time in the 150  $\mu\text{m}$  in four heterogeneous experiments, error bars represent standard deviation of the average values of the hydraulic conductivity.**

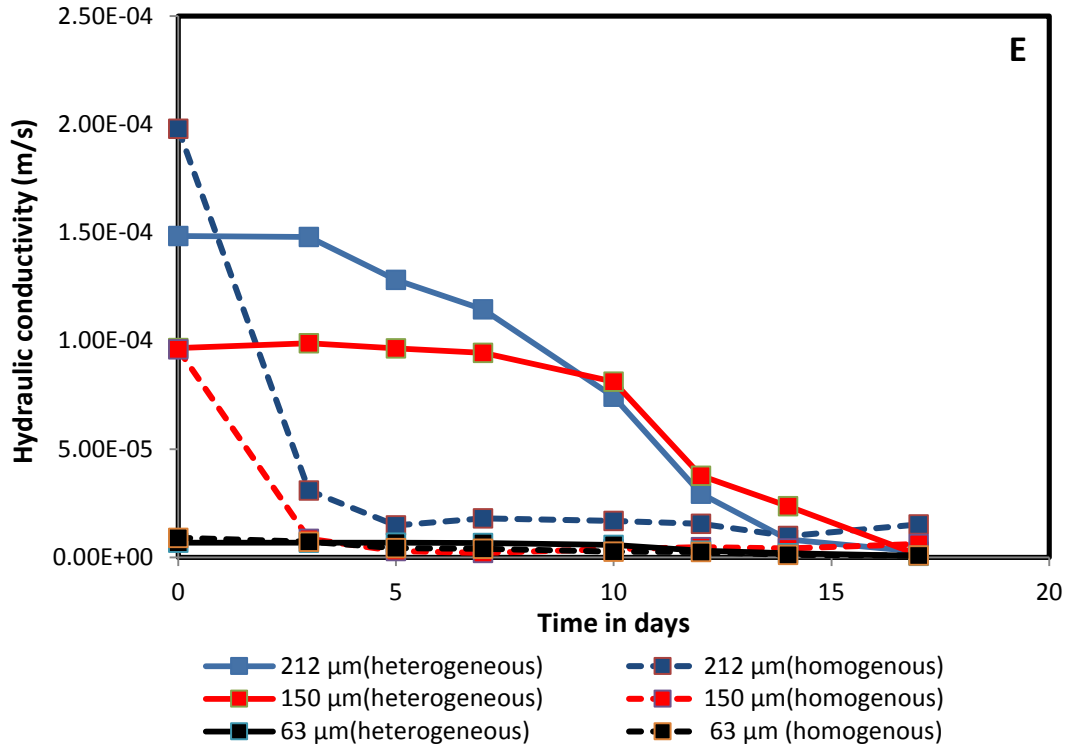


**Figure 5.17F: The changes of the hydraulic conductivity via time in the 63 μm in one heterogeneous experiment, error bars represent standard deviation of the average values of the hydraulic conductivity.**

By comparing the heterogeneous and homogenous experiments for the same sand fractions as shown in Figure 5.18A-E, it can be observed that the hydraulic conductivity in the homogenous experiments decreased sharply after three days of the nutrients delivery. In contrast, it takes more time to decrease in the heterogeneous experiments. The reason behind that can be attributed to the preferential flow in the heterogeneous columns which affects the amount of nutrients that delivered to each sand column.

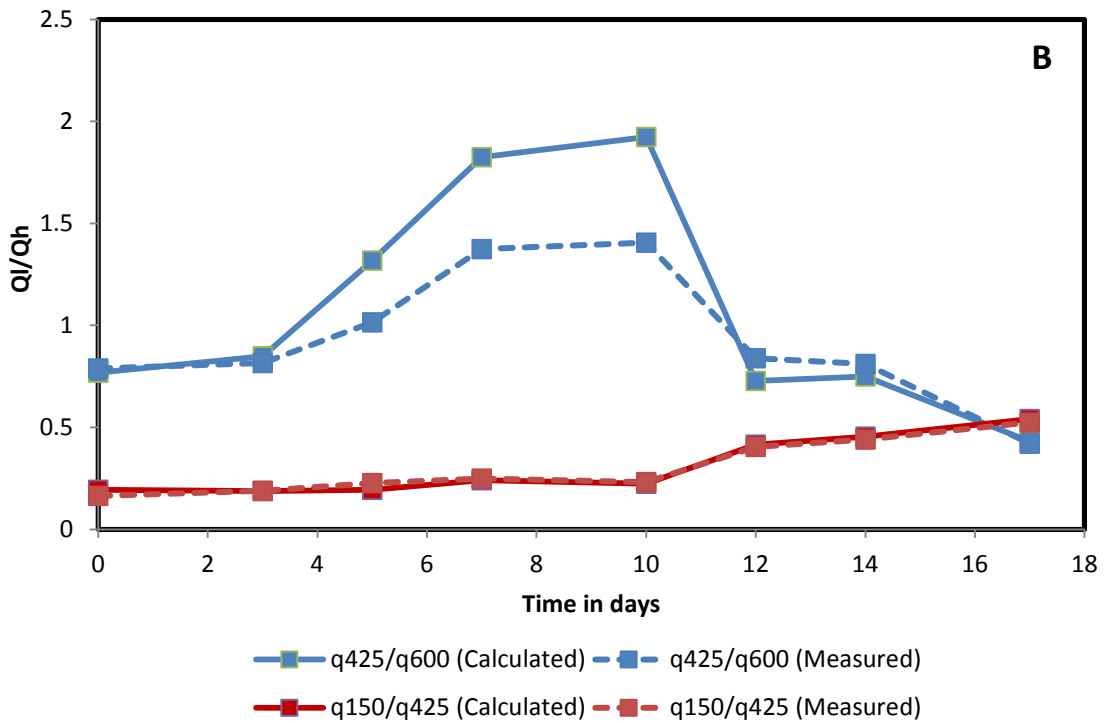
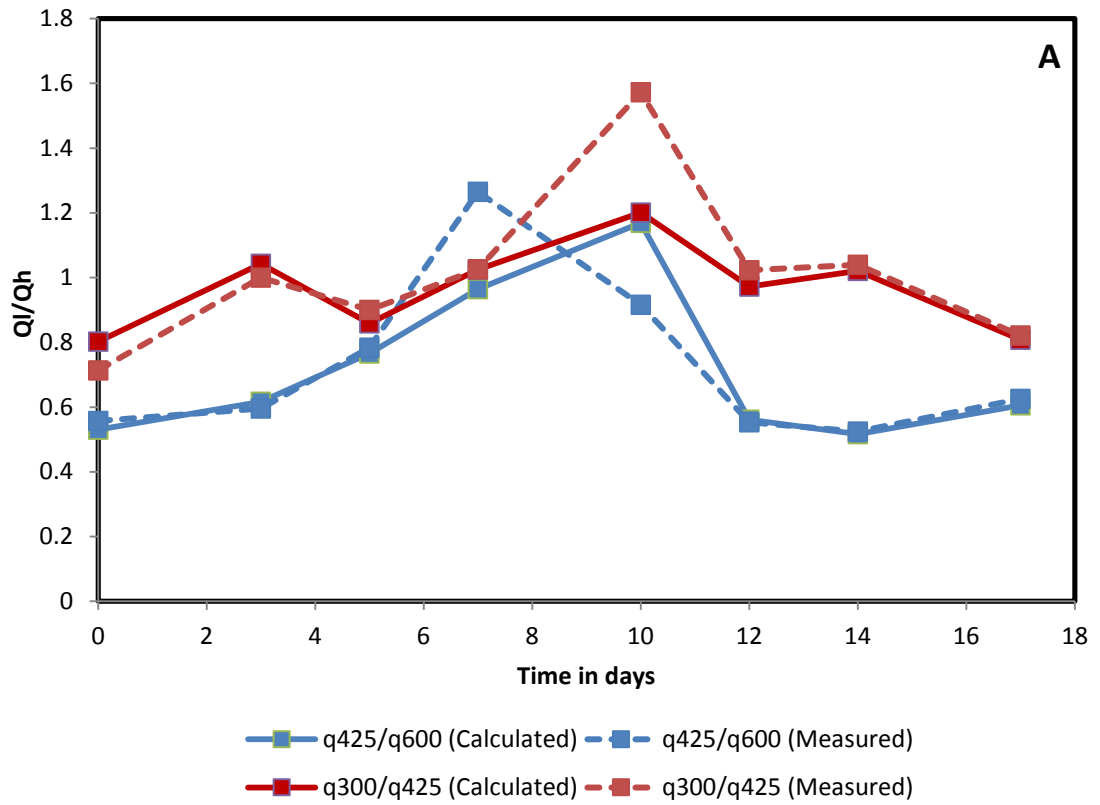


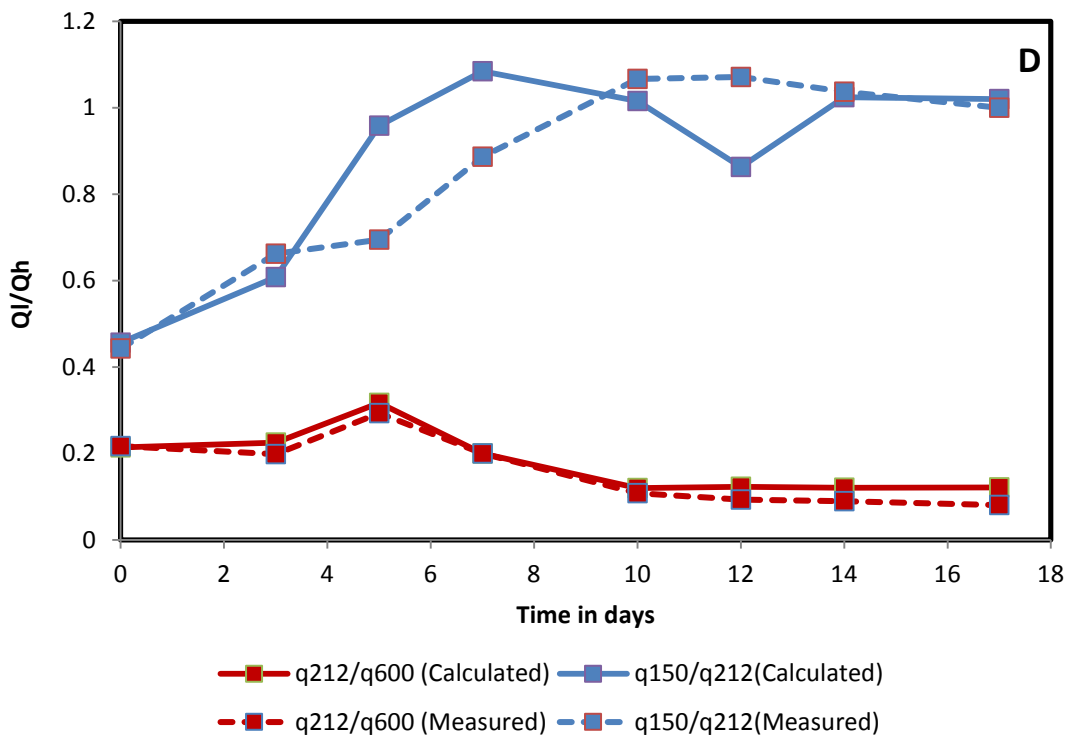
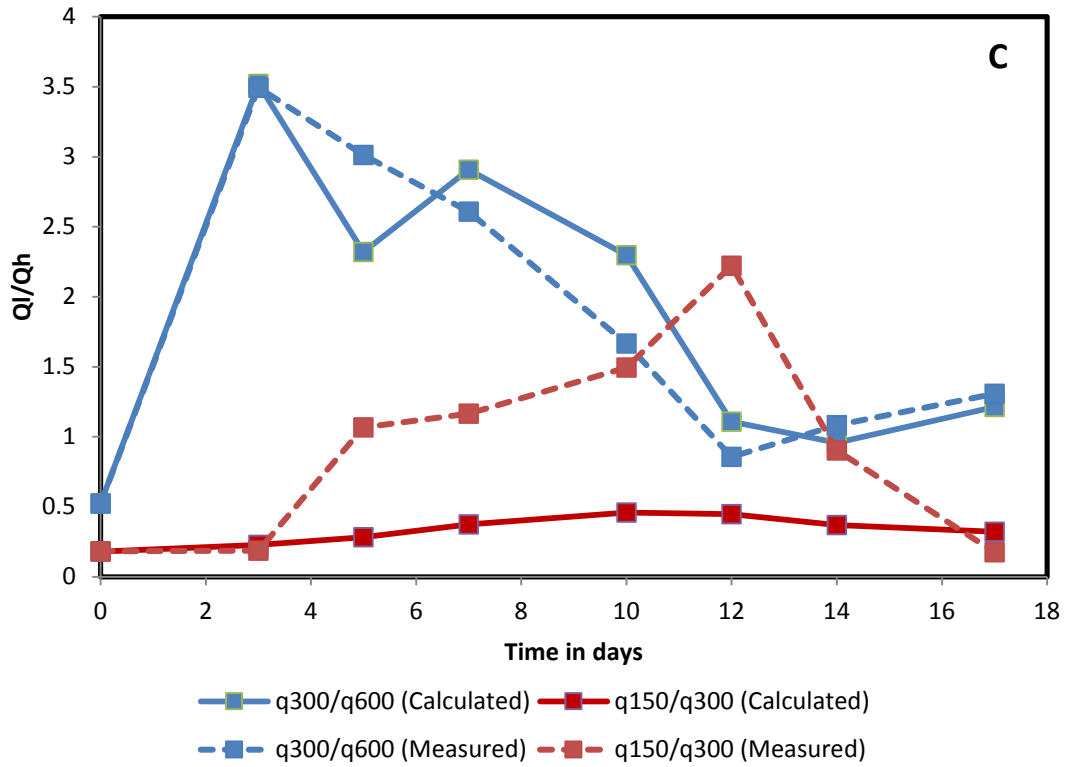




**Figure 5.18A-E: Comparisons between the homogenous and heterogeneous experiments for the same sand fractions.**

In order to monitor the flow rate fluctuations in each sand fraction, a ratio of the flow rate of the less permeable sand fraction ( $Q_l$ ) to that of the more permeable sand fractions ( $Q_h$ ) as a function with time calculated for each heterogeneous experiment as shown in Figure 5.19A-E.





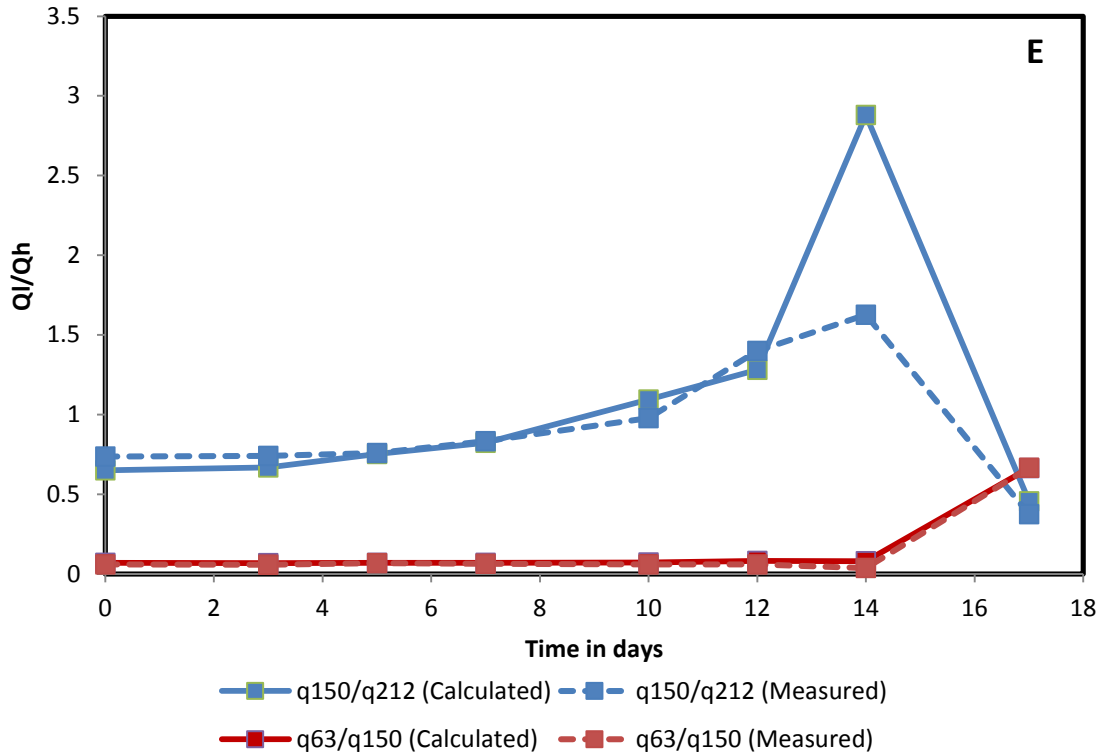


**Figure 5.19: Ratio of low to high flow rate via time for all heterogeneous experiments. A: EXP.(1), B: EXP.(2), C: EXP. (3), D: EXP.(4) and E: EXP.(5).**

Generally speaking, in all the heterogeneous experiments, the total flow rate decreased gradually with time until the end of each experiment, but the ratio of flow rate ( $Q_l$ ) the less permeable sand fraction of that of the more permeable sand fraction ( $Q_h$ ) was different depending on the range of the sand permeability in each experiment.

Regarding the first heterogeneous experiment EXP. (1), Figure 5.19A shows that the ratio of the flow rate ( $Q_{425}/Q_{600}$ ) is 1.17, whereas the ratio of flow rate ( $Q_{300}/Q_{425}$ ) was 1.20 by the end of day 10. These figures show that there is no clear change between the ratio of flow in 300 and 425 micron which means there is no apparent flow diversion between them.

With continuous feeding, the ratio of flow ( $Q_{425}/Q_{600}$ ) then decreased more by the end of day 12, remaining nearly constant until the end of the experiment. This trend

referred to the fact that the clogging of the 600 micron by the end of day 10 was due to the biomass accumulation possibly affecting the flow path and diverting it into the 425 and 300 micron, whilst the flow rate ratio ( $Q_{300}/Q_{425}$ ) stayed constant for the same period.

The results of the second experiment EXP. (2) as shown in Figure 5.19B indicate that by the end of day 5, the ratio of the flow ( $Q_{425}/Q_{600}$ ) was greater than 1.0 which further indicates that the 600 $\mu\text{m}$  became less permeable than the 425  $\mu\text{m}$  due to the clogging that was caused by the biomass accumulation. This situation continued until the end of day 12 where the ratio of flow ( $Q_{425}/Q_{600}$ ) declined and became less than 1.0. This decline of flow ratio might have occurred due to the clogging of the 425  $\mu\text{m}$  that resulted in the flow diversion from the 425  $\mu\text{m}$  into the 600  $\mu\text{m}$ .

On the contrary, the situation was different in the 150 micron where the ratio of flow rate ( $Q_{150}/Q_{425}$ ) gradually increased from 0.19 by day 3 into 0.54 by the end of the experiment. This trend indicated that the amount of the accumulated biomass might be not enough to clog the 150  $\mu\text{m}$  sand fraction at this time due to the high surface area of this sand fraction which needs more biomass to accumulate.

The results of the third experiment EXP.(3) as shown in Figure 5.19C reveal that the ratio of flow rate ( $Q_{300}/Q_{600}$ ) increased significantly from 0.5 to 3.5 after only three days of nutrients delivery; this great increasing might have attributed to the large reduction in the hydraulic conductivity of the 600  $\mu\text{m}$  sand fractions which consequently reduced the nutrient flow rate in this sand fraction. The significant reduction in hydraulic conductivity in the 600  $\mu\text{m}$  sand fraction could be the reasons that divert the flow from the 600  $\mu\text{m}$  into the 300  $\mu\text{m}$ , and resulted in more growth of

bacteria in the 300  $\mu\text{m}$  sand fractions thereby reduce the difference in permeability between 600 and 300  $\mu\text{m}$  by the end of the experiment.

On the other hand, the flow rate ratio ( $Q_{150}/Q_{300}$ ) increased slightly over time from an initial value of 0.17 to a final value of 0.32. This small increase of the flow rate ratio referred to the fact that the least permeable sand fraction 150  $\mu\text{m}$  possibly need more time to clog due to the high surface area of this sand fraction.

The results of the fourth experiment EXP.(4) as shown in Figure 5.19D show that the flow rate ratio ( $Q_{212}/Q_{600}$ ) experienced an initial increase during the first five days, then gradually decreased towards the end of the experiment to get a final value similar to the initial one. Whilst, the flow rate ratio ( $Q_{150}/Q_{212}$ ) increased to approximately 1.0 by the end of day 5 until the end of the experiment which means that the flow rate is nearly the same for the 150 and 212  $\mu\text{m}$  sand fractions. The increase of the flow rate ratio ( $Q_{212}/Q_{600}$ ) during the five days of the experiment could be occurred due to the fast clogging of the 600  $\mu\text{m}$  sand fractions compared to the slow reduction in the 212  $\mu\text{m}$  sand fractions. While, the following decrease of the flow rate ratio ( $Q_{212}/Q_{600}$ ) could be resulted from flow diversion from the 212 to 150  $\mu\text{m}$  sand fractions.

The results showed that the difference in the permeability between the 600 $\mu\text{m}$  sand fraction and the other two sand fractions (212 and 150 micron) is still high despite the continuous pumping of nutrients. This high difference in permeability could be attributed to the large surface area of the 212 and 150  $\mu\text{m}$  sand fractions that need more biomass to accumulate.

As regards the last experiment, Figure 5.19E shows that the ratio of flow rate for the 150  $\mu\text{m}$  sand fraction relative to the 212  $\mu\text{m}$  sand fraction ( $Q_{150}/Q_{212}$ ), and the ratio of the flow rate of the 63  $\mu\text{m}$  sand fraction relative to that of the 150  $\mu\text{m}$  sand fraction

(Q63/Q150). The results of this experiment show that on day14, the ratio of flow rate (Q150/Q212) was equal to 2.28 which mean that the 212  $\mu\text{m}$  at this time was almost clogged and became less permeable than the 150  $\mu\text{m}$  due to the accumulation of biomass which led to divert the nutrient solution into the 150  $\mu\text{m}$ . With continuous feeding the ratio of flow rate (Q150/Q212) decreased again, which means that the flow was diverted again into the 212 $\mu\text{m}$  sand fraction. Whilst the flow rate ratio (Q63/Q150) started to increase on day 14 of the experiment which means that the 63  $\mu\text{m}$  need more time to clog than the other sand fractions 212  $\mu\text{m}$  and 150  $\mu\text{m}$ .

The results of the loss on ignition for each experiment as illustrated in the Figure 5.4A-E, which shows the biomass distributed in each zone for each sand fraction. In these figures it can note that biomass amount throughout each sand column distributed in a homogeneous way. The results of this study are relatively consistent with results observed by Seki (2013) who concluded that biological clogging may start from the middle or bottom of the flow column and with the results of Cunningham *et al.* (1991) who also reported that the biomass distributed in a homogeneous way throughout each sand column.

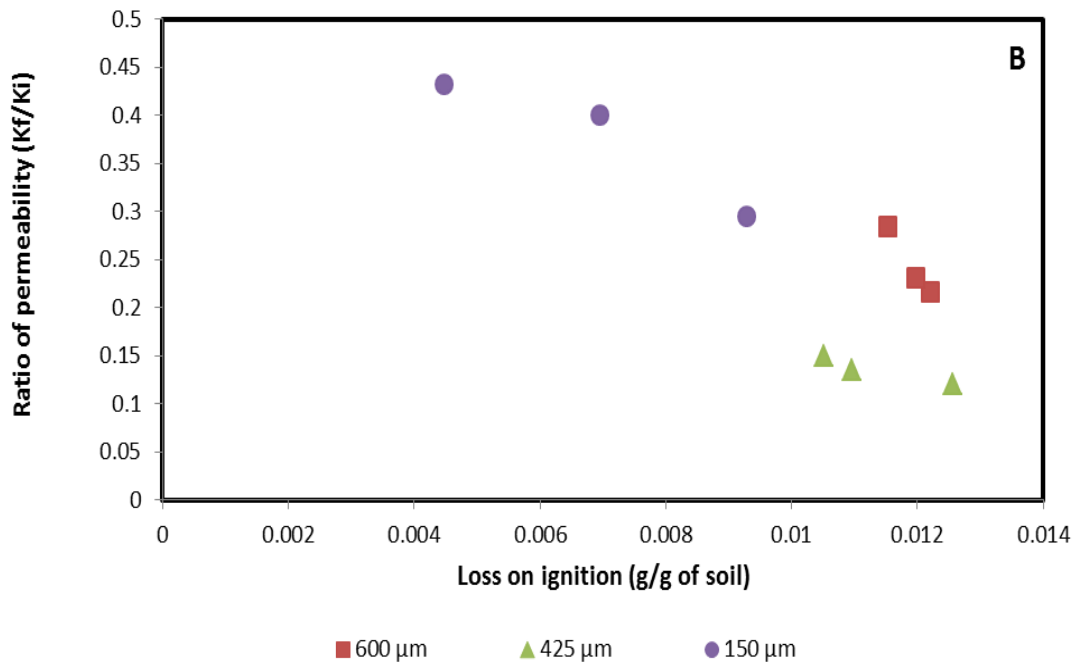
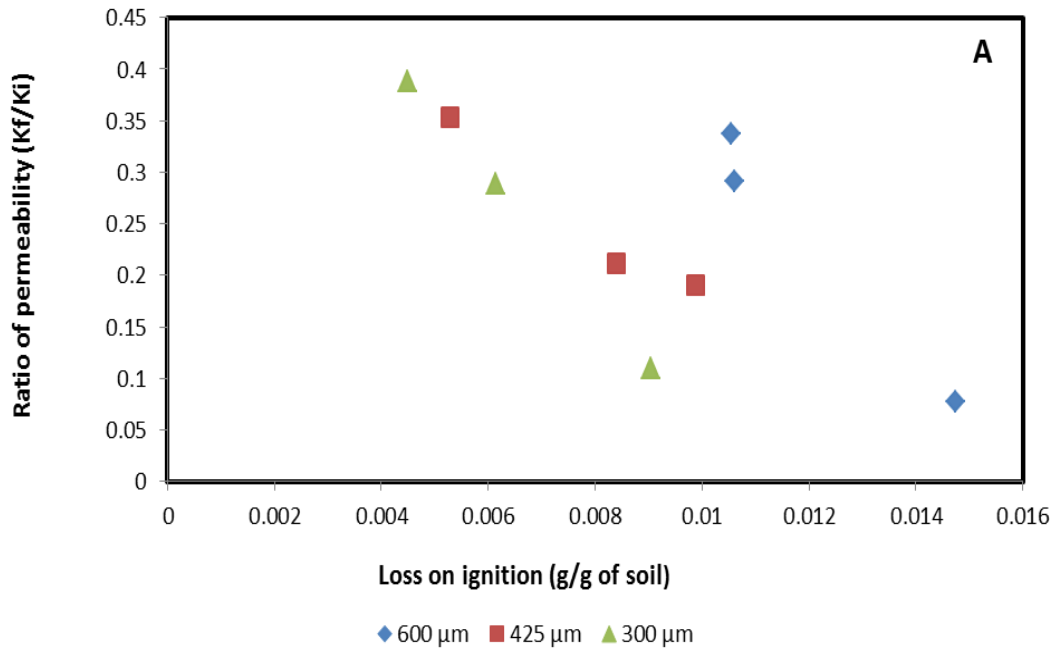
Furthermore, soil samples which were collected at the end of each experiment and analysis for loss on ignition indicated that the amount of average biomass accumulation for the larger particles was greater than the small particles as shown in Figure 5.5A-E.

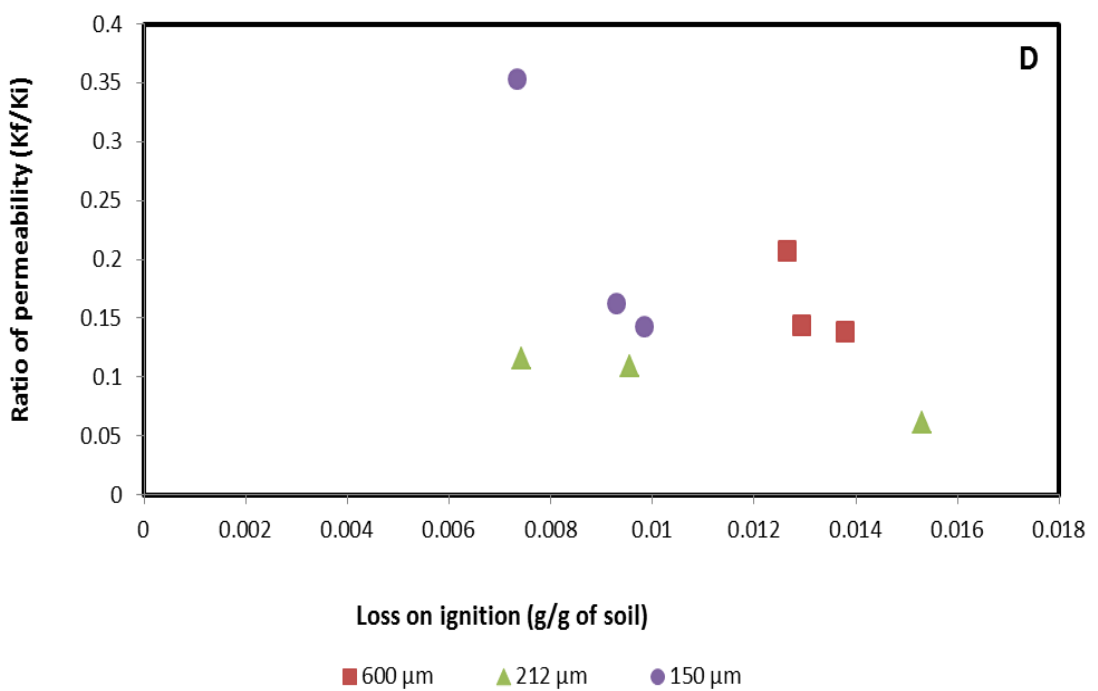
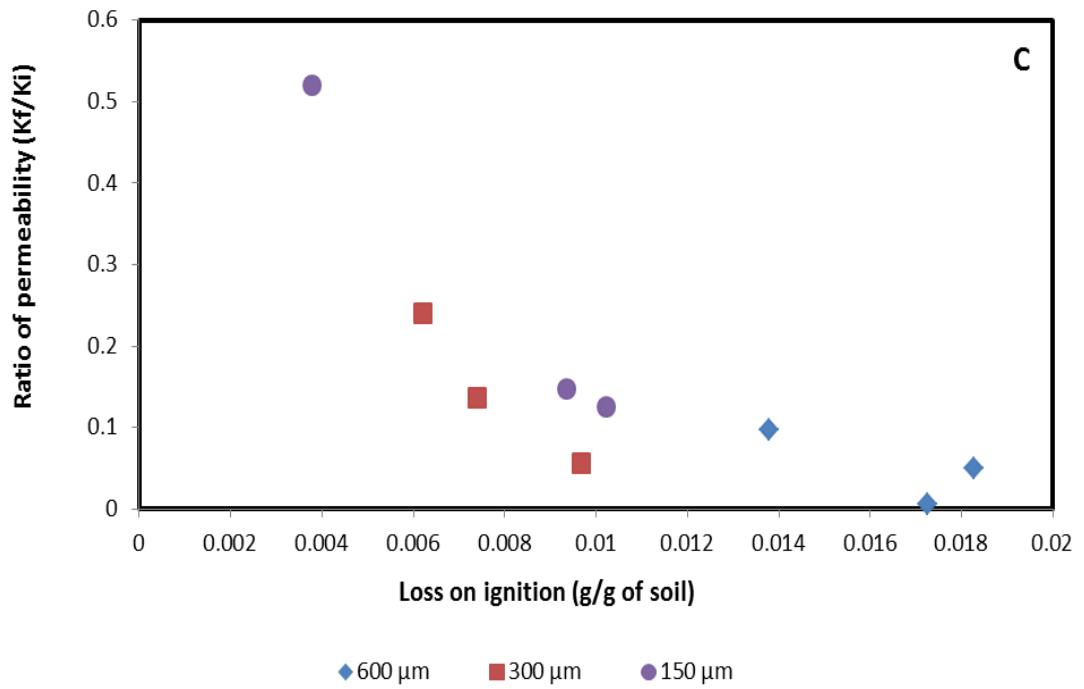
By using these data, loss on ignition was correlated with the relative hydraulic conductivity ( $K_{rel}$ ) for each set of heterogeneous experiments as shown in Figures 5.20A-E. The relative hydraulic conductivity ( $K_{rel}$ ) can be defined as the hydraulic conductivity of the clogged porous media at each time interval divided by the

hydraulic conductivity of the clean porous media. Figure 5.20A, presents the relation between the loss on ignition and relative hydraulic conductivity ( $K_{rel}$ ) for three columns of the three sand fractions 600, 425, and 300  $\mu\text{m}$ .

Regarding the heterogeneous experiment which included the use of two high permeable sand fractions 600 and 425  $\mu\text{m}$  and one low permeable one 150  $\mu\text{m}$ , the results indicated that the large sand fraction has the greatest amount of biomass as shown in Figure 5.19B which links relative hydraulic conductivity with loss on ignition for three columns for each sand fraction. Similar trends can be detected for the other heterogeneous experiments as shown in Figure 5.20C-E.

In general, these figures show that it is not easy to link between the loss on ignition and relative hydraulic conductivity ( $K_{rel}$ ) for the six sand fractions. This could be attributed to the pore structure of each sand fraction which affects the relation between the hydraulic conductivity and biomass and vary from fraction to fraction. But it could be noticed that the larger grain size has the greatest amount of biomass as mentioned previously. This might be occurred due to the large void volume, where the bacteria have the access to much more amounts of nutrients. These findings agree with the literature (Cunningham *et al.*, 1991 and Bielefeldt *et al.*, 2002) who all reported that the larger sand fraction has the greater amount of biomass.





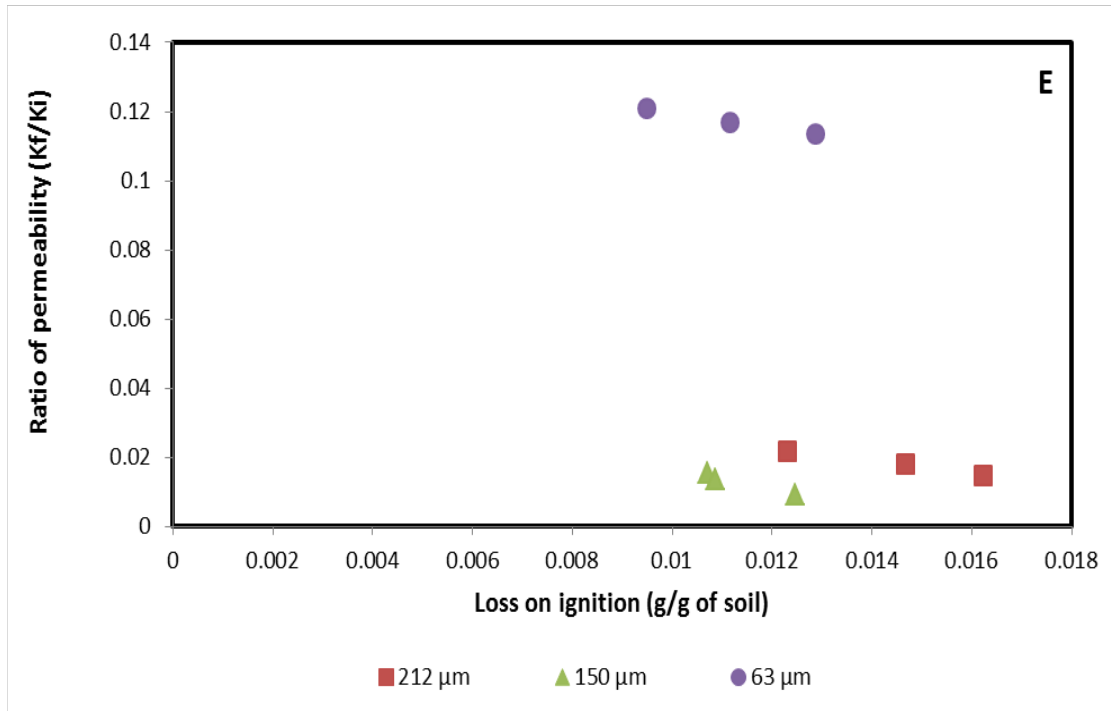


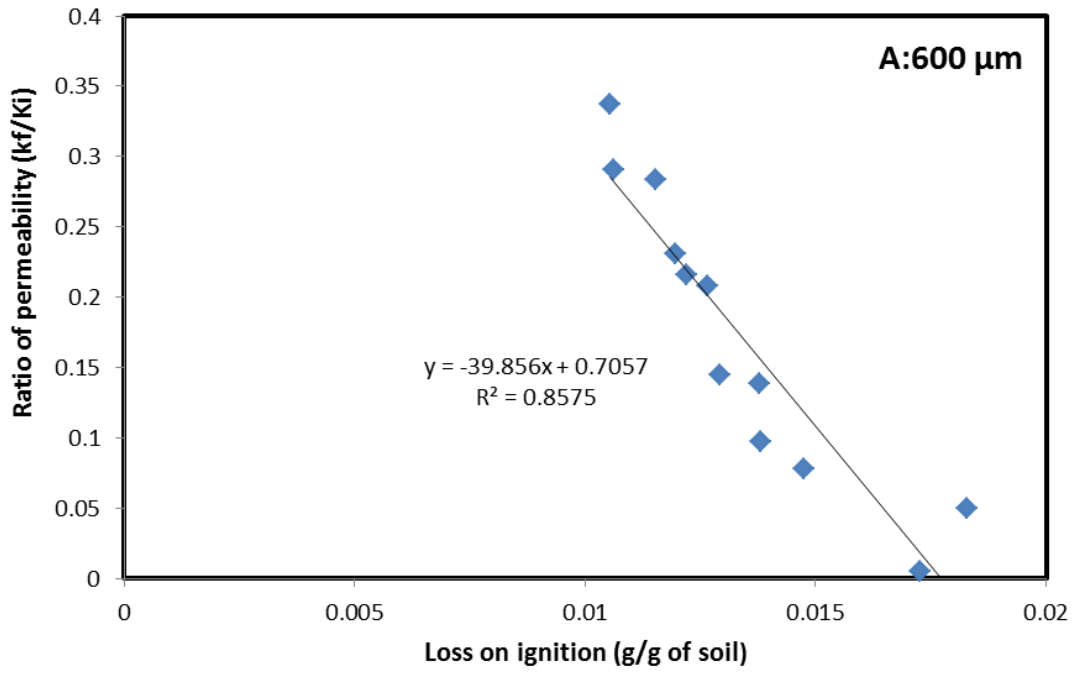
**Figure 5.20: Relation between relative hydraulic conductivity and loss on ignition for the three columns of each set of sand fractions and for all heterogeneous experiments.**

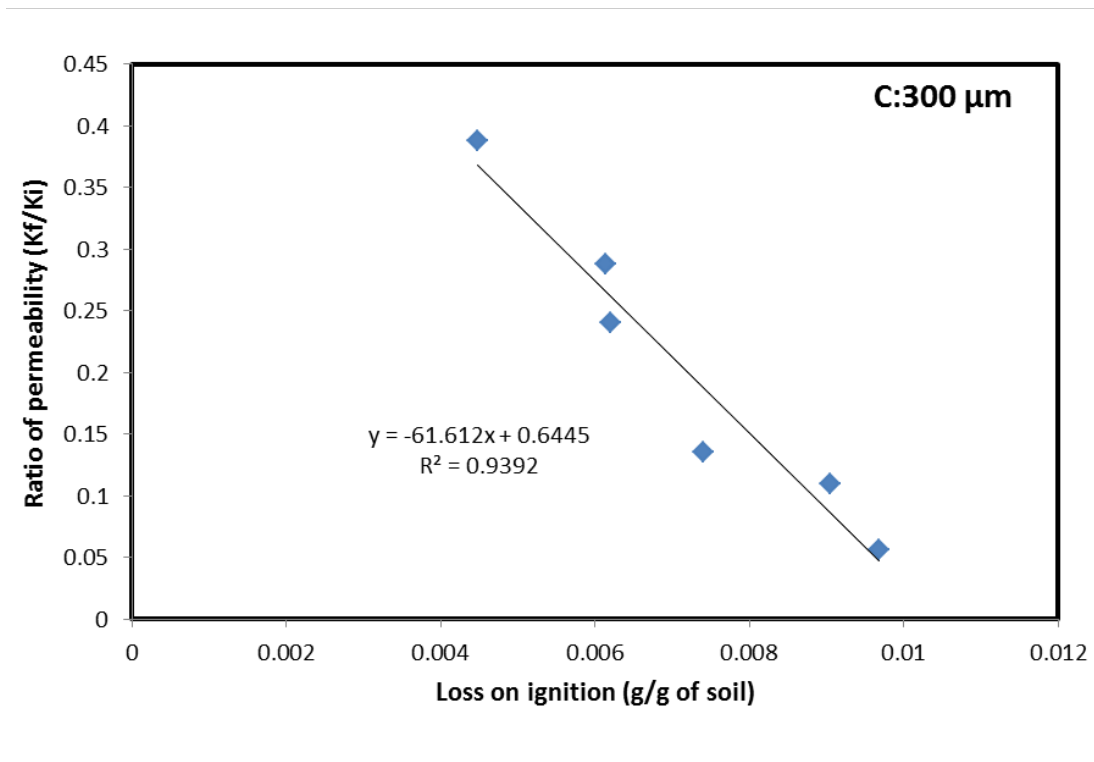
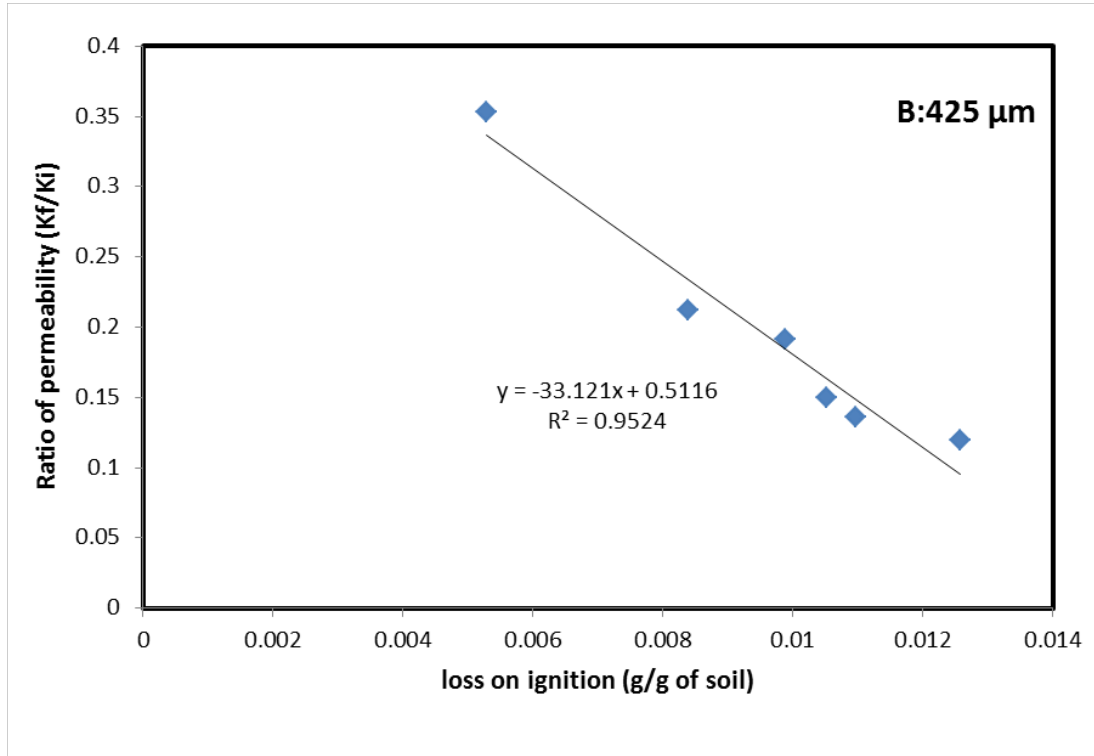
On the other hand, the relation between relative hydraulic conductivity and loss on ignition for each sand fraction was calculated by using the values of the loss on ignition and the corresponding values of the relative hydraulic conductivity for the six sand fractions as illustrated in Figures 5.21A-E

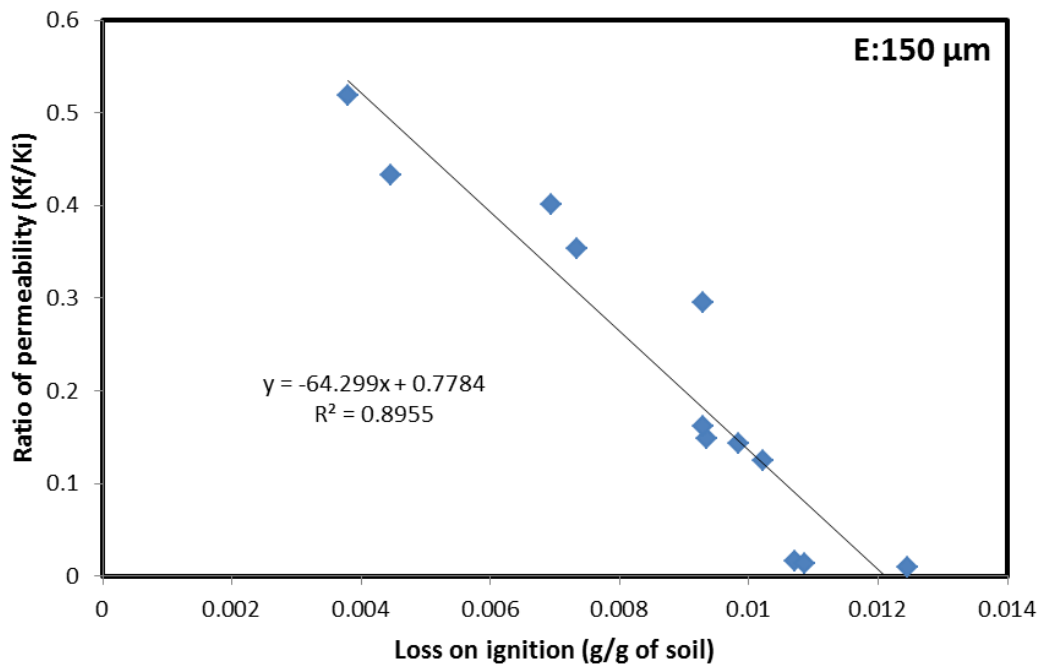
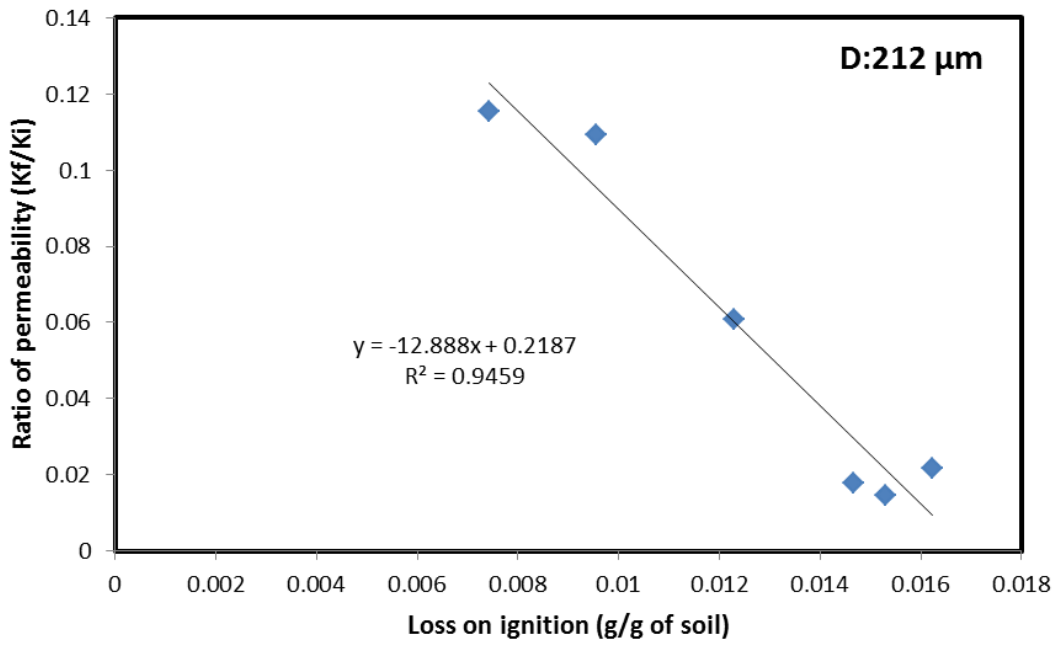
In these figures it can be observed that the hydraulic conductivity values decreased with the increase of loss on ignition for the six sand fractions 600, 425, 300, 212, 150, and 63 μm. This indicates that the biomass accumulation is responsible for the decline in hydraulic conductivity values.

This outcome agrees with the results of Bielefeldt *et al.* (2002) who confirm that bioclogging account for the reduction in hydraulic conductivity because there was more biomass clogging the pores in the larger grain size. Seki *et al.* (2005) also detected that hydraulic conductivity decreased exponentially with the loss on ignition

which suggests that the organic matter was responsible for the decrease in hydraulic conductivity values.







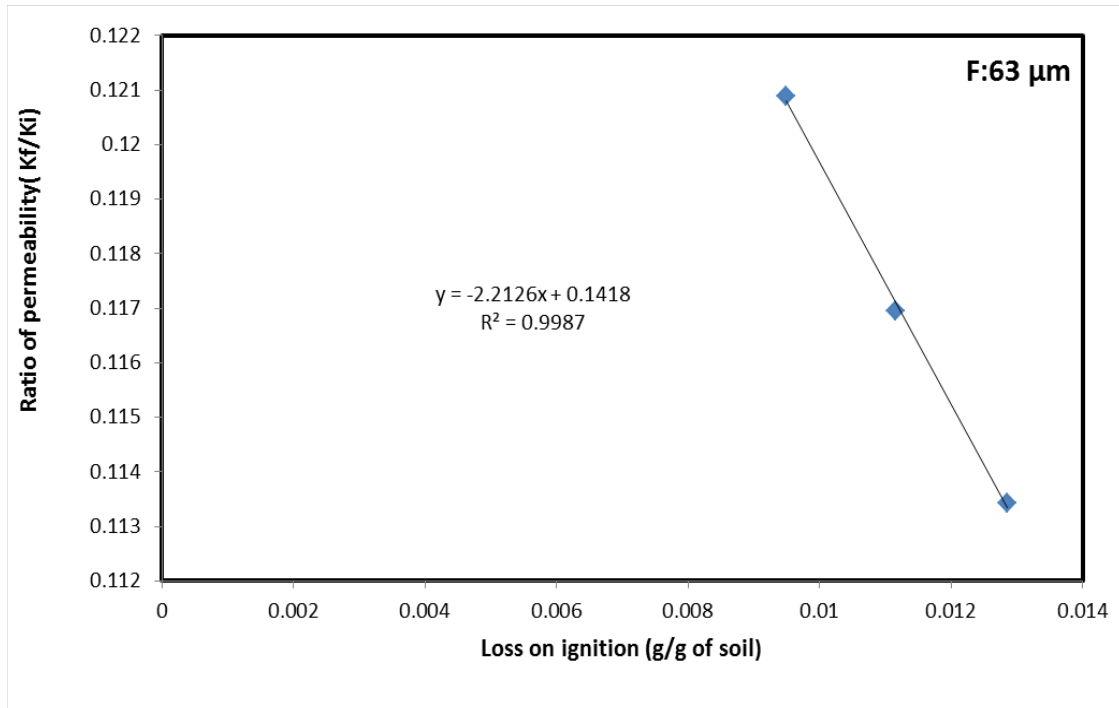


**Figure 5.21: Relation between loss on ignition values and relative hydraulic conductivity for six sand fractions.**

These relationships could be used to calculate the relation between the loss on ignition and relative hydraulic conductivity for another set of sand fractions which were not focused on in this study due to the time frame. The analysis of the total number of bacteria for each sand column was carried out to estimate how the cells were distributed at the end of each experiment.

In all the column heterogeneous experiments the number of cells significantly increased compared to the control columns that did not show any changes in the number of cells for the three sand fractions. The increase of cell numbers in the biological columns probably occurred due to the nutrient availability which enhanced the growth of bacteria in each sand column.

As for the links between the cells number and loss on ignition, the results showed that there is no remarkable correlation between the total number of cells and the

corresponding loss on ignition values which indicates that the reduction of the hydraulic conductivity attributed only to the biomass accumulation which formed by EPS not cells.

The results of the preliminary experiment which was carried out to investigate the effect of the different concentrations of zinc 0.1-0.5 mM on the bacterial growth showed that the concentration of 0.1 mM of zinc resulted in increasing the optical density of the bacterial suspension. Whilst, the optical density of the bacterial suspension, decreased by increasing zinc concentrations.

The increase of the optical density of the bacterial suspension could be ascribed to the resistance of cells to the low concentrations of zinc, whereas the decreased of it could be attributed to the toxicity of cells with increasing the concentrations of zinc.

The outcomes of this experiment greatly match with the results of Mittal and Goal (2010) who reported that microbes show greater optical density values in the absence of metal ions.

In relation to the results of the bioclogging experiments in the contaminated heterogeneous porous media which were carried out to investigate how the biological control of groundwater could be used in the treatment of contaminated land. It can observe that the reduction in hydraulic conductivity in the 600  $\mu\text{m}$  resulted in diverting much of the nutrient solution into the less permeable sand fraction 300  $\mu\text{m}$  which has a smaller permeability than 600  $\mu\text{m}$ , thereby caused a more growth of cells and subsequently more production of EPS which filled the pore volume and caused bioclogging in this sand fraction as well.

The same scenario was noted in the least permeable sand fraction 150  $\mu\text{m}$  which clogged significantly after receiving enough amount of nutrient solution. On the other

hand, the hydraulic conductivity values in all sand fractions remained constant over time in the control experiment.

By comparing the results of this experiment with the previous experiment EXP.(3) as shown in Figure 5.22 it can notice that the reduction of the hydraulic conductivity in both experiments almost the same for the three sand fractions.

The analysis of the outflow water samples which were collected regularly during the measurements of the hydraulic conductivity showed that the highest sorption capacity of zinc was detected in 150  $\mu\text{m}$  the least permeable sand fraction, whereas the lowest sorption capacity of zinc was detected in 600  $\mu\text{m}$  the high permeable sand fraction.

The explanation of this difference could be related to the adsorption capacity of each sand fraction which increased by decreasing the particle grain size. This outcome considerably match with the results of Kumar *et al.* (2013) who reported that the adsorption capacity of soil increased by decreasing the particle grain size due to high surface area of fine particle grain size that absorbs more metal ions.

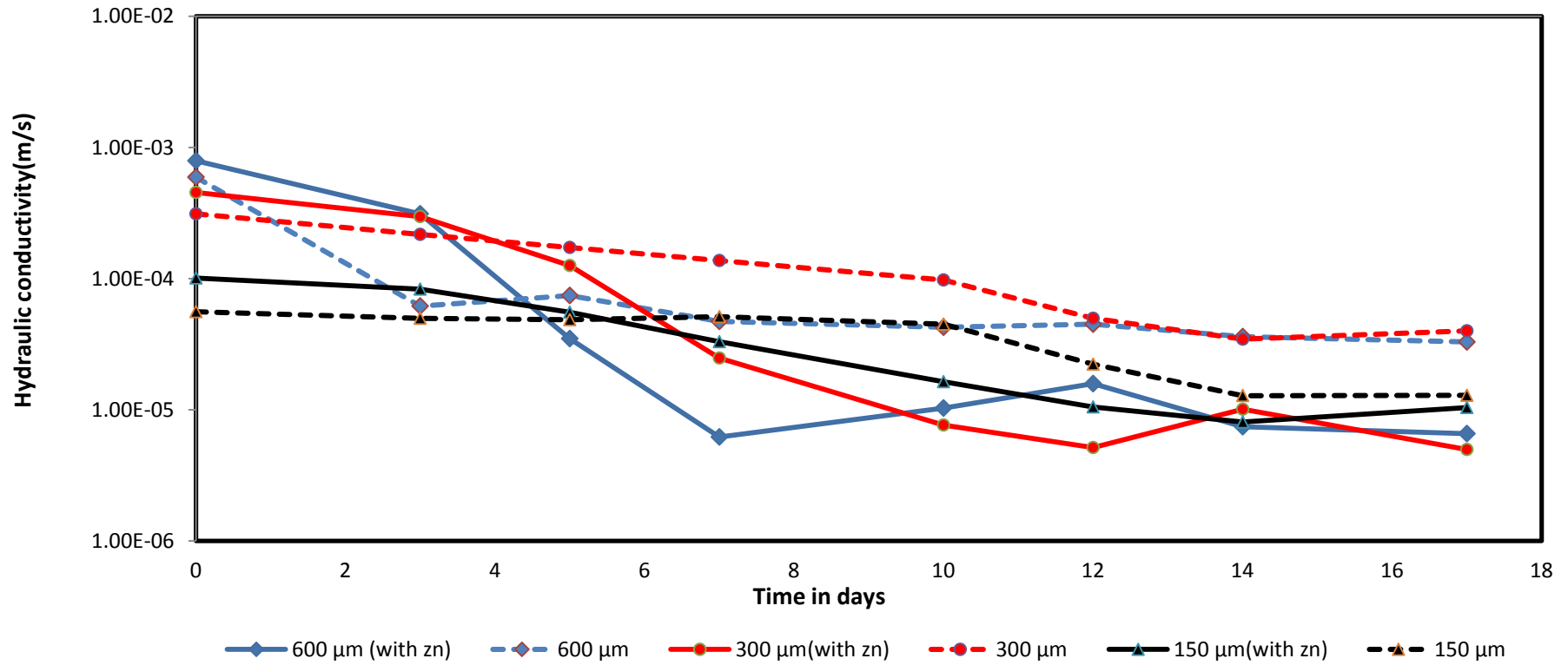


Figure5.22: Comparison between the changes of the hydraulic conductivity values for three sand fractions in clean and contaminated porous media.

On the contrary, the control experiment that did not show any significant changes of zinc concentrations with time; this could be attributed to the high adsorption capacity of sand for zinc with the absence of bacteria.

As for the loss on ignition, the results of this analysis showed slightly similar trend for the previous five heterogeneous experiments, where the largest sand fraction has the large amount of biomass.

**THEORETICAL ANALYSIS OF THE EXPERIMENTAL WORK**

**6.1 Introduction**

Generally mathematical bioclogging models are used to improve the understanding of bioclogging processes in porous media. There are many approaches to model the changes of the hydraulic conductivity in porous media. Most of these models link the changes of the hydraulic conductivity with the related changes in porosity due to the accumulation of the amount of biomass in porous media.

The aim of this chapter is to calculate the theoretical hydraulic conductivity changes with time, depending on the development of mathematical models and in cooperation with the previous mathematical models which linking the relative hydraulic conductivity with the relative porosity.

Table 6.1: Parameters used in the bioclogging models

Parameter	Description
$k$	The saturated hydraulic conductivity
$Q$	The flow rate (cm/sec)
$t$	The time (sec)
$dh/dl$	The hydraulic gradient
$A$	The cross section area (cm <sup>2</sup> )
$Q_i$	The flow rate (ml/min)
$k_{rel}$	The relative hydraulic conductivity
$n_{rel}$	The relative porosity
$k_c$	The relative hydraulic conductivity of the plug
$n_c$	Critical porosity change at which biofilm growth switches into plug growth
$\emptyset(\eta_{rel})$	Distribution function describing how many pores show biofilm growth and plug growth, respectively
$V_t$	The volume of the sand column (cm <sup>3</sup> )
$V_s$	The volume of sand particles (cm <sup>3</sup> )
$r$	The radius of the soil particles (cm)
$a$	The unit cell dimension (cm)
$y$	The thickness of the cylinder which fits inside the pore body of the body centred cubic unit cell (cm)
$x$	The radius of the cylinder which fits inside the pore body of the body centred cubic unit cell (cm)
$G_m$	Glucose mass (g)
$G_c$	Glucose concentration (g/l)
$EPS_m$	EPS mass in (g/l)
$EPS_v$	EPS volume in (cm <sup>3</sup> )
$EPS_d$	EPS density (g /cm <sup>3</sup> )
$V_{pf}$	Final pore throat volume (cm <sup>3</sup> )
$V_{pi}$	Initial pore throat volume (cm <sup>3</sup> )
$\eta_f$	Final porosity
$\eta_o$	Initial porosity

## 6.2 Pore bioclogging model

In this study, the observed changes of hydraulic conductivity with time were compared with the predicted values using different bioclogging models such as the biofilm or plugs (Vandevivere *et al.*, 1995), micro-colony (Okubo and Matsumoto, 1979), and macroscopic (Clement *et al.*, 1996) models. The changes of the hydraulic conductivity with the related changes in porosity due to the accumulation of the amount of biomass in porous media was

modelled by assuming bioclogging occurs in the pore throat due to the accumulation of biomass. Moreover, it was assumed that the amount of EPS produced due to the consuming of the entire substrate by the bacteria, and by assuming that the EPS density equal to  $1.1\text{g/cm}^3$ , the volume of EPS was calculated to use after for calculating the final porosity of the porous media.

The pore volume is based on the pore shape which certainly depends on the shape and the arrangements of the soil particles. These particles were assumed spherical with constant diameter because the spherical shape is an ideal model. The particles can be arranged in different ways such as; simple cubic, body centred cubic and face centred cubic. These terms usually used in materials science to describe the atomic packing and called crystal system. Crystal system is composed of three space lattices, or unit cells *simple cubic (SC)*, *body centred cubic (BCC)*, and *face-centred cubic (FCC)* (Mitchell, 2004).

In this model the porous media particles were assumed to line up in a body centred cubic way as shown in Figure 6.1. This assumption depends on the value of the porosity of this structure which is about 0.32 according to equation (6.12). The porosity of this structure is slightly close to the porosity of the porous media which were calculated in the bioclogging experiments. The porosities of the other packing models (simple cubic and face centred cubic) structure are 0.48 and 0.26 respectively (Mitchell, 2004).

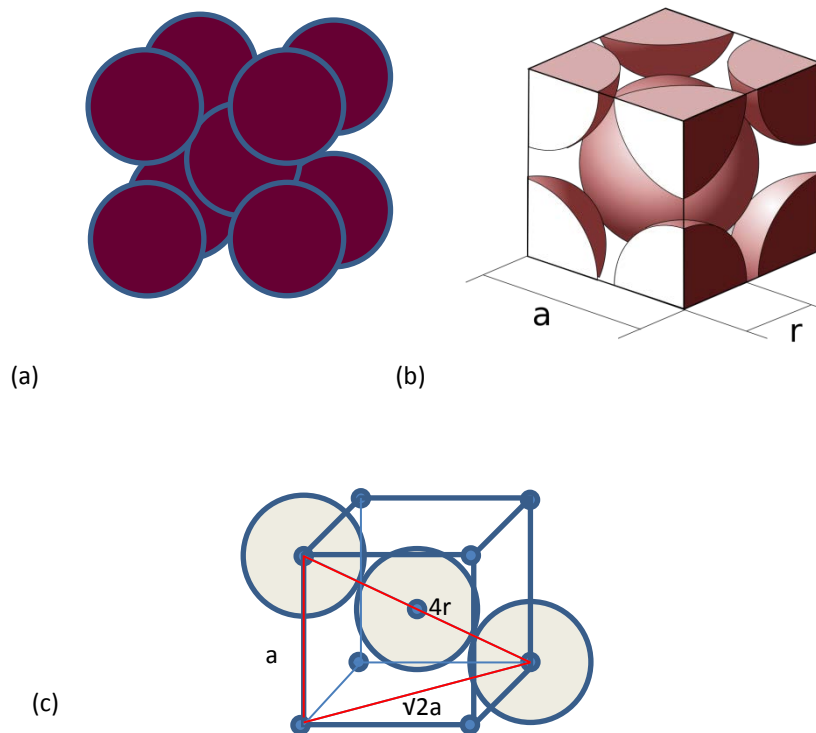


**Figure 6.1: (a) Body-centred cubic (b) Body-centred cubic unit cell (c) Section in body-centred cubic.**

The volume of the body centred cubic cell is  $a^3$ , and according to Figure 6.1, the number of atoms or spheres in the body centred cubic BCC unit cell:

Pythagoras's theorem can be used to link the unit cell dimension ( $a$ ) with the radius of the particle ( $r$ ).

$$(4r)^2 = a^2 + (2\sqrt{a})^2 \quad 6.1$$

$$a = \frac{4r}{\sqrt{3}} \quad 6.2$$

The total pore volume can be calculated by subtracting the volume,  $V_s$  of the sand particles from the unit cell volume. The volume of sand particles is equal to the volume of two spheres.

$$V_s = 2 \cdot \left(\frac{4}{3}\right)\pi r^3 \quad 6.3$$

$$V_s = \left(\frac{8}{3}\right)\pi r^3 \quad 6.4$$

The total volume of the unit cell,  $V_t$  is  $a^3$ , and by substituting the value of  $a$  in the equation 6.4 can be defined as:

$$V_t = \left(\frac{4r}{\sqrt{3}}\right)^3 \quad 6.5$$

The porosity of the body centred cubic unit cell which is equal to 0.32 can be calculated as:

$$\text{Unit cell porosity} = 1 - \frac{V_s}{V_t} \quad 6.6$$

$$\text{Unit cell porosity} = 1 - \frac{\left(\frac{8}{3}\pi r^3\right)}{a^3} \quad 6.7$$

$$\text{Unit cell porosity} = 1 - \frac{\left(\frac{8}{3}\pi r^3\right)}{\left(\frac{4r}{\sqrt{3}}\right)^3} \quad 6.8$$

$$\text{Unit cell porosity} = 0.32 \quad 6.9$$

The total void volume  $V_v$ , can be defined as:

$$V_v = \left(\frac{4r}{\sqrt{3}}\right)^3 - \left(\frac{8}{3}\right)\pi r^3 \quad 6.10$$

$$V_v = \frac{r^3(64-8\pi\sqrt{3})}{3\sqrt{3}} \quad 6.11$$

Through Figure 6.2 the appropriate large shape that could fit inside the pore throat was assumed to be an ellipsoid. The ellipsoid is the more realistic shape because in this model the pore throat volume was assumed to fill up first and approximately the only realistic shape that could fill up all the pore throat spaces is the ellipsoid shape.

The pore throat volume can be calculated by subtracting the volume of the largest ellipsoid which can be drawn inside the total pore volume from the total pore volume. Six ellipsoids with semi-principal axes of length,  $x$ ,  $x$  and  $y/2$  can be fit inside the body centred cubic unit cell.

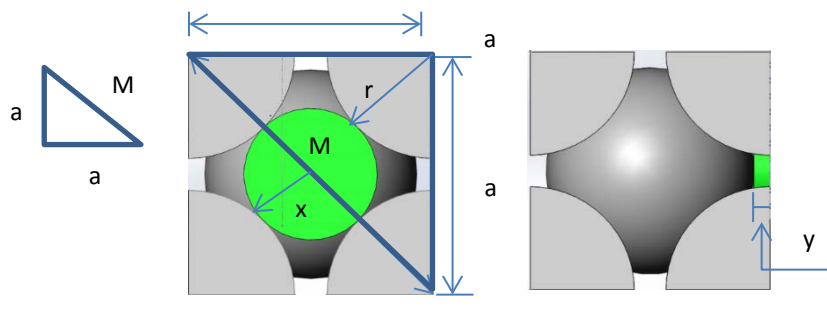


**Figure 6.2: The Pore body inside the body centred cubic unit cell.**

According to Figure 6.2 the following relations can be written:

$$x = (a\sqrt{2} - 2r)/2$$

$$y = (a-2r)/2$$

And so

$$x = \frac{r(2\sqrt{2}-\sqrt{3})}{\sqrt{3}} \tag{6.12}$$

$$y = \frac{r(2-\sqrt{3})}{\sqrt{3}} \tag{6.13}$$

The volume of the large ellipsoid which can be fitted inside the void volume is calculated as below:

$$\text{Ellipsoid volume} = \frac{4\pi}{3} x \cdot x \cdot \frac{y}{2}$$

$$\text{Ellipsoid volume} = \frac{2\pi r^3 (2-\sqrt{3})(2\sqrt{2}-\sqrt{3})^2}{9\sqrt{3}} \quad 6.14$$

According to Figure 6.2, there are six ellipsoids and therefore the total volume of the larger voids will be as below:

$$\text{Ellipsoid volumes} = \frac{4\pi r^3 (2-\sqrt{3})(2\sqrt{2}-\sqrt{3})^2}{3\sqrt{3}} \quad 6.15$$

Then the pore throat volume can be calculated by subtracting the ellipsoids volume from the total void volume.

$$\text{SmallPore volume} = \left[ \frac{r^3 (64-8\pi\sqrt{3})}{3\sqrt{3}} \right] - \left[ \frac{4\pi r^3 (2-\sqrt{3})(2\sqrt{2}-\sqrt{3})^2}{3\sqrt{3}} \right] \quad 6.16$$

The ratio of the small pore volume to the total void volume is approximately 0.8.

### 6.3 Model calculations

For each experiment and by applying Darcy's law the hydraulic gradient ( $dh/dl$ ) was calculated using the initial observed values of both hydraulic conductivity and initial flow rate for each sand fraction.

$$Q = -KA \frac{dh}{dl} \quad 6.17$$

The amount of glucose ( $G_m$ ) in gram which was delivered into each sand column was calculated by multiplying the initial flow rate ( $Q_i$ ) in ml/minutes, which delivered to each sand fraction by ( $t$ ) in minutes the feeding period and the initial concentration of glucose ( $G_c$ ) ( $10.0 \text{ g l}^{-1}$ ).

$$G_m = Q_i \cdot t \cdot G_c \quad 6.18$$

By assuming that *B. indica* consumed the entire amount of glucose and converted it to EPS. In this study, EPS was assumed to consist of a heteropolysaccharide (PS-7) because *B. indica* has the ability to produce copious amount of bacterial heteropolysaccharide (designed as PS-7) which is mainly composed of glucose (Wu *et al.*, 2006).

The chemical formula for this heteropolysaccharide is (C<sub>40</sub>H<sub>53</sub>O<sub>29</sub>) and the glucose chemical formula is (C<sub>6</sub>H<sub>12</sub>O<sub>6</sub>). Based on the chemical formula of glucose and EPS, 20.0 molecules of glucose are needed to obtain 3.0 molecules of EPS. The amount of EPS ( $EPS_m$ ) in grams produced in each sand column was calculated by multiplying the glucose amount ( $G_m$ ) in grams by 2990 g/mole (the weight of 20.0 moles of glucose) and dividing the result by 3600 g/mole (the weight of 3.0 moles of EPS).

$$EPS_m = G_m \left( \frac{2990}{3600} \right) \quad 6.19$$

The EPS volume ( $EPS_v$ ) in cubic centimetre was calculated by dividing the EPS mass ( $EPS_m$ ) by the EPS density ( $EPS_d$ ) which was assumed to be 1.1g cm<sup>-3</sup> (Vandevivere and Baveye, 1992).

$$EPS_v = EPS_m / EPS_d \quad 6.20$$

By assuming that bioclogging only occurs in small pore, the final small pore volumes are calculated by subtracting the EPS volume from the total initial small pore volumes.

$$Vp_f = Vp_i - EPS_v \quad 6.21$$

The new porosity was calculated by dividing the final small pore volume by the total void volume

$$\eta_f = \frac{V_{pf}}{V_t} \quad 6.22$$

Afterwards, the relative porosity values ( $\eta_{rel}$ ) were calculated by dividing the new or final porosity ( $\eta_f$ ) by the initial porosity ( $\eta_o$ ) of each sand fraction at each time step.

$$\eta_{rel} = \frac{\eta_f}{\eta_o} \quad 6.23$$

On the other hand, the relative hydraulic conductivity values ( $k_{rel}$ ) were calculated by using equations 2.1- 2.4, which are repeated below:

$$k_{rel} = \phi_{(\eta_{rel})} \eta_{rel}^2 + (1 - \phi_{(\eta_{rel})}) \frac{k_c}{1 - \eta_{rel}(1 - k_c)} \quad 2.1$$

$$\phi_{(nrel)} = \frac{\exp(-0.5(1 - \eta_{rel}))}{\eta_c} \quad 2.2$$

$$k_{rel} = (\eta_{rel})^2 \quad 2.3$$

$$k_{rel} = (\eta_{rel})^{19/6} \quad 2.4$$

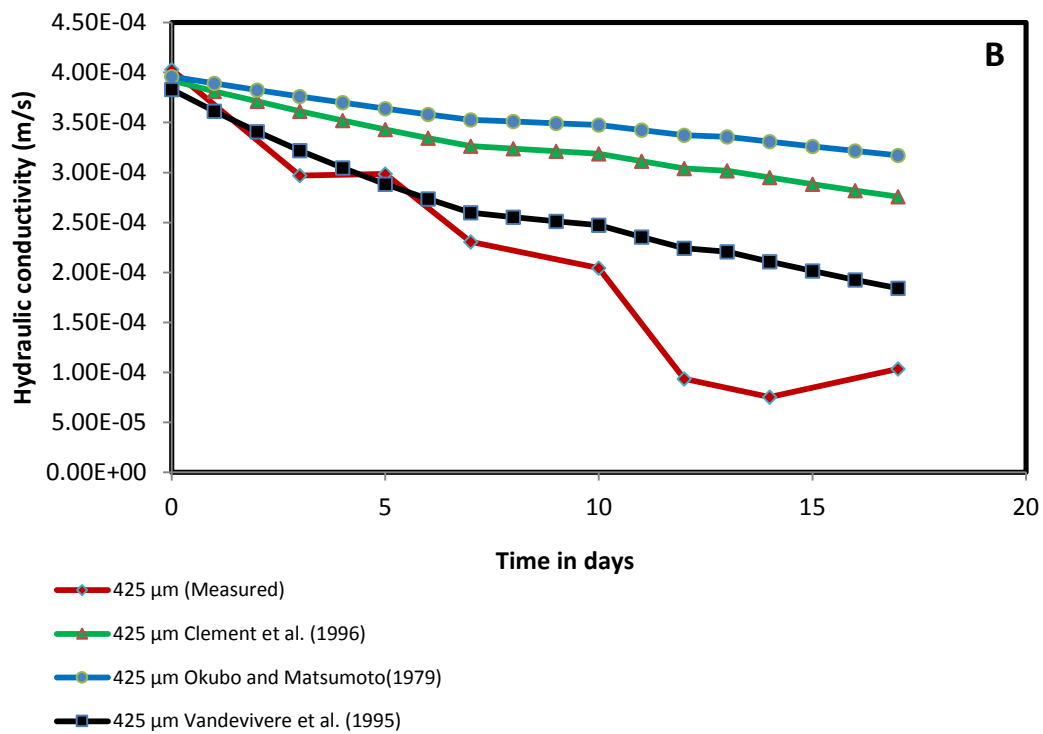
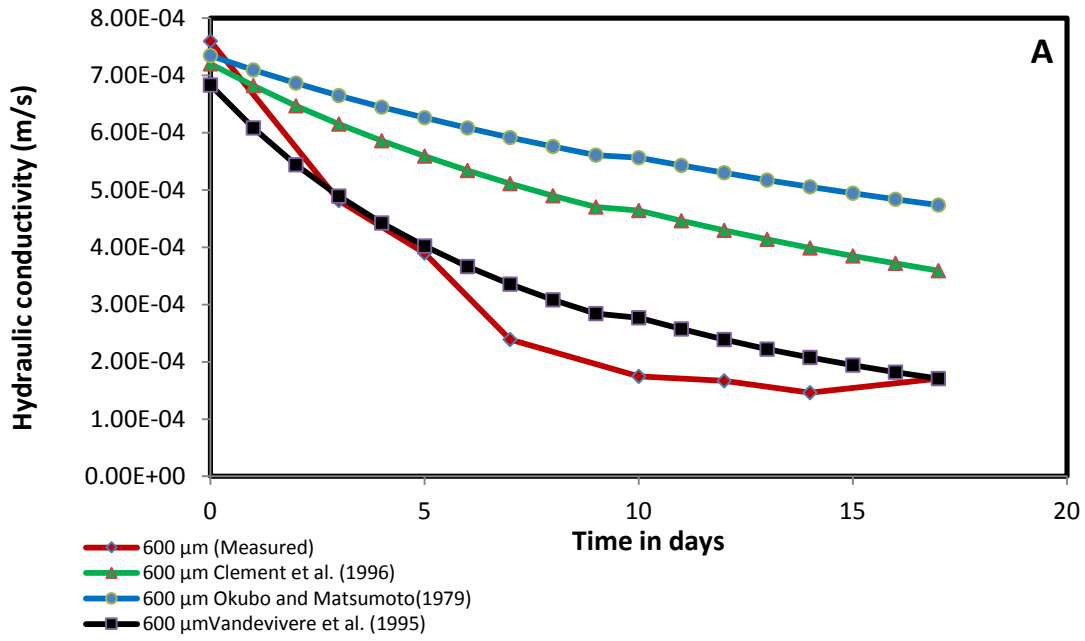
In the end, the final hydraulic conductivity values were calculated by multiplying the relative hydraulic conductivity by the initial hydraulic conductivity values.

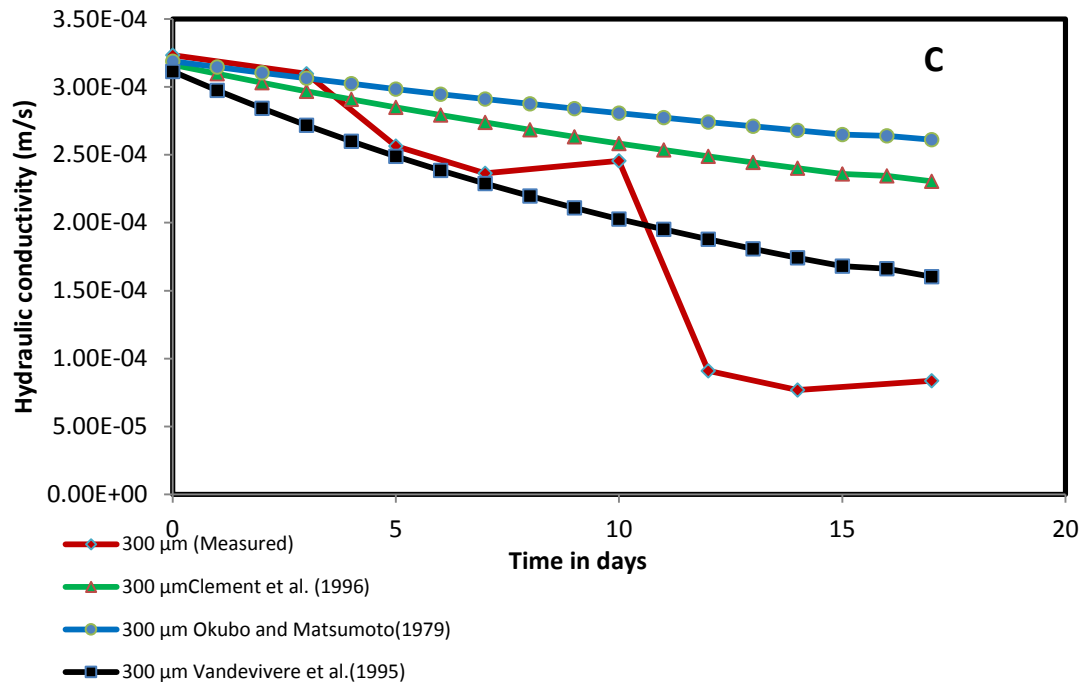
The predicted changes of the hydraulic conductivity using different clogging models were compared with the measured results from the five heterogeneous experiments as shown in Figures 6.3-6.7. Generally the results that have represented in these figures showed that amongst the three models the measured values of the hydraulic conductivity relatively match with the predicted values which were obtained by using Vandevivere *et al.* (1995) model. In addition to that, these figures illustrate that for larger sand fractions, both predicted and

measured results of hydraulic conductivity look very close to each other in value. While, for smaller sand fractions the measured value start to drop away from the predicted value which give an indication that these models could not be generalised for all sand fractions because of different assumptions of each bioclogging model. These assumptions can be applied if the pore structure is the same for all sand fractions but in fact the pore structure dissimilar from fraction to fraction.

For example, Okubo and Matsumoto (1979) calculated the effect of biological clogging of the reduction of hydraulic conductivity by assuming that pore space is in the bundle of straight pore and uniform biofilm is formed in the pore. Whilst, Vandevivere *et al.* (1995) assumed the porous medium to be represented by a bundle of parallel pores all having the same radius and also assumed that the biomass within a pore is present either as a biofilm or a plug.

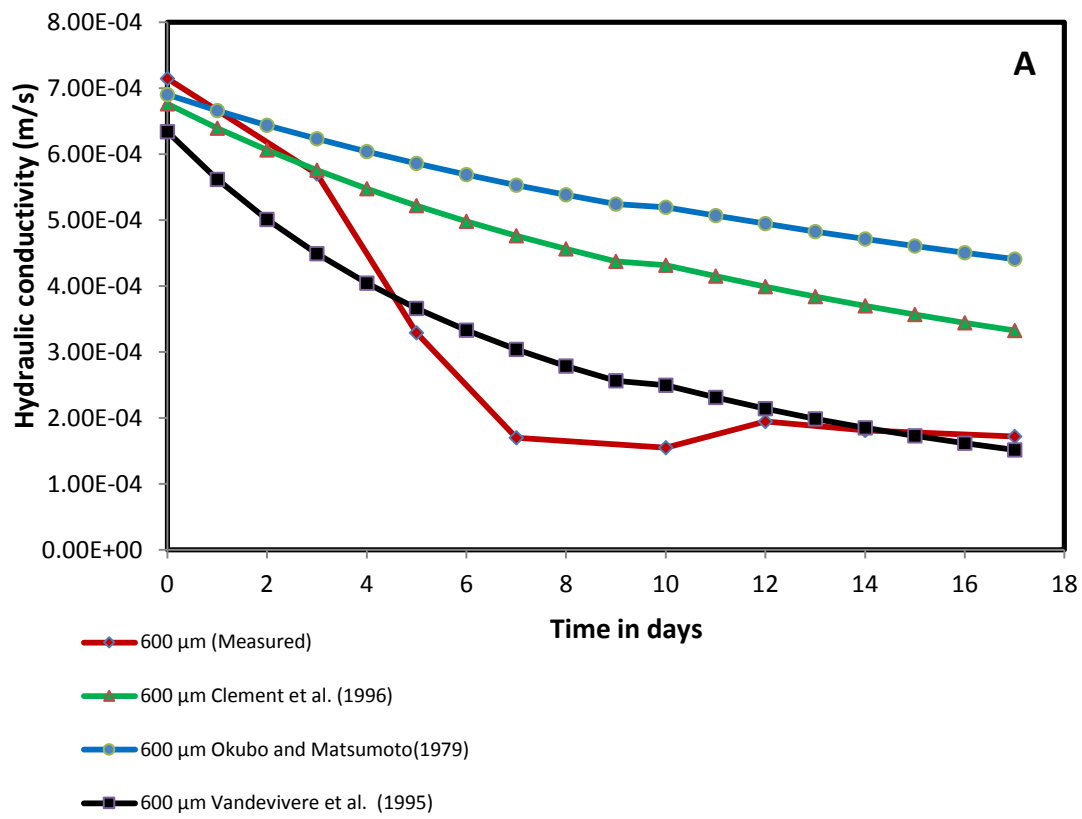
The results of the first experiment EXP.(1) described in Figure 6.3 shows that both of the measured and the predicted values of the hydraulic conductivity of the 600 $\mu$ m sand fraction are nearly similar. While, for the 300  $\mu$ m and 425  $\mu$ m sand fractions the measured values of the hydraulic conductivity were matching the predicted values for a period of time but started to move away after a certain time.

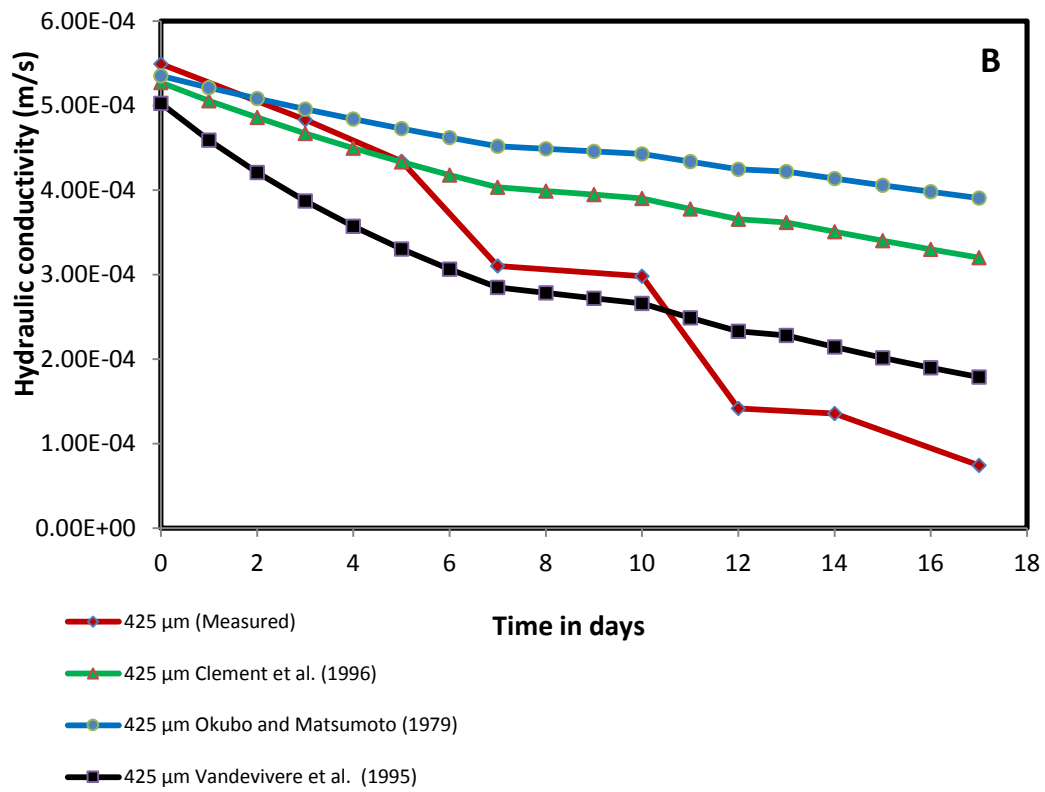




**Figure 6.3: Comparison between the predicted and the measured changes of the hydraulic conductivity with time for A: 600, B: 425, and C: 300 μm sand fractions.**

As for the second experiment EXP. (2) results shown in Figure 6.4 indicate that both of the measured and the predicted values of the hydraulic conductivity of the 600μm and 425 μm sand fractions coincide more with those obtained by applying Vandevivere *et al.* (1995) model. Whilst, the 150 μm sand fraction and despite the fact that the initial measured values of the hydraulic conductivity were very close to the predicted values, but they started to move away from the measured values after little time of the experiment start.





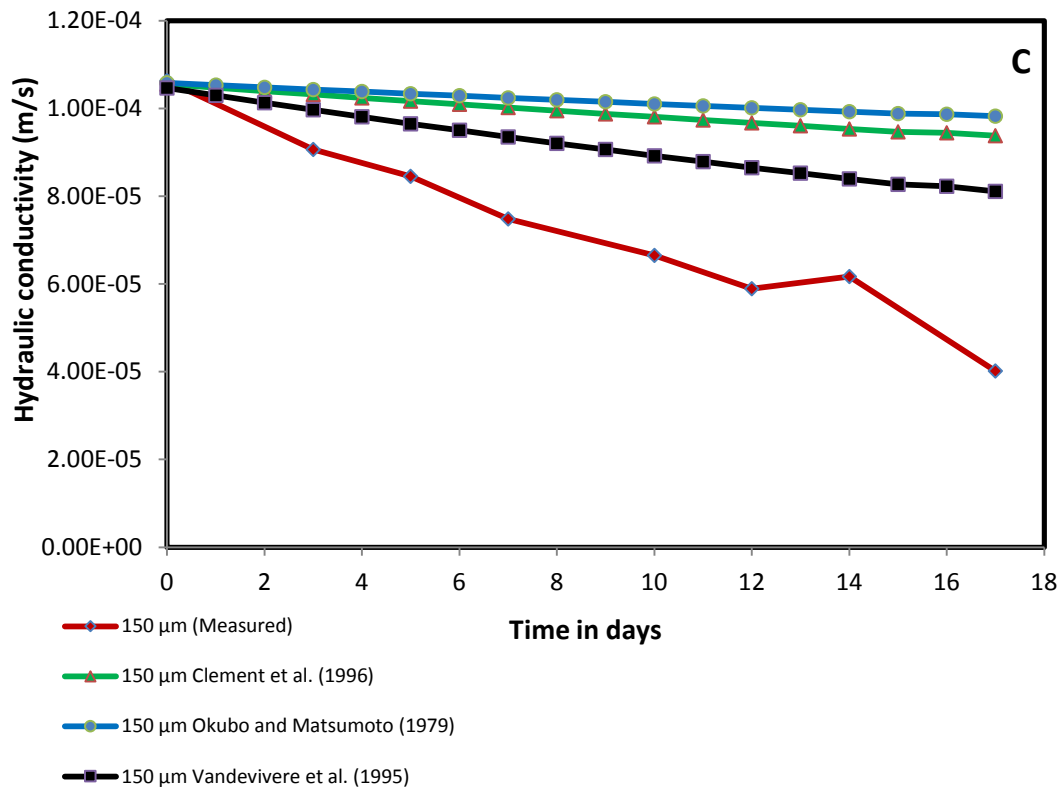
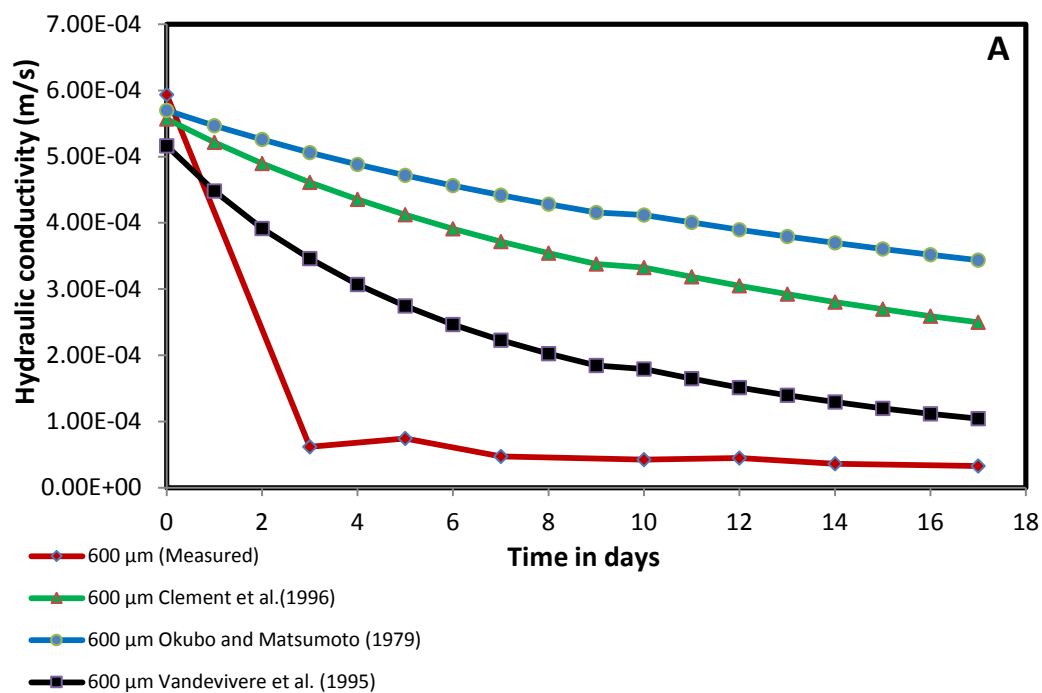


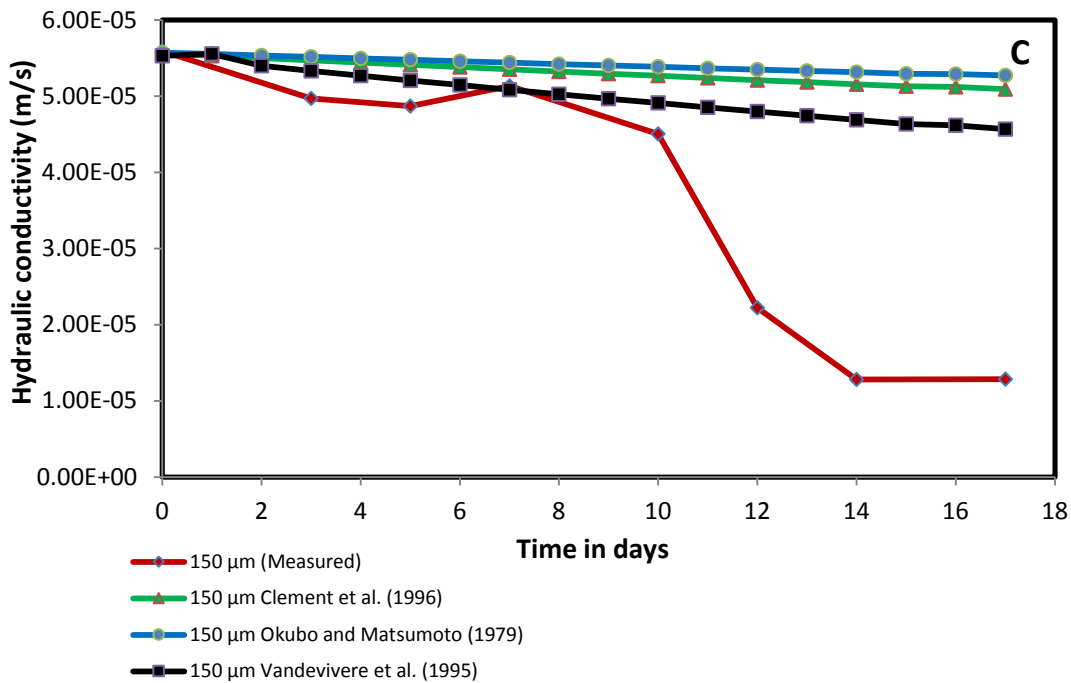
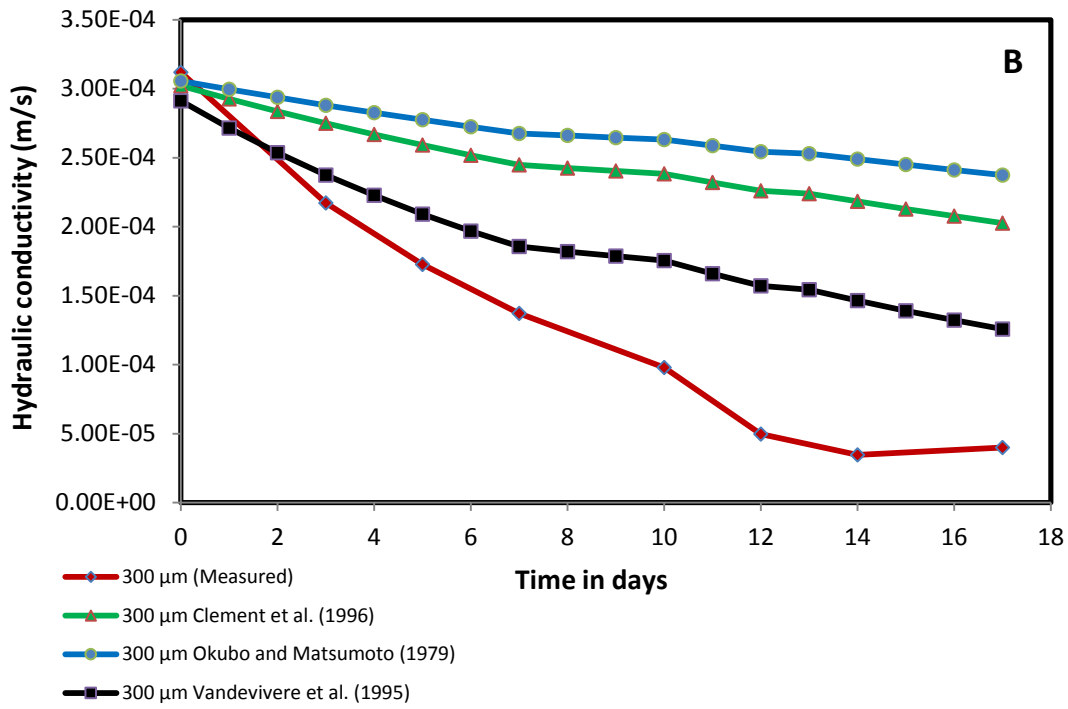
**Figure 6.4: Comparison between the predicted and the measured changes of the hydraulic conductivity with time for A: 600, B: 425, and C: 150 μm sand fractions.**

For the third experiment EXP.(3), the measured values of the hydraulic conductivity for the 600μm sand fraction as shown in Figure 6.5 dropped sharply during the first three days of the experiment, then they started to decrease steadily until the end of the experiment, unlike the predicted values of the hydraulic conductivity which decreased gradually. Despite this difference between the measured and the predicted values during the first three days, it can see that both measured and predicted values of the hydraulic conductivity ended up to the same value.

On the other hand, a different trend can be noted in the 300  $\mu\text{m}$ , where the measured values and the predicted values of the hydraulic conductivity started at similar values, and then they gradually moved away from each other.

As for the 150  $\mu\text{m}$  sand fraction, the measured and the predicted values of the hydraulic conductivity also started at values close to each other, but the measured values suddenly fell away from the predicted values after day 10.

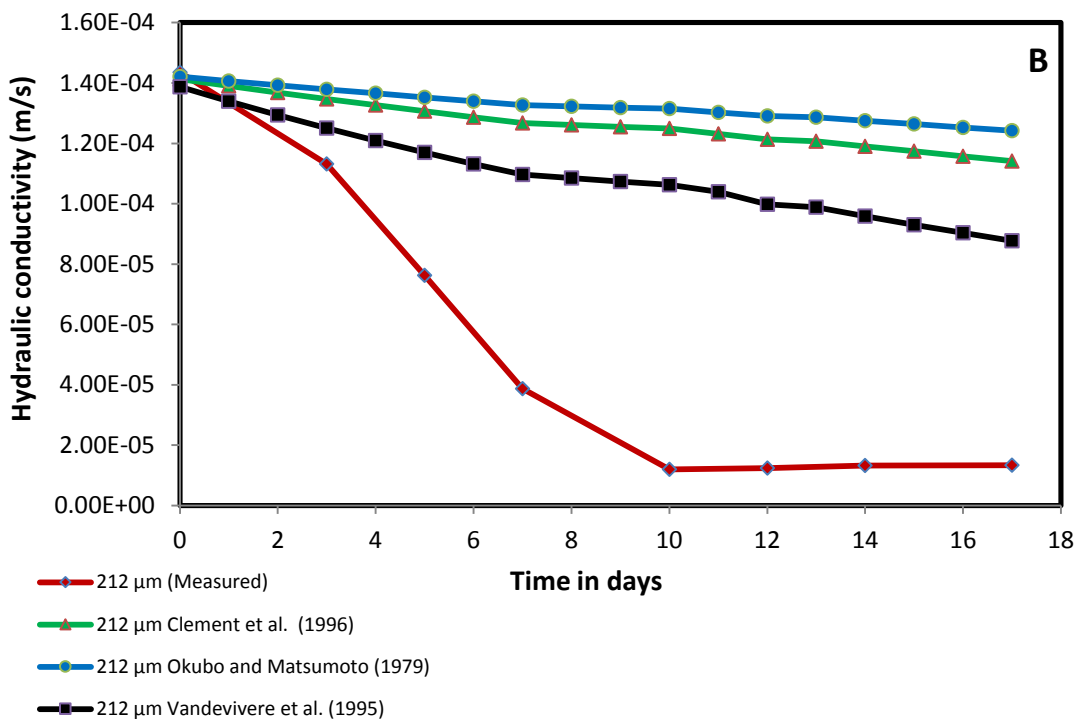
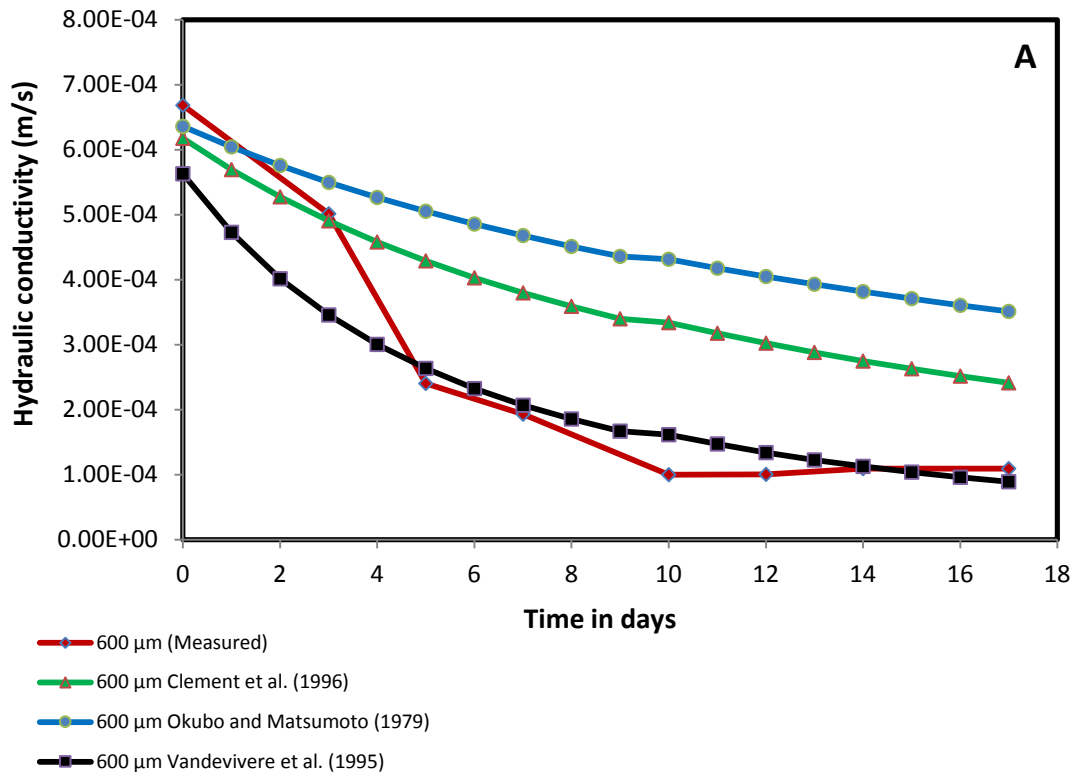




**Figure 6.5: Comparison between the predicted and the measured changes of the hydraulic conductivity with time for A: 600, B: 300, and C: 150 μm sand fractions.**

Figure 6.6 shows the predicted and the measured values of the hydraulic conductivity which obtained from the fourth experiment EXP.(4). By comparing the measured values of the hydraulic conductivity with the predicted values for the three sand fractions which were used in this experiment, it can be detected that the measured values of the hydraulic conductivity coincide well with the predicted values for the 600 $\mu\text{m}$ , whereas the measured values did not match the predicted values for the other sand fractions 212 and 150  $\mu\text{m}$ .

In the case of the 212  $\mu\text{m}$  sand fraction, the measured values of the hydraulic conductivity dramatically dropped down away from the predicted values after day 3, then they decreased steadily after day 10. But for the 150  $\mu\text{m}$  sand fraction the measured values of the hydraulic conductivity started to rise higher than the predicted values during the first five days, then sharply started to decrease away from the predicted values after day 5. The reason behind this different behaviour of both of 212 and 150 $\mu\text{m}$  sand fractions could be attributed to the fact that most of bioclogging models failed to predict the changes of the hydraulic conductivity for the finest materials which might be because of the idealised assumption of these models that assumed a uniform structure of the pore distribution.



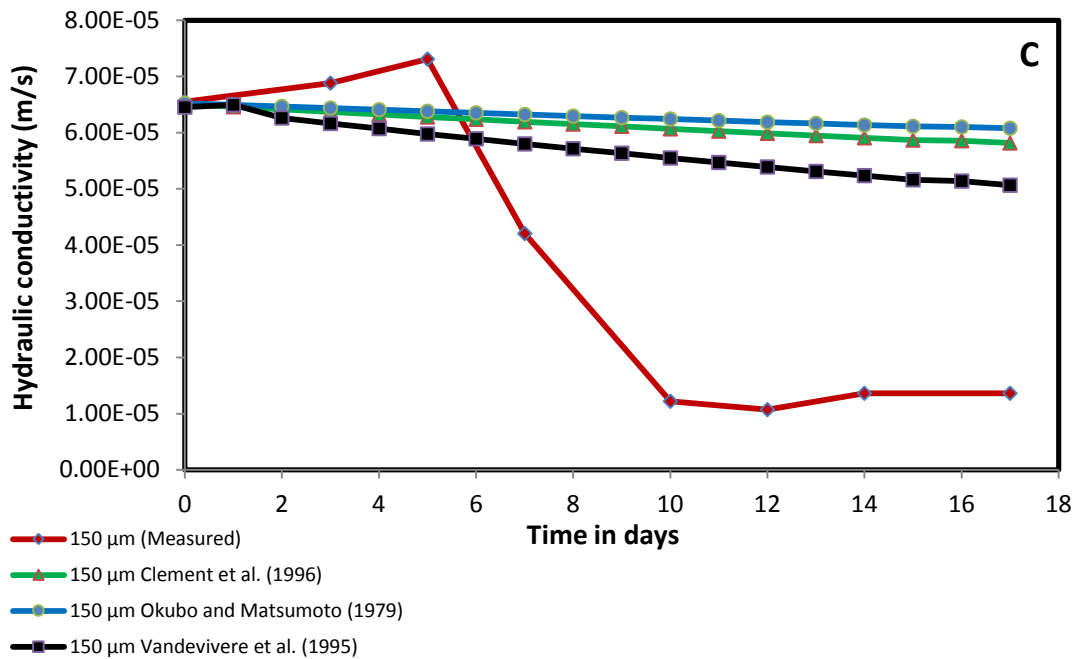


**Figure 6.6: Comparison between the predicted and the measured changes of the hydraulic conductivity with time for A: 600, B: 212, and C: 150 μm sand fractions.**

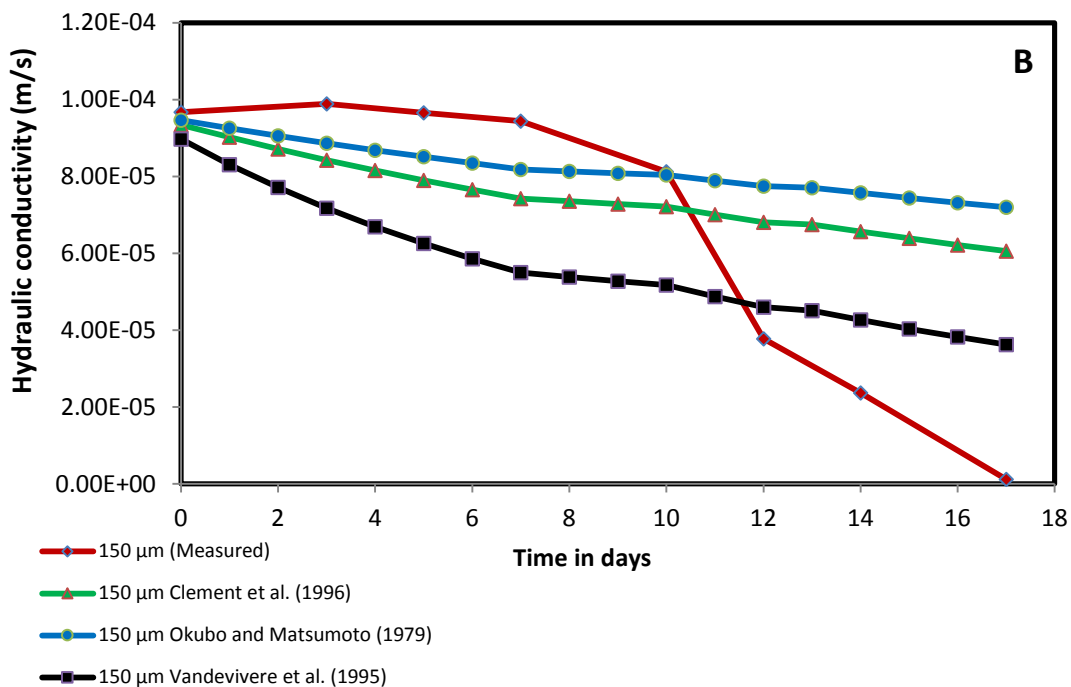
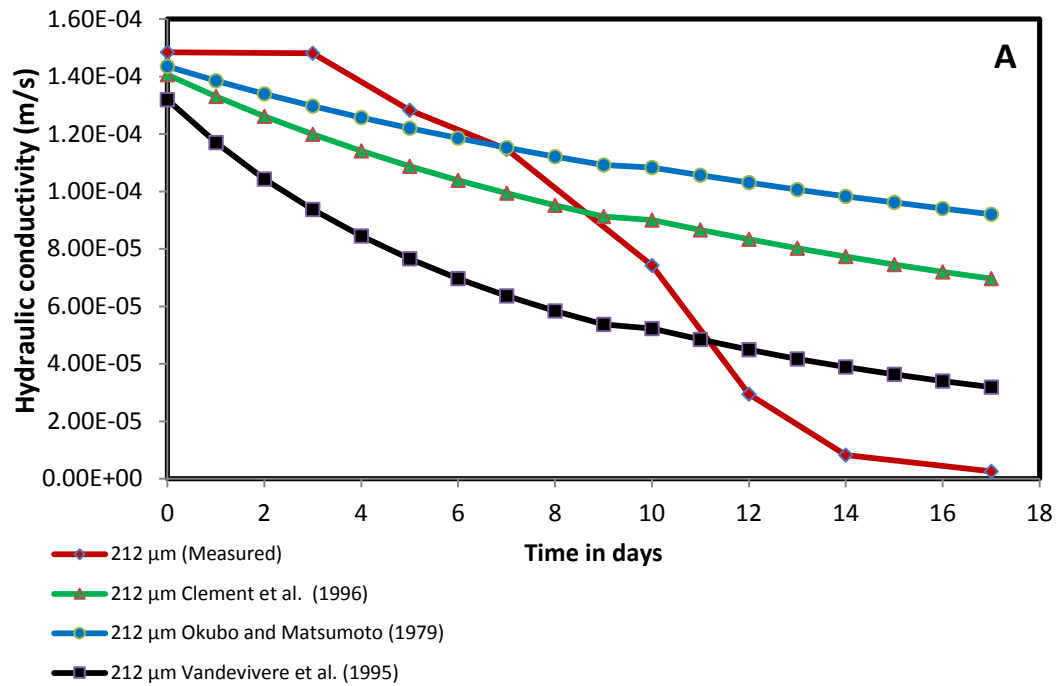
The results of the fifth experiment EXP.(5) as shown in Figure 6.7 specify that the measured values of the hydraulic conductivity of the 212 μm and 150 μm sand fraction relatively match the predicted values from the bioclogging models. Whereas, the measured values of the hydraulic conductivity relatively did not match the predicted values for the 63μm sand fraction. For 212 μm sand fraction, the measured hydraulic conductivity values remained steady in the first three days, but they seem to fall suddenly and between day 7 and day 12, they began to decrease dramatically to intersect with the predicted values which continued to decrease gradually. From day 12 till the end of the experiment, the decrease of the measured values of the hydraulic conductivity continued to fall, until it ended up with values lower than the predicted values.

For the 150  $\mu\text{m}$  sand fraction, there were no significant changes in the measured values of the hydraulic conductivity during the first seven days of the experiment, whereas the predicted values showed a gradual reduction of the hydraulic conductivity. After this period, the measured values of the hydraulic conductivity started to decrease to intersect with the predicted values in day 10. Following day 10 and up until the end of the experiments, the measured values of the hydraulic conductivity experienced a sharp decrease compared to the decrease in the predicted values which continued decreasing gradually.

For the 63 $\mu\text{m}$  sand fraction, the predicted values and measured values were very much similar to each other until the end of day 7. This could be attributed to the small amount of nutrients that was delivered to this sand fraction which affected the growth of bacteria and resulted in the reduction in the hydraulic conductivity. Despite the fact, there is no clear evidence on what's going on in this sand fraction, but it could be that the small pore volume has the large resistance to the flow which might be reduce the chance of cell to grow and form biofilm quickly.

Subsequently, the measures values started to fall slightly till it reached day 10, where measured values were experiencing a sharp fall until the end of the experiment. This sharp drop in the measured values of the hydraulic conductivity could be attributed to the diverted amount of nutrients which is coming from the 150  $\mu\text{m}$ .

Overall, it can be detected that the bioclogging models are relatively applicable for the most permeable sand fractions and by decreasing the sand fractions these models failed to predict the changes of the hydraulic conductivity. This prompts the conclusion that mathematical models, including the model developed in this study are inadequate for predicting the change of the hydraulic conductivity for all sand fractions. The reasons behind that could be related to the structure of the fine material which differs from the structure of the coarse material.



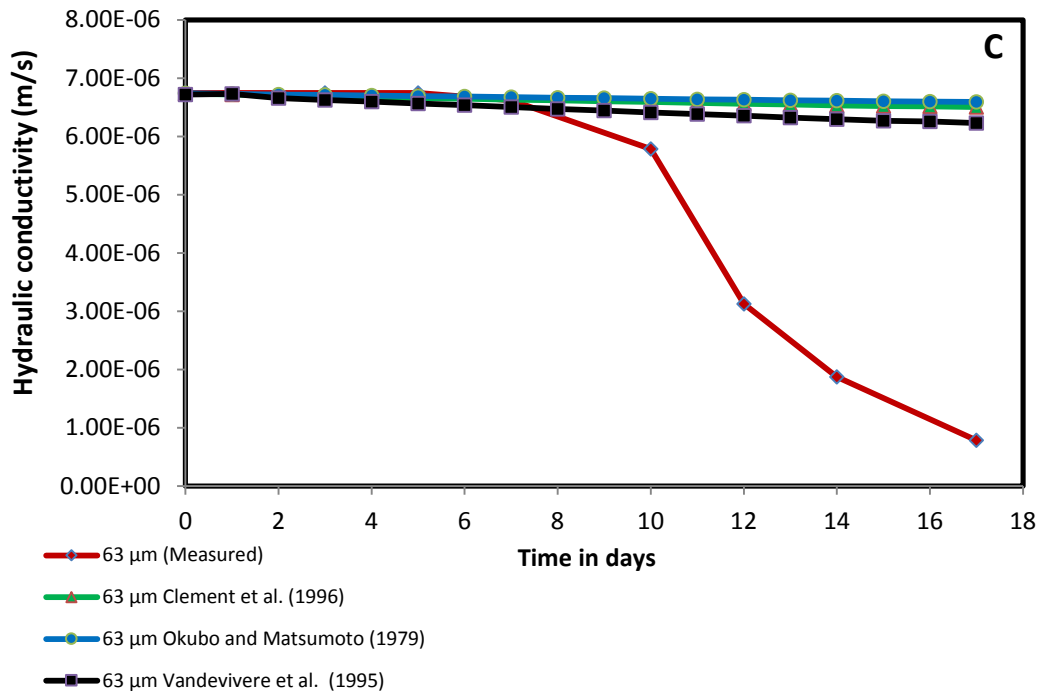


**Figure 6.7:** Comparison between the predicted and the measured changes of the hydraulic conductivity with time for A: 212, B: 150 and C: 63 μm sand fractions.

## 6.4 Overall discussion

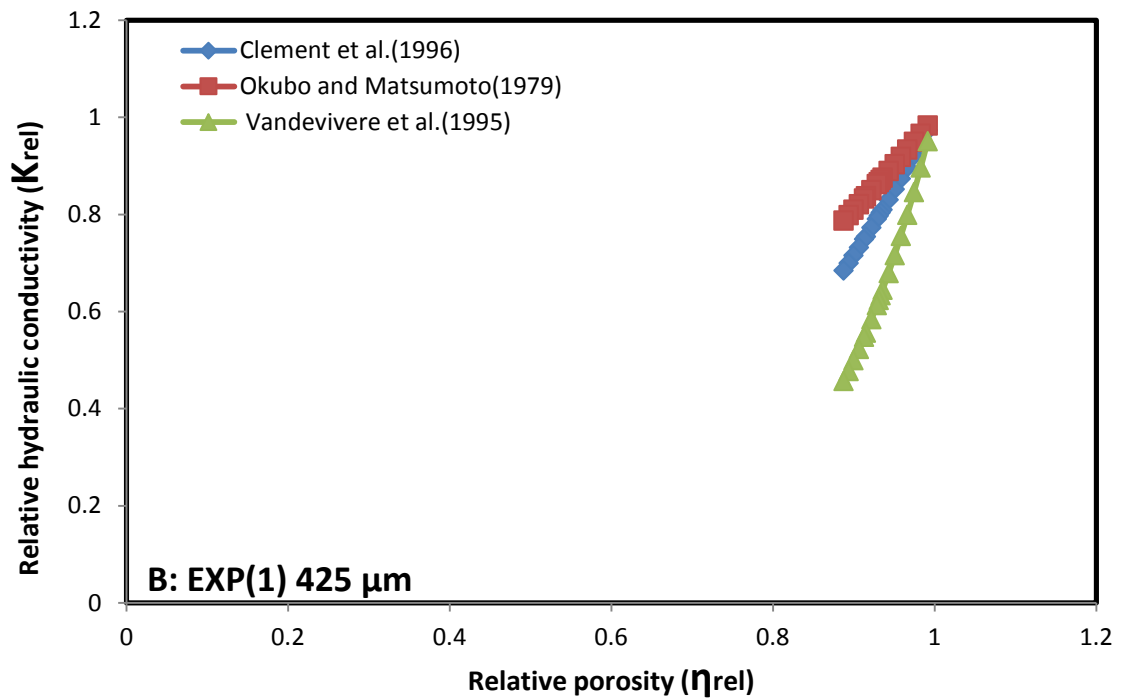
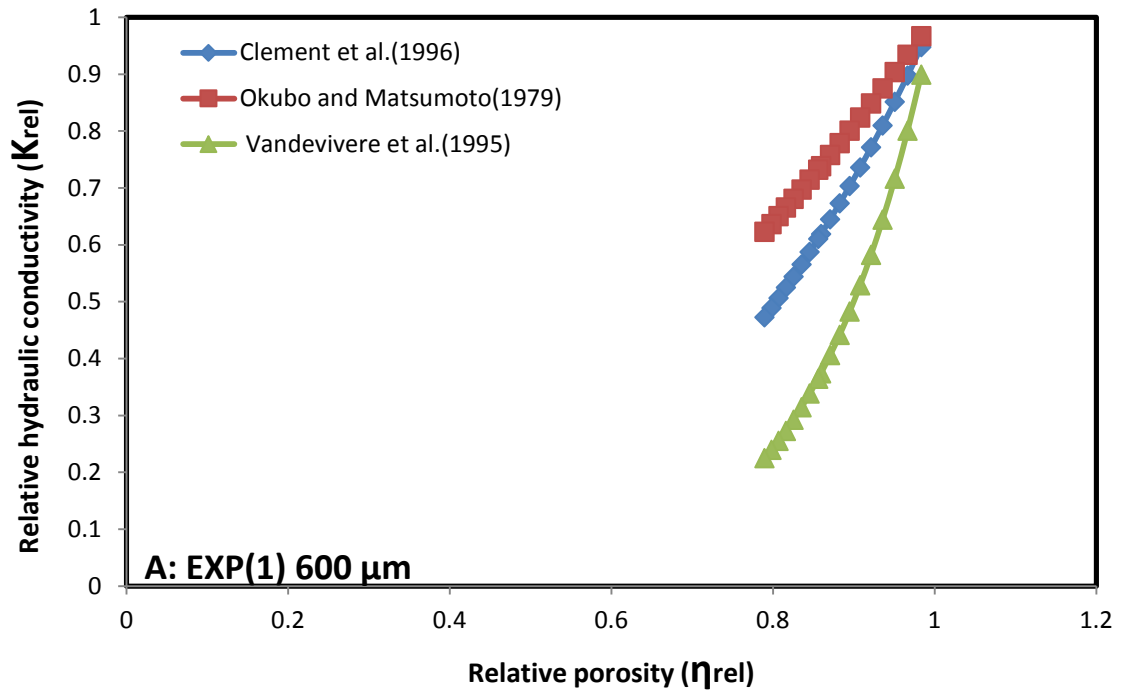
By comparing sand column results with the predicted results which were obtained by linking the changes of the hydraulic conductivity with the changes in the porosity of the porous media using three bioclogging models, it can be observed that the predicted values of the hydraulic conductivity coincide to some extent with the measured values of the hydraulic conductivity for the large sand fractions. On the contrary, for wide ranges of fine sand fractions these models showed a big difference or far predictions for the hydraulic conductivity changes with time.

The observed changes of the hydraulic conductivity for the large sand fractions relatively matches well with the bioclogging models, especially the biofilm/plug model which suggested by Vandivereve *et al.* (1995). The reason behind that could be attributed to the similarity

between the assumption of Vandivereve *et al.* (1995) model and this model. Vandivereve *et al.* (1995) model included a function of the pore distribution and our model assumed that the bioclogging occurred in the pore throats. However, as the grain size decreases, there is an increasing variance between the predicted values of the hydraulic conductivity and the measured values. This could be attributed to the shape of the larger pore which assumed to present as an ellipsoid which means that the biomass assumed to be distributed uniformly in the pore throat whilst the biomass might be distributed in non-homogenous way inside the pore throat.

By comparing the model results with the literature, it can be detected that biofilm models all assumed that the biomass is distributed uniformly on pore walls, as a biofilm or plugs and none of these models could predict satisfactorily the saturated hydraulic conductivity reductions observed in fine sands, whereas they fared somewhat better in coarser materials. The failure of these models was mainly attributed to the fact that biomass may not grow as a uniform biofilm or plugs only. Also, the idealized geometry could be one of the main reasons which led to this failure where most of bioclogging models as well as our model assumed that the pore space is distributed in a homogenous way.

This can be clearly seen in Figures 6.8-6.12 which correlate the relative hydraulic conductivity ( $K_{rel}$ ) and the relative porosity ( $\eta_{rel}$ ) for the five experiments using three bioclogging models. For example, Figure 6.8 shows that the model of Vandivereve *et al.* (1995) much more effective than the models of both Clement *et al.* (1996) and Okubo and Matsumoto (1979), where much higher reductions of hydraulic conductivity for a given porosity reduction for the coarse sand fraction.



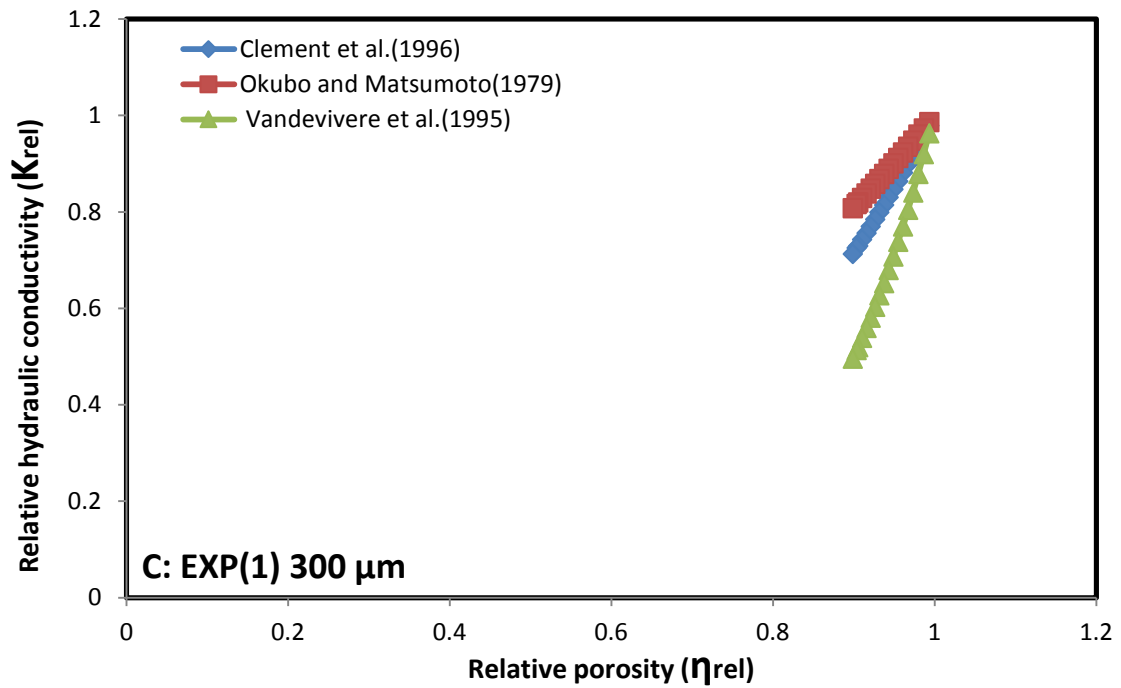
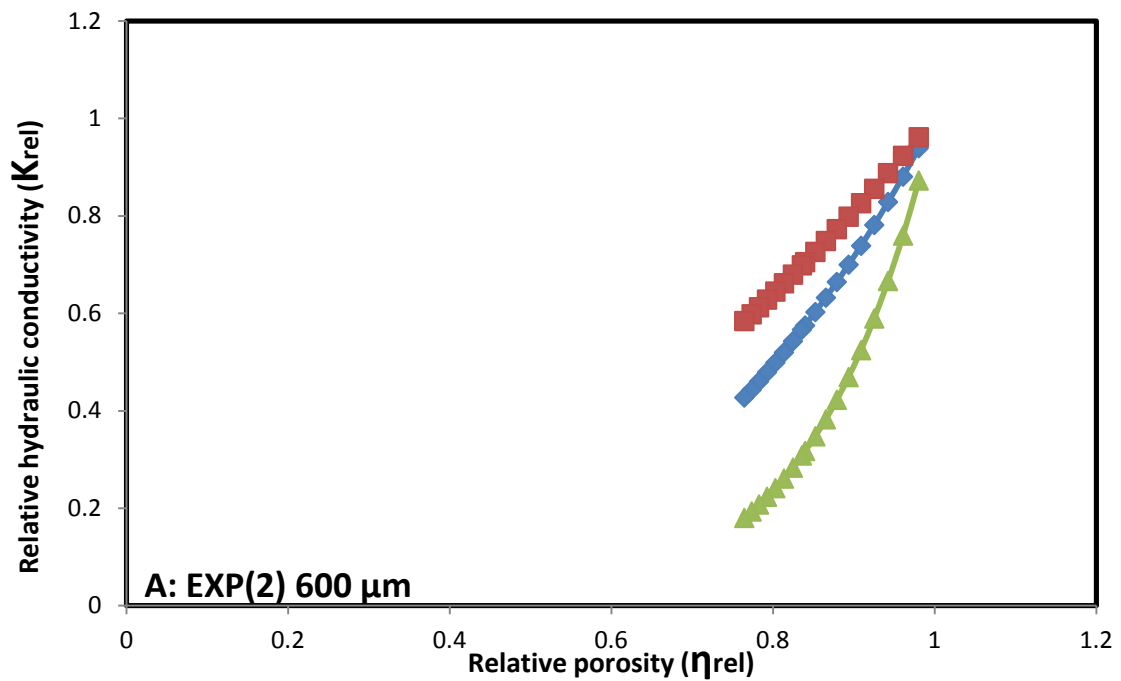
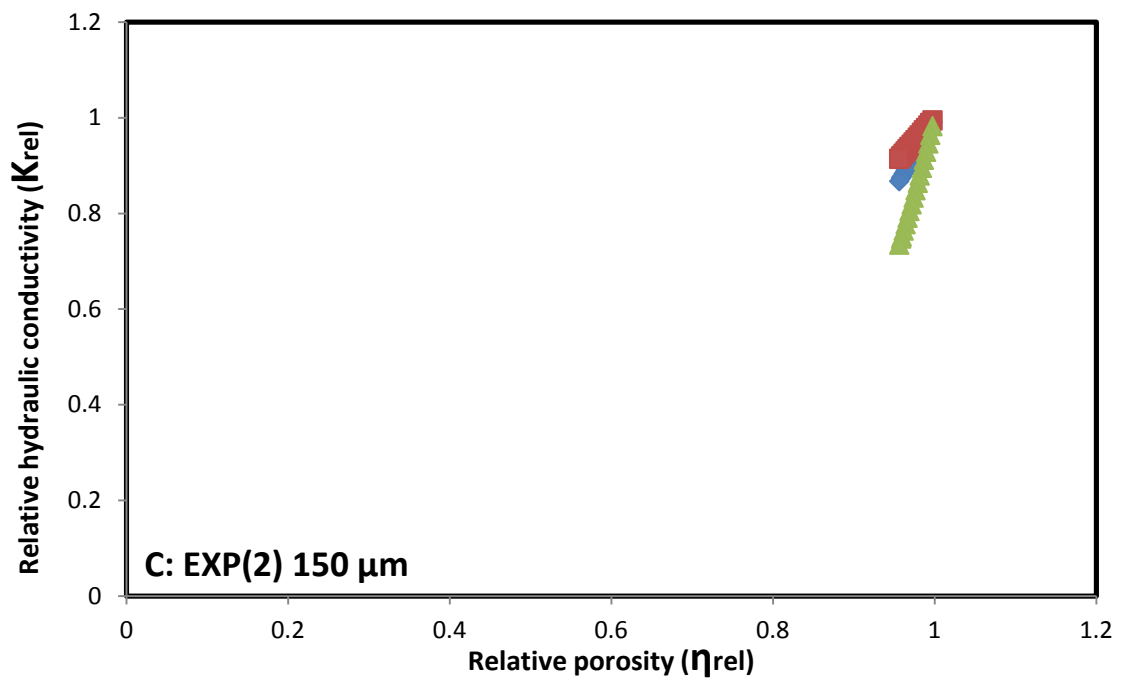
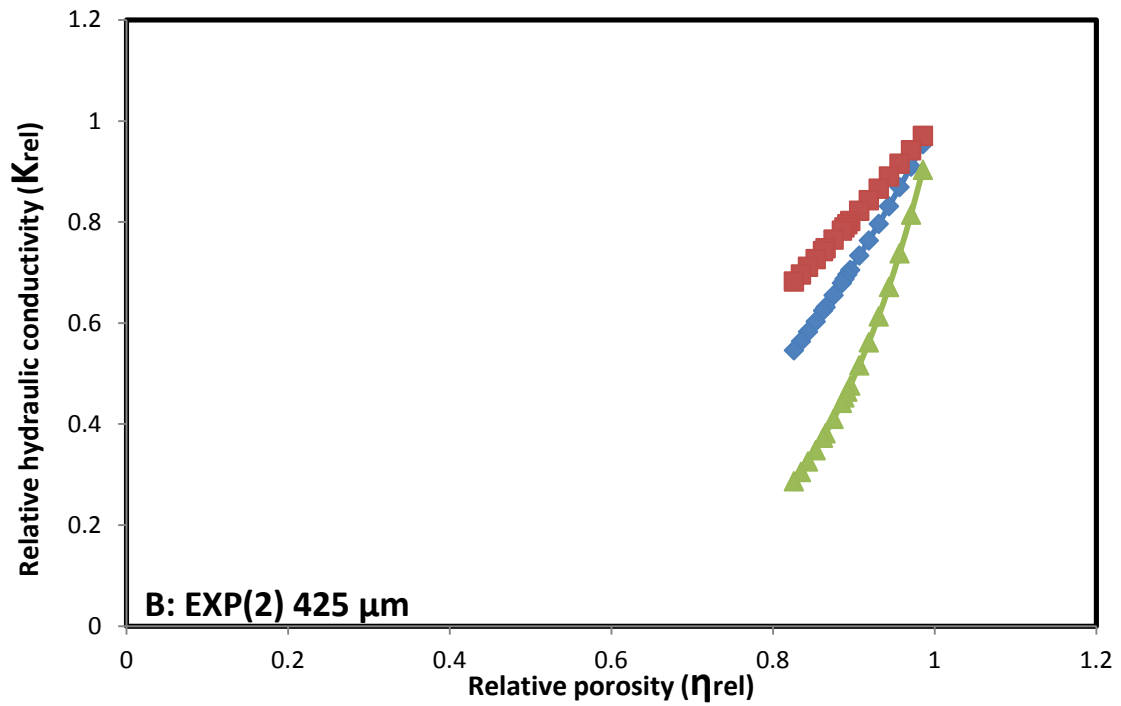
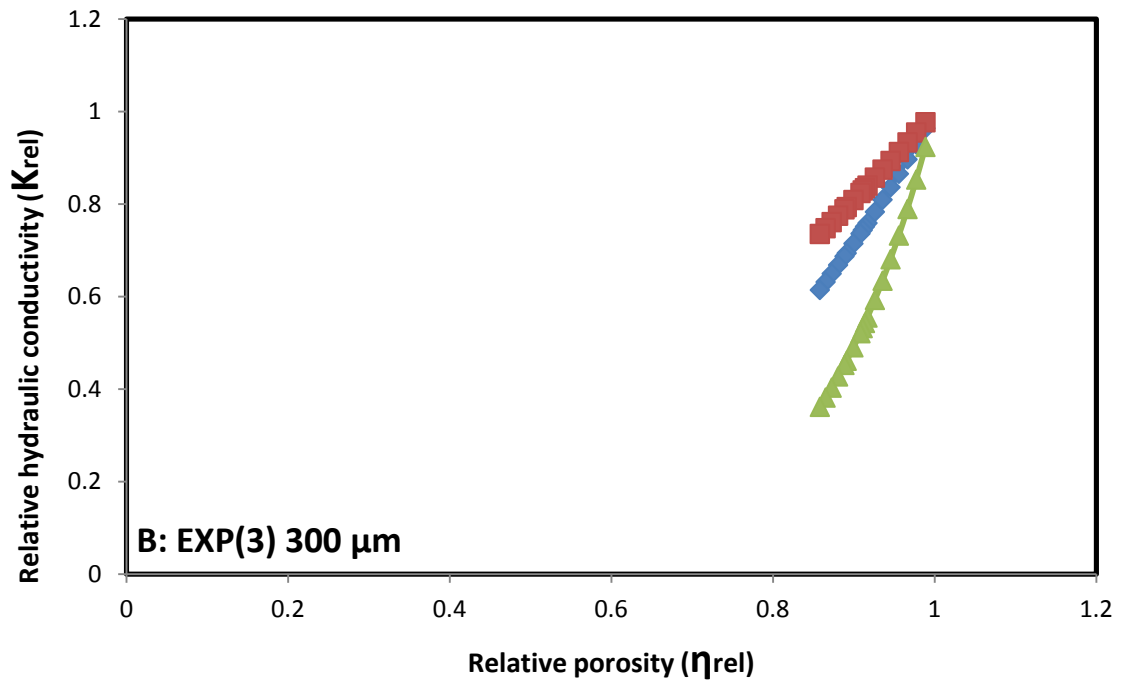
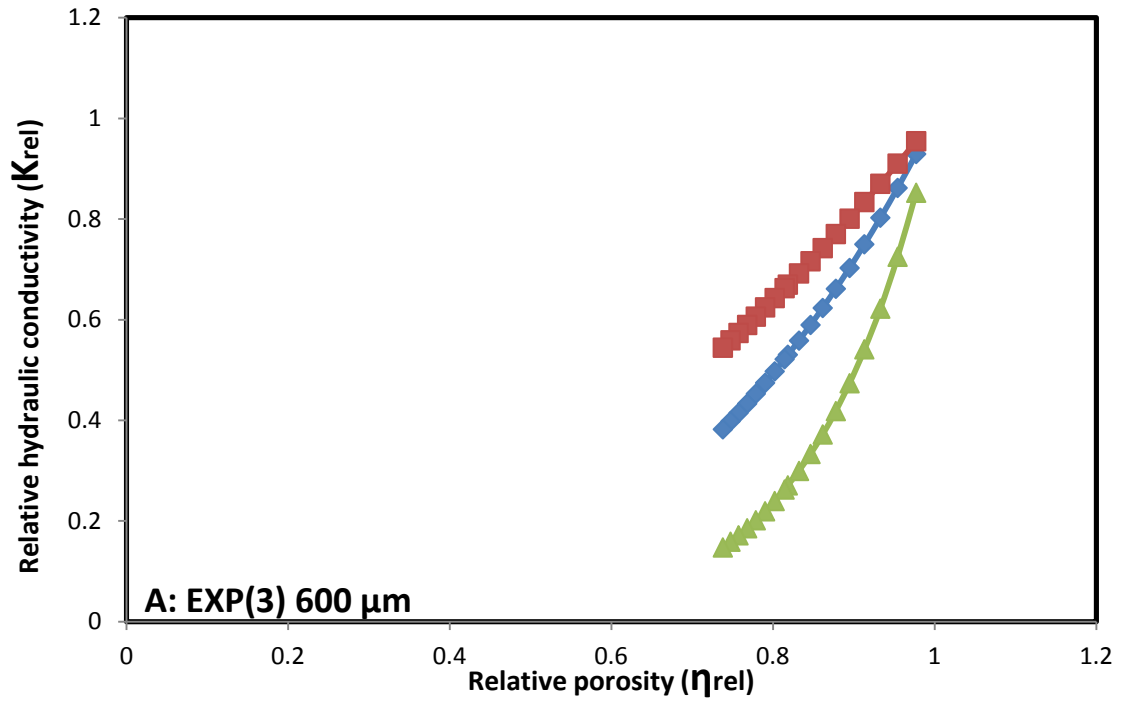


Figure 6.8: The relation between the relative hydraulic conductivity ( $K_{rel}$ ) and relative porosity ( $\eta_{rel}$ ) for the for EXP.(1) using three bioclogging models.





**Figure 6.9:** The relation between the relative hydraulic conductivity ( $K_{rel}$ ) and relative porosity ( $\eta_{rel}$ ) for the for EXP.(2) using three bioclogging models.



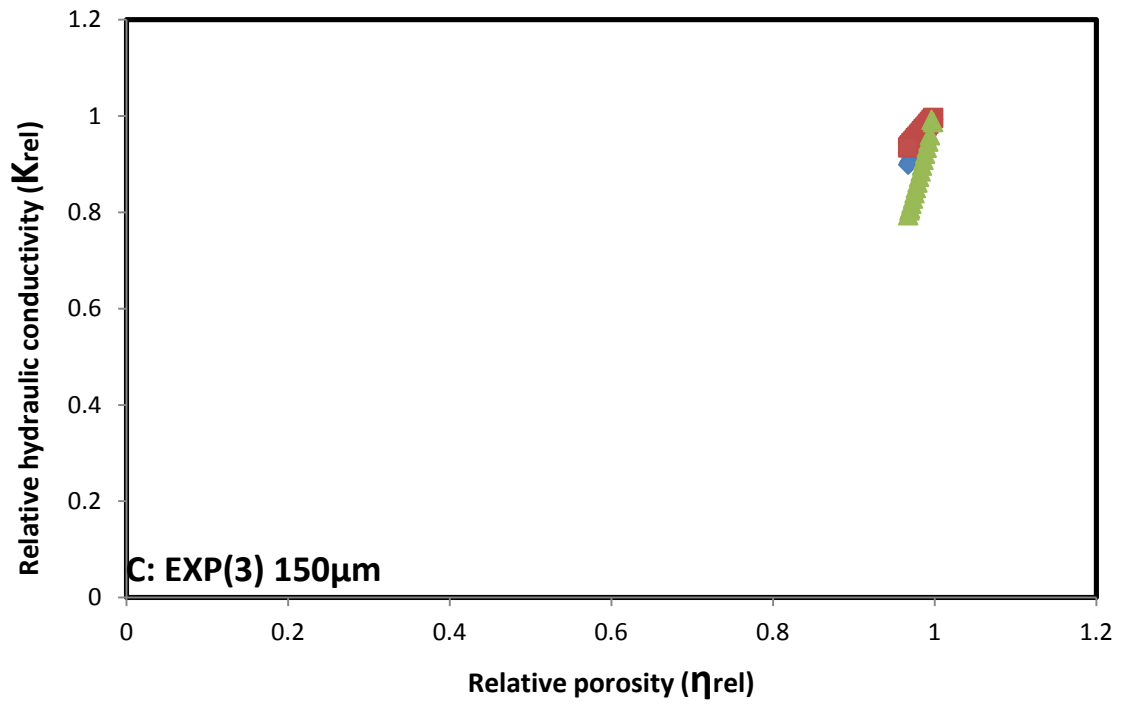
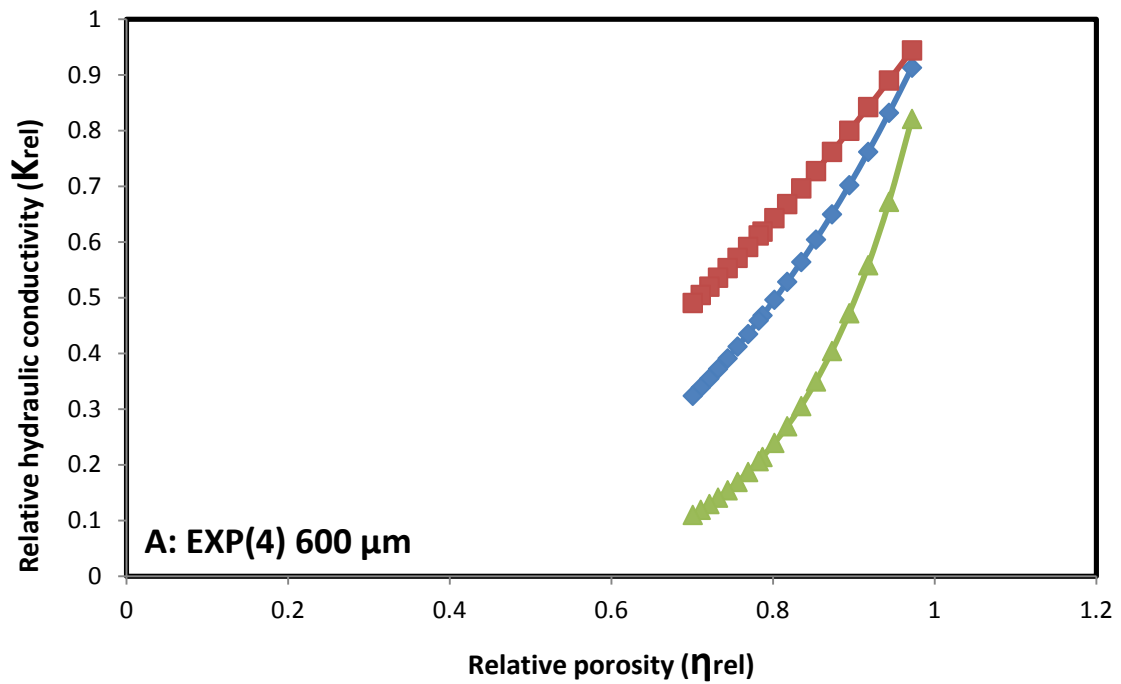


Figure 6.10: The relation between the relative hydraulic conductivity ( $K_{rel}$ ) and relative porosity ( $\eta_{rel}$ ) for the for EXP.(3) using three bioclogging models.



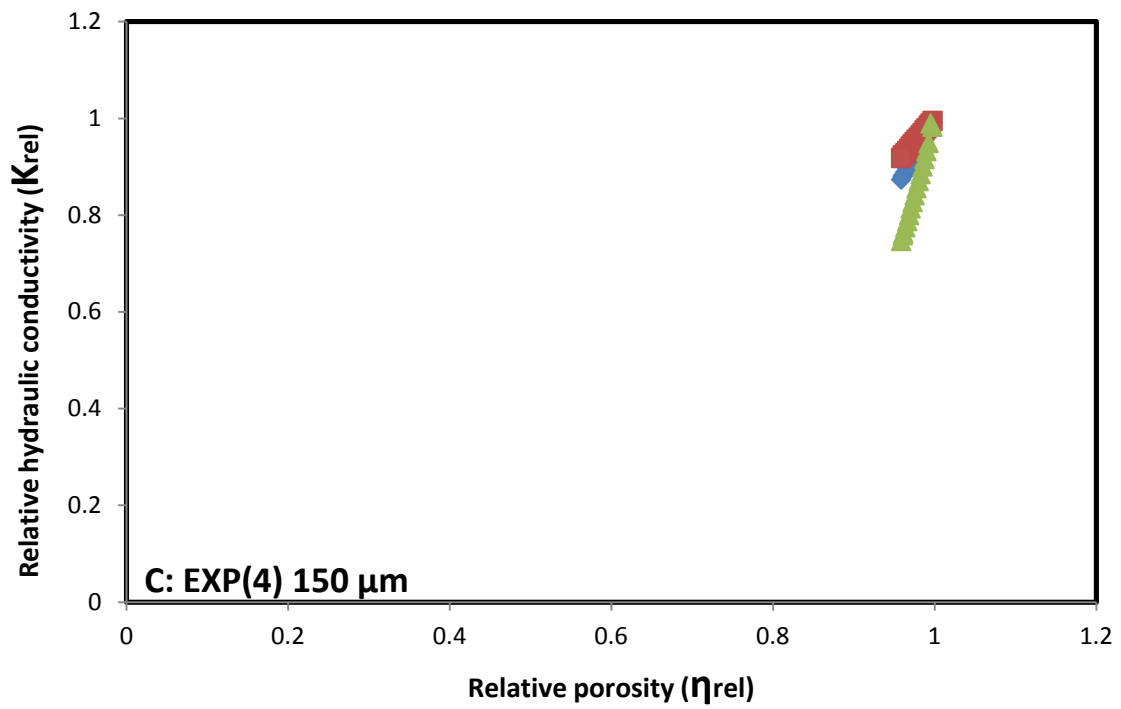
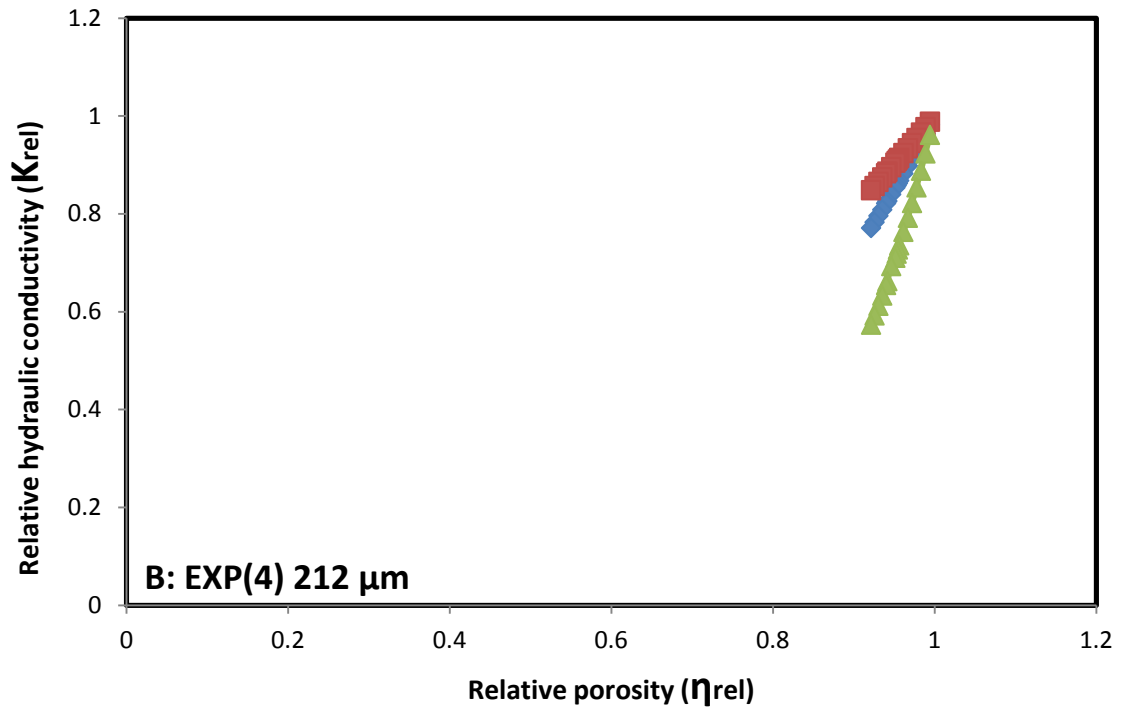
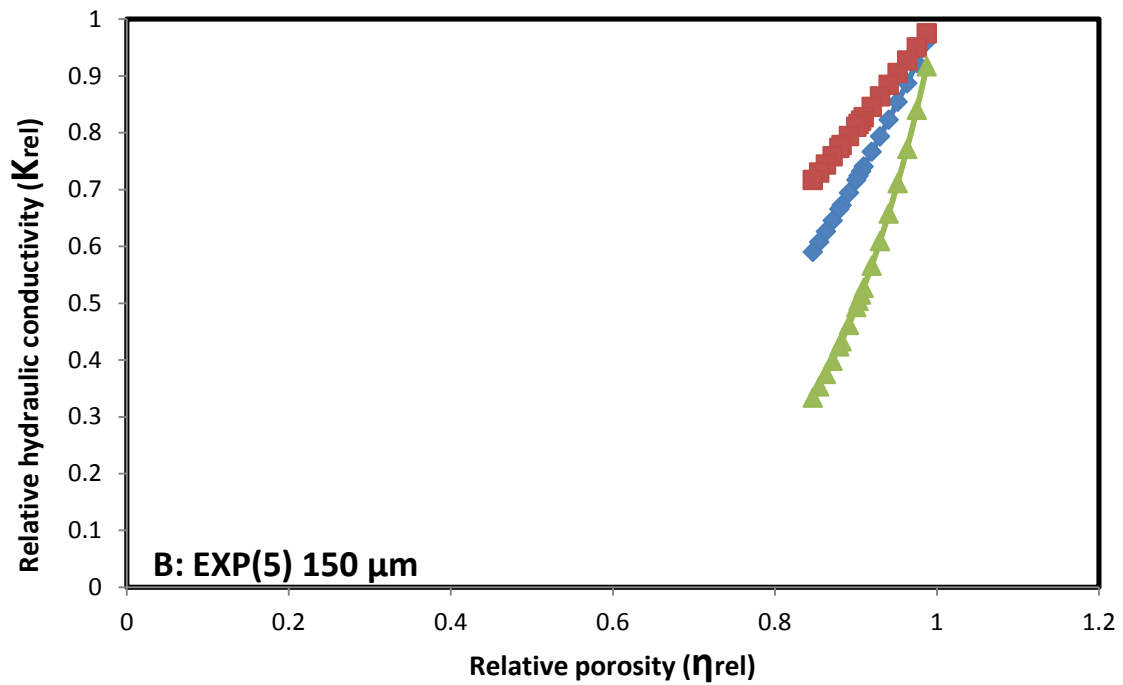
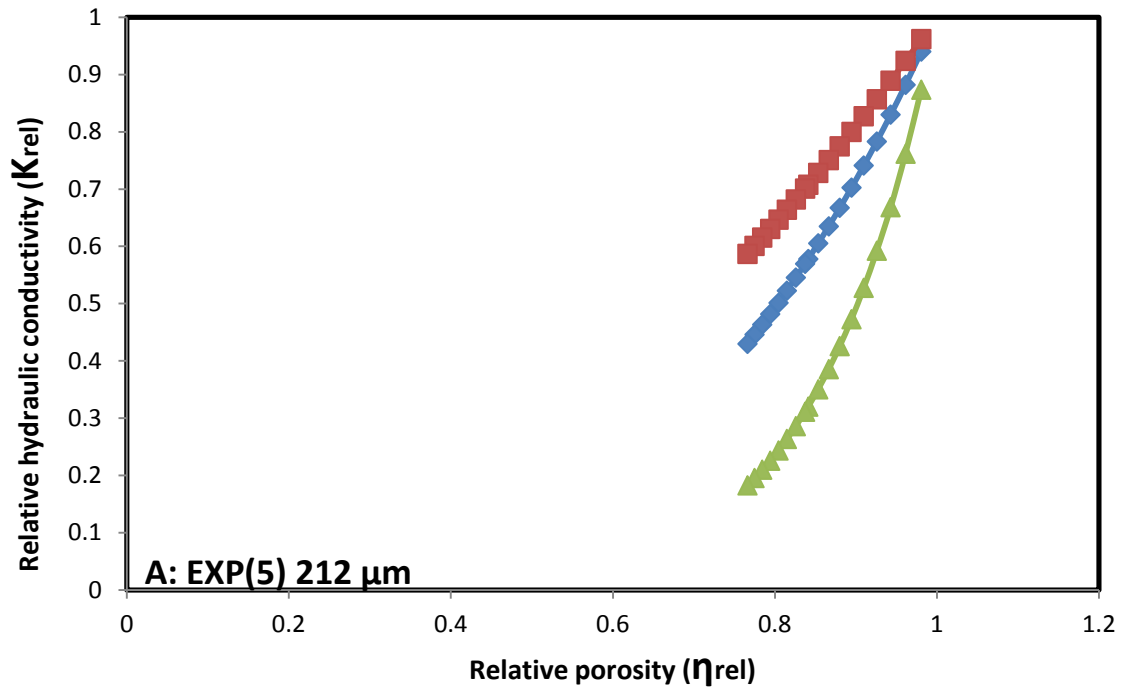
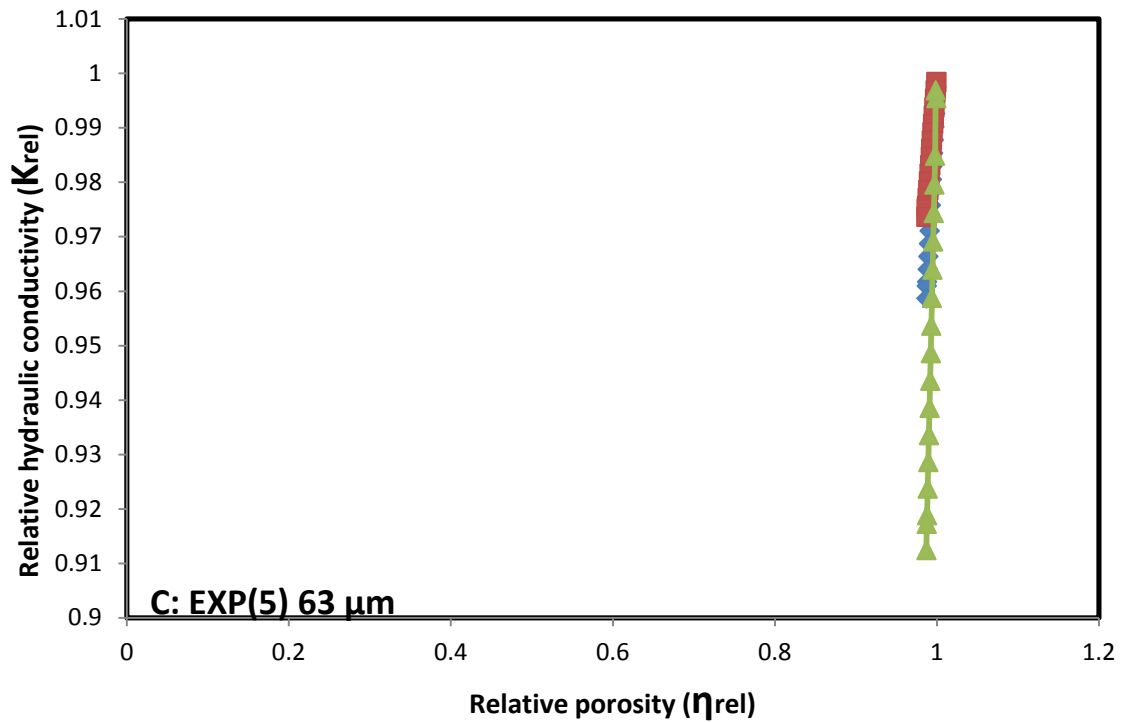


Figure 6.11: The relation between the relative hydraulic conductivity ( $K_{rel}$ ) and relative porosity ( $\eta_{rel}$ ) for the for EXP.(4) using three bioclogging models.





**Figure 6.12:** The relation between the relative hydraulic conductivity ( $K_{rel}$ ) and relative porosity ( $\eta_{rel}$ ) for the for EXP.(5) using three bioclogging models.

The reason behind that can be attributed to the assumption of Clement *et al.* (1996) who introduced a macroscopic model for bioclogging, which does not assume a specific distribution of the biomass within the pores. To incorporate biomass growth into this concept, Clement *et al.* (1996) followed a macroscopic approach, not making specific assumptions on the structure of the biomass accumulation in the porous medium. Nevertheless, it was assumed that the biomass was preferentially plugging larger pores, as observed in a porous medium reactor experiment by Torbati *et al.* (1986). It was, therefore, assumed that the pore size distribution was not changed due to biomass growth, but only the maximum pore radius was reduced. The model described above was criticized for not accounting the effect of plug formation. Therefore, Vandevivere *et al.* (1995) presented a simple model, assuming the porous medium

being represented as a bundle of parallel pores. Vandevivere *et al.* (1995) assumed that in case biofilm and plug formation occur simultaneously in a porous medium.

## **CONCLUSIONS AND RECOMMENDATIONS**

### **7.1 Introduction**

Biological clogging in homogeneous porous media was investigated by several authors, but only few of them addressed the effect of grain size on the bioclogging process. However, controversy still exists about the importance of the sand grain size effect on bioclogging efficiency.

Some studies demonstrated that biofilm accumulation preferentially plug large sand pore size, and biofilm thickness increases with the increase of the sand grain size (Clement *et al.*, 1996; Torbati *et al.*, 1986; Cunningham *et al.*, 1991). This could be attributed to the tendency of bacteria growing in high permeable sand fractions due to the great amount of nutrients (Jenneman *et al.*, 1984)

On the contrary, Vandevivere *et al.*(1992) indicated that the clogging efficiency is greater for small particle diameters but this conclusion was reported without any explanation. Nevertheless, they reported that it was likely that coarse textured material clogged earlier due to the less surface area which allowed more biofilm to form. In order to address this issue, the effect of grain size on bacterial growth (*P. putida* mt-2 and *B. indica*) on EPS production and on the subsequent reduction of hydraulic conductivity in porous media was investigated using sand column experiments.

On the other hand, most of the previous bioclogging studies were performed mainly in homogeneous porous media. However, the field sites are primarily heterogeneous. Therefore, this study aims to study the bioclogging process in porous media and the

factors that can affect this process, also to understand how all aspects of flow are affected by the clogging process, and finally to investigate the potential of biological growth to control direction and location of subsurface hydraulic flow to overcome the problems of preferential flow.

The major objectives of this study were to evaluate experimentally the effect of bacterial growth on the hydraulic conductivity of the porous media, and the factors that can affect the bioclogging process such as the grain size and bacterial growth conditions.

An extensive experimental and theoretical work was undertaken using different sand fractions ranging from 63-1180 micron in size and two bacterial strains (*P. putida* mt-2 and *B. indica*). Sand column experiments were conducted to study the bioclogging process in both homogeneous and heterogeneous porous media.

### **7.1.2 Conclusions of the bioclogging experiments in homogeneous porous media**

The following conclusions can be drawn.

- (1) Depending on the results of the preliminary experiments it could be claimed that biofilm growth was observed with both species used here. EPS production with *P. putida* was maximised at the highest levels of glucose and ammonium sulphate tested, but was still at a much lower level than that produced by *B.indica*. The latter was therefore used for subsequent experiments.
- (2) The results of the experiments which included the use of *B.indica*, the reduction of the hydraulic conductivity was similar for the sand fractions that ranging from (150-1180 $\mu$ m), whereas the 63  $\mu$ m the fine sand fraction showed a gradual reduction of the hydraulic conductivity throughout the whole period which is slower reduction than with the other sand fractions. The gradual decrease in the hydraulic conductivity was only

observed in the 63  $\mu\text{m}$  sand fraction, whereas for other fine sand fractions 150 and 212  $\mu\text{m}$  the hydraulic conductivity values decreased in a similar trend to the coarse sand fractions. This lag in reduction of the hydraulic conductivity could be attributed to the large surface area of this fine sand fraction (63  $\mu\text{m}$ ) which needs more biofilm to form and clog the pore volume. The other potential reason is the less amount of biomass in this sand fraction compared to other sand fractions, as suggested previously that may be the presence of more preferential flow paths in the fine sand fraction could lead to less chance of bacteria to grow, thus less biomass production.

### **7.1.3 Conclusions of the bioclogging experiments in heterogeneous porous media**

The following conclusions can be drawn from the results of the heterogeneous experiments.

- (1) Results from all sand column heterogeneous experiments clearly showed that the hydraulic conductivity decreased significantly in the columns that were injected with live cells, while there were no signs of any significant changes in hydraulic conductivity in the control columns.
- (2) In general, the results of five experiments that were running for seventeen days showed that the hydraulic conductivity values decreased considerably up to 90.0 % after three days of nutrient delivery in the more permeable sand fractions, there appears to be an increased lag with smaller grain sizes, then the final values end up being quite similar. This behaviour can be attributed to the structure of the pore of each sand fraction, perhaps the large pore, there more chance for nutrient to flow in a straight paths that conduct the nutrients quickly, while in fine grain size there may be more preferential

flow paths then the nutrients has to go around the particles thus less chance for cell to have access to the nutrients.

- (3) Regarding the relation between the loss on ignition and the relative hydraulic conductivity. The relative hydraulic conductivity ( $K_{rel}$ ) is inversely proportional to the loss on ignition for each experiment; however, it can be clearly observed that it is not easy to generalize this for the five heterogeneous experiments. Also, it can be noticed that the larger grain size has the largest amount of biomass, which caused the reduction of the hydraulic conductivity of each sand fraction. As mentioned previously, this might be occurred due to the passing of more amounts of the nutrient in the large pore void than the small pore voids, this could be due to the presence of preferential flow paths in the fine sand fractions that divert the flow around the soil particles. Consequently, the cells which reside in the small pore have less chance to access the nutrients, which result in less formation of biofilm.

Although many studies support the finding of this study, but none of these studies gave a clear explanation behind the ability of biomass to accumulate more in the large grain size. Nevertheless, it can be suggested that the lower amount of biomass in the fine grain size could be related to the lack of connectivity in the fine grain size compared to the more connectivity to the large grain size allow the nutrients to spread around the soil particles and thereby enhance the growth of bacteria which is responsible for clogging through the formation of biofilm. Also, it can suggest that maybe there is less preferential flow in the coarse grain size, which lead to more mix of nutrients around the soil particle, hence more biomass production.

(4) It can conclude from the results of the five heterogeneous experiments that the flow diverted from sand fraction to another in some of the heterogeneous experiments. For instance, the 600  $\mu\text{m}$  which used in four heterogeneous experiments, the results show that there was a flow diversion from the 600  $\mu\text{m}$  sand fractions into other sand fractions in three of the heterogeneous experiments, as the first experiment no flow diversion happens.

Although the reason behind that different behaviour is hard to explain, but the narrow range of the initial permeability between the three sand fractions which used in the first experiment could be the one of the reasons that diminishes the opportunity of the flow to divert the flow from the 600  $\mu\text{m}$  to other sand fractions.

(5) By comparing the results of heterogeneous experiment in contaminated porous media with the previous experiment Exp. (3), it can notice that the hydraulic conductivity in contaminated porous media decreased by the same. In addition to that, the results indicate that flow diversion can work in heterogeneous soils. Zinc is initially only removed from the 600 micron fraction, but then starts to be removed from the other fractions too, suggesting that flow must be occurring in these columns too, but that it requires a certain amount of biofilm growth before it happens.

Moreover, the results showed that the highest sorption capacity of zinc was detected in 150  $\mu\text{m}$  the least permeable sand fraction, whereas the lowest sorption capacity of zinc was detected in 600  $\mu\text{m}$  the high permeable sand fraction.

The explanation of this difference could be related to the adsorption capacity of each sand fraction which increased by decreasing the particle grain size due to high surface area of fine particle grain size that absorbs more metal ions.

#### **7.1.4 Conclusions of the theoretical analysis of the experimental works**

- (1) Sand column results and the predicted results which obtained by linking the changes of the hydraulic conductivity with the changes in the porosity of the porous media using three bioclogging models reveals that the predicted values of the hydraulic conductivity coincided to some extent with the measured values of the hydraulic conductivity for the large sand fractions.
- (2) Generally amongst the three models it can be observed that the measured values of the hydraulic conductivity relatively match with the predicted values obtained by using Vandevivere *et al.* (1995) model more than matching with other values. This likely account for the similarity between the assumption of Vandivereve *et al.* (1995) model and this model. Vandivereve *et al.* (1995) model included a function of the pore distribution and our model assumed that the bioclogging mainly occurs in the pore throats. However, this only applicable for the large sand fractions, whereas for the fine sand fractions the predicted values are sometimes far away from the measured values. This corresponds with the findings of several previous studies which also confirmed that bioclogging models can only predict the change of the hydraulic conductivity for the large sand fractions. The failure of these models could be related to the assumptions that made by each model, which is possible that are somehow less appropriate in fine-textured materials than they are in coarse textured ones. The second possible reason for the disparities between observations and model predictions is related to the assumption

made in some of these models that the microorganisms which is responsible of clogging forms biofilms of constant thickness which uniformly coated the particle surface.

## **7.2 Recommendations and Future works**

This study provided significant information regarding the bioclogging process in homogenous and heterogeneous porous media and the factors that have a great effect on this process such as the effect of grain size and the optimal growth conditions of bacteria. Furthermore, this study highlighted the need for additional works and future researches.

Some of the recommendations of this study are:

1. Due to the limited time frame, the experiments for the heterogeneous porous media were performed for a short time while the clean-up process could be lasting for long periods. It is recommended to conduct a similar experiment but for long periods to explore the effect of time on the bioclogging process and also to investigate for how long the bioclogging of the porous media will last.
2. Once more due to the limited time frame, the heterogeneous bioclogging experiments were performed in only one dimension. The one dimension column experiments allow studying the flow along the column only and this will limit the study of the subsurface flow. The subsurface flow is definitely more than one dimension, therefore these experiments should be scaled up into two or three dimensions in order to link between the vertical and the horizontal flow, which was neglected or assumed that the flow is only in one dimension.
3. In this study, bioclogging heterogeneous experiments were conducted for the inorganic contaminated porous media; however, further tests should be performed on different

types of contaminants such as the organic contaminants to assess the general applicability of the proposed procedure.

4. The influence of changes in the hydraulic conductivity due to the biological clogging can be used in the clean-up process to control the development of the preferential flow. As many studies confirmed that the preferential flow can be developed due to the soil heterogeneity. In this study, bacteria and their nutrients were used to reduce the difference between the highly permeable and the low permeable sand fractions. When these sand fractions have nearly similar permeability then the clean-up process of the contaminated porous media will be quicker. It is recommended to scale up the experimental works which were performed in this thesis to focus on the possibility of applying the bioclogging process to control the problem of preferential flow in heterogeneous porous media.

## **REFERENCES**

- Abu-Ashour, J., Joy, D. M., Lee, H., Whiteley, H. R. and Zelin, S. (1994) 'Transport of microorganisms through soil', *Water, Air, and Soil Pollution*, 75(1-2), 141-158.
- Allaire, S. E., Roulier, S. and Cessna, A. J. (2009) 'Quantifying preferential flow in soils: A review of different techniques', *Journal of Hydrology*, 378(1), 179-204.
- Allan, V. J., Callow, M. E., Macaskie, L. E. and Paterson-Beedle, M. (2002) 'Effect of nutrient limitation on biofilm formation and phosphatase activity of a *Citrobacter* sp', *Microbiology*, 148(1), 277-288.
- Amalfitano, S. and Fazi, S. (2008) 'Recovery and quantification of bacterial cells associated with streambed sediments', *Journal of microbiological methods*, 75(2), 237-243.
- Armitage, J. P. (2005) 'Understanding the Development and Formation of Biofilms', *Dept. of Biochemistry: Oxford University*.
- Arnon, S., Ronen, Z., Adar, E., Yakirevich, A. and Nativ, R. (2005) 'Two-dimensional distribution of microbial activity and flow patterns within naturally fractured chalk', *Journal of contaminant hydrology*, 79(3), 165-186.
- Augustin, M., Ali-Vehmas, T. and Atroshi, F. (2004) 'Assessment of enzymatic cleaning agents and disinfectants against bacterial biofilms'.
- Baveye, P., Vandevivere, P., Hoyle, B. L., DeLeo, P. C. and de Lozada, D. S. (1998) 'Environmental impact and mechanisms of the biological clogging of saturated soils and aquifer materials', *Critical reviews in environmental science and technology*, 28(2), 123-191.
- Bayer, P., Finkel, M. and Teutsch, T. (2002) 'Reliability of hydraulic performance and cost-estimates of barrier-supported pump-and-treat systems in heterogeneous aquifers', *ACTA-UNIVERSITATIS CAROLINAE GEOLOGICA*, (2/3), 290-294.
- Beven, K. and Germann, P. (1982) 'Macropores and water flow in soils', *Water resources research*, 18(5), 1311-1325.
- Bielefeldt, A. R., McEachern, C. and Illangasekare, T. (2002) 'Hydrodynamic changes in sand due to biogrowth on naphthalene and decane', *Journal of Environmental Engineering*, 128(1), 51-59.

- Bonala, M. V. and Reddi, L. N. (1998) *Physicochemical and biological mechanisms of soil clogging: an overview*, translated by ASCE, 43-68.
- Bouwer, H. (1991) 'Simple derivation of the retardation equation and application to preferential flow and macrodispersion', *Groundwater*, 29(1), 41-46.
- Brough, M., Al-Tabbaa, A. and Martin, R. (2001) *Laboratory investigation of optimum conditions for sub-surface biofilm barriers*, translated by 177-182.
- Brovelli, A., Malaguerra, F. and Barry, D. (2009) 'Bioclogging in porous media: Model development and sensitivity to initial conditions', *Environmental Modelling & Software*, 24(5), 611-626.
- Brown, L., Vadie, A. and Stephens, J. (2000) *Slowing production decline and extending the economic life of an oil field: new MEOR technology*, translated by Society of Petroleum Engineers.
- Brusseau, M. and Rao, P. (1990) 'Modeling solute transport in structured soils: A review', *Geoderma*, 46(1), 169-192.
- Bryant, R. S., Burchfield, T. E., Dennis, D. and Hitzman, D. (1990) 'Microbial-enhanced waterflooding: Mink unit project', *SPE Reservoir Engineering*, 5(01), 9-13.
- Bryers, J. D. and Characklis, W. G. (1982) 'Processes governing primary biofilm formation', *Biotechnology and bioengineering*, 24(11), 2451-2476.
- Characklis, W. G. and Marshall, K. C. (1990) 'Biofilms'.
- Chen-Charpentier, B. M., Dimitrov, D. T. and Kojouharov, H. V. (2009) 'Numerical simulation of multi-species biofilms in porous media for different kinetics', *Mathematics and Computers in Simulation*, 79(6), 1846-1861.
- Chen, X., Hou, W., Song, G. and Wang, Q. (2011) 'Adsorption of Cu, Cd, Zn and Pb Ions from Aqueous Solutions by Electric Arc Furnace Slag and the Effects of pH and Grain Size', *Chemical and Biochemical Engineering Quarterly*, 25(1), 105-114.
- Choi, Y. and Morgenroth, E. (2003) 'Monitoring biofilm detachment under dynamic changes in shear stress using laser-based particle size analysis and mass fractionation', *Water Science & Technology*, 47(5), 69-76.

- Clement, T., Hooker, B. and Skeen, R. (1996) 'Macroscopic models for predicting changes in saturated porous media properties caused by microbial growth', *Groundwater*, 34(5), 934-942.
- Costerton, J. W., Cheng, K., Geesey, G. G., Ladd, T. I., Nickel, J. C., Dasgupta, M. and Marrie, T. J. (1987) 'Bacterial biofilms in nature and disease', *Annual Reviews in Microbiology*, 41(1), 435-464.
- Cote, C. M., Bristow, K. L., Charlesworth, P. B., Cook, F. J. and Thorburn, P. J. (2003) 'Analysis of soil wetting and solute transport in subsurface trickle irrigation', *Irrigation Science*, 22(3-4), 143-156.
- Crane, S. R. and Moore, J. A. (1984) 'Bacterial pollution of groundwater: a review', *Water, Air, and Soil Pollution*, 22(1), 67-83.
- Crecente, C., Rasmussen, K., Torsaeter, O., Strom, A. and Kowalewski, E. (2005) *An experimental study of microbial improved oil recovery by using Rhodococcus sp. 094*, translated by.
- Crespo, F., Reddy, B., Eoff, L., Lewis, C. and Pascarella, N. (2014) *Development of a Polymer Gel System for Improved Sweep Efficiency and Injection Profile Modification of IOR/EOR Treatments*, translated by.
- Cunningham, A. B., Characklis, W. G., Abedeen, F. and Crawford, D. (1991) 'Influence of biofilm accumulation on porous media hydrodynamics', *Environmental science & technology*, 25(7), 1305-1311.
- Cusack, F., Singh, S., Novosad, J., Chmilar, M., Blenkinsopp, S. and Costerton, J. (1992) *The use of ultramicrobacteria for selective plugging in oil recovery by waterflooding*, translated by Society of Petroleum Engineers.
- Das, N. and Chandran, P. (2010) 'Microbial degradation of petroleum hydrocarbon contaminants: an overview', *Biotechnology research international*, 2011.
- Davey, M. E. and O'toole, G. A. (2000) 'Microbial biofilms: from ecology to molecular genetics', *Microbiology and molecular biology reviews*, 64(4), 847-867.
- Dean Jr, W. E. (1974) 'Determination of carbonate and organic matter in calcareous sediments and sedimentary rocks by loss on ignition: comparison with other methods', *Journal of Sedimentary Research*, 44(1).

- DeJong, J. T., Fritzges, M. B. and Nüsslein, K. (2006) 'Microbially induced cementation to control sand response to undrained shear', *Journal of Geotechnical and Geoenvironmental Engineering*, 132(11), 1381-1392.
- Dennis, M. L. and Turner, J. P. (1998) 'Hydraulic conductivity of compacted soil treated with biofilm', *Journal of Geotechnical and Geoenvironmental Engineering*, 124(2), 120-127.
- Desouky, S., Abdel-Daim, M., Sayyouh, M. and Dahab, A. (1996) 'Modelling and laboratory investigation of microbial enhanced oil recovery', *Journal of Petroleum Science and Engineering*, 15(2), 309-320.
- Díaz, J., Rendueles, M. and Díaz, M. (2010) 'Straining phenomena in bacteria transport through natural porous media', *Environmental Science and Pollution Research*, 17(2), 400-409.
- DiCarlo, D. A., Bauters, T. W., Darnault, C. J., Steenhuis, T. S. and Parlange, J. (1999) 'Lateral expansion of preferential flow paths in sands', *Water resources research*, 35(2), 427-434.
- Donlan, R. M. and Costerton, J. W. (2002) 'Biofilms: survival mechanisms of clinically relevant microorganisms', *Clinical microbiology reviews*, 15(2), 167-193.
- Dupin, H. J., Kitanidis, P. K. and McCarty, P. L. (2001) 'Simulations of two-dimensional modeling of biomass aggregate growth in network models', *Water resources research*, 37(12), 2981-2994.
- Dupin, H. J. and McCarty, P. L. (2000) 'Impact of colony morphologies and disinfection on biological clogging in porous media', *Environmental science & technology*, 34(8), 1513-1520.
- Elkateb, T., Chalaturnyk, R. and Robertson, P. K. (2003) 'An overview of soil heterogeneity: quantification and implications on geotechnical field problems', *Canadian Geotechnical Journal*, 40(1), 1-15.
- Engesgaard, P., Seifert, D. and Herrera, P. (2006) 'Bioclogging in porous media: tracer studies' in *Riverbank Filtration Hydrology*, Springer, 93-118.
- EPA, J. (1996) *Pump-and-Treat Ground-Water Remediation: A Guide for Decision Makers and Practitioners*, EPA/625/R-95/005, Office of Research and Development, Washington DC, <http://www.epa.gov/ORD/WebPubs/pumptreat>.
- Environmental Security Technology Certification Program (ESTCP) 2005. [Bioaugmentation for Remediation of Chlorinated Solvents: Technology Development Status and Research Needs](#).

- Evanko, C.R. and Dzombak, D.A., (1997) *Remediation of metals-contaminated soils and groundwater*. Ground-water remediation technologies analysis center.
- Fialho, A. M., Moreira, L. M., Granja, A. T., Popescu, A. O., Hoffmann, K. and Sá-Correia, I. (2008) 'Occurrence, production, and applications of gellan: current state and perspectives', *Applied microbiology and biotechnology*, 79(6), 889-900.
- Folch, A., Vilaplana, M., Amado, L., Vicent, T. and Caminal, G. (2013) 'Fungal permeable reactive barrier to remediate groundwater in an artificial aquifer', *Journal of hazardous materials*, 262, 554-560.
- Fritsche, W. and Hofrichter, M., 2005. Aerobic degradation of recalcitrant organic compounds by microorganisms. *Environmental Biotechnology Concepts and Applications*.
- Fuchs, S., Hahn, H. H., Roddewig, J., Schwarz, M. and Turković, R. (2004) 'Biodegradation and bioclogging in the unsaturated porous soil beneath sewer leaks', *Acta hydrochimica et hydrobiologica*, 32(4-5), 277-286.
- Gadd, G. M. (2007) 'Geomycology: biogeochemical transformations of rocks, minerals, metals and radionuclides by fungi, bioweathering and bioremediation', *Mycological research*, 111(1), 3-49.
- Gadd, G. M. and Raven, J. A. (2010) 'Geomicrobiology of eukaryotic microorganisms', *Geomicrobiology Journal*, 27(6-7), 491-519.
- Gargiulo, G., Bradford, S., Šimůnek, J., Ustohal, P., Vereecken, H. and Klumpp, E. (2007) 'Bacteria transport and deposition under unsaturated conditions: The role of the matrix grain size and the bacteria surface protein', *Journal of contaminant hydrology*, 92(3), 255-273.
- Grishchenkov, V.G., Townsend, R.T., McDonald, T.J., Autenrieth, R.L., Bonner, J.S. and Boronin, A.M., 2000. Degradation of petroleum hydrocarbons by facultative anaerobic bacteria under aerobic and anaerobic conditions. *Process Biochemistry*, 35(9), pp.889-896.
- Green, D. and Willhite, G. 'Enhanced Oil Recovery; SPE Textbook Series, Vol. 6; Society of Petroleum Engineers (SPE): Richardson, TX, 1998', *There is no corresponding record for this reference*.
- Ham, Y. J., Kim, S. B. and Park, S.-J. (2007) 'Numerical experiments for bioclogging in porous media', *Environmental technology*, 28(10), 1079-1089.
- Hand, V. L., Lloyd, J. R., Vaughan, D. J., Wilkins, M. J. and Boulton, S. (2008) 'Experimental studies of the influence of grain size, oxygen availability and organic carbon availability on bioclogging in porous media', *Environmental science & technology*, 42(5), 1485-1491.

- Harbottle, M., Sills, G., Thompson, I. and Jackman, S. (2004) *The use of electrokinetics to enhance the degradation of organic contaminants in soils*, University of Oxford.
- Hardie, M. A., Cotching, W. E., Doyle, R. B., Holz, G., Lisson, S. and Mattern, K. (2011) 'Effect of antecedent soil moisture on preferential flow in a texture-contrast soil', *Journal of Hydrology*, 398(3), 191-201.
- Hashim, M.A., Mukhopadhyay, S., Sahu, J.N. and Sengupta, B.(2011) Remediation technologies for heavy metal contaminated groundwater.*Journal of environmental management*, 92(10), pp.2355-2388.
- Hendricks, D. W., Post, F. J. and Khairnar, D. R. (1979) 'Adsorption of bacteria on soils: experiments, thermodynamic rationale, and application', *Water, Air, and Soil Pollution*, 12(2), 219-232.
- Hendrickx, J. M. and Flury, M. (2001) 'Uniform and preferential flow mechanisms in the vadose zone', *Conceptual models of flow and transport in the fractured vadose zone*, 149-187.
- Hicks, M. A. and Nuttall, J. D. (2012) *Influence of Soil Heterogeneity on Geotechnical Performance and Uncertainty: A Stochastic View on EC7*, translated by 215-227.
- Hill, D. D. and Sleep, B. E. (2002) 'Effects of biofilm growth on flow and transport through a glass parallel plate fracture', *Journal of contaminant hydrology*, 56(3), 227-246.
- Ho, C. K. and Udell, K. K. (1992) 'An experimental investigation of air venting of volatile liquid hydrocarbon mixtures from homogeneous and heterogeneous porous media', *Journal of contaminant hydrology*, 11(3), 291-316.
- Holliger, C., Gaspard, S., Glod, G., Heijman, C., Schumacher, W., Schwarzenbach, R. P. and Vazquez, F. (1997) 'Contaminated environments in the subsurface and bioremediation: organic contaminants', *FEMS Microbiology Reviews*, 20(3-4), 517-523.
- Holm, J. (2000) 'Effect of biomass growth on the hydrodynamic properties of groundwater aquifers, Series Papers 72, Dept', *Hydrodynamics and Water Resources, Technical University of Denmark*.
- Hutton, M. and Symon, C. (1986) The quantities of cadmium, lead, mercury and arsenic entering the UK environment from human activities. *Science of the total environment*, 57, pp.129-150.
- Hunter, R. C. and Beveridge, T. J. (2005) 'High-resolution visualization of *Pseudomonas aeruginosa* PAO1 biofilms by freeze-substitution transmission electron microscopy', *Journal of bacteriology*, 187(22), 7619-7630.

International Centre for Soil and Contaminated Sites (ICSS) 2006. [Manual for Biological Remediation Techniques](#).

Ivanov, V. and Chu, J. (2008) 'Applications of microorganisms to geotechnical engineering for bioclogging and biocementation of soil in situ', *Reviews in Environmental Science and Bio/Technology*, 7(2), 139-153.

Jarvis, N. and Dubus, I. (2006) 'State-of-the-art review on preferential flow', *Report DI*, 6.

Jenneman, G. E., Knapp, R. M., McInerney, M. J., Menzie, D. and Revus, D. (1984) 'Experimental studies of in-situ microbial enhanced oil recovery', *Society of Petroleum Engineers Journal*, 24(01), 33-37.

Joutey, N.T., Bahafid, W., Sayel, H. and El Ghachtouli, N. (2013) Biodegradation: involved microorganisms and genetically engineered microorganisms. *Biodegradation-life of science. In Tech, Rijeka*, pp. 289-320.

Jury, W. A. and Horton, R. (2004) *Soil physics*, John Wiley & Sons.

Kao, C., Chen, S. and Liu, J. (2001) 'Development of a biobarrier for the remediation of PCE-contaminated aquifer', *Chemosphere*, 43(8), 1071-1078.

Keely, J. F. (1996) 'Performance evaluations of pump-and-treat remediations', *EPA environmental engineering sourcebook Edited by JR Boulding, Ann Arbor Press, Chelsea, Michigan*, 31-57.

Khan, F. I., Husain, T. and Hejazi, R. (2004) 'An overview and analysis of site remediation technologies', *Journal of environmental management*, 71(2), 95-122.

Kim, D.-S. and Fogler, H. S. (2000) 'Biomass evolution in porous media and its effects on permeability under starvation conditions'.

Kim, G. (2004) 'Hydraulic conductivity change of bio-barrier formed in the subsurface by the adverse conditions including freeze-thaw cycles', *Cold regions science and technology*, 38(2), 153-164.

Kim, G., Lee, S. and Kim, Y. (2006) 'Subsurface biobarrier formation by microorganism injection for contaminant plume control', *Journal of bioscience and bioengineering*, 101(2), 142-148.

Kim, J.-W., Choi, H. and Pachepsky, Y. A. (2010) 'Biofilm morphology as related to the porous media clogging', *Water Research*, 44(4), 1193-1201.

- Kim, J., Park, H.-D. and Chung, S. (2012) 'Microfluidic approaches to bacterial biofilm formation', *Molecules*, 17(8), 9818-9834.
- Kim, S. B. (2006) 'Numerical analysis of bacterial transport in saturated porous media', *Hydrological processes*, 20(5), 1177-1186.
- Knox, A., Seaman, J., Pierzynski, G. and Adriano, D. (2000) 'Chemophytostabilization of metals in contaminated soils', *ENVIRONMENTAL SCIENCE AND POLLUTION CONTROL SERIES*, 811-836.
- Kokare, C., Chakraborty, S., Khopade, A. and Mahadik, K. (2009) 'Biofilm: Importance and applications', *Indian Journal of Biotechnology*, 8(2), 159-168.
- Komlos, J., Cunningham, A., Warwood, B. and James, G. (1998) *Biofilm barrier formation and persistence in variable saturated zones*, translated by.
- Komlos, J., Cunningham, A. B., Camper, A. K. and Sharp, R. R. (2004) 'Biofilm barriers to contain and degrade dissolved trichloroethylene', *Environmental progress*, 23(1), 69-77.
- Kowalewski, E., Rueslåtten, I., Steen, K., Bødtker, G. and Torsæter, O. (2006) 'Microbial improved oil recovery—bacterial induced wettability and interfacial tension effects on oil production', *Journal of Petroleum Science and Engineering*, 52(1), 275-286.
- Kumar, A., Bisht, B., Joshi, V. and Dhewa, T. (2011) 'Review on Bioremediation of Polluted Environment:: A Management Tool', *International journal of environmental sciences*, 1(6), 1079.
- Lappan, R. E. and Fogler, H. S. (1994) 'Leuconostoc mesenteroides growth kinetics with application to bacterial profile modification', *Biotechnology and bioengineering*, 43(9), 865-873.
- Lappan, R. E. and Fogler, H. S. (1996) 'Reduction of porous media permeability from in situ Leuconostoc mesenteroides growth and dextran production'.
- Lazar, I., Petrisor, I. and Yen, T. (2007) 'Microbial enhanced oil recovery (MEOR)', *Petroleum Science and Technology*, 25(11), 1353-1366.
- Lembre, P., Lorentz, C. and Di Martino, P. (2012) *Exopolysaccharides of the biofilm matrix: A complex biophysical world*, INTECH Open Access Publisher.

- Lim, C.-P., Zhao, D., Takase, Y., Miyanaga, K., Watanabe, T., Tomoe, Y. and Tanji, Y. (2011) 'Increased bioclogging and corrosion risk by sulfate addition during iodine recovery at a natural gas production plant', *Applied microbiology and biotechnology*, 89(3), 825-834.
- Liu, Y., Steenhuis, T. S. and Parlange, J. (1994) 'Closed-form solution for finger width in sandy soils at different water contents', *Water resources research*, 30(4), 949-952.
- MacLeod, F., Lappin-Scott, H. and Costerton, J. (1988) 'Plugging of a model rock system by using starved bacteria', *Applied and Environmental Microbiology*, 54(6), 1365-1372.
- Malone, R. W., Ahuja, L. R., Ma, L., Don Wauchope, R., Ma, Q. and Rojas, K. W. (2004) 'Application of the Root Zone Water Quality Model (RZWQM) to pesticide fate and transport: an overview', *Pest management science*, 60(3), 205-221.
- Manual, E. (2004) 'How to Evaluate Alternative Cleanup Technologies for Underground Storage Tank Sites: A Guide for Corrective Action Plan Reviewers', *US Environmental Protection Agency*.
- Manuel, C., Nunes, O. and Melo, L. (2007) 'Dynamics of drinking water biofilm in flow/non-flow conditions', *Water Research*, 41(3), 551-562.
- Matthess, G. and Pekdeger, A. (1981) 'Concepts of a survival and transport model of pathogenic bacteria and viruses in groundwater', *Studies in Environmental Science*, 17, 427-437.
- Mayer, C., Moritz, R., Kirschner, C., Borchard, W., Maibaum, R., Wingender, J. and Flemming, H.-C. (1999) 'The role of intermolecular interactions: studies on model systems for bacterial biofilms', *International journal of biological macromolecules*, 26(1), 3-16.
- McCarty, P. L., Goltz, M. N., Hopkins, G. D., Dolan, M. E., Allan, J. P., Kawakami, B. T. and Carrothers, T. (1998) 'Full-scale evaluation of in situ cometabolic degradation of trichloroethylene in groundwater through toluene injection', *Environmental science & technology*, 32(1), 88-100.
- McCaulou, D. R., Bales, R. C. and McCarthy, J. F. (1994) 'Use of short-pulse experiments to study bacteria transport through porous media', *Journal of contaminant hydrology*, 15(1), 1-14.
- Mitchell, B. S. (2004) *An introduction to materials engineering and science for chemical and materials engineers*, John Wiley & Sons.
- Mitchell, J. K. and Santamarina, J. C. (2005) 'Biological considerations in geotechnical engineering', *Journal of Geotechnical and Geoenvironmental Engineering*, 131(10), 1222-1233.

- Mittal, A., Mittal, J. and Kurup, L. (2007) 'Utilization of hen feathers for the adsorption of indigo carmine from simulated effluents', *J. Environ. Prot. Sci*, 1, 92-100.
- Nagata, T. and Watanabe, Y. (1990) 'Carbon-and nitrogen-to-volume ratios of bacterioplankton grown under different nutritional conditions', *Applied and Environmental Microbiology*, 56(5), 1303-1309.
- Nasrazadani, A., Tahmourespour, A. and Hoodaji, M. (2011) 'Determination of bacteria resistance threshold to lead, zinc and cadmium in three industrial wastewater samples', *J Environ Studies*, 36, 75-86.
- Nielsen, D. R., Biggar, J. W. and Erh, K. T. (1973) *Spatial variability of field-measured soil-water properties*, University of California, Division of Agricultural Sciences.
- Nies, D. H. (1999) 'Microbial heavy-metal resistance', *Applied microbiology and biotechnology*, 51(6), 730-750.
- Oberdorfer, J. A. and Peterson, F. L. (1985) 'Waste-Water Injection: Geochemical and Biogeochemical Clogging Processes', *Groundwater*, 23(6), 753-761.
- Omenn, G.S., 1992. Environmental biotechnology: biotechnology solutions for a global environmental problem, hazardous chemical wastes. *Asia-Pacific Journal of Public Health*, 6(2), pp.40-45.
- Okubo, T. and Matsumoto, J. (1979) 'Effect of infiltration rate on biological clogging and water quality changes during artificial recharge', *Water resources research*, 15(6), 1536-1542.
- Pal, A. and Paul, A. (2013) 'Optimization of cultural conditions for production of extracellular polymeric substances (EPS) by serpentine rhizobacterium *Cupriavidus pauculus* KPS 201', *Journal of Polymers*, 2013.
- Palmer, C. D. and Fish, W. (1992) *Chemical enhancements to pump-and-treat remediation*, Superfund Technology Support Center for Ground Water, Robert S. Kerr Environmental Research Laboratory.
- Patel, S. and Kasture, A. (2014) E (Electronic) Waste Management using Biological systems-overview. *Int. J. Curr. Microbiol. App. Sci*, 3(7), pp.495-504.
- Peyton, B. M. and Characklis, W. (1993) 'A statistical analysis of the effect of substrate utilization and shear stress on the kinetics of biofilm detachment', *Biotechnology and bioengineering*, 41(7), 728-735.

- Porter, K. G. and Feig, Y. S. (1980) 'The use of DAPI for identifying and counting aquatic microflora1', *Limnology and oceanography*, 25(5), 943-948.
- Prakash, B., Veeregowda, B. and Krishnappa, G. (2003) 'Biofilms: a survival strategy of bacteria', *Current science*, 85(9), 1299-1307.
- Pyne, R. D. G. (1995) *Groundwater recharge and wells: a guide to aquifer storage recovery*, CRC press.
- Qi, M.-C., Hu, J., Zou, S.-J., Chen, H.-Q., Zhou, H.-X. and Han, L.-C. (2008) 'Mechanical strain induces osteogenic differentiation: Cbfa1 and Ets-1 expression in stretched rat mesenchymal stem cells', *International journal of oral and maxillofacial surgery*, 37(5), 453-458.
- Ray, C., Vogel, T. and Dusek, J. (2004) 'Modeling depth-variant and domain-specific sorption and biodegradation in dual-permeability media', *Journal of contaminant hydrology*, 70(1), 63-87.
- Reddy, K. R. (2008) 'Physical and chemical groundwater remediation technologies' in *Overexploitation and contamination of shared groundwater resources*, Springer, 257-274.
- Rice, R. C. (1974) 'Soil clogging during infiltration of secondary effluent', *Journal (Water Pollution Control Federation)*, 708-716.
- Rittmann, B. E. (1993) 'The significance of biofilms in porous media', *Water resources research*, 29(7), 2195-2202.
- Rochex, A. and Lebeault, J.-M. (2007) 'Effects of nutrients on biofilm formation and detachment of a *Pseudomonas putida* strain isolated from a paper machine', *Water Research*, 41(13), 2885-2892.
- Ross, N., Villemur, R., Deschênes, L. and Samson, R. (2001) 'Clogging of a limestone fracture by stimulating groundwater microbes', *Water Research*, 35(8), 2029-2037.
- Rutherford, S. T. and Bassler, B. L. (2012) 'Bacterial quorum sensing: its role in virulence and possibilities for its control', *Cold Spring Harbor perspectives in medicine*, 2(11), a012427.
- Ryan, J. N. and Elimelech, M. (1996) 'Colloid mobilization and transport in groundwater', *Colloids and surfaces A: Physicochemical and engineering aspects*, 107, 1-56.

- Sanin, S. L., Sanin, F. D. and Bryers, J. D. (2003) 'Effect of starvation on the adhesive properties of xenobiotic degrading bacteria', *Process Biochemistry*, 38(6), 909-914.
- Sauer, K., Camper, A. K., Ehrlich, G. D., Costerton, J. W. and Davies, D. G. (2002) 'Pseudomonas aeruginosa displays multiple phenotypes during development as a biofilm', *Journal of bacteriology*, 184(4), 1140-1154.
- Schmitt, J., Nivens, D., White, D. C. and Flemming, H.-C. (1995) 'Changes of biofilm properties in response to sorbed substances-an FTIR-ATR study', *Water Science and Technology*, 32(8), 149-155.
- Seifert, D. and Engesgaard, P. (2007) 'Use of tracer tests to investigate changes in flow and transport properties due to bioclogging of porous media', *Journal of contaminant hydrology*, 93(1), 58-71.
- Steve, K. and Erika, T. (1998) Activated Carbon M Reynold T., Paul A., " Unit Operations and Processes of Activated Carbon. *Environmental Engineering*", 2nd Ed. PWS Publishing Co. p, 25(350), p.749.
- Zabochnicka-Świątek, M. and Krzywonos, M. (2014) Potentials of biosorption and bioaccumulation processes for heavy metal removal. *Mercury*, 6(5,245), pp.1-145.
- Seki, K. (2013) 'Biological Clogging of Sand Columns'.
- Seki, K., Kamiya, J. and Miyazaki, T. (2005) 'Temperature dependence of hydraulic conductivity decrease due to biological clogging under ponded infiltration', *TRANSACTIONS-JAPANESE SOCIETY OF IRRIGATION DRAINAGE AND RECLAMATION ENGINEERING*, 73(3), 13.
- Seki, K. and Miyazaki, T. (2001) 'A mathematical model for biological clogging of uniform porous media', *Water resources research*, 37(12), 2995-2999.
- Seki, K., Miyazaki, T. and Nakano, M. (1998) 'Effects of microorganisms on hydraulic conductivity decrease in infiltration', *European Journal of Soil Science*, 49(2), 231-236.
- Seki, K., Suko, T. and Miyazaki, T. (2002) *Bioclogging of glass beads by bacteria and fungi*, translated by 1244-1.
- Sen, R. (2008) 'Biotechnology in petroleum recovery: the microbial EOR', *Progress in Energy and Combustion Science*, 34(6), 714-724.
- Shackelford, C. D. and Daniel, D. E. (1991) 'Diffusion in saturated soil. I: Background', *Journal of Geotechnical Engineering*.

- Shafahi, M. and Vafai, K. (2009) 'Biofilm affected characteristics of porous structures', *International Journal of Heat and Mass Transfer*, 52(3), 574-581.
- Shaw, J. C., Bramhill, B., Wardlaw, N. and Costerton, J. (1985) 'Bacterial fouling in a model core system', *Applied and Environmental Microbiology*, 49(3), 693-701.
- Simunek, J. and Van Genuchten, M. (2007) 'Contaminant transport in the unsaturated zone: theory and modelling', *The Handbook of Groundwater Engineering*, 22, 22-38.
- Singh, R., Paul, D. and Jain, R. K. (2006) 'Biofilms: implications in bioremediation', *Trends in microbiology*, 14(9), 389-397.
- Slichter, C. S. (1905) *Field measurements of the rate of movement of underground waters*, Govt. Print. Off.
- Smith, E. A. (2012) *Spatial and temporal variability of preferential flow in a subsurface-drained landscape in north-central Iowa*, UNIVERSITY OF MINNESOTA.
- Soares, M. I. s. M., Braester, C., Belkin, S. and Abeliovich, A. (1991) 'Denitrification in laboratory sand columns: carbon regime, gas accumulation and hydraulic properties', *Water Research*, 25(3), 325-332.
- Stevik, T. K., Aa, K., Ausland, G. and Hanssen, J. F. (2004) 'Retention and removal of pathogenic bacteria in wastewater percolating through porous media: a review', *Water Research*, 38(6), 1355-1367.
- Stewart, T. L. and Fogler, H. S. (2001) 'Biomass plug development and propagation in porous media'.
- Stone, W. W. and Wilson, J. T. (2006) 'Preferential flow estimates to an agricultural tile drain with implications for glyphosate transport', *Journal of Environmental Quality*, 35(5), 1825-1835.
- Stoodley, P., Dodds, I., Boyle, J. and Lappin-Scott, H. (1999) 'Influence of hydrodynamics and nutrients on biofilm structure', *Journal of applied microbiology*, 85, 19S-28S.
- Suchomel, B. J., Chen, B. M. and Allen III, M. B. (1998) 'Network model of flow, transport and biofilm effects in porous media', *Transport in Porous Media*, 30(1), 1-23.

- Suslow, T. V. (2004) 'Oxidation-reduction potential (ORP) for water disinfection monitoring, control, and documentation', *Division of Agriculture and National Resources, University of California, Davis*.
- Suthar, H., Hingurao, K., Desai, A. and Nerurkar, A. (2009) 'Selective plugging strategy-based microbial-enhanced oil recovery using *Bacillus licheniformis* TT33', *Journal of microbiology and biotechnology*, 19(10), 1230-1237.
- Tangahu, B. V., Sheikh Abdullah, S. R., Basri, H., Idris, M., Anuar, N. and Mukhlisin, M. (2011) 'A review on heavy metals (As, Pb, and Hg) uptake by plants through phytoremediation', *International Journal of Chemical Engineering*, 2011.
- Tark, M., Tover, A., Tarassova, K., Tegova, R., Kivi, G., Horak, R. and Kivisaar, M. (2005) 'A DNA polymerase V homologue encoded by TOL plasmid pWW0 confers evolutionary fitness on *Pseudomonas putida* under conditions of environmental stress', *Journal of bacteriology*, 187(15), 5203-5213.
- Taylor, S. W. and Jaffé, P. R. (1990a) 'Biofilm growth and the related changes in the physical properties of a porous medium: 1. Experimental investigation', *Water resources research*, 26(9), 2153-2159.
- Taylor, S. W. and Jaffé, P. R. (1990b) 'Substrate and biomass transport in a porous medium', *Water Resour. Res.*, 26(9), 2181-2194.
- Thomas, J. and Ward, C. (1989) 'In situ bioremediation of organic contaminants in the subsurface', *Environmental science & technology*, 23(7), 760-766.
- Thullner, M. (2010) 'Comparison of bioclogging effects in saturated porous media within one- and two-dimensional flow systems', *Ecological Engineering*, 36(2), 176-196.
- Thullner, M., Mauclaire, L., Schroth, M. H., Kinzelbach, W. and Zeyer, J. (2002) 'Interaction between water flow and spatial distribution of microbial growth in a two-dimensional flow field in saturated porous media', *Journal of contaminant hydrology*, 58(3), 169-189.
- Thullner, M., Schroth, M. H., Zeyer, J. and Kinzelbach, W. (2004) 'Modeling of a microbial growth experiment with bioclogging in a two-dimensional saturated porous media flow field', *Journal of contaminant hydrology*, 70(1), 37-62.
- Thullner, M. C. (2001) *Experimental and numerical investigations of bioclogging in porous media using two-dimensional flow fields*, unpublished thesis Diss., Naturwissenschaften ETH Zürich, Nr. 14372, 2002.

- Torbati, H., Raiders, R., Donaldson, E., McInerney, M., Jenneman, G. and Knapp, R. (1986) 'Effect of microbial growth on pore entrance size distribution in sandstone cores', *Journal of Industrial Microbiology*, 1(4), 227-234.
- Trefry, M. G. and Johnston, C. D. (1998) 'Pumping test analysis for a tidally forced aquifer', *Groundwater*, 36(3), 427-433.
- Vaid, Y. and Negussey, D. (1988) 'Preparation of reconstituted sand specimens', *Advanced triaxial testing of soil and rock, ASTM STP, 977*, 405-417.
- Van der Ruyt, M. and van der Zon, W. (2009) 'Biological in situ reinforcement of sand in near-shore areas', *Proceedings of the ICE-Geotechnical Engineering*, 162(1), 81-83.
- Vandevivere, P. and Baveye, P. (1992) 'Saturated hydraulic conductivity reduction caused by aerobic bacteria in sand columns', *Soil Science Society of America Journal*, 56(1), 1-13.
- Vandevivere, P., Baveye, P., Lozada, D. S. and DeLeo, P. (1995) 'Microbial clogging of saturated soils and aquifer materials: Evaluation of mathematical models', *Water resources research*, 31(9), 2173-2180.
- Vilcáez, J., Li, L., Wu, D. and Hubbard, S. S. (2013) 'Reactive transport modeling of induced selective plugging by leuconostoc mesenteroides in carbonate formations', *Geomicrobiology Journal*, 30(9), 813-828.
- Villasenor, J., Van Loosdrecht, M., Picioreanu, C. and Heijnen, J. (2000) 'Influence of different substrates on the formation of biofilms in a biofilm airlift suspension reactor', *Water Science & Technology*, 41(4), 323-330.
- Vu, B., Chen, M., Crawford, R. J. and Ivanova, E. P. (2009) 'Bacterial extracellular polysaccharides involved in biofilm formation', *Molecules*, 14(7), 2535-2554.
- Wang, D., Han, P., Shao, Z. and Seright, R. S. (2006) *Sweep improvement options for the Daqing oil field*, translated by Society of Petroleum Engineers.
- Wang, J. and Chen, C. (2009) 'Biosorbents for heavy metals removal and their future', *Biotechnology advances*, 27(2), 195-226.

- Weidner, C., Henkel, S., Lorke, S., Rde, T. R., Schttrumpf, H. and Klauder, W. (2012) 'Experimental modelling of chemical clogging processes in dewatering wells', *Mine Water and the Environment*, 31(4), 242-251.
- Wu, J.-R., Son, J. H., Kim, K. M., Lee, J.-W. and Kim, S.-K. (2006) 'Beijerinckia indica L3 fermentation for the effective production of heteropolysaccharide-7 using the dairy byproduct whey as medium', *Process Biochemistry*, 41(2), 289-292.
- Wu, J., Gui, S., Stahl, P. and Zhang, R. (1997) 'Experimental study on the reduction of soil hydraulic conductivity by enhanced biomass growth', *Soil Science*, 162(10), 741-748.
- Yakimov, M. M., Amro, M. M., Bock, M., Boseker, K., Fredrickson, H. L., Kessel, D. G. and Timmis, K. N. (1997) 'The potential of Bacillus licheniformis strains for in situ enhanced oil recovery', *Journal of Petroleum Science and Engineering*, 18(1), 147-160.
- Yates, M. V. and Yates, S. (1991) 'Modeling microbial transport in the subsurface: A mathematical discussion'.
- Yuan, S., Wei, S. and Chang, B. (2000) 'Biodegradation of polycyclic aromatic hydrocarbons by a mixed culture', *Chemosphere*, 41(9), 1463-1468.
- Zhang, T. C., Fu, Y., Bishop, P. L., Kupferle, M., FitzGerald, S., Jiang, H. H. and Harmer, C. (1995) 'Transport and biodegradation of toxic organics in biofilms', *Journal of hazardous materials*, 41(2), 267-285.
- Zhong, X., Wu, Y. and Xu, Z. (2013) 'Bioclogging in porous media under discontinuous flow condition', *Water, Air, & Soil Pollution*, 224(5), 1-12.

